Phenomenology and collider constraints of Supersymmetric models in the Run 2 era of the LHC

Sophie Williamson

▶ **To cite this version:**

HAL Id: tel-03010490
https://theses.hal.science/tel-03010490

Submitted on 17 Nov 2020

THÈSE DE DOCTORAT
DE SORBONNE UNIVERSITÉ

Spécialité : Physique Théorique

École doctorale n564: Physique en Île-de-France

réalisée

au Laboratoire de Physique Théorique et Hautes Energies

sous la direction de Mark D. Goodsell

présentée par

Sophie Louise Soulsby Williamson

pour obtenir le grade de :

DOCTEUR DE SORBONNE UNIVERSITÉ

Phenomenology and collider constraints of Supersymmetric models in the Run 2 era of the LHC

soutenue le 12$^{\text{ème}}$ Septembre 2019

devant le jury composé de :

M.	Adam FALKOWSKI	Examinateur
M.	Mark D. GOODSELL	Directeur de thèse
M$^{\text{me}}$	Gudrid MOORTGAT-PICK	Rapporteuse
M$^{\text{me}}$	Lydia ROOS	Examinatrice
M.	Michael SPANNOWSKY	Rapporteur

To the man who gave me life and all he could for me to live it well.
My father.
30.09.1951 – 29.06.2018.

Acknowledgements

The saying goes that behind every great man, there is a great woman. While I believe this line of thought to be entirely outdated, I think it is quite true that behind every scientist, from the moderate to the genius, there is an active team of collaborators, intellectual adversaries and curious coffee-break conversationalists. It is along this vein that I must acknowledge all of those that have contributed to my being able to compose this thesis.

Undeniably, the person to whom I owe the most is my supervisor, Mark, who helped me make the transition from somewhat petrified student to physicist going out in the world to try and hold their own. I know having me as your student has not always been the most straight-forward of options, but without your support, kindness, generosity, interest, trust and expertise[1], I certainly would not be in the position I am today. Thank you for always leaving your door open for me, and for making it so pleasant to be your student. I will always appreciate how welcome you made me feel in the early days, responding to "I have a number of very stupid questions" with "Oh, I love a good stupid question. The more stupid the better". Thank you for always being so positive, and for being a role-model who does physics for the love of physics itself.

I am entirely grateful to the reviewers of my thesis, Gudrid Moortgat-Pick and Michael Spannowsky, for taking the time to go over my manuscript and for their very kind and helpful feedback. I thank you both for accepting to travel to Paris to take part in my jury. I am also thankful to the other members of my jury, Adam Falkowski and Lydia Roos, for participating in my thesis defence.

A great deal of thanks must also go to my collaborators, for so wilfully sharing their scientific knowledge with me, and for their patience in doing so.

I owe a lot to Sabine Kraml, for the time she has spent with me during our many international encounters, essentially taking on the roll of a second supervisor and welcoming me into the world of reinterpretation and LHC physics. Along with Mark, I must reiterate my thanks for your support, advice and reference-writing in helping me obtain my post-doctoral position. Not only have I learnt a lot through my collaborations with you, but have felt privileged to absorb from you a love of mountains, scrambling and rock-climbing. I wish for many more fruitful collaborations in the future, not only because you still have yet to teach me how to cross-country ski.

My thanks must also go to the other members of the LPSC in Grenoble, for inviting me to give my first seminar and accommodating me in their lab for a visit. I thank Humberto, for his efforts to our multiple finished and ongoing projects together, and for always being a friendly face. You are only a year my PhD junior, but it has been so nice to watch you grow, and to collaborate, learn and share with you throughout our mutual doctoral journeys. I also thank Guillaume, for imparting with me his

---

[1]I could expand this list, but at the risk of you blushing.

knowledge on recasting.

I am altogether grateful to Karl Knordström, for answering my many (MANY) questions on all things collider physics, and for always explaining everything so well[2]. I truly appreciate all the details you would go into, and for always finding a way to help me understand what I was struggling with. You were great fun to work with, and I thank you for always making me feel comfortable in my question-asking.

I must also thank Richard Ruiz, for bringing me on board his project looking at dynamic jet vetoes, and for sharing with me his knowledge in this domain of physics. While the world of QCD is still almost an entire unconquered land to me, I thank you for helping me take my first steps. I am grateful to you and your lab for your invitation to visit you at CP3, Louvain, and for being so generous with your beer buying. Thank you for being such an active and interested collaborator.

I thank Benjamin Fuks, for his enthusiasm throughout our collaborations and meetings, and sharing with me his expertise in physics tools and collider physics. My gratitude also goes to the other members of my group, Karim Benakli and Pietro Slavich, for integrating me into the group at LPTHE and for various discussions.

My unreserved thanks go to Johannes Braathen: my PhD brother, good friend, and physics genie. Thank you for all you did helping me settle into lab life at LPTHE, for your friendship, kindness, incessant teasing, mochi providing, physics discussions and helping me advance through the sea of post-doctoral applications. Without a doubt, my first few years at Jussieu would not have been so enjoyable without you, and I wish to continue tolerating you in future.

I thank Yann Mambrini and Claude Viallet for taking on the roles of my scientific advisor and mentor respectively, and for taking the time to see me through the various stages of my PhD. I thank Benoit Douçot, for his support and benevolence during some of the hardest times of my PhD. I very much enjoyed our interactions, and I am truly grateful for how you helped me. I thank Julia Harz, for all her assistance, patience and kindness during the early days of my PhD. I thank Stephan Huber, my master's supervisor and all-round awesome person, for without him it is unlikely I would have considered undertaking a thesis to start with. I thank Claire Adby, my high school physics teacher, for guilting me into coming and talking with her at the A-level choices meeting, for encouraging me to take on physics when I found it so daunting and for convincing me I could do it.

There are numerous members of the lab that I must acknowledge – Mathieu Boudaud, Marco Cirelli, Benoit Estienne, Françoise Got, Andreas Goudelis, Isabelle Nicolaï, Sebastian Passehr, Marco Picco, Hua-sheng Shao, Marjorie Stievenart-Ammour – for without them my experience there would not have been the same. This is not to mention the many PhD students with whom my studies have overlapped - Constantin, Damien, Guillaume, Yifan, Yoan, Gregoire, Osmin, Gaetan, Colin, Ruben, Enrico, Giovanni, Manuel, Kang, Hugo, Oscar, Chrysoula, Mathieu, Thomas, Alessandro, Maxence and Alexis.

Finally, my sincere thanks go to my family and closest friends: to my brothers, Matthew and Andrew, for always making me feel like the smart one in the family; to my auntie Melanie and uncle John, for always being there for me; to Jess, for coming to Paris to cheer me on during races and defences; to Edouard, for his support, acceptance, care, and tolerance; to my mum, for everything she has done and will continue to do to help me realise my life's goals. Mum, you have always been my biggest female role-model, and I find it inspiring what you have managed to achieve in life and in science, despite being told physics was "no subject for a girl". Not that

---

[2]Maybe if you'd done so a bit worse, life would have been more peaceful for you.

Abbreviations

NLO	Next-to-Leading Order
NNLO	Next-to-Next-to-Leading Order
PDF	Parton Distribution Function
PS	Parton Shower
QCD	Quantum Chromodynamics
QFT	Quantum Field Theory
RG(E)	Renormalisation Group (Equation)
S/B	Signal Over Background
SLHA	Supersymmetry Les Houches Accord
SM	Standard Model
SUSY	Supersymmetry/Supersymmetric
THDM	Two-Higgs-Doublet Model
UFO	Universal FeynRules Output
UV	Ultra-violet
VEV	Vacuum Expectation Value
WIMP	Weakly Interacting Massive Particle

Contents

Introduction

"Don't knock the weather. If it didn't change once in a while, nine out of ten people couldn't start a conversation". - Kin Hubbard

While a seemingly arbitrary way to open a thesis, this quote resembles in some way the modern state of particle physics. All the components of the Standard Model (SM) have, to this day, been experimentally observed, yet unanswered questions mean that the domain of particle theory goes far beyond experimental capabilities: the conversation in the Beyond the Standard Model (BSM) community is thriving because the Standard Model does not completely conform to expectations. While the SM has successfully been predicting experimental outcomes since the 1970's, it is clearly lacking an integrated description of gravity, and among many other issues, runs into the problem of unobserved Planck-scale sized quantum corrections to the Higgs mass (assuming the miraculous cancellation of which does not occur) if the SM is not capped at some lower energy scale and absorbed into some higher energy theory.

The theoretical predictions of the Standard Model were finally satisfied in 2012 with the discovery of the Brout-Englert-Higgs boson – short-named Higgs – at the Large Hadron Collider (LHC) in CERN, when not only was the particle content polished off, but the part played by electroweak symmetry breaking (EWSB) in the establishment of gauge boson and fermion masses substantiated. The 125 GeV Higgs boson mass is now known to a precision of $\sim 0.1\%$ and, as the only scalar in the SM, is sensitive to new physics which would have an impact on its mass, couplings and behaviour. In turn, the parameter space of any SM-extended model can be explored and constrained and, as such, the Higgs can be seen as a gateway to new discoveries.

Many models propose effective solutions to the dilemmas of the SM, from extra dimensional and string theories to composite Higgs and technicolour, but supersymmetry has long been established as a theoretical ring-leader with proposed explanations for almost all of these. Supersymmetry (SUSY) is an elegant theory, that essentially doubles the Standard Model particle content by levelling off the bosonic-fermionic antisymmetry. Integer and half-integer spin particles are paired together in *super-multiplets*, thus eliminating each other's radiative loop divergent diagrams. However, nature clearly has other ideas, and SUSY must be broken at some energy level above what we can currently probe, resulting in superpartners heavier than their Standard Model counterparts. It is therefore timely to consider non-minimal supersymmetry, with additional particle content added to the minimal supersymmetric standard model (MSSM). Such models can help alleviate the tension between the electroweak and increasing supersymmetry scales, by physically justifying why some particle content can be heavier (*e.g.* gluinos - the supersymmetric partners to the gluons), and simultaneously allowing some particle content to be lighter than in the minimal version (*e.g.* squarks - the supersymmetric partners to the quarks). One such model is the Dirac gaugino supersymmetric standard model (MDGSSM), which will be the focus

of chapters 2 and 3. Simplified minimal models will also be considered in chapters 3 and 4.

This thesis will begin with an introductory chapter 1 on the Standard Model and a glance at the Higgs mechanism, which is responsible for generating the masses of the Standard Model particle spectrum. This section will segway, via a short summary of motivations for beyond the standard model physics, into a discussion of the basic supersymmetry formalism and the models that will be discussed in this text - namely the MSSM, the MDGSSM and the minimal R-symmetric supersymmetric standard model (MRSSM) - with particular attention paid to the Higgs sectors. The central 3 chapters are based on 3 articles:

- Karim Benakli, Mark Dayvon Goodsell and Sophie Louise Williamson, *Higgs alignment from extended supersymmetry*, Eur. Phys. J. C **78** (2018) no.8, 658, `arXiv:1801.08849 [hep-ph].`

which corresponds to the content of chapter 2;

- Guillaume Chalons, Mark Dayvon Goodsell, Sabine Kraml, Humberto Reyes-González and Sophie Louise Williamson, *LHC limits on gluinos and squarks in the minimal Dirac gaugino model*, JHEP **1904** (2019) 113, `arXiv:1812.09293 [hep-ph],`

which correlates to chapter 3; and

- Benjamin Fuks, Karl Nordström, Richard Ruiz and Sophie Louise Williamson, *Sleptons without Hadrons*, `arXiv:1901.09937 [hep-ph]`, *To appear in PRD.*

which constitutes the work of chapter 4.

The first of these investigates the Higgs sector of a two-Higgs doublet model extension immersed within a higher energy SUSY theory. Owing to the additional content in the MDGSSM, it is possible to group together the particles in $\mathcal{N} = 2$ multiplets. The resulting $\mathcal{N} = 2$ symmetry between the gauge and new Yukawa couplings means that, as long as the symmetry is unbroken, the Higgs sector is always in *alignment* and fully agrees with that of the Standard Model. This chapter looks at the effect on the Higgs mass and properties of running down from a higher energy $\mathcal{N} = 2$ scale to electroweak energies, including the inclusion of radiative corrections to the scalar effective potential. A simplistic comparison is also performed in the MRSSM, where alignment in the Higgs sector is not predicted.

As one of an abundance of SM-extensions, BSM model-specific limits are understandably not all provided by the experimental collaborations. Following this thread, chapter 3 aims to derive and compare the limits on the squarks and gluinos in the MDGSSM with those in the MSSM, in the context of Run 2 of the LHC. This study is motivated from the basis that, by virtue of the extended Higgs sector in the MDGSSM, the neutralino and chargino spectrum is enlarged creating a more elaborate decay spectrum. Additionally, the production mechanisms across the two models differ, as gluino pair-production is enhanced and squark production is suppressed in the MDGSSM relative to the MSSM.

Chapter 4 explores the impact of introducing dynamic jet vetoes in searches for colourless superpartners in weak-scale supersymmetry models. Despite the traditional application of central static jet vetoes, searches at hadron colliders are impeded by large top quark pair and diboson backgrounds. However, it can be shown that by employing a jet veto which is adjusted dynamically based on relative measures of leptonic and hadronic activities present in an event, the signal-to-background efficiency

increases and the sensitivity of searches for colourless superpartners can be improved. A representative scenario considering the Drell-Yan production of a pair of right-handed smuons decaying into a dimuon system accompanied by missing transverse energy is discussed; however the results should be applicable to all searches for new, heavy, uncoloured physics that is searched for using jet vetoes at the LHC.

This thesis will then be wrapped up with a short conclusion (chapter 4.6), with additional calculations and details available in the appendix.

1 – The SM and beyond

1.1 The Standard Model

The core of the work presented in the following chapters will establish itself on the foundation of supersymmetry, and supersymmetric models. But before justifying why we want to go beyond the standard model (BSM), we should motivate why this may be necessary to start with. This section will very briefly cover the electroweak sector of the standard model (SM) and, in particular, the Higgs sector and its electroweak symmetry breaking (EWSB) mechanism. There are numerous good references on the SM out there, with examples being [1–6].

1.1.1 Its fields and content

The standard model is, to date, undoubtedly the most convincing theory we have that describes the fundamental interactions between matter and the forces of nature. It is neatly summarised as an $SU(3)_c \times SU(2)_L \times U(1)_Y$ gauge theory, which describes the interactions of elementary particles charged under the strong (coloured), weak (left) and electromagnetic (hypercharge) forces respectively. Matter fields can be separated into those that are charged under the strong force (the quarks) and those that are not (the leptons). Together, they make up the fermionic fields of the SM (fermions, named after the Fermi-Dirac statistics they obey), and possess 1/2 integer spin. The bosons (that follow Bose-Einstein statistics) get instead an integer spin, and can be subdivided into four vector (gauge) bosons of spin-1; a scalar boson (the Higgs) of spin-0; and the hypothetical force carrier for gravity, the graviton, of spin-2.

Each of the gauge boson fields is associated with a gauge symmetry, where there is one gauge field for each of the gauge group generators: B_μ corresponds to the hypercharge generator, Y, of the $U(1)_Y$ group; W_μ^a correspond to the three weak generators $\sigma^a/2$ ($a = 1, 2, 3$) - given by the Pauli matrices - of the $SU(2)_L$ group, and G_μ^a correspond to the eight strong generators λ^a ($a = 1...8$) - given by the Gell-mann matrices - of the $SU(3)_c$ group. The number of gauge fields is a consequence of the fact that they live in the adjoint representation - hence 3 for $SU(2)$ (each members of a weak isospin triplet) and 8 for $SU(3)$. A gauge symmetry is a symmetry that allows states that cannot be physically distinguished from each other to be connected, with a gauge *transformation* linking each location in the parameter space with a change of co-ordinates. As such, the transformation parameter in gauge theories is space-time dependent and gauge symmetries are described as *local* symmetries. This is compared to global symmetries where the transformation parameter is constant across all space-time. Taking a function $\phi(x) = \rho(x)e^{i\lambda(x)}$, consider a global and local U(1) symmetry:

- If the action is invariant under a local $U(1)$ symmetry, under a translation

$$\phi(x) \to e^{i\alpha(x)\phi(x)}$$

$$= e^{i\alpha(x)}\rho(x)e^{i\lambda(x)} = \phi'(x)\,, \tag{1.1.1}$$

the parameter $\alpha(x)$ can be chosen such that for each value of $\lambda(x)$, $\phi'(x) = \lambda(x)$. In other words, it is always possible to choose a transformation such that the theory's dependency on the parameter $\lambda(x)$ is redundant.

- If the action is invariant under a global $U(1)$ symmetry, the parameter α is constant and, under the translation

$$\phi(x) \to e^{i\alpha\phi(x)}$$
$$= e^{i\alpha}\rho(x)e^{i\lambda(x)} = \phi'(x)\,, \tag{1.1.2}$$

α cannot be chosen to eliminate the theory's dependency on $\lambda(x)$ for all values of x. The theory then has a true dependency on $\lambda(x)$ - a dependency which cannot be gauged away.

In the theories that will be considered in this text, the standard model gauge group is a local symmetry, whereas supersymmetry is a global one. Local invariance under a gauge symmetry is required as a feature of the theory so as to get rid of redundant degrees of freedom. For example, the 4 d.o.f that accompany a four-vector are more d.o.f than is necessary to describe massive (3 d.o.f) or massless (2 d.o.f) bosons. In the case of massless bosons, it is possible to remove one degree of freedom by the imposition that they be physical (*e.g.* a photon spinning in line with its direction of motion would theoretically be travelling faster than the speed of light!), but there is still one redundant d.o.f. This is where gauge invariance is implemented, so that the physical quantity being measured is identical regardless of the field being transformed. Unless the gauge symmetry is spontaneously broken, then the associated gauge bosons will be massless. This follows from gauge invariance: if one takes a gauge field $A^\mu(x)$ which transforms under a gauge transformation like

$$A^\mu(x) \to A'^\mu(x) = A^\mu(x) + \partial^\mu\phi(x) \tag{1.1.3}$$

then it follows that the mass term $m_A^2 A_\mu A^\mu$ would transform like

$$m_A^2 A_\mu A^\mu \to m_A^2 A_\mu A^\mu + 2m_A^2 A_\mu \partial^\mu\phi + m_A^2 \partial_\mu\phi\partial^\mu\phi\,, \tag{1.1.4}$$

which only holds for arbitrary ϕ if m_A vanishes. This is exactly what happens in the cases of quantum electrodynamics (mediated by the photon) and quantum chromodynamics (mediated by the gluons) which are massless fields with helicity, or (transverse) polarisations, ± 1. However, the story continues for the electroweak gauge groups: experimental measurements of the $W-$ and $Z-$ boson masses reveal they are not equal, and hence $SU(2)_L$ cannot be the group the governs the observed weak interactions. Indeed, after EWSB, the SM gauge group is further broken down from $SU(2)_L \times U(1)_Y \to U(1)_{EM}$. The *Goldstone theorem* states that a theory with spontaneous symmetry breaking has a massless particle in its spectrum [7, 8]: these are known as Goldstone bosons ($G^\pm, G^0$), and they constitute the extra degrees of freedom (d.o.f) that go into making up the longitudinal polarisations of the then massive $W^\pm, Z$ bosons. The electroweak bosons can then possess helicities $0, \pm 1$. Technically speaking, these 3 longitudinal polarisations *are* Higgs bosons - just not *the* Higgs boson, h, that acquires a vacuum expectation value (VEV), v, that we spent such a long time searching for at the LHC.

The Higgs doublet, denoted by

$$\Phi = \begin{pmatrix} \phi^+ \\ \phi^0 \end{pmatrix}\,, \tag{1.1.5}$$

where

$$\phi^0 = \frac{1}{\sqrt{2}}(\phi_1 + i\phi_2)\,, \qquad \phi^+ = \frac{1}{\sqrt{2}}(\phi_3 + i\phi_4)\,, \tag{1.1.6}$$

is the only scalar field of the SM, where $T_3 = \sigma_3/2$ is the 3rd component of the weak isospin generators $T^a = \sigma^a/2$, with σ^a the Pauli matrices given by

$$\sigma_0 = \begin{pmatrix} 1 & 0 \\ 0 & 1 \end{pmatrix}, \qquad \sigma_1 = \begin{pmatrix} 0 & 1 \\ 1 & 0 \end{pmatrix}, \tag{1.1.7}$$

$$\sigma_2 = \begin{pmatrix} 0 & -i \\ i & 0 \end{pmatrix}, \qquad \sigma_3 = \begin{pmatrix} 1 & 0 \\ 0 & -1 \end{pmatrix}. \tag{1.1.8}$$

Its upper component, ϕ^+ has weak isospin $T_3 = 1/2$ and electric charge $Q = 1$, whilst its lower component ϕ^0 has $T_3 = -1/2$ and is neutral. From

$$Y = Q - T_3\,, \tag{1.1.9}$$

one can then deduce that the Higgs doublet has weak hypercharge $Y_\Phi = 1/2$ (breaking $U(1)_Y$ symmetry), and is therefore charged under the $SU(2)_L \times U(1)_Y$ gauge group having the quantum numbers $(2, 1/2)$. This mechanism through which the gauge bosons obtain mass is referred to as the *Higgs mechanism*. The next question we want to answer is: how is the electroweak symmetry broken, and what does the Higgs have to do with it? Fermionic particles have spin and thus necessarily 2 d.o.f, and therefore could not constitute the one missing d.o.f needed by the electroweak bosons to make them massive. In fact, only a scalar particle with 1 d.o.f can be eaten by the to-be-massive electroweak bosons. Moreover, for the electroweak bosons to annex an extra degree of freedom, these scalars must be charged under the electroweak force: the Higgs boson is obviously the ideal candidate. There is then one scalar d.o.f remaining from the complex Higgs doublet, and *this* Higgs gets a VEV, triggering EWSB.

This occurs when the minimum of the Higgs potential,

$$V(\Phi) = -\mu^2 \Phi^\dagger \Phi + \lambda (\Phi^\dagger \Phi)^2 \tag{1.1.10}$$

$$= -\frac{\mu^2}{2}\left(\phi_1^2 + \phi_2^2 + \phi_3^2 + \phi_4^2\right) + \frac{\lambda}{4}\left(\phi_1^2 + \phi_2^2 + \phi_3^2 + \phi_4^2\right)^2 \tag{1.1.11}$$

gets a non-zero field value, with μ^2 being the Higgs mass term and λ the Higgs quartic coupling representing an interaction of strength λ. It should be noted that $\lambda > 0$ to ensure a stable vacuum (ground state), and that no higher order terms in Φ are permitted if the Standard Model is to be a renormalisable theory. When the potential is minimised one finds that

$$\frac{\partial V(\Phi)}{\partial \Phi} = \Phi\left(-\mu^2 + 2\lambda \Phi^\dagger \Phi\right) = 0\,, \tag{1.1.12}$$

which can be satisfied by two solutions:

- $\mu^2 < 0$ and the minimisation condition is given by $\Phi = 0$, corresponding to a theory of quantum electrodynamics with a supplementary charged scalar with mass μ where electroweak symmetry is preserved both by the Lagrangian and the vacuum.

- $\mu^2 > 0$, and the minimisation condition is given by the non-zero value

$$\Phi^\dagger \Phi = \frac{\mu^2}{2\lambda}\,. \tag{1.1.13}$$

The Higgs potential then takes the form of a "mexican hat", and the origin of Φ is no longer at the minimum of the potential. Instead, the Higgs particle will "roll" off the origin to a lower energy configuration: this then means that the shape of the potential is no longer symmetric under the electroweak symmetry. In other words, the electroweak symmetry preserved by the Lagrangian is not preserved by the vacuum.

The latter is what occurs in the Standard Model when the direction of the vacuum is chosen to be

$$\Phi_{\text{groundstate}} = \langle 0|\Phi|0\rangle = \begin{pmatrix} 0 \\ \frac{v}{\sqrt{2}} \end{pmatrix} \tag{1.1.14}$$

$$\longrightarrow \Phi(x) = \frac{1}{\sqrt{2}} \begin{pmatrix} 0 \\ v + h(x) \end{pmatrix}, \tag{1.1.15}$$

and is what is meant by "the Higgs gets a VEV". In fact, it is possible to choose a basis of ϕ in whichever orientation compared to the local vacuum, but conservation of electric charge means that only a neutral scalar should acquire a VEV. Typically, as in (1.1.14), the vacuum is chosen to lie along the real part of ϕ^0, but this selection is arbitrary. Then, $\phi_1 = \phi_2 = \phi_4 = 0$ and $\phi_3 = v$ where the VEV satisfies

$$v = \sqrt{\frac{\mu^2}{\lambda}} > 0\,; \qquad \mu^2 > 0\,, \lambda > 0. \tag{1.1.16}$$

The value of v is not predicted in the SM, but is measured by experiment as $v = 246$ GeV. In fact, only one of the four Higgs gets a VEV meaning that the four scalars are no longer on the same footing: this is why the $SU(2)$ symmetry is broken. However, since the vacuum is invariant under the electric charge,

$$\left(\frac{\sigma_3}{2} + Y\right) \Phi_{\text{groundstate}} = \frac{1}{2}\left(\begin{pmatrix} 1 & 0 \\ 0 & -1 \end{pmatrix} + \begin{pmatrix} 1 & 0 \\ 0 & 1 \end{pmatrix}\right) \frac{v}{\sqrt{2}} = 0\,, \tag{1.1.17}$$

$U(1)_{\text{EM}}$ remains a symmetry of the theory and the photon remains massless.

The matter fields are coupled to the gauge fields via the covariant derivative, D_μ,

$$D_\mu = \partial_\mu + igW_\mu^a \frac{\sigma^a}{2} + ig_Y Y_\Phi B_\mu\,. \tag{1.1.18}$$

The second term in (1.1.18) is suppressed when D_μ is acting on right-handed fields: the weak isospin group is so-called "$SU(2) - \text{left}$" as only the left- (and anti-right-) handed fermions couple to the $SU(2)_L$ gauge bosons - the left-handed fermions being arranged in doublets, while the right-handed fields are singlets: this is what is meant by the weak interaction being *chiral*. On the other hand, both left- and right- handed species need to interact with the photon, and thus both chiralities are charged under the weak hypercharge group.

Electroweak symmetry breaking ensures that the electroweak bosons mix among themselves, meaning that B_μ and W_μ^a are not physically measurable states. The scalar contributions to the SM Lagrangian arise through the terms,

$$\mathcal{L}_{\text{scalars}} = (D^\mu \Phi)^\dagger (D_\mu \Phi) - V(\Phi)\,, \tag{1.1.19}$$

where, substituting Φ for the Higgs doublet field, the first piece generates the masses for the gauge bosons:

$$
\begin{aligned}
(D^\mu\Phi)^\dagger(D_\mu\Phi) &= \left| \left(\partial_\mu + igW^a_\mu \frac{\sigma^a}{2} + i\frac{g_Y}{2}B_\mu \right) \frac{1}{\sqrt{2}} \begin{pmatrix} 0 \\ v+h \end{pmatrix} \right|^2 \\
&= \left| \begin{pmatrix} \partial_\mu + i\frac{g}{2}W^3_\mu + i\frac{g_Y}{2}B_\mu & i\frac{g}{2}W^1_\mu + \frac{g}{2}W^2_\mu \\ i\frac{g}{2}W^1_\mu - \frac{g}{2}W^2_\mu & \partial_\mu - i\frac{g}{2}W^3_\mu + i\frac{g_Y}{2}B_\mu \end{pmatrix} \frac{1}{\sqrt{2}} \begin{pmatrix} 0 \\ v+h \end{pmatrix} \right|^2 \\
&= \left| \begin{pmatrix} i\frac{g}{2}W^+_\mu(v+h) \\ \frac{1}{\sqrt{2}} \left[\partial_\mu h - \frac{i}{2}(v+h)\left(gW^3_\mu - g_Y B_\mu\right) \right] \end{pmatrix} \right|^2 \\
&= \frac{1}{2}\partial_\mu h \partial^\mu h + \frac{g^2}{4}W^+_\mu W^{\mu-}(v+h)^2 + \frac{1}{8}(v+h)^2(gW^3_\mu - g_Y B_\mu)(gW^{\mu3} - g_Y B^\mu) \\
&= \frac{1}{2}\partial_\mu h \partial^\mu h + \frac{g^2}{4}(v+h)^2 W^+_\mu W^{-\mu} + \frac{1}{8}(v+h)^2(g^2+g^2_Y)Z_\mu Z^\mu \,,
\end{aligned}
$$
(1.1.20)

where

$$
W^\pm_\mu \equiv \frac{1}{\sqrt{2}}\left[W^1_\mu \mp W^2_\mu \right] , \qquad Z_\mu \equiv \frac{gW^3_\mu - g_Y B_\mu}{\sqrt{g^2+g^2_Y}} ,
$$
(1.1.21)

and

$$
B^\dagger_\mu = B_\mu \,, \qquad W^{3\dagger}_\mu = W^3_\mu \,, \qquad W^{+\dagger}_\mu = W^-_\mu \,.
$$
(1.1.22)

The remaining vector boson state not written above is A_μ,

$$
A_\mu \equiv \frac{gW^3_\mu + g_Y B_\mu}{\sqrt{g^2+g^2_Y}} ,
$$
(1.1.23)

which is a state orthogonal to Z_μ and also comes from the mixing of W^3_μ and B_μ. The transformation between the bases $\{W^3_\mu, B_\mu\}$ to $\{Z_\mu, A_\mu\}$ is given by the weak mixing angle, θ_W,

$$
\tan\theta_W = \frac{g_Y}{g} \,.
$$
(1.1.24)

The masses[1] for the gauge bosons can then be read off from the Lagrangian,

$$
\mathcal{L}_{\text{scalars}} \supset m^2_W W^+_\mu W^{\mu-} + \frac{1}{2}m^2_Z Z_\mu Z^\mu + \frac{1}{2}m^2_A A_\mu A^\mu \,,
$$
(1.1.25)

such that

$$
m_W = g\frac{v}{2} \,, \qquad m_Z = \frac{v}{2}\sqrt{g^2_Y + g^2} \,, \qquad m_A = 0 \,.
$$
(1.1.26)

Finally, the Higgs boson mass can be found by plugging (1.1.15) into the scalar potential and taking the second derivative with respect to the Higgs field, h, yielding

$$
m^2_h = 2\mu^2 = 2v^2\lambda \,.
$$
(1.1.27)

---

[1]Note that the factor $1/2$ in the definition of the Z-boson and photon fields comes from the fact that those fields are real, whereas the W-bosons are complex.

Particle	Field	$(SU(3),\ SU(2),\ U(1)_Y)$	T_3	Y
Quarks	$Q_{i,L} = (u_{i,L}, d_{i,L})$	($\mathbf{3}$, $\mathbf{2}$, 1/6)	(1/2, -1/2)	(2/3, -1/3)
	$u_{i,R}^c$	($\bar{\mathbf{3}}$, $\mathbf{1}$, -2/3)	0	-2/3
	$d_{i,R}^c$	($\bar{\mathbf{3}}$, $\mathbf{1}$, 1/3)	0	1/3
Leptons	$L_{i,L} = (\nu_{i,L}, e_{i,L})$	($\mathbf{1}$, $\mathbf{2}$, -1/2)	(1/2, -1/2)	(0, -1)
	$e_{i,R}^c$	($\mathbf{1}$, $\mathbf{1}$, 1)	0	1

Table 1.1: Matter content of the Standard Model.

The Higgs mass value is not predetermined, as λ is a free parameter and only v is phenomenologically fixed (from the W- and $Z-$ boson masses).

The coupling of the Higgs field to the covariant derivative cannot be the cause of fermionic masses for the simple reason that fermionic fields do not appear in D_μ: but these couplings can be added manually to the Lagrangian:

$$-\mathcal{L}_{\text{matter}} = y_e^{ij} \bar{L}_{L,i}^\alpha \Phi_\alpha e_{R,j}^c + y_d^{ij} \bar{Q}_{L,i}^\alpha \Phi_\alpha d_{R,j}^c + y_u^{ij} \epsilon^{\alpha\beta} \bar{Q}_{L,i,\alpha} \Phi_\beta^\dagger u_{R,j}^c + \text{h.c.} \qquad (1.1.28)$$

where $(i,j) = 1,2,3$ are family indices, (α,β) are $SU(2)$ indices, ϵ^{ij} is the totally antisymmetric tensor and where the SM matter fields are displayed in table 1.1. As is the case with gauge boson mass terms, fermionic mass terms are also absent from the $SU(3)_c \times SU(2)_L \times U(1)_Y$ invariant Lagrangian. This is because the fermions adhere to a chiral symmetry, under which the left and right handed components have opposite charge: $\psi_L \to e^{-i\alpha}\psi_L$, $\psi_R \to e^{i\alpha}\psi_R$. Generally this can be written

$$\psi \to e^{i\alpha\gamma_5}\psi\,, \qquad (1.1.29)$$

where γ_5 is a hermitean matrix that anticommutes with the four gamma matrices,

$$\gamma_5 = \begin{pmatrix} \mathbb{1} & 0 \\ 0 & -\mathbb{1} \end{pmatrix}\,, \qquad (1.1.30)$$

and is used to project the Dirac field into its left- and right-handed components

$$\psi_L = \frac{1-\gamma^5}{2}\psi\,, \qquad \psi_R = \frac{1+\gamma^5}{2}\psi\,. \qquad (1.1.31)$$

As such, a fermionic mass term would break the chiral symmetry:

$$m_\psi \bar{\psi}\psi \to m_\psi \bar{\psi} e^{2i\alpha\gamma_5}\psi \neq m_\psi \bar{\psi}\psi. \qquad (1.1.32)$$

The symmetry is referred to as a *custodial* chiral symmetry because it is owing to the fact that the left and right handed components act differently under the gauge symmetry that means they cannot receive gauge-invariant mass terms in the Lagrangian. It also means that, even when the symmetry is not exact and $m_\psi \neq 0$, the mass shift to the fermion will always be proportional to the mass of the fermion itself, and hence the fermion masses are protected from large corrections. It is through the Yukawa interactions between the fermions and the Higgs field the fermion fields acquire masses. After EWSB one finds that

$$-\mathcal{L}_{\text{fermion masses}} = m_u^{ij} \bar{u}_{L\,i} u_{R\,j}^c + m_d^{ij} \bar{d}_{L\,i} d_{R\,j}^c + m_e^{ij} \bar{e}_{L\,,i} e_{R\,j}^c\,, \qquad (1.1.33)$$

where the masses are proportional to the Higgs VEV,

$$m_u^{ij} = y_u^{ij} \frac{v}{\sqrt{2}}, \qquad m_d^{ij} = y_d^{ij} \frac{v}{\sqrt{2}}, \qquad m_e^{ij} = y_e^{ij} \frac{v}{\sqrt{2}}. \tag{1.1.34}$$

The above discussion is an entirely classical picture of the Standard Model. When one considers a quantum description of the theory, then the freedom afforded in choosing co-ordinates must be fixed so that one representative state is picked from all possible physically identical states. Quantisation of the gauge fields, $A^\mu(x)$, removes any redundant degrees of freedom by imposing a local constraint at each point in space-time: this process is called *gauge fixing*. The procedure of gauge fixing leads to the inclusion of additional terms in the Lagrangian parametrised by the ζ which vanish in the limit of classical physics. This choice of value for this parameter is arbitrary, and it should not appear in any physically measurable quantities such as for the scattering amplitudes. Without gauge fixing, it is not possible to write down an expression for the gauge boson propagators. For example, take the Lagrangian for a classical electromagnetic field plus some gauge fixing term which vanishes in the classical limit $\zeta \to \infty$,

$$S_0 = \int d^4x \left[-\frac{1}{4} F_{\mu\nu} F^{\mu\nu} - \frac{1}{2\zeta} (\partial_\mu A^\mu)^2 \right],$$

where $F_{\mu\nu}$ is the gauge field strength of the abelian $U(1)$ field,

$$F_{\mu\nu} = \partial_\mu A_\nu - \partial_\nu A_\mu. \tag{1.1.35}$$

Expanding the field strength tensor and transforming to Fourier space one finds that

$$\begin{aligned}
S_0 &= \int d^4x \left[-\frac{1}{2} \partial_\mu A_\nu \left(\partial^\mu A^\nu - \partial^\nu A^\mu \right) - \frac{1}{2\zeta} (\partial_\mu A^\mu)(\partial_\nu A^\nu) \right] \\
&= \frac{1}{2} \int d^4x \Big\{ A_\nu \left[\partial^2 g^{\mu\nu} - \left(1 - \frac{1}{\zeta} \right) \partial^\mu \partial^\nu \right] A_\mu + \text{total derivative terms} \Big\} \\
&= \frac{1}{2} \int \frac{d^4p}{(2\pi)^4} A_\nu(p) \left[-p^2 g^{\mu\nu} + \left(1 - \frac{1}{\zeta} \right) p^\mu p^\nu \right] A_\mu(p), \tag{1.1.36}
\end{aligned}$$

where one assumes that the photon field vanishes at infinity. The photon propagator, $D_{\mu\lambda}$, for which one uses the ansatz $D_{\mu\lambda} = A g_{\mu\lambda} + B p_\mu p_\lambda$, is then found from

$$i \left(-p^2 g^{\mu\nu} + \left(1 - \frac{1}{\zeta} \right) p^\mu p^\nu \right) D_{\mu\lambda}(p) = \delta_\mu^\lambda. \tag{1.1.37}$$

Matching up the coefficients on either side of the equation one finds that

$$A = -\frac{1}{p^2}, \qquad B = -\frac{1}{p^4}(\zeta - 1), \tag{1.1.38}$$

so that the propagator is given by

$$iD_{\mu\lambda}(p) = -\frac{i}{p^2} \left(g_{\mu\lambda} - \frac{1}{p^2}(1 - \zeta) p_\mu p_\lambda \right). \tag{1.1.39}$$

As one can see, in the classical limit that $\zeta \to \infty$, the photon propagator becomes undefined: this is why gauge fixing is necessary, even though the final results do not depend on the gauge fixing choice. There are multiple gauge choices possible: for $\zeta = 1$ this propagator corresponds to the 't Hooft-Feynman gauge; for $\zeta = 0$ to the Lorentz gauge *etc*. Different choices of gauge are employed when calculating the gauge boson propagators in the Standard Model, but this is not something that will be detailed here.

1.1.2 Motivation for BSM models

It is largely believed within the physics community that the Standard Model does not paint the whole picture of our universe. While the SM is in excellent agreement with experimental measurements, it is widely thought that the SM exists as the low energy limit of some higher energy theory that would provide justification for the observed shortcomings or unanswered questions of the SM. The origin of this is not down (just) to weary and ambitious theorists, but also due to experimental indications. For one, the discovery of neutrino masses [9] - predicted to be vanishing in the SM - won Takaaki Kajita and Aurthur McDonald the 2015 Nobel prize in physics, while further observational signs of dark matter and energy prompt raised eyebrows as the SM provides no viable candidate. Theoretically, it is also concerning that the SM does nothing to integrate the theory of gravity into its framework, or suggest reasonable explanations for various sources of required fine-tuning. One example of the latter is the hierarchy of masses between the Planck and electroweak scales that opens up the Higgs mass to large corrections from heavy physics. Another is the "strong CP problem" (see *e.g.* [10–13], where, unlike in the electroweak sector, CP symmetry has been consistently measured as a feature of QCD despite the fact that the QCD Lagrangian does admit such violating terms. This leads to the question of why this CP-violating parameter θ_{QCD} should be so tiny when it is not required to be.

There are copious reviews on these "issues" in the SM, so only a brief overview of SM shortcomings related to the rest of this text will be given in what follows. A (considerably) more thorough discussion can be found in most quantum field theory and Standard Model textbooks, as well as various review articles such as [14–17].

The Hierarchy Problem

The hierarchy problem originates in the Higgs sector and relates to the fact that the accuracy of the SM is capped at some energy scale, Λ. The Higgs boson mass becomes vulnerable to quantum corrections from this scale, which could be where new physics takes over, or equivalently, the Planck scale. If no new physics were out there, it would suggest that the Higgs mass should be of the order of the Planck mass, yet with its measurement of 125 GeV, this would imply the occurrence of cancellations of an incredulous manner. As previously discussed, gauge bosons and fermion masses are protected by the gauge-chiral symmetry present in the SM and are forbidden from having mass terms in the $SU(3)_c \times SU(2)_L \times U(1)_Y$ invariant Lagrangian. When the Higgs scalar provokes EWSB, they acquire masses proportional to the Higgs VEV and not to the scale of new physics, Λ. On the contrary, there is no symmetry present that protects scalar masses, and so even if a Higgs mass term were written in the SM Lagrangian $\propto v$, it would be sensitive to quantum corrections of the order of the heaviest particle coupling to it, *i.e.* at the scale of new physics. Experimental results suggest that new physics is at least of the $\mathcal{O}(\text{TeV})$, and there is nothing that prevents $\Lambda \gg v$: in this case the theory would require a large amount of fine-tuning to keep the Higgs mass around a few hundred GeV. Notably, the defining scale of quantum gravity, the Planck scale $\sim 10^{19}$ GeV$/c^2$ is much greater than the electroweak scale, and this caveat is often referred to as the *hierarchy problem*.

Vacuum Stability

One can also query whether there are other vacuums than the electroweak vacuum at $v = 246$ GeV. At large values of the Higgs field, where $h \gg v$, the effective potential

can be approximated by [18]

$$V_{\text{eff}}^{\text{tree}}(h) = \frac{\lambda_{\text{eff}}(h)}{4}h^4\,, \qquad (1.1.40)$$

where the two-loop expression for λ_{eff} is given in (85) of [18] and can be approximated by $\lambda(\mu)$ for large field values. If all the SM couplings are run to high energies, it is possible to investigate the RG evolution of λ to see whether the vacuum at v is stable, unstable (with a life-time shorter than the age of the universe) or meta-stable (a long-lived vacuum greater than the age of the universe, but not the final vacuum state configuration of the universe). If λ becomes negative at high energy scales, then it indicates that the scalar potential is unbounded from below and that at some point the Higgs scalar will tunnel from our EW vacuum to a (more) stable one. The top-quark and Higgs masses are the most important parameters for determining the EW phases of the SM, and studies performed in [18, 19], suggest that, for the current measured values of m_t and m_h, the SM vacuum would sit in a metastable state, but that the Higgs quartic becomes negative before the Planck scale (roughly between $10^9 - 10^{12}$ GeV - see figure 5 of [18]). The stability conditions phrased in terms of m_h and m_t are given in equations (65) and (66) of [19] respectively. One possible explanation for this is that new physics arises around the point that $\lambda < 0$ before the instability region, stabilising the potential.

Unification of gauge couplings

An additional motivation for BSM physics is the idea that the Standard Model gauge couplings unify at some Grand Unified Theory (GUT) scale. This is well-motivated from the fact that the electromagnetic and weak interactions unify into the electroweak force at low energies, in which the strong force plays no part. Embedding the SM as a subgroup in a GUT theory is a concept that has been around since the 1970's [20] (with further considerations made on the embedding of the Higgs scalars in [21]), when it was hypothesised that all the SM couplings originate from a from an $SU(5)$ interaction involving one coupling strength,

$$\sqrt{\frac{5}{3}}g_1(M_{\text{GUT}}) = g_2(M_{\text{GUT}}) = g_3(M_{\text{GUT}}) \equiv g_{\text{GUT}}\,. \qquad (1.1.41)$$

In the Standard Model, the $U(1), SU(2)$ and $SU(3)$ couplings do not unify at a GUT scale, however such convergence is much improved in models such as supersymmetry (SUSY) where the additional particle content changes the behaviour of the running couplings. One of the beauties of SUSY is how unexpected yet natural this result is.

Dark Matter/Energy

Dark matter (DM) and energy (DE) constitute almost 95% of the matter in the universe, but because it has not been observed directly, it must not interact with the strong force; must minimally interact with observable electromagnetic radiation; must not be electrically charged, and is thus difficult to detect. As such, dark matter and energy makes its fingerprint on the universe through gravitational effects. There are multiple sources of dark matter evidence, with a comprehensive review being given in *e.g.* [22], with indications of DM dating as far back as the 1920's [23]. One of the big pieces of evidence in favour of the existence of DM comes from observations of the rotation curves of galaxies, namely that the amount of observed matter present in spiral galaxies fails to explain the rate of their rotation [24]. While these observations

do not allow us to determine the amount of DM in the universe, such information can be derived from measurements of the Cosmic Microwave Background (CMB). Dark matter objects are theorised to span multiple orders of magnitude in size, from being very large (*e.g.* black holes) to very small (*e.g.* weakly interacting particles (WIMPS) and axions). Interestingly, it is widely believed that very large objects cannot contribute to more than a small fraction of the DM out there [25], meaning that there needs to be a dark matter candidate particle in the fundamental description of the universe. The Standard Model does not propose such a particle, but BSM offers many. In particular, supersymmetry presents the lightest supersymmetric particle (LSP) - a neutral, stable particle called a neutralino.

One of the neat things about supersymmetry is that is proposes solutions to many of the quandaries of the SM, instead of being designed in an ad-hoc way to target one single issue. With this, the basics of supersymmetry will now be addressed.

1.2 Supersymmetry

This chapter aims to give a brief overview of a small sample of supersymmetry models, and the required background to understand how they come to life. There are many aspects of supersymmetry that will not be covered, but fortunately there are many good (and less good) supersymmetry reviews out there, of which the reader may wish to refer to any of the following: [26–32].

The Standard Model picture of particle physics classifies particles into two groups: those with half-integer spin (fermions) and those with integer spin (bosons). The fundamental concept of supersymmetry is to establish a relationship between these two fundamental classes of particles, which transforms one into the other. In other words, supersymmetry dictates that for each boson their should be a fermionic corresponding superpartner, and vice versa.

Thus far, supersymmetry continues to be a hypothetical symmetry, and evidence for it has not (yet) been found by experiment, despite high expectations. But that has not (yet) prevented experimentalists, phenomenologists and theorists around the globe from conjuring up models based on its existence. As long as parameter space exists in SUSY models which could have evaded the current constraints so far, these communities will continue in their quest for supersymmetry.

1.2.1 SUSY basics

1.2.1.1 Two-component fermion notation

In the context of supersymmetric field theories, it is typical to choose notation in terms of two-component Weyl spinors instead of four-component Dirac spinors. A Dirac spinor, Ψ, can always be written in terms of a left- and a right-handed Weyl spinor,

$$\Psi = \begin{pmatrix} \psi_\alpha \\ \bar{\chi}^{\dot{\alpha}} \end{pmatrix}, \tag{1.2.1}$$

with chiralities +1 and -1 respectively, where $\alpha, \dot{\alpha}$ are spinor indices and can each take the values $1, 2$. The Weyl spinors ψ_α and $\bar{\chi}_{\dot{\alpha}}$ are complex Grassmann numbers, and are not in the same $(SU(2))$ representations, that is, it is not possible to turn ψ_α into $\bar{\chi}_{\dot{\alpha}}$ by contracting it with another tensor. On the other hand, within a single $SU(2)$, the fundamental (ψ_α) and anti-fundamental $(\bar{\chi}^{\dot{\alpha}})$ representations are the same as they can be transformed one to the other via

$$\psi^\alpha = \epsilon^{\alpha\beta}\psi_\beta, \qquad \bar{\psi}^{\dot{\alpha}} = \epsilon^{\dot{\alpha}\dot{\beta}}\bar{\psi}_{\dot{\beta}}, \qquad \psi_\alpha = \epsilon_{\alpha\beta}\psi^\beta, \qquad \bar{\psi}_{\dot{\alpha}} = \epsilon_{\dot{\alpha}\dot{\beta}}\bar{\psi}^{\dot{\beta}}, \tag{1.2.2}$$

where $\epsilon_{\alpha\beta} = -\epsilon^{\alpha\beta}$, $\epsilon_{\dot{\alpha}\dot{\beta}} = -\epsilon^{\dot{\alpha}\dot{\beta}}$ is the $SU(2)$ antisymmetric tensor. Unlike bosonic variables, fermionic variables anti-commute such that $\psi_1\chi_2 = -\chi_2\psi_1$. When spinors are written without indices, it is because they are contracted like

$$\psi\chi \equiv \psi^\alpha\chi_\alpha = \epsilon^{\alpha\beta}\psi_\beta\chi_\alpha = \epsilon^{\beta\alpha}\psi_\alpha\chi_\beta = -\psi_\alpha\epsilon^{\alpha\beta}\chi_\beta = -\psi_\alpha\chi^\alpha = \chi^\alpha\psi_\alpha \equiv \chi\psi$$

$$\bar{\psi}\bar{\chi} \equiv \bar{\psi}_{\dot{\alpha}}\bar{\chi}^{\dot{\alpha}} = \epsilon_{\dot{\alpha}\dot{\beta}}\bar{\psi}^{\dot{\beta}}\bar{\chi}^{\dot{\alpha}} = \epsilon_{\dot{\beta}\dot{\alpha}}\bar{\psi}^{\dot{\alpha}}\bar{\chi}^{\dot{\beta}} = -\bar{\psi}^{\dot{\alpha}}\epsilon_{\dot{\alpha}\dot{\beta}}\bar{\chi}^{\dot{\beta}} = -\bar{\psi}^{\dot{\alpha}}\bar{\chi}_{\dot{\alpha}} = \bar{\chi}_{\dot{\alpha}}\bar{\psi}^{\dot{\alpha}} \equiv \bar{\chi}\bar{\psi}. \tag{1.2.3}$$

As will be seen later, the relationship between the two components of Ψ will determine what type of mass terms one is able to write for the fermions.

1.2.1.2 SUSY algebra and superspace

The fundamental symmetry group of particle physics, the Poincaré group, is the group under which all relativistic quantum field theory actions must be invariant. The group has ten generators: three associated to spatial rotations, J_i (i=1,2,3); three to boosts, K_i (i=1,2,3); and four to translations in space and time, P^μ ($\mu = 0, 1, 2, 3$). These first two combine to make the Lorentz group $SO(1,3)$. Supersymmetry arises from the question of whether it is possible to extend the Poincaré group with any more symmetries of spacetime (*global* symmetries), and not just those that commute with it such as internal (*local*) symmetries.

In the 1960's, Coleman and Mandula showed in [33] that in a quantum field theory, under a set of reasonable assumptions[2], that the largest viable symmetry group was that of the Poincaré group plus some internal symmetry groups. However, the Coleman-Mandula theorem only considered symmetries whose form could be described by commutation relations between their generators - bosonic symmetry generators. It came later that Haag, Lopuszanski and Sonius [34] tried relaxing this constraint and allowed for the possibility of fermionic symmetry generators which obeyed anti-commutation relations instead. This paved the way for *supersymmetry*, which lead to the possibility of the largest symmetry group of particle physics could instead be that of *superPoincaré* plus some internal symmetry groups. These supersymmetry generators are denoted $Q_\alpha^A, \bar{Q}_{\dot\alpha}^A$, where A indicates the number of supersymmetries $1...\mathcal{N}$ – generally taken to be 1 in realistic theories. Two generators (Q and its complex conjugate) are necessary owing to the fact that fermions are complex states. Along with the commutation relations for the Poincaré group and internal symmetries, the supersymmetry algebra includes the anti-commutation relations

$$\{Q_\alpha^A, Q_\beta^B\} = \epsilon_{\alpha\beta} Z^{AB}\,, \tag{1.2.4}$$

$$\{\bar{Q}_{\dot\alpha}^A, Q_{\dot\beta}^B\} = \epsilon_{\dot\alpha\dot\beta} \left(Z^{AB}\right)^*\,, \tag{1.2.5}$$

$$\{Q_\alpha^A, \bar{Q}_{\dot\beta}^B\} = 2\sigma_{\alpha\dot\beta}^\mu P_\mu \delta^{AB}\,, \tag{1.2.6}$$

$$\left[P_\mu, Q_\alpha^A\right] = \left[P_\mu, \bar{Q}_{\dot\alpha}^A\right] = 0\,, \tag{1.2.7}$$

where $Z^{AB} = -Z^{BA}$ are Lorentz scalars, more commonly known as *central charges*, which commute with the whole supersymmetry algebra and within themselves.

To describe our four-dimensional spacetime we use four bosonic coordinates x^μ, which are associated with the generator P_μ. To equal this number in fermionic coordinates as is the fundamental principle of supersymmetry, a new variable must be introduced and a set of rules to describe its behaviour established. Specifically, these four fermionic coordiates are called *Grassmann* coordinates, and are a set of two two-component anti-commuting spinors θ_α and $\bar{\theta}_{\dot\alpha}$ ($\alpha = 1, 2$) associated to the supersymmetry generators $Q_\alpha, \bar{Q}_{\dot\alpha}$ that obey

$$\{\theta^\alpha, \theta^\beta\} = \{\bar{\theta}^{\dot\alpha}, \bar{\theta}^{\dot\beta}\} = \{\theta^\alpha, \bar{\theta}^{\dot\alpha}\} = 0\,, \tag{1.2.8}$$

with θ_α left-handed, $\bar{\theta}_{\dot\alpha}$ right-handed, and both having the mass dimension $-1/2$. Being Grassmann variables, θ and $\bar{\theta}$ are swapped between representations according to the relations in eqs .(1.2.2), (1.2.3). Together, the four bosonic and four fermionic coordinates live in an eight-dimensional manifold called *superspace*. There are numerous identities involving Grassmann coordinates which can be found in any comprehensive book or set of lecture notes on supersymmetry, but important to the following will be

---

[2]Locality; causality; positive particle energy; particle spectrum finiteness; among others

the derivative,

$$\frac{\partial}{\partial\theta^\beta}(\theta^\alpha) = \delta^\alpha_\beta, \qquad \frac{\partial}{\partial\bar\theta^{\dot\beta}}(\bar\theta^{\dot\alpha}) = \delta^{\dot\alpha}_{\dot\beta},$$

$$\frac{\partial}{\partial\theta_\beta}(\theta_\alpha) = \delta^\beta_\alpha, \qquad \frac{\partial}{\partial\bar\theta_{\dot\beta}}(\bar\theta_{\dot\alpha}) = \delta^{\dot\beta}_{\dot\alpha},$$

$$\frac{\partial}{\partial\theta_\beta}(\theta^\alpha) = \epsilon^{\alpha\beta}, \qquad \frac{\partial}{\partial\bar\theta_{\dot\beta}}(\bar\theta^{\dot\alpha}) = \epsilon^{\dot\alpha\dot\beta}, \qquad (1.2.9)$$

$$\frac{\partial}{\partial\theta^\beta}(\theta_\alpha) = \epsilon_{\alpha\beta}, \qquad \frac{\partial}{\partial\bar\theta^{\dot\beta}}(\bar\theta_{\dot\alpha}) = \epsilon_{\dot\alpha\dot\beta},$$

having used that $\epsilon_{\alpha\beta}\epsilon^{\beta\gamma} = \delta^\gamma_\alpha$, where ϵ is the 2-dimensional anti-symmetric tensor and δ is the Kronecker delta. It should be noted that any derivative of $\theta(\bar\theta)$ with respect to $\bar\theta(\theta)$ is zero,. They are the basis of the chiral covariant derivative, *i.e.* the *superderivative*, which will be a fundamental tool in constructing the types of supersymmetric fields that will live in the manifold. They are given by

$$D_\alpha = \frac{\partial}{\partial\theta^\alpha} - i\left(\sigma^\mu\bar\theta\right)_\alpha \partial_\mu, \qquad D^\alpha = -\frac{\partial}{\partial\theta_\alpha} + i\left(\bar\theta\bar\sigma^\mu\right)^\alpha \partial_\mu,$$

$$\bar D^{\dot\alpha} = \frac{\partial}{\partial\bar\theta_{\dot\alpha}} - i\left(\bar\sigma^\mu\theta\right)^{\dot\alpha} \partial_\mu, \qquad \bar D_{\dot\alpha} = -\frac{\partial}{\partial\bar\theta^{\dot\alpha}} + i\left(\theta\sigma^\mu\right)_{\dot\alpha} \partial_\mu, \qquad (1.2.10)$$

and obey the anti-commutation relations

$$\{D_\alpha, Q_\beta\} = \{D_\alpha, \bar Q_{\dot\beta}\} = \{\bar D_{\dot\alpha}, Q_\beta\} = \{\bar D_{\dot\alpha}, \bar Q_{\dot\beta}\} = 0,$$

$$\{D_\alpha, D_\beta\} = \{\bar D_{\dot\alpha}, \bar D_{\dot\beta}\} = 0, \qquad (1.2.11)$$

$$\{D_\alpha, D_{\dot\beta}\} = 2i\sigma^\mu_{\alpha\dot\beta}\partial_\mu.$$

Indeed, the supersymmetry generators Q are themselves differential operators and are written

$$\hat Q_\alpha = i\frac{\partial}{\partial\theta^\alpha} - (\sigma^\mu\bar\theta)_\alpha\partial_\mu, \qquad \hat Q^\alpha = -i\frac{\partial}{\partial\theta_\alpha} + (\bar\theta\bar\sigma^\mu)^\alpha\partial_\mu,$$

$$\hat{\bar Q}^{\dot\alpha} = i\frac{\partial}{\partial\bar\theta_{\dot\alpha}} - (\bar\sigma^\mu\theta)^{\dot\alpha}\partial_\mu, \qquad \hat{\bar Q}_{\dot\alpha} = -i\frac{\partial}{\partial\bar\theta^{\dot\alpha}} + (\theta\sigma^\mu)_{\dot\alpha}\partial_\mu. \qquad (1.2.12)$$

A thorough derivation of (1.2.12) is given, for example, in sections 4.1 of [35] and 4.2 of [32]. As can be seen, the superderivatives and SUSY generators in eqs. (1.2.11) and (1.2.12) mix the Grassmann and Lorentz algebras, which is expected - having expanded 4-dimensional Minkowski space to 8-dimensional superspace.

Lastly, one needs to define integration in superspace so as to preserve translational invariance. The type of integral used for integration over functions of Grassmann coordinates is the Berezin integral, and is defined as

$$1 = \int d\theta\, \theta = \int d^2\theta\, \theta\theta = \int d\bar\theta\, \bar\theta = \int d^2\bar\theta\, \bar\theta\bar\theta,$$

$$0 = \int d\theta = \int d\bar\theta. \qquad (1.2.13)$$

This concludes the set of tools allowing us to contruct supersymmetric fields and their interactions in superspace.

1.2.1.3   Superfields and representations of SUSY algebra

Superfields are the means through which supersymmetric theories are represented: they are simply fields in superspace, and are the names given to the groupings of particles and their supersymmetric friends along with the auxilliary fields that that exist in the off-shell Lagrangian. There are two kinds of superfields in a four-dimensional $\mathcal{N} = 1$ supersymmetric field theory that does not describe gravitational interactions: chiral superfields and vector superfields, which are the supersymmetric extensions of spin-1/2 and spin-1 fields respectively. A chiral superfield contains the physical degrees of freedom of a fermion and a complex scalar (a scalar and pseudoscalar), and describes the lepton-slepton, quark-squark and Higgs-Higgsino multiplets. A vector superfield is composed of a gaugino and gauge-boson and describes the gauge-boson-gaugino multiplets, *i.e.* of the $U(1)_Y$ gauge-boson-bino multiplet, the three $W^\pm, Z$-wino multiplets and the gluon-gluino multiplet.

The most general superfield possible, which can, if desired, be a complex function, has a parameter for each possible combination in θ and $\bar{\theta}$. Each grassmann co-ordinate has two components ($\alpha = 1, 2$), and they anti-commute with each other. The fact that $\theta_\alpha \theta_\beta = -\theta_\beta \theta_\alpha$ implies that $\theta_\alpha \theta_\beta = 0$ for $\alpha = \beta$. Hence if one combined more than two grassmann co-ordinates, there would necessarily be two or more of the same component, and this combination would vanish. It follows that the possible combinations of θ and $\bar{\theta}$ are restricted in the superfield to be

$$
\begin{aligned}
S(x, \theta, \bar{\theta}) = &\, a(x) + \theta \xi(x) + \bar{\theta} \bar{\chi}(x) + \theta\theta b(x) + \bar{\theta}\bar{\theta} c(x) \\
&+ \theta \sigma^\mu \bar{\theta} v_\mu(x) + \theta\theta\bar{\theta}\bar{\lambda}(x) + \bar{\theta}\bar{\theta}\theta \psi(x) + \theta\theta\,\bar{\theta}\bar{\theta} d(x) \,,
\end{aligned}
\tag{1.2.14}
$$

where a, b, c, d are scalar fields; $\xi, \psi, (\chi, \lambda)$ are left(right)-handed fermionic (or spinor) fields and v_μ is a vector field. These different fields are called *component* fields, and are ordinary fields in Minkowski space. In this way, it is easy to see that a superfield is just a finite assembly of fields in the usual space-time. This expression for a general superfield contains many more degrees of freedom than are necessary to describe a chiral or vector multiplet, and some of them are not physical. The expansion in eq. (1.2.14) is a *reducible* representation of SUSY. Chiral and vector superfields are two *irreducible* representations of SUSY.

Chiral superfields are superfields that obey the condition

$$
\bar{D}_{\dot{\alpha}} \Phi = 0 \,,
\tag{1.2.15}
$$

whilst anti-chiral superfields are superfields that obey

$$
D_\alpha \bar{\Phi} = 0 \,,
\tag{1.2.16}
$$

where the superderivatives were defined in eq. (1.2.10). The reason for requiring the construction of the superderivative arises from the fact that the standard derivatives $\partial_{\alpha, \dot{\alpha}}$ are not supersymmetric covariant, which means that acting them on a superfield would not return a superfield. By the very definition of chirality, chiral and anti-chiral superfields are distinct, and $\Phi \neq \bar{\Phi}$. As such, chiral and anti-chiral fields cannot be real. Matter fields and their superpartners are described by a complex scalar and a fermion, and so straight away it is obvious that there is no place for v_μ in the definition of the chiral superfield: but in fact, v_μ can be defined in terms of bosonic fields. Using eq. (1.2.15) and matching terms according to their parametrisation in θ and $\bar{\theta}$, the excess degrees of freedom can be eliminated. Then, by performing the simple rescaling $a \to \phi$, $\xi \to \sqrt{2}\psi$ and $b \to F$, one finds the general expression for a chiral superfield:

$$
\Phi(x, \theta, \bar{\theta}) = \phi(x) + \sqrt{2}\theta\psi(x) + \theta\theta F(x) - i\bar{\theta}\bar{\sigma}^\mu\theta\partial_\mu\phi - \frac{i}{\sqrt{2}}\theta\theta\bar{\theta}\bar{\sigma}^\mu\partial_\mu\psi(x) - \frac{1}{4}\theta\theta\bar{\theta}\bar{\theta}\partial_\mu\partial^\mu\phi(x).
\tag{1.2.17}
$$

This expression represents the expansion in superspace of the degrees of freedom in a chiral superfield – two complex scalars, (ϕ, F), each with 2 degrees of freedom, and a complex spinor ψ with 4 degrees of freedom. As it can be seen from eq. (1.2.17), the F-terms do not possess a kinetic term, and thus are not dynamical degrees of freedom. Along with the D-terms that will manifest themselves in the vector superfields, the F-terms are called auxilliary fields and their purpose is to allow the supersymmetry algebra to close off-shell. They can be integrated out trivially using the Euler-Lagrange equations to bring the Lagrangian on-shell. The Lagrangian density for the F-auxilliaries is then

$$\mathcal{L}_{\text{aux}} \supset F^* F \,, \tag{1.2.18}$$

and thus they have the vanishing equations of motion $F = 0$ and $F^* = 0$.

The criteria for a vector superfield is illuminated by the fact that it is often referred to as *real* superfield, *i.e.* that

$$V^a = V^{a*} \,. \tag{1.2.19}$$

To determine the general form of the vector superfield this condition is applied to eq.(1.2.14) to find relationships between the coefficients. The excess degrees of freedom remaining appear as a result of supergauge invariance, but they can be "supergauged away" under a supergauge transformation. One particular gauge choice, and the one that will be employed for the rest of this section is the Wess-Zumino gauge,

$$V^a(x, \theta, \bar{\theta}) = \theta \sigma^\mu \bar{\theta} v_\mu^a(x) + \bar{\theta}\bar{\theta}\theta\lambda^a(x) + \theta\theta\bar{\theta}\bar{\lambda}^a(x) + \frac{1}{2}\theta\theta\bar{\theta}\bar{\theta}D^a(x) \,, \tag{1.2.20}$$

which fixes the supergauge without affecting the ordinary gauge freedoms. Under the Wess-Zumino gauge, there is one gauge boson (first term); one (massive) gaugino (the second and third terms) and an auxilliary field D (the last term). Notably, the Wess-Zumino gauge fixing constraints are not conserved under supersymmetry transformations, but a supergauge transformation can always restore them. The D-auxilliary field, similarly to the F-term, has the Lagrangian density

$$\mathcal{L}_{\text{aux}} \supset \frac{1}{2}\sum_a D^a D^a \,, \tag{1.2.21}$$

with the D-term fields also satisfying the trivial equations of motion, $D^a = 0$.

The dimension of the vector superfield is zero, which means that it is possible to exponentiate the field to create supergauge invariant kinetic terms for the gauge (and charged chiral) multiplets when considering non-abelian gauge groups - the result of course still holds and simplifies for abelian gauge groups. From eq. (1.2.20) it can be seen that the lowest component has a $\bar{\theta}\theta$ parametrisation, which contributes to the beauty of the Wess-Zumino gauge, namely that

$$V^2 = \frac{1}{2}\theta\theta\bar{\theta}\bar{\theta}v^\mu_a v^a_\mu \,, \tag{1.2.22}$$

and any terms with $V^{n>2}$ vanish. From this it follows that the Taylor expansion of the exponentiated vector field is restricted to

$$e^V = 1 + V + \frac{1}{2}V^2, \tag{1.2.23}$$

which greatly simplifies calculations.

A summary of the components of the chiral and vector supermultiplets can be seen in table 1.2. While there will be no further talk about the gravity multiplet, it has been included in the table for completeness. Now that all the basic types of superfields have been seen, it is possible to move on and construct $\mathcal{N} = 1$ supersymmetric Lagrangians.

Supermultiplet	Spin-0	Spin-1/2	Spin-1	Spin-3/2	Spin-2
Chiral	Complex scalar	Weyl fermion	–	–	–
Vector/gauge	–	Weyl fermion/gaugino	Gauge boson	–	–
Gravity	–	–	–	Gravitino	Graviton

Table 1.2: Table showing the basic types of $\mathcal{N} = 1$ multiplets.

1.2.1.4 Superpotentials and SUSY Lagrangians

Section 1.2.1.3 discussed the two types of fundamental superfields that can be used to describe $\mathcal{N} = 1$ supersymmetric theories in the absence of gravitational interactions, the chiral and vector superfields. This section will start by discussing theories with chiral (matter) superfields, and move onto vector superfields below.

In the most general renormalisable $\mathcal{N} = 1$ actions, the two types of terms involving chiral superfields are the kinetic terms, K, and the *superpotential*, W. However, K and W cannot be just any combination of Φ and $\bar{\Phi}$. In order for the kinetic terms, to be supersymmetrically invariant, the function K must be a superfield, and more specifically, a *real* superfield. A real superfield can be composed of a chiral and anti-chiral superfield, whilst the product of two (anti-) chiral superfields is a (anti-) chiral superfield: hence, $K = K(\Phi, \bar{\Phi})$ must be a function of both. The kinetic terms for chiral superfields can be described by a Kähler potential,

$$S_{\text{matter, kinetic}} = \int d^4x \int d^2\theta \, d^2\bar{\theta} \, K\left(\Phi, \bar{\Phi}\right) , \qquad (1.2.24)$$

where K is a real function of chiral and anti-chiral superfields. Moreover, the Lagrangian density should transform as a scalar quantity under space-time symmetry, and hence requires K - or, more accurately, its $\theta^2\bar{\theta}^2$ component which remains after the superspace integral - to be a scalar function. Renormalisability determines the mass dimension of K: as $[\mathcal{L}] = 4$ and $[\theta] = [\bar{\theta}] = -\frac{1}{2}$, then it is required that $[K(\Phi, \bar{\Phi})] = 2$. An obvious guess, and in fact the most general Kähler potential for a renormalisable $\mathcal{N} = 1$ theory, is

$$S_{\text{matter, kinetic}} = \int d^4x \int d^2\theta \, d^2\bar{\theta} \, \bar{\Phi}\Phi . \qquad (1.2.25)$$

However, the Standard Model is a gauged quantum field theory, and the action also needs to describe the dynamics of vector (gauge) superfields, V^a. Not only is it then necessary to add kinetic terms for the gauge bosons and gauginos (see below), but the kinetic terms for the chiral superfields in eq. (1.2.25) will no longer be supergauge invariant if the chiral superfields are charged under some local gauge symmetry. This is because the chiral superfields living in some representation R of the gauge group a, will now transform under a gauge transformation,

$$\Phi \to e^{i\Lambda_a T_R^a}\Phi , \qquad (1.2.26)$$

where Λ_a is also a chiral superfield and T_R^a are the generator matrices of the representation R. The action written in eq. (1.2.25) for non-gauged chiral-superfields will no longer be supergauge invariant: denoting $\Lambda = \Lambda_a T_R^a$, it is clear that

$$\bar{\Phi}\Phi \to \bar{\Phi}e^{-i\bar{\Lambda}}e^{i\Lambda}\Phi \neq \bar{\Phi}\Phi , \qquad (1.2.27)$$

and it follows that our description of non-gauged chiral interactions will need to be modified. In fact, the correct supergauge invariant expression for the chiral kinetic terms (for fields charged under either abelian or non-abelian groups) is

$$\mathcal{L}_{\text{gauged-matter, kinetic}} = \int d^2\theta\, d^2\bar{\theta}\, \bar{\Phi}\, e^{2g_a T^a V^a}\, \Phi\,, \tag{1.2.28}$$

where under a supergauge transformation, $e^{2g_a T^a V^a} \to e^{-i\bar{\Lambda}} e^{2g_a T^a V^a} e^{i\Lambda}$. It is known from eq. (1.2.23) that the expansion of the vector field is constrained to the order V^2, meaning that in components, the kinetic terms for the matter fields are

$$\begin{aligned}
\mathcal{L}_{\text{gauged-matter, kinetic}} &= \int d^2\theta\, d^2\bar{\theta}\, \left[\bar{\Phi}\Phi + 2g_a \bar{\Phi} T^a V^a \Phi + 2g_a^2 \bar{\Phi} T^2 V^2 \Phi\right]_{\theta\theta\bar{\theta}\bar{\theta}} \\
&= \bar{F}F + \partial^\mu \bar{\phi}\partial_\mu \phi + i\bar{\psi}\bar{\sigma}^\mu \partial_\mu \psi \\
&\quad + g(\bar{\phi}T^a \phi)D^a - \sqrt{2}g_a\left\{(\bar{\phi}T^a \psi)\lambda^a + \bar{\lambda}^2(\bar{\psi}T^a \phi)\right\} \\
&\quad + ig_a(\bar{\phi}T^a \partial^\mu \phi)v_\mu^a + g_a(\bar{\psi}T^a \bar{\sigma}^\mu \psi)v_\mu^a + ig_a(\partial_\mu \bar{\phi}T^a \phi)v^{\mu,a} \\
&\quad + g_a^2 \bar{\phi}v_a^\mu v_\mu^a \phi\,,
\end{aligned} \tag{1.2.29}$$

where the first line shows the $\bar{\Phi}\Phi$ terms (up to an integration by parts); the second and third lines show the $2g\bar{\Phi}TV\Phi$ terms, and the last line shows the term quadratic in V^2 (given by eq. (1.2.22) multiplied by $2g^2$).

The other piece of the Lagrangian describing the chiral interactions is the superpotential, which deterimines all the non-gauge couplings and masses of the model. Thus, the superpotential generates the SM Yukawa couplings; positive mass-squared terms for the Higgs doublet fields; fermion mass terms; scalar self interaction terms, and any other interactions between additional matter and the Higgs fields.

The kinetic terms described by eq. (1.2.25) contain the combinations of chiral superfields that transform in field space. The components for which there has not yet been written an interaction are the ones that do not propagate (*i.e.* they do not contain any field-space derivatives): the auxilliary fields, namely the F-terms. The F-terms are parameterised by $\theta\theta$ in a chiral superfield, or $(\bar{\theta}\bar{\theta})$ in an anti-chiral superfield, but can be made up of other component combinations when dealing with multiple chiral superfields. The simplest description of chiral superfield actions is given by

$$S_{\text{matter, interactions}} = \int d^4x \int d^2\theta\, W(\Phi) + \text{h.c}, \tag{1.2.30}$$

where W is a holomorphic function. Given that a holomorphic function of a (anti)-chiral superfield is still a (anti)-chiral superfield, then from eqs. (1.2.15,1.2.16) one can see that

$$\overline{D}_{\dot{\alpha}} W(\Phi) = 0\,, \qquad D_\alpha \overline{W}(\bar{\Phi}) = 0\,. \tag{1.2.31}$$

Evidently, $W(\Phi)$ must therefore not contain any convariant derivatives, as D_α and $\bar{D}_{\dot{\alpha}}$ do not commute, and eqs. (1.2.31) would no longer hold. As $[d^2\theta] = 1$, it is also required that $[W] = 3$. Assuming a renormalisable Lagrangian, as $[\Phi] = 1$, the superpotential should be at most cubic. This leaves the superpotential with the general form

$$W(\Phi_i) \equiv a^i \Phi_i + \frac{1}{2}M^{ij}\Phi_i \Phi_j + \frac{1}{6}y^{ijk}\Phi_i \Phi_j \Phi_k\,, \tag{1.2.32}$$

which means that in terms of component fields, the piece of the Lagrangian devoted to chiral interactions is

$$\mathcal{L}_{\text{matter, interactions}} = \left[a^i \Phi_i + \frac{1}{2} M^{ij} \Phi^i \Phi^j \frac{1}{6} y^{ijk} \Phi^i \Phi^j \Phi^k \right]_{\theta\theta} + \text{h.c.} \tag{1.2.33}$$

$$= a^i F_i + \frac{1}{2} M^{ij} \left(\phi_i F_j - \psi_i \psi_j \right) + \frac{1}{6} \left(\phi_i \phi_j F_k - \phi_i \psi_j \psi_k \right) + \text{h.c.} \tag{1.2.34}$$

$$= -\frac{1}{2} M^{ij} \psi_i \psi_j - \frac{1}{6} y^{ijk} \phi_i \psi_j \psi_k + \text{h.c.}, \tag{1.2.35}$$

where $\theta\psi_i \theta\psi_j = -\frac{1}{2}\theta\theta\psi_i\psi_j$ and F has been set to 0 from its equations of motion. Unlike for the matter kinetic terms, the matter interaction Lagrangian does not need any modification to account for gauge covariance. Each term in the superpotential should be individually gauge covariant (with any tadpole terms only existing for gauge singlet chiral superfields). Hence, as the superpotential is holomorphic, it will always be gauge invariant under a supergauge transformation. Take, for example, 3 chiral superfields charged under a $U(1)$ symmetry with charge e, such that under a translation $\Phi \to e^{ie\Lambda}\Phi$; then $\Phi_i \Phi_j \Phi_k \to e^{(e_i + e_j + e_k)\Lambda} \Phi_i \Phi_j \Phi_k$ will be gauge invariant given that $e_i + e_j + e_k = 0$.

Next, it is time to consider the supersymmetric version of the gauge Lagrangian. The kinetic terms for spin-1 fields are defined using the field strength tensor $F_{\mu\nu}^a$,

$$\mathcal{L} \supset -\frac{1}{4} F_{\mu\nu}^a F_a^{\mu\nu}, \tag{1.2.36}$$

where

$$F_{\mu\nu}^a = \partial_\mu v_\nu^a - \partial_\nu v_\mu^a + g f^{abc} v_\mu^b v_\nu^c, \tag{1.2.37}$$

with f^{abc} the structure constants defined in section A; a the index of the gauge group for a given gauge field v, and g the appropriate gauge coupling. As the gauge boson appears explicitly in the lowest component of the vector superfield, (see eq. (1.2.20)), two spacetime derivatives acting on the vector field $\partial_\mu v^\mu \partial^\mu v_\mu$ will give rise to the gauge boson kinetic terms required. However, this method would never induce the kinetic terms for the gauginos, $\lambda\bar{\sigma}^\mu\partial_\mu\bar{\lambda}$. Instead it is necessary to define the supersymmetric field strength tensor using superderivatives:

$$\mathcal{W}_\alpha \equiv -\frac{1}{8}\bar{D}_{\dot{\alpha}}\bar{D}^{\dot{\alpha}} \left(e^{-2gV^aT^a} D_\alpha e^{2gV^aT^a} \right), \qquad \bar{\mathcal{W}}_{\dot{\alpha}} \equiv \frac{1}{8} D_\alpha D^\alpha \left(e^{2gV^aT^a} \bar{D}_{\dot{\alpha}} e^{-2gV^aT^a} \right). \tag{1.2.38}$$

Using eqs. (1.2.22, 1.2.23), the SUSY field strength (chiral) superfield in the adjoint representation of the gauge group, $\mathcal{W}_\alpha^a$, can be derived:

$$\mathcal{W}_\alpha^a = \lambda_\alpha^a + \theta_\alpha D^a - (\sigma^{\mu\nu}\theta)_\alpha F_{\mu\nu}^a + i\theta\theta \left(\sigma^\mu \nabla_\mu \bar{\lambda}^a \right)_\alpha. \tag{1.2.39}$$

where the fundamental and adjoint representations are linked through

$$\mathcal{W}_\alpha = 2g_a \mathcal{W}_\alpha^a T^a, \tag{1.2.40}$$

and the Wess-Zumino gauge (as discussed in section 1.2.1.3) has been used. Employing (1.2.40), the kinetic and self-interaction terms are obtained from

$$\text{Tr}\left[\mathcal{W}_\alpha^a \mathcal{W}^{a\alpha}\right] = \frac{1}{4g_a^2 \text{Tr}[T^a T^a]} \text{Tr}[\mathcal{W}_\alpha \mathcal{W}^\alpha]$$

$$= \frac{1}{4S_a g_a^2} \mathrm{Tr}[\mathcal{W}_\alpha \mathcal{W}^\alpha] \,, \tag{1.2.41}$$

where S_a is the normalisation for the generators (defined in appendix A) and is typically given by $S_a = 1/2$.

The SUSY field strength tensor is a chiral superfield, but instead of a scalar as its bottom component, it has now a gaugino: this means that W_α can also be referred to as the gaugino superfield. It is now possible to write the kinetic (and self-interaction) terms for the gauge fields,

$$S_{\mathrm{gauge}} = \int d^4x \int d^2\theta \; \mathcal{W}_\alpha^a \mathcal{W}_a^\alpha + \mathrm{h.c.} \tag{1.2.42}$$

$$= \int d^4x \left[D^a D_a + 2i\lambda^a \sigma^\mu \nabla_\mu \bar{\lambda}_a - \frac{1}{2} F^{a\mu\nu} F_{a\mu\nu} + \frac{i}{4} \epsilon^{\mu\nu\tau\kappa} F_{\mu\nu} F_{\tau\kappa} + \mathrm{h.c} \right] . \tag{1.2.43}$$

The expressions describing the interactions and propagation of the gauge and (gauged) matter fields in a renormalisable $\mathcal{N} = 1$ SUSY theory have now been presented. The only other allowable addition to these terms is the *Fayet-Iliopulos* term which can occur for Abelian gauge groups,

$$\mathcal{L}_{\mathrm{FI}} = - \int d^2\theta d^2\bar{\theta} \sum_A \kappa_A V^A \,, \tag{1.2.44}$$

where κ_A are the constants associated with the vector superfields, V^A, corresponding to the abelian factors $A = 1, 2, 3 ... n$. As will be discussed later, the presence of a Fayet-Iliopulos terms can induce SUSY breaking. For one $U(1)$ vector gauge field one would get

$$\mathcal{L}_{\mathrm{FI}} = -\frac{1}{2} D^a \,. \tag{1.2.45}$$

Collecting all this together, the most general $\mathcal{N} = 1$ SUSY lagrangian is given by

$$\mathcal{L} = \int d^2\theta \, d^2\bar{\theta} \, \left[\bar{\Phi} \, e^{2g_a T^a V^a} \, \Phi \right]_{\theta^2 \bar{\theta}^2} + \int d^2\theta \, [W(\Phi)]_{\theta^2} + \int d^2\bar{\theta} \, \left[\overline{W}(\bar{\Phi}) \right]_{\bar{\theta}^2}$$
$$+ \int d^2\theta \, [\mathcal{W}_\alpha^a \mathcal{W}_a^\alpha]_{\theta^2} + \int d^2\bar{\theta} \, \left[\overline{\mathcal{W}}_a^{\dot{\alpha}} \overline{\mathcal{W}}_{\dot{\alpha}}^a \right]_{\bar{\theta}^2} - \sum_A \kappa_A V^A \,. \tag{1.2.46}$$

Obviously, the terms in the Lagrangian will depend on the chosen SUSY model, and importantly, on the symmetries the model is desired to possess. The next sections will look at theories that allow for a global gauge symmetry, and how this can be desirable in SUSY models.

1.2.1.5 R-symmetry

Some supersymmetric Lagrangians can, in addition, accommodate a global $U(N)_R$ symmetry - an *R-symmetry* - where N is determined by the number of supersymmetry generators in the theory. For a typical $\mathcal{N} = 1$ supersymmetry, this symmetry group is simply $U(1)_R$, but as one moves to extended supersymmetries one gets the non-abelian groups $U(2)_R = SU(2)_R \times U(1)$ for $\mathcal{N} = 2$; $U(4)_R = SU(4)_R \times U(1)$ for $\mathcal{N} = 4$ etc. In the case of $\mathcal{N} = 2$ for example; $SU(2)_R$ rotates the supercharges, while $U(1)$ changes the phase. Needless to say, as the number of supersymmetries increases, so do the constraints on the action.

An R-symmetry is a group that commutes with the Lorentz group whilst leaving the SUSY algebra invariant, and can be a symmetry of the theory - but it is neither assured nor required. For any R-symmetry, the associated charges carried by the superfields are called *R-charges*.

The R-charges of matter fields depend on the model (as will be seen in section 1.2.4.1), in contrast to the fields in a (*real*) vector multiplet which are uniquely fixed - see eqs. (1.2.50, 1.2.51). Real fields have an R-charge of 0, which means that any Lagrangian terms manifesting themselves from the Kahler potential (which, recall, is real) are by default invariant under the R-symmetry. The Lagrangian as a whole is only invariant under R-symmetry if the superpotential transforms with an R-charge of 2, *i.e.* $W \to e^{2i\alpha}W$. Sometimes, R-charge assignments for the chiral multiplets allow this, but in other cases a consistent choice of R-charges for the superfields does not exist, and R-symmetry will be explicitly broken in the Lagrangian. If a supersymmetric Lagrangian does accommodate R-symmetry, then its superspace coordinates $\theta, \bar{\theta}$ transform as

$$\theta \xrightarrow{\text{R}} e^{i\alpha}\theta, \qquad \bar{\theta} \xrightarrow{\text{R}} e^{-i\alpha}\bar{\theta}, \tag{1.2.47}$$

with R-charges +1 and -1 respectively, where α parametrises the global R-transformation, and the superspace derivatives inversely, with $R_{d\theta} = -1$, $R_{d\bar{\theta}} = 1$. From this one can see that the covariant derivatives D_α and $\bar{D}^{\dot{\alpha}}$ will have R-charge assignments +1 and -1 respectively. The spacetime coordinates must not be affected when an internal rotation of the supercharges is made which means that, in order for the SUSY algebra to remain invariant, the SUSY generators must also transform under the R-symmetry simultaneously,

$$\hat{Q} \xrightarrow{\text{R}} e^{-i\alpha}\hat{Q}, \qquad \hat{\bar{Q}} \xrightarrow{\text{R}} e^{i\alpha}\hat{\bar{Q}}, \tag{1.2.48}$$

with R-charges -1 and +1 respectively. It follows that as the supersymmetry generators (often used interchangeably with supercharges) are charged under the $U(N)_R$ symmetry, they will *not* commute with the R-symmetry generator, R:

$$[R, Q] = -Q, \qquad [R, \bar{Q}] = \bar{Q}. \tag{1.2.49}$$

Consequently, the R-symmetry acts differently on the different components of the superfields, which will each have individual R-charges. As the vector field is real (while R-symmetry is a chiral symmetry), $V^a \xrightarrow{\text{R}} V^a$, it must not carry any R-charge and it is straightforward to see that its components must transform under the R-symmetry like

$$v^a_\mu \xrightarrow{\text{R}} v^a_\mu$$
$$\lambda^a \xrightarrow{\text{R}} e^{i\alpha}\lambda^a \tag{1.2.50}$$
$$D^a \xrightarrow{\text{R}} D^a.$$

with R-charges 0, 1 and 0 respectively. The R-charge for the chiral superfields can, on the other hand, be chosen, $\Phi \xrightarrow{\text{R}} e^{ir_\Phi\alpha}\Phi$, which means that

$$\phi \xrightarrow{\text{R}} e^{ir_\Phi\alpha}\phi$$
$$\psi \xrightarrow{\text{R}} e^{i(r_\Phi-1)\alpha}\psi \tag{1.2.51}$$
$$F \xrightarrow{\text{R}} e^{i(r_\Phi-2)\alpha}F$$

with R-charges r_Φ, $r_\Phi - 1$ and $r_\Phi - 2$ respectively.

Quantum gravity arguments [36] tell us[3] however, that no continuous global symmetries should be exact, and so the R-symmetry should be broken at some scale. R-symmetry cannot be broken spontaneously in the visible sector as this would lead to a massless R-axion which has not been observed by experiment, meaning that it must be broken explicitly. It is possible to break R-symmetry in a specific sector, and as R-symmetry is an extended chiral symmetry, it makes sense that it be broken in the Higgs sector rather than the matter sector. It will be looked at how R-symmetry plays a role in a variety of models later on, and how it can be explicitly broken as in the MSSM; explicitly broken in the Higgs sector as in the MDGSSM, and conserved in the MRSSM.

1.2.1.6 Extended $\mathcal{N} = 2$ supersymmetry

It has already been motivated why supersymmetry is worth studying, but why supersymmetry with $\mathcal{N} > 1$ generators? For one, more supersymmetry results in simpler theories with fewer degrees of freedom, as physical observables and parameters are more highly constrained. For this reason, theories with extended supersymmetry are often studied for their interesting mathematical properties (see *i.e.* works by Seiberg and Witten [37, 38]), such as for the interplay between geometry and quantum mechanics, with many such examples being looked at in the context of string theory. As the number of supersymmetries increases, particle content is grouped together in representations that is not seen in the standard model *e.g.* with fermions in real representations while the quarks and leptons of the standard model live in chiral representations. It is for this reason that phenomenologically viable supersymmetric models tend to possess only $\mathcal{N} = 1$ supersymmetry. However, there are exceptions, and this text will discuss $\mathcal{N} = 2$ supersymmetry which will be explored in the context of minimal Dirac gaugino models in section 1.2.4.

First and foremostly, an $\mathcal{N} = 2$ supersymmetric theory *is* an $\mathcal{N} = 1$ supersymmetric theory: an $\mathcal{N} = 2$ multiplet contains two sub-$\mathcal{N} = 1$ supersymmetries. In other words, an $\mathcal{N} = 2$ hypermultiplet can be constructed out of two $\mathcal{N} = 1$ chiral multiplets, while an $\mathcal{N} = 2$ vector multiplet can be formed from an $\mathcal{N} = 1$ chiral and vector multiplets:

$$
\begin{aligned}
\mathcal{N} &= 2 \,\text{vector multiplet}: \Phi = (\phi, \psi_\alpha, F) \oplus V = (\lambda_\alpha, A_\mu, D) \\
\mathcal{N} &= 2 \,\text{hypermultiplet}: \Phi_{H_1} = (\phi_{H_1}, \psi_{1_\alpha}, F_1) \oplus \Phi_{H_2} = (\bar{\phi}_{H_2}, \bar{\psi}_{2_{\dot{\alpha}}}, \bar{F}_1).
\end{aligned}
\tag{1.2.52}
$$

Both $\mathcal{N} = 2$ supermultiplets can be seen as the direct sum of two $\mathcal{N} = 1$ multiplets - both with the same internal quantum numbers. Hence, ϕ and ψ_α need to be in the same representation as λ_α and A_μ - the adjoint representation - as they are now in the same supermultiplet. For this reason, the chiral multiplet Φ will transform under the adjoint representation of the gauge group, whereas $(\bar{\Phi}_{H_2})\, \Phi_{H_1}$ will transform in the (anti-) fundamental representation of the gauge group.

The two supersymmetries can exist entirely independently, and indeed it is possible to have an $\mathcal{N} = 1$ SUSY theory with many independent $\mathcal{N} = 1$ multiplets. It is when there is an additional symmetry (or symmetries) linking the multiplets that one gets $\mathcal{N} > 1$ SUSY. This work will feature the case where two sets of supersymmetry generators are related by an R-symmetry - an $SU(2)_R$ symmetry (see section 1.2.1.5). The two $\mathcal{N} = 1$ supersymmetries become connected when the theory remains symmetric under an $SU(2)_R$ rotation acting on the Weyl fermions (in a vector supermultiplet)

---

[3]Or rather, strongly suggest.

(a)

$\mathcal{N} = 1$ chiral multiplet

Q^1_α ψ_{1_α} Q^2_α

ϕ_{H_1} $\bar{\phi}_{H_2}$

$\bar{Q}^2_{\dot\alpha}$ $\bar{Q}^1_{\dot\alpha}$

$\bar\psi_{2_{\dot\alpha}}$

$\mathcal{N} = 1$ anti-chiral multiplet

(b)

$\mathcal{N} = 1$ vector multiplet

Q^1_α A_μ Q^2_α

λ_α ψ_α

Q^2_α Q^1_α

ϕ

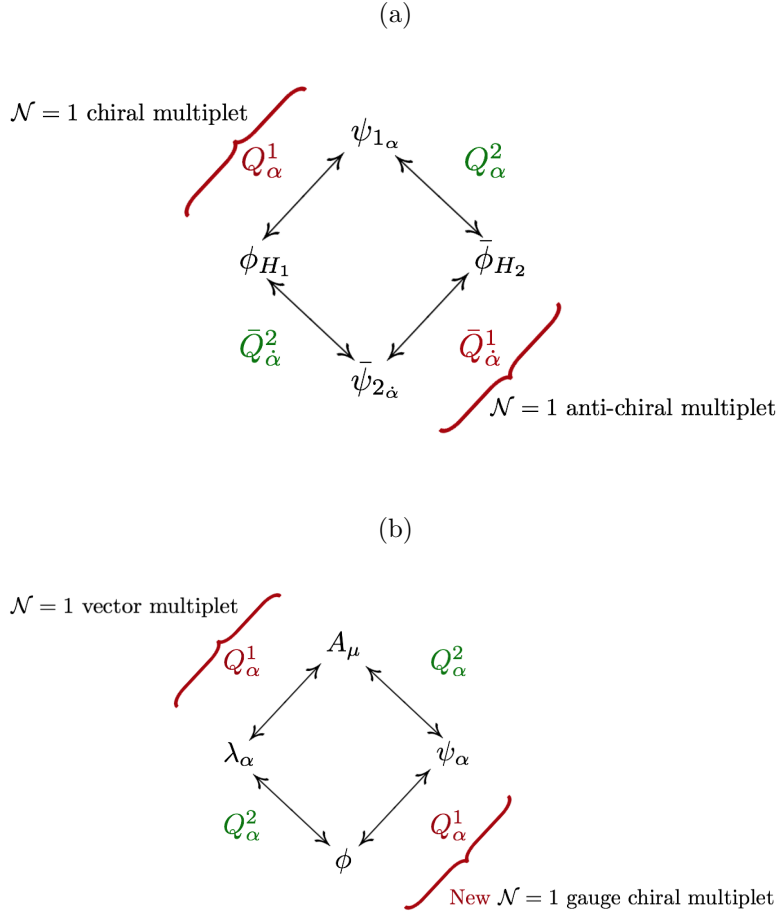New $\mathcal{N} = 1$ gauge chiral multiplet

Figure 1.1: Diagrams depicting the relationships between the $\mathcal{N} = 1$ supermultiplets to form an $\mathcal{N} = 2$ symmetry in the case of (a) an $\mathcal{N} = 2$ hypermultiplet and (b) an $\mathcal{N} = 2$ vector supermultiplet.

or the complex scalars (in the hypermultiplet). Pictorially, using the notation of eq. (1.2.52), this can be visualised as in fig. 1.1, where Q^i_α ($i = 1, 2$) is as defined in section 1.2.1.1.

This means that, in the hypermultiplet, the fermionic fields ψ_1 and $\bar\psi_2$ transform as singlets, while the complex scalars $\phi_{H_1}, \bar\phi_{H_2}$ transform as doublets. In the $\mathcal{N} = 2$ vector multiplet, the gaugino from the $\mathcal{N} = 1$ gauge multiplet and the chiral fermion from the new $\mathcal{N} = 1$ chiral multiplet transform as a doublet $(\lambda_\alpha, \psi_\alpha)$ under the $SU(2)_R$ symmetry, while the bosonic fields, A_μ and ϕ, transform as singlets.

However, for these supermultiplets to be related in this way, additional restrictions need to be placed on the $\mathcal{N} = 1$ Lagrangian. As λ_α and ψ_α can be rotated into each other under the $SU(2)_R$ symmetry, they need to be treated symmetrically by the structure of the Lagrangian. For example, the Lagrangian should be invariant under transformations of the chiral superfield Φ both proportional to λ_α and to ψ_α, and the kinetic terms for both should have the same normalisation. As such, the presence of a non-zero superpotential would give rise to mass and interaction terms for the chiral fermion, that are absent for the gaugino: this is forbidden by R-symmetry, and hence the superpotential in this case must vanish. In fact, for renormalisable theories, the superpotential is entirely forbidden and all interactions are given by

gauge interactions. While there is no superpotential, there will still be a potential coming from the D-terms (recall that the auxilliary field F is proportional to the derivative of the superpotential, which vanishes in $\mathcal{N} = 2$).

As one goes from $\mathcal{N} = 2$ SUSY to $\mathcal{N} = 4$ SUSY the separation between matter and vector multiplets disappears, and instead they are replaced by one multiplet containing a vector, 4 fermions and 3 complex scalars, *i.e.* 3 $\mathcal{N} = 1$ chiral multiplets and an $\mathcal{N} = 1$ vector multiplet, or an $\mathcal{N} = 2$ hypermultiplet and an $\mathcal{N} = 2$ vector multiplet. There is just one gauge coupling for the theory, and in fact it does not run at all. Mathematically speaking, it is possible to have any number of fermionic generators: while $\mathcal{N} = 4$ SUSY is the largest amount of supersymmetry possible in a renormalisable theory, the physical limit (if renormalisability is not an issue) in reality is $\mathcal{N} = 8$. When $\mathcal{N} > 8$, the multiplets contain massless particles (superpartners) of helicity $|\lambda| > 2$, at which point it becomes very difficult to harmonise the theory with restrictions from QFT. In a (hazelnut sized) nutshell: the generalised Coleman-Mandula theorem forbids long-range interactions of particles with spin $|\lambda| > 2$, because the higher spin particles would need to be coupled to a current with a rank higher than is permitted in order to preserve Lorentz covariance [33, 34, 39, 40].

For a more extensive description of extended supersymmetries, in particular in $\mathcal{N} = 2$ supersymmetries, the reader may wish to consult [31, 32, 41] among others. Models possessing more than 2 supersymmetries are, however, beyond the scope of this text.

1.2.2 SUSY breaking

With supersymmetry, as with all BSM theories, there's a caveat: as the SUSY generators commute with the momentum operator, and by extension $P^2 = P_\mu P^\mu$, it implies that all particles sitting in the same multiplet have the same mass, *i.e.* that the SM particles enjoy the same mass as their superpartners. Only, we would have been hard-pressed to *avoid* seeing much of this extra particle content, what with selectrons hanging around at 511 keV. Obviously, if SUSY were to exist, it would need to be broken at some low energy scale.

Mechanisms of SUSY breaking could provide an entire thesis and beyond just on their own, so in this chapter only a very primitive overview of the two general methods will be discussed: spontaneous and explicit SUSY breaking.

Whether supersymmetry in a model will be spontaneously broken or not is determined by the absolute value of the scalar potential at its minima. The energy in these vacua is only zero if the associated vacuum preserves supersymmetry - as supersymmetry is a global symmetry, any SUSY preserving vacua will be global minima of the scalar potential. If the vacuum energy (of any global or local minima of the potential) is non-zero,

$$Q_\alpha |\text{vac}\rangle \neq 0, \qquad \bar{Q}_{\dot\alpha} |\text{vac}\rangle \neq 0 \,.$$

then supersymmetry is spontaneously broken at that order in the perturbative theory[4]. This means that SUSY is spontaneously broken if any of the scalar component fields acquire VEVs. From eq.(1.2.6), it can be seen that the SUSY generators are related to the momentum operator P_μ, whose lowest component is the energy, P_0 (equivalently,

---

[4]Interestingly, non-renormalisation theorems [42, 43] tell us that if a theory preserves SUSY at tree-level, then it will be supersymmetric at all orders in the perturbation theory.

the Hamiltonian, $P_0 \equiv \mathcal{H}$), and thus

$$\sum_{\alpha=\dot{\beta}=1,2} \left\{ Q_\alpha, \bar{Q}_{\dot{\beta}} \right\} = 2(\sigma_{11}^\mu + \sigma_{22}^\mu)P_\mu$$

$$= 2\left((P_0 + P_3) + (P_0 - P_3)\right) = 4P_0 \equiv \mathcal{H}\,. \tag{1.2.53}$$

The last line in (1.2.53) arises from the fact that the only components of σ^μ which have a non-vanishing 11/22 entry are $(\sigma^0)_{11} = 1$, $(\sigma^3)_{11} = 1$, $(\sigma^0)_{22} = 1$ and $(\sigma^3)_{22} = -1$ as can be read off of the Pauli matrices given in (1.1.8). This means that

$$\langle \text{vac}|\mathcal{H}|\text{vac}\rangle = \frac{1}{4}\left[\langle\text{vac}|Q_1\bar{Q}_1|\text{vac}\rangle + \langle\text{vac}|\bar{Q}_1Q_1|\text{vac}\rangle + \langle\text{vac}|Q_2\bar{Q}_2|\text{vac}\rangle + \langle\text{vac}|\bar{Q}_2Q_2|\text{vac}\rangle\right]$$

$$= \frac{1}{4}\left[|\bar{Q}_1|\text{vac}\rangle|^2 + |Q_1|\text{vac}\rangle + |^2|\bar{Q}_2|\text{vac}\rangle|^2 + |Q_2|\text{vac}\rangle|^2\right] \geq 0\,, \tag{1.2.54}$$

such that the vacuum energy in a SUSY breaking vacuum is definite positive. This turns the question of whether the vacuum state is invariant under supersymmetry into the question of whether the Hamiltonian is invariant under it. Assuming there are no space-time dependent effects nor fermionic condensates (such as those that can and do arise in QCD) then the Hamiltonian directly corresponds to the scalar potential. Using eq. (1.2.61), one finds

$$\mathcal{H}|\text{vac}\rangle = V|\text{vac}\rangle \tag{1.2.55}$$

which implies that SUSY will be broken if any of the fields in the scalar potential obtain VEVs that do not vanish in the ground state. The scalar potential is composed of non-dynamical degrees of freedom in the theory *i.e.* the D-component from the real (gauge) superfields, and the F-components of the chiral superfields (and their conjugates) defined in eqs.(1.2.18, 1.2.21) respectively. The F-terms of the potential are derived from the superpotential, and thus contain all the interaction terms,

$$V_F = F_i^*(\Phi_i^*)F(\Phi_i) \tag{1.2.56}$$

where

$$F_i = -\frac{\partial W^*}{\partial \Phi_i^*}|_{\bar{\Phi}_i = \bar{\phi}_i}, \qquad F_i^* = -\frac{\partial W}{\partial \Phi_i}|_{\Phi_i = \phi_i}\,, \tag{1.2.57}$$

with ϕ denoting the scalar field component of the chiral superfield Φ (*i.e.* H_u^0, S *etc*), and the subscript i implying an implicit sum over all fields contributing to the superpotential. The D-terms are parametrised by the gauge couplings: for the $U(1)_Y$ and $SU(2)_L$ gauge groups respectively these are

$$D_Y = -g_Y' \sum_j Y_j \phi_j^* \phi_j\,, \tag{1.2.58}$$

$$D_2^a = -g_2 \sum_j \phi_j^* \frac{\sigma^a}{2} \phi_j\,, \tag{1.2.59}$$

where Y_j is the hypercharge of the field and σ^a are the usual Pauli matrices. Together they give the D-term potential,

$$V_D^{EW} = \frac{1}{2}\sum_{a=1}^{3}(D_2^a)^2 + \frac{1}{2}D_Y^2\,, \tag{1.2.60}$$

and in turn $V_F + V_D$ make up the electroweak scalar potential,

$$V(\phi_i, \phi_i^*) = F^* F + \frac{1}{2} \sum_a D^a D^a \qquad (1.2.61)$$

$$= \left| \frac{\partial W}{\partial \Phi_i} \right|^2_{|_{\Phi_i \to \phi_i}} + \frac{1}{2} \sum_a g_a^2 \left(\phi_i^* T_{ij}^a \phi_j \right)^2 , \qquad (1.2.62)$$

where T_{ij} are the group generators ($= Y_i, \sigma^a / 2$). It can now be seen, more specifically, that if either of the F- or D-terms gets a VEV, then SUSY will be spontaneously broken:

$$\langle \mathrm{vac} | \mathcal{H} | \mathrm{vac} \rangle = \langle F^* \rangle \langle F \rangle + \frac{1}{2} \sum_a \langle D^a \rangle \langle D^a \rangle \neq 0. \qquad (1.2.63)$$

These terms can break SUSY in any combination[5]:

$$\begin{aligned} \langle F_i \rangle &\neq 0 , \\ \langle D^a \rangle &\neq 0 , \\ \langle F_i \rangle = 0 \text{ and } \langle D^a \rangle &\neq 0 . \end{aligned} \qquad (1.2.64)$$

In order to preserve Lorentz invariance the field obtaining a VEV should be a scalar, as only such VEVs are invariant under Lorentz transformations. Furthermore, so as to respect gauge symmetry, it should also be a gauge singlet.

The first type of SUSY breaking above is more commonly known as called the O'Raifeartaigh breaking, in which the auxilliary field F of a gauge singlet (a field with all gauge quantum numbers equal to zero) chiral superfield obtains a VEV. SUSY cannot be broken by a superpotential of the form of (1.2.32), as the only evident minimum arises from $\Phi = 0$. For a field in the superpotential to develop a non-trivial VEV, then an additional term would need to be added such that no choices for the superfields can lead them to simultaneously vanish. Specifically, this should be a linear term that does not contain any dependence on the field.

The second type of spontaneous SUSY breaking is Fayet-Iliopoulos breaking, which comes about if the auxilliary field D^a of a gauge singlet vector field obtains a VEV. D-terms like those in eqs.(1.2.58, 1.2.59) will not break SUSY, but as mentioned in section 1.2.1.4, a Fayet-Iliopulous term can be added which will break SUSY in the U(1) gauge case. This mechanism can not be used for non-Abelian groups as it is not possible to have a term $\propto D^a$ in the Lagrangian without it breaking gauge invariance.

It is, in fact, not straight-forward to generate SUSY breaking in the visible sector without unwanted consequences, and many methods typically involve spontaneous SUSY breaking being triggered by fields in a hidden sector and being propagated through to the visible sector, such as through gravity and gauge mediation. For further reading on mechanisms for spontaneous supersymmetry breaking, see for example [47–50] and references therein.

Whatever the method effecting SUSY breaking, it is always possible to look at its remnants in the low energy theory when the hidden sectors have been integrated out. The Lagrangian, which will no longer be UV complete but an effective description, will then contain *soft* terms that break SUSY explicitly. It is possible to derive the soft terms from some higher scale constraint, by matching the effective theory with the complete theory, and run them down to the low-energy scale, or one can simply

---

[5] In this text, spontaneous SUSY breaking by means of gauge, fermionic or gravitino condensates will not be considered (see *e.g.* [44], [45] and [46] respectively).

write them at the low energy scale without knowing anything about the method of SUSY breaking. These new operators are of positive mass dimension, so that the theory remains renormalisable, and do not add any quadratic divergences, for example in quantum corrections to scalar masses [51]. After all, if terms were added involving dimensionless couplings to the Lagrangian, then quadratic divergences would be reintroduced at the UV scale - the elimination of which is one of the attractive motivators for supersymmetry! - and one would forgo the stabilising of the mass hierarchy between the electroweak and Planck scales. Phenomenologically, it is always possible to study supersymmetry models in this way without knowing the method of SUSY breaking, however the scale at which SUSY is broken will explicitly appear in the Lagrangian. This scale then becomes the scale at which the cancellation of UV divergences is no longer true.

The most general soft supersymmetry breaking terms that can be added to the Lagrangian of a general theory are

$$\mathcal{L}_{\text{soft}} = -\left(\frac{1}{6} a^{ijk} \phi_i \phi_j \phi_k + \frac{1}{2} b^{ij} \phi_i \phi_j + t^i \phi_i \right) + \text{h.c.} + \left(\frac{1}{2} M_a \lambda^a \lambda^a \right) + \text{h.c.} - \left(m^2 \right)^i_j \phi^{j*} \phi_i \,,$$

$$(1.2.65)$$

which are (from left to right) scalar trilinear coupling, scalar bilinear coupling, tadpole, Majorana gaugino mass, and scalar mass terms respectively. The first, second and third in brackets would each be allowed in a soft SUSY breaking model on the condition their counterparts in the superpotential ((1.2.32)) were also allowed by gauge invariance. The last of these, the tadpole term, will not be present in any model that is discussed in this text as it is required to be a gauge singlet (of which there will be none). Majorana mass terms (the fourth term) and diagonal $(i = j)$ scalar masses (the last term) will always preserve gauge invariance and be allowed, but the former will always break R-symmetry (as mentioned earlier, the R-charges of vector field components are uniquely fixed, and $R[\lambda^a] = 1$): whether the latter preserves or breaks R-symmetry will be determined by the choices of R-charge for the chiral superfields.

Now that the fundamental description and principles of supersymmetry have been covered it is possible to move on to study the most minimal supersymmetric extension of the SM; the minimal supersymmetric standard model (MSSM).

1.2.3   The MSSM

The most minimal theoretically consistent supersymmetric extension of the SM is the Minimal Supersymmetric Standard Model (MSSM), which is an $\mathcal{N} = 1$ supersymmetric theory. In essence, the particle content is (approximately) "doubled", and each SM particle then sits in a supersymmetric multiplet with its superpartner. All the particle content of the MSSM is described in table 1.4. SUSY transformations do not change the SM $SU(3)_c \times SU(2)_L \times U(1)_Y$ quantum numbers, and so each SM particle and its superpartner carry the same ones. It is not possible to form these supermultiplets out of already existing particle content as it simply wouldn't be possible to group together all the particle content by quantum number: for example, there is no fermionic octet of SU(3) in the SM which could be grouped with the gluon to form a supermultiplet, and similar arguments hold for the quarks and leptons. Instead, the fermionic quarks and leptons are embedded in chiral multiplets with their scalar superpartners - the squarks and sleptons - and the gauge bosons are put into vector multiplets with their fermionic superpartners - the gauginos. As a spin zero particle,

the Higgs boson should theoretically reside in a chiral multiplet with its superpartner, the higgsino, however the Higgs bosons are a special exception to this pattern.

In the MSSM, it is necessary to have two separate Higgs doublets[6]. There are two reasons for this: the first is that in the SM the Higgs field generates masses for up-type fermions, whilst its complex conjugate generates the masses for the down-types[7]. In SUSY, the superpotential must be a holomorphic function of the fields, and therefore must be a function of Φ_i but not $\bar{\Phi}_i$. The second argument is that adding just one higgsino (the superpartner to the Higgs) would make $SU(2)$ and $U(1)$ anomalous, which would destroy the consistency of the model. Gauge anomalies occur when the gauge symmetry is preserved by the classical Lagrangian but is violated at loop-level. They can be seen in triangle diagrams, specifically those (at 1-loop) in which there are three gauge bosons on the vertices with fermions running inside the loop. The condition for the cancellation of anomalies[8] is that the trace over the generator matrices associated with the gauge coupling at each vertex vanishes, *i.e.* that $\mathrm{tr}\, T_\alpha T_\beta T_\gamma = 0$, where $T_{\alpha,\beta,\gamma}$ could be generators of the same group or different ones. Real (vector-like) representations do not contribute to gauge anomalies: only chiral representations do. For this reason, the cancellation of anomalies can seem more apparent when the fermions are split into their left- and right-handed components: for example, cancellation of the $U(1)$ anomalies (at a vertex $U(1) \times U(1) \times U(1)$) is ensured by $\mathrm{Tr}[Y_R^3] - \mathrm{Tr}[Y_L^3] = 0$, where Y is the hypercharge which is related to the electric charge, Q, and spin, T_3, of the particles through $Q = T_3 + Y$. For each generation of particles, one must then have that (using the values in table 1.4)

$$\mathrm{Tr}[Y_R^3] = 3\left(\frac{2}{3}\right)^3 + 3\left(-\frac{1}{3}\right)^3 + (-1)^3 = -\frac{2}{9}\,, \tag{1.2.66}$$

$$\underset{u_R}{} \qquad \underset{d_R}{} \qquad \underset{e_R}{}$$

$$\mathrm{Tr}[Y_L^3] = 3\left(\frac{1}{6}\right)^3 + 3\left(\frac{1}{6}\right)^3 + \left(-\frac{1}{2}\right)^3 + \left(-\frac{1}{2}\right)^3 + \left(\frac{1}{2}\right)^3 + \left(-\frac{1}{2}\right)^3 = -\frac{2}{9}\,, \tag{1.2.67}$$

$$\underset{u_L}{} \qquad \underset{d_L}{} \qquad \underset{e_L}{} \qquad \underset{\nu_L}{} \qquad \underset{H_u}{} \qquad \underset{H_d}{}$$

$$\longrightarrow \mathrm{Tr}[Y_R^3] - \mathrm{Tr}[Y_L^3] = 0\,,$$

which would evidently not be true if the second higgsino had not been included in the particle content (where the annotations in blue denote the hypercharge for the individual fields contributing to the trace). Removing the last two contributions to $\mathrm{Tr}[Y_L^3]$ from the Higgs doublets, which as stated essentially cancel each other's contributions, one regains the loop contributions for the SM. The end result is that in the MSSM, the Higgs must form one particle across two chiral multiplets with opposite hypercharge, $\mathbf{H_u}$ and $\mathbf{H_d}$, which couple differently to the up- and down-type quark fields. Together these form a vector-like pair such that the MSSM is anomaly free under $U(1)$ and $SU(2)$.

The possible gauge invariant terms that can be added to the MSSM superpotential,

---

[6]The vast majority of supersymmetric theories possess two Higgs doublets, although there are exceptions, *e.g.* [52].

[7]Despite this, a number of efforts have been made to construct supersymmetric models with tree-level couplings only to one Higgs doublet such as where down-type fermion masses are loop-induced through couplings to the up-type Higgs doublet [53], [54], [55].

[8]For a complete discussion of anomalies, see [56].

in all their indexed glory, are

$$
\begin{aligned}
W_{\mathrm{MSSM}} &= \mu(\mathbf{H_u})_\alpha(\mathbf{H_d})_\beta\epsilon^{\alpha\beta} + (y_u)_i^j\bar{\mathbf{u}}^{ia}\mathbf{Q}_{j\alpha a}(\mathbf{H_u})_\beta\epsilon^{\alpha\beta} \\
&\quad - (y_d)_i^j\bar{\mathbf{d}}^{ia}\mathbf{Q}_{j\alpha a}(\mathbf{H_d})_\beta\epsilon^{\alpha\beta} - (y_e)_i^j\bar{\mathbf{e}}^{ia}\mathbf{L}_{j\alpha a}(\mathbf{H_d})_\beta\epsilon^{\alpha\beta} \\
&= \mu\mathbf{H_u}\cdot\mathbf{H_d} + y_u\bar{\mathbf{u}}\mathbf{Q}\cdot\mathbf{H_u} - y_d\bar{\mathbf{d}}\mathbf{Q}\cdot\mathbf{H_d} - y_e\bar{\mathbf{e}}\mathbf{L}\cdot\mathbf{H_d}\,, \quad\quad (1.2.68)
\end{aligned}
$$

where $y_{u,d,e}$ are 3×3 matrices in family space with the family indexes i,j as in the SM; a denotes colour indices, which are (raised) lowered in the (anti-) fundamental representations of $SU(3)$, $(\bar{\mathbf{3}})\mathbf{3}$; $\alpha, \beta = 1, 2$ are $SU(2)_L$ indices which can be substituted in notation by "·" to denote an $SU(2)$ contraction of two doublets, and μ parametrises the $SU(2)$ invariant coupling between the two-Higgs doublets and is akin to a supersymmetric mass term for the Higgs fields (more on this to follow). The superpotential here is expressed in terms of superfields, but recall that only the $\theta\theta$ ($\bar{\theta}\bar{\theta}$) components survive from $W(\bar{W})$ in the Lagrangian. These couplings generate masses for the fermions when the neutral Higgs fields of $\mathbf{H_u}$ and $\mathbf{H_d}$ acquire VEVs. It should be noted that no mass terms for the quarks and leptons occur in the Lagrangian, as this would explicitly break the electroweak gauge symmetry.

The MSSM is defined by the choice of terms that are allowed in the superpotential. There are additional gauge invariant, renormalisable terms that violate baryon/lepton number that could be added, but they can be forbidden in the MSSM (which is by definition the most minimal SUSY model possible) by the implementation of a discrete symmetry; *R-parity* [57,58], which is defined by

$$
R_P = (-1)^{3B+L+2s}\,, \quad\quad (1.2.69)
$$

where s denotes particle spin. Without R-parity, it would mean that the $B-L$ violating couplings such as

$$
W_{\not{R}_p} \supset \mu^i\mathbf{L}_i\cdot\mathbf{H_u} + \lambda_e^{ijk}\mathbf{L}_i\cdot\mathbf{L}_j\bar{\mathbf{e}}_k + \lambda_B^{ijk}\bar{\mathbf{u}}_i\bar{\mathbf{d}}_j\bar{\mathbf{d}}_k + \lambda_L^{ijk}\mathbf{L}_i\cdot\mathbf{Q}_j\bar{\mathbf{d}}_k \quad\quad (1.2.70)
$$

would allow the decay of SUSY particles to SM particles. From using the fact that $B[\mathbf{Q}_i] = 1/3$, $B[\bar{\mathbf{u}}_i, \bar{\mathbf{d}}] = -1/3$, $L[\mathbf{L}_i] = 1$ and $L[\bar{\mathbf{e}}_i] = -1$, in the examples above one can see that the couplings μ, λ_e and λ_L all violate lepton number, while λ_B violates baryon number. These are examples of violations of baryon/lepton number by 1 unit, but of course there are many more examples. There is good reason to suspect that R-parity would be a symmetry of supersymmetric theories: foremostly, B and L violating processes have not been observed experimentally. Notably, the most obvious source of $B-L$ violating processes would come from proton decay which would violate B and L by one unit each. However, considering that the lifetime of the proton has been measured to be $> 10^{33}$ years [59], the couplings parametrizing $B-L$ processes would have to be tiny indeed. Consequently, the non-detection of $B-L$ decays places very strict limits on the types of terms in (1.2.70).

The imposition of R-parity results in some interesting consequences on the phenomenology of the model. All SM matter must have an R-parity of $+1$ (even R-parity), while each superpartner has R-parity -1 (odd R-parity). A particle with R-parity -1 cannot decay into one with R-parity $+1$, which means that the lightest superpartner in the decay chain will not be able to decay: it must be stable. This type of supersymmetric particle is termed a "lightest supersymmetric particle" (LSP). Furthermore, R-parity assignments (recall that R-parity is multiplicative) mean that supersymmetric particles produced in collider experiments must be pair-produced (an initial state matter particle will have R-parity $+1$, as do squark-antisquark and slepton-antislepton pairs which have parity $(-1)^2 = 1$). The consquence of this latter point is that any

R-parity conserving supersymmetric events occurring in colliders will have an associated missing energy of *at least* $2m_{\tilde{\chi}_0}$, with $\tilde{\chi}_0$ being the LSP. If this LSP is neutral under the gauge groups, it becomes an attractive dark matter candidate.

The MSSM can also contain soft-SUSY breaking terms in its Lagrangian, given generally by

$$
\begin{aligned}
-\mathcal{L}_{\text{soft}} = {} & (\tilde{Q}^i)^\dagger (\mathbf{m_Q}^2)_i^j \tilde{Q}_j + \tilde{u}_R^{ci}(\mathbf{m_{\bar{u}}}^2)_i^j (\tilde{u}_{Rj}^c)^\dagger + \tilde{d}_R^{ci}(\mathbf{m_{\bar{d}}}^2)_i^j (\tilde{d}_{Rj}^c)^\dagger \\
& + (\tilde{L}^i)^\dagger (\mathbf{m_L}^2)_i^j \tilde{L}_j + \tilde{e}_R^{ci}(\mathbf{m_{\bar{e}}}^2)_i^j (\tilde{e}_{Rj}^c)^\dagger \\
& + m_{H_u}^2 |H_u|^2 + m_{H_d}^2 |H_d|^2 + B_\mu(H_u \cdot H_d + \text{h.c}) \\
& + \frac{1}{2}\left(M_3 \tilde{g}^a \tilde{g}^a + M_2 \tilde{W}^b \tilde{W}^b + M_1 \tilde{B}\tilde{B} + \text{h.c.}\right) \\
& + \left(\mathbf{a_u}^{ij}\tilde{u}_{Ri}^c \tilde{Q}_j \cdot H_u + \mathbf{a_d}^{ij}\tilde{d}_{Ri}^c \tilde{Q}_j \cdot H_d + \mathbf{a_e}^{ij}\tilde{d}_{Ri}^c \tilde{L}_j \cdot H_d + \text{c.c.}\right),
\end{aligned}
\tag{1.2.71}
$$

where (with all colour indices surpressed) lines 1-2 show the squark and slepton mass squared terms where $\mathbf{m_Q}^2, \mathbf{m_L}^2, \mathbf{m_{\bar{u}}}^2, \mathbf{m_{\bar{d}}}^2, \mathbf{m_{\bar{e}}}^2$ are 3×3 hermitian matrices in family space; line 3 shows the Higgs mass squared terms; line 4 shows the complex Majorana gaugino mass terms for each gauge group (for the gluinos, winos and binos respectively) where $a = 1...8$ and $b = 1...3$, and line 5 shows the trilinear scalar couplings where $\mathbf{a_{u,d,e}}$ are 3×3 complex matrices in family space. These terms represent all those that can be added to the MSSM Lagrangian to break SUSY softly without any base assumptions about the mechanism of SUSY breaking. It is interesting to note that the 105 [60] new parameters of the MSSM (compared to the SM) are almost entirely due to the fact that SUSY is broken: $\mathbf{m_{Q,\bar{u},\bar{d},\bar{e},L}}$ each have 9 independent entries; $\mathbf{a_{u,d,e}}$ each have 18 independent entries; each gaugino mass consists of 2 d.o.f, and both B_μ and μ are complex and contribute 2 d.o.f each. Of these 111 new parameters, 105 are physical and cannot be removed. If SUSY were unbroken, the only additional parameter would be μ. If one has more knowledge about the breaking mechanism, then these terms can be constrained further. Evidently, the terms in eq.(1.2.71) must break SUSY as only the masses and couplings are given for the scalars and gauginos, and not for their respective superpartners.

The Majorana gaugino masses above are the only type of gaugino mass generated in the MSSM. Majorana mass terms are composed of just two Weyl fermions,

$$
\Psi_M = \begin{pmatrix} \lambda_\alpha \\ \bar{\lambda}^{\dot{\alpha}} \end{pmatrix}, \qquad \bar{\Psi}_M = (\lambda^\alpha, \bar{\lambda}_{\dot{\alpha}}),
\tag{1.2.72}
$$

and lead to the soft SUSY breaking mass terms,

$$
\mathcal{L}_{\text{soft}} \supset -\frac{1}{2}M_a \bar{\Psi}_M \Psi_M = -\frac{1}{2}M_a\left(\lambda^\alpha \lambda_\alpha + \bar{\lambda}_{\dot{\alpha}}\bar{\lambda}^{\dot{\alpha}}\right),
\tag{1.2.73}
$$

that can be seen in eq.(1.2.71) (with M_a a Majorana gaugino mass for each gauge group). The reason that gauginos can acquire masses through the soft terms, whilst the SM fermions cannot, is because they live in the same representation of the gauge group as their respective gauge bosons and are hence real, and not chiral. In order to conjure a type of mass that does not break SUSY - a *Dirac mass* - one would need an extra set of fermions in the adjoint representation. As will be seen in later chapters, the addition of such particles is part and parcel of a type of model called *Dirac gaugino* models. In those chapters the focus will be on the Higgs sector of extended supersymmetry models, and for that reason this section will delve further into the electroweak sector (with particular attention paid to the Higgs sector) of the MSSM.

1.2.3.1   The Higgs sector (and EWSB) in the MSSM

As previously mentioned, there are two complex $SU(2)_L$ Higgs doublets in the MSSM,

$$H_u = \begin{pmatrix} H_u^+ \\ H_u^0 \end{pmatrix} , \qquad H_d = \begin{pmatrix} H_d^0 \\ H_d^- \end{pmatrix} . \tag{1.2.74}$$

As in the Standard Model, if the Higgs obtain appropriate VEVs, then $SU(2)_L \times U(1)_Y$ is broken, and the SM fermions acquire masses (recall the gauginos - the only new fermions - get their masses through soft SUSY breaking terms). We are now interested in the role of the Higgs in EWSB.

As the Higgs is no longer the only scalar in the model, the general MSSM scalar potential contains not only Higgs-centric terms but also those with sfermions. Considering that the squarks and sleptons do not obtain VEVs and play a role in EWSB, they shall be neglected here for our purposes. The Higgs scalar potential gets contributions from three sources: the F-terms, the D-terms and the soft terms, such that

$$
\begin{aligned}
V_{\mathrm{MSSM}}^{\mathrm{Higgs}} =& V_F + V_D + V_{\mathrm{soft}} \\
=& \left| \frac{\partial W}{\partial \mathbf{H_u}} \right|^2_{|\mathbf{H_u} \to H_u} + \left| \frac{\partial W}{\partial \mathbf{H_d}} \right|^2_{|\mathbf{H_d} \to H_d} \\
&+ \frac{1}{2} g_Y^2 \left(H_u^* Y_{H_u} H_u + H_d^* Y_{H_d} H_d \right)^2 + \frac{1}{2} g_2^2 \left(H_{ui}^* \frac{\sigma_{ij}^a}{2} H_{uj} + H_{di}^* \frac{\sigma_{ij}^a}{2} H_{dj} \right)^2 \\
&+ V_{\mathrm{soft}}|_{\mathbf{H_u}, \mathbf{H_d}} \\
=& |\mu|^2 \left(|H_d|^2 + |H_u|^2 \right) \\
&+ \frac{1}{8} \left(g_Y^2 + g_2^2 \right) \left(|H_u|^2 - |H_d|^2 \right) + \frac{1}{2} g_2^2 |H_d^* H_u|^2 \\
&+ m_{H_u}^2 |H_u|^2 + m_{H_d}^2 |H_d|^2 + B_\mu (H_u \cdot H_d + \mathrm{h.c.}) ,
\end{aligned}
\tag{1.2.75}
$$

where V_F corresponds to the first line, V_D to the second and V_{soft} to the third; $Y_{H_u} = \frac{1}{2}$, $Y_{H_d} = -\frac{1}{2}$, and where it has been used that $\sigma_{ij}^a \sigma_{kl}^a = \sum_{i=1}^3 \sigma_{ij}^i \sigma_{jk}^i = 2\delta_{il}\delta_{jk} - \delta_{ij}\delta_{kl}$. Here it should be noted that, while μ^2 is defined as positive and is invariant under supersymmetry, $m_{H_u}^2$ and $m_{H_d}^2$ arise from SUSY breaking and can be of either sign. One of the interesting features of the MSSM is that, unlike in the Standard Model, the Higgs quartic coupling - and by extension the Higgs masses - is predetermined at tree-level by the gauge couplings and is no longer a free parameter. At the minimum of the potential $V_{\mathrm{MSSM}}^{\mathrm{Higgs}}$, it is always possible to rotate away the VEV of one component of the two Higgs doublets because of $SU(2)$ symmetry. If one chooses, e.g. $\langle H_u^+ \rangle = 0$ and take the derivative of the potential with respect to that component field, then the resulting equation implies that indeed $\langle H_d^- \rangle = 0$ also. This means that at the minimum of the potential, electroweak gauge symmetry can be broken while preserving $U(1)_{\mathrm{QED}}$: i.e. an electrically neutral vacuum can be maintained. The Higgs scalar potential can hence be written solely in terms of its neutral components:

$$
\begin{aligned}
V_{\mathrm{MSSM}}^{\mathrm{Higgs}} =& \left(|\mu|^2 + m_{H_u}^2 \right) |H_u^0|^2 + \left(|\mu|^2 + m_{H_d}^2 \right) |H_d^0|^2 - \left(B_\mu H_u^0 H_d^0 + \mathrm{h.c.} \right) \\
&+ \frac{1}{8} (g_Y^2 + g_2^2) \left(|H_u^0|^2 + |H_d^0|^2 \right)^2 .
\end{aligned}
\tag{1.2.76}
$$

The minimum of the potential is required to be stable in all directions of field space, which means that

$$2|\mu|^2 + m_{H_d}^2 + m_{H_u}^2 > 2B_\mu > 0 , \tag{1.2.77}$$

must be constrained so as to avoid a potential unbounded from below when $H_u^0 = H_d^0$ - deemed the D-flat direction, *i.e.* the point in field space at which V_D vanishes. From this it follows that $(|\mu|^2 + m_{H_u}^2)$ and $(|\mu|^2 + m_{H_d}^2)$ cannot simultaneously be negative if condition (1.2.77) is to hold true. Furthermore, for explicit EWSB to occur (and for there to be a negative mass squared term in the Lagrangian), $H_u^0 = H_d^0 = 0$ cannot be a stable (or unstable if (1.2.77) doesn't hold) minimum of the potential. This equates to saying that the mass of the Higgs at the minimum of the potential is negative - but of course, as the Higgs mass is parameterised by three coefficients $(m_{H_u}^2, m_{H_d}^2, |\mu|^2)$ it is not obvious how to read off the condition. Using $V_H = V_{\text{MSSM}}^{\text{Higgs}}$ for the rest of this chapter, one can get a constraint on the Higgs mass by requiring that

$$\det \begin{pmatrix} \frac{\partial^2 V}{\partial H_d^0 \partial H_d^{0*}} & \frac{\partial^2 V}{\partial H_d^0 \partial H_u^0} \\ \frac{\partial^2 V}{\partial H_u^{0*} \partial H_d^0} & \frac{\partial^2 V}{\partial H_u^{0*} \partial H_u^0} \end{pmatrix}_{|H_u^0 = H_d^0 = 0} < 0 \,, \tag{1.2.78}$$

which translates into the condition

$$(|\mu|^2 + m_{H_d}^2)(|\mu|^2 + m_{H_u}^2) < B_\mu^2 \,. \tag{1.2.79}$$

This means that the point at which $H_u^0 = H_d^0$ is a saddle point, and that the minimum of the potential can occur for non-zero H_u^0, H_d^0.

Let us suppose for a moment that the Higgs doublet soft masses are the same, $m_{H_u}^2 = m_{H_d}^2 = m_H^2$. In this instance, condition (1.2.77) becomes

$$2|\mu|^2 + 2m_H^2 > 2B_\mu \longrightarrow (|\mu|^2 + m_H^2)^2 > B_\mu^2 \,.$$

However, this obviously conflicts with condition (1.2.79): $(|\mu|^2 + m_H^2)^2$ cannot be both greater than and smaller than B_μ^2. In other words, for the stability and EWSB conditions to make any sense, it must be required that

$$m_{H_u}^2 \neq m_{H_d}^2 \,. \tag{1.2.80}$$

It is interesting that, in order to break electroweak symmetry, SUSY must also be broken. Both of the Higgs doublet neutral components can obtain VEVs,

$$\langle H_u^0 \rangle = \frac{v_u}{\sqrt{2}} \equiv \frac{v \sin \beta}{\sqrt{2}} \,, \qquad \langle H_d^0 \rangle \equiv \frac{v_d}{\sqrt{2}} = \frac{v \cos \beta}{\sqrt{2}} \,,$$
$$\to \tan \beta \equiv \frac{v_u}{v_d} \,, \tag{1.2.81}$$

where v is the SM Higgs VEV and, as v_u and v_d are real and positive, $0 \leq \tan \beta \leq \pi/2$. In fact, to be even more explicit, it is specifically only the *real* components in the neutral Higgs doublets that obtain VEVs,

$$\langle H_{u_R}^0 \rangle = v_u \,, \qquad \langle H_{u_R}^0 \rangle = v_d \,, \tag{1.2.82}$$

while

$$\langle H_{u_I}^0 \rangle = \langle H_{d_I}^0 \rangle = \langle H_u^+ \rangle = \langle H_d^- \rangle = 0 \,. \tag{1.2.83}$$

The combination of the Higgs doublet VEVs are experimentally fixed owing to their relation to the Z-boson mass via

$$v^2 = v_u^2 + v_d^2 = \frac{4m_Z^2}{g^2 + g'^2} \,, \tag{1.2.84}$$

and here recall that the relation between the SM Higgs VEV and the W-boson mass is given by

$$m_W^2 = \frac{1}{4} v^2 g_2^2 \,. \tag{1.2.85}$$

As long as (1.2.77) and (1.2.79) are satisfied, then it is possible to write down the minimum conditions of the potential:

$$
\begin{aligned}
\left.\frac{\partial V_H}{\partial H_u^0}\right|_{\min} &= m_{H_u}^2 + |\mu|^2 - B_\mu \cot\beta - \frac{m_Z^2}{2}\cos 2\beta = 0 \,, \\
\left.\frac{\partial V_H}{\partial H_d^0}\right|_{\min} &= m_{H_d}^2 + |\mu|^2 - B_\mu \tan\beta + \frac{m_Z^2}{2}\cos 2\beta = 0 \,.
\end{aligned}
\tag{1.2.86}
$$

1.2.3.2   The Higgs mass spectrum

So far the focus has been only on the gauge eigenstates $H_u^0, H_d^0, H_u^+, H_d^-$ in the Higgs sector of the MSSM, but to see how SUSY would manifest itself in reality one needs to transform the focus to the corresponding mass eigenstates. To obtain the physical Higgs masses and fields from the Higgs doublets one needs to decompose the doublet fields into their real and imaginary parts, which for the neutral components is

$$H_u^0 = \frac{H_{u_R}^0 + iH_{u_I}^0}{\sqrt{2}} \,, \qquad H_d^0 = \frac{H_{d_R}^0 + iH_{d_I}^0}{\sqrt{2}} \,, \tag{1.2.87}$$

$$\tag{1.2.88}$$

which means that each Higgs doublet, H_u and H_d, contains 4 real scalar degrees of freedom. From these 8 d.of. one gets 2 CP-even Higgs, h, H; a CP-odd Higgs A^0; two charged Higgs $H^\pm$ and 3 would-be Goldstone bosons $G^0, G^\pm$. Although a SUSY theory is now being considered, the number of Goldstones after EWSB is the same as in the SM as it remains the same symmetry group, $SU(2)_L \times U(1)_Y \to U(1)_{\text{QED}}$, is being broken. There is only mixing between fields of the same charge, *i.e.* between h, H, A and G^0; H^+ and G^+; and H^- and G^-. In essence this means that the unphysical degrees of freedom of the gauge eigenstates can be traded for physical ones: H_u^+ being a combination of H^+ and G^+; H_d^- a combination of H^- and G^-, and both H_u^0 and H_d^0 a combination of h, H, A and G^0. All in all, the Higgs doublets can then be rewritten as

$$H_u = \begin{pmatrix} c_\beta H^+ - s_\beta G^+ \\ \frac{1}{\sqrt{2}}\left[s_\beta v + c_\alpha h + s_\alpha H + i(c_\beta A - s_\beta G^0) \right] \end{pmatrix} \,, \tag{1.2.89}$$

$$H_d = \begin{pmatrix} \frac{1}{\sqrt{2}}\left[c_\beta v - s_\alpha h + c_\alpha H + i(s_\beta A + c_\beta G^0) \right] \\ c_\beta G^- + s_\beta H^- \end{pmatrix} \,, \tag{1.2.90}$$

where the shorthand $c_x = \cos x, s_x = \sin x$ has been employed. The new mixing angle α has also been introduced, which parametrises the mixing between the CP-even neutral Higgs,

$$\begin{pmatrix} H_{u_R}^0 \\ H_{d_R}^0 \end{pmatrix} = \begin{pmatrix} c_\alpha & s_\alpha \\ -s_\alpha & c_\alpha \end{pmatrix} \begin{pmatrix} h \\ H \end{pmatrix} \,. \tag{1.2.91}$$

For the duration of the work that follows CP-conservation will be assumed, but it should be noted that if CP is violated then the CP-odd Higgs will also mix with the

other neutral scalars. After EWSB, the three Goldstone boson d.o.f get absorbed by the vector bosons $Z, W^{\pm}$, rendering them massive, leaving behind a 5-piece extended Higgs sector. In this work, the CP-odd Higgs mass, m_A, is often referred to as the pseudoscalar mass, and throughout the assumption that $m_h < m_H$, with h resembling the SM-like Higgs, will be used.

What is really useful when making concrete model predictions is to have real expressions for the physical scalar particles that are being postulated: it is desirable to derive the mass matrices,

$$\mathcal{M}_{ij} = \left. \frac{\partial^2 V_H}{\partial \phi_i \partial \phi_j} \right|_{\min} . \tag{1.2.92}$$

Starting with the CP-odd Higgs mass matrix, one needs to take second derivatives of the potential with respect to the imaginary components of the neutral Higgs doublet fields and get rid of any contributions that will vanish at the minimum of the potential,

$$\left. \frac{\partial^2 V_H}{\partial H^0_{u_I} \partial H^0_{u_I}} \right|_{\min} = |\mu|^2 + m^2_{H_u} + \frac{1}{8}(g_Y^2 + g_2^2)(v_u^2 - v_d^2) , \tag{1.2.93}$$

$$\left. \frac{\partial^2 V_H}{\partial H^0_{d_I} \partial H^0_{d_I}} \right|_{\min} = |\mu|^2 + m^2_{H_d} + \frac{1}{8}(g_Y^2 + g_2^2)(v_d^2 - v_u^2) , \tag{1.2.94}$$

$$\left. \frac{\partial^2 V_H}{\partial H^0_{u_I} \partial H^0_{d_I}} \right|_{\min} = B_\mu . \tag{1.2.95}$$

Using (1.2.84) and substituting in for the masses using the minimum conditions (1.2.86), the pseudoscalar mass matrix reduces to

$$\mathcal{M}_A^2 = \begin{pmatrix} B_\mu \cot\beta & B_\mu \\ B_\mu & B_\mu \tan\beta \end{pmatrix} , \tag{1.2.96}$$

where the usual convention that B_μ is real[9] has been taken. The two physical masses can be found by diagonalising the mass matrix and finding two eigenvalues, yielding

$$\lambda_1 \equiv m^2_{G^0} = 0 , \tag{1.2.97}$$

$$\lambda_2 \equiv m^2_A = B_\mu(\tan\beta + \cot\beta) = 2\frac{B_\mu}{\sin 2\beta} . \tag{1.2.98}$$

The same process is followed for the charged Higgs masses. As the charged Higgs transform among one another under charge, they are not CP-eigenstates. For this reason, the masses of the positive and negative components will be equal, and the fields H^+_u and H^-_d are not decomposed into their real and imaginary parts when finding the mass matrix. Instead, the eigenvalues are those of $m^2_{H^\pm}, m^2_{G^\pm}$. One gets that

$$\left. \frac{\partial^2 V_H}{\partial H^+_u \partial H^+_u} \right|_{\min} = \left(|\mu|^2 + m^2_{H_u}\right) + \frac{1}{8}(g_Y^2 + g_2^2)(v_u^2 - v_d^2) + \frac{1}{4}g_2^2 v_d^2 , \tag{1.2.99}$$

$$\left. \frac{\partial^2 V_H}{\partial H^-_d \partial H^-_d} \right|_{\min} = (|\mu|^2 + m^2_{H_d}) + \frac{1}{8}(g_Y^2 + g_2^2)(v_d^2 - v_u^2) + \frac{1}{4}g_2^2 v_u^2 , \tag{1.2.100}$$

$$\left. \frac{\partial^2 V_H}{\partial H^+_u \partial H^-_d} \right|_{\min} = B_\mu + \frac{1}{4}g_2^2 v_u v_d , \tag{1.2.101}$$

---

[9]Generally, B_μ may be taken as real and positive as any possible associated phase can be absorbed into those of H_u and H_d.

so that, in the basis (H_u^+, H_d^-), the charged Higgs mass matrix is

$$
\begin{aligned}
\mathcal{M}_{H^\pm} &= \begin{pmatrix} B_\mu \cot\beta + m_W^2 \cos^2\beta & B_\mu + m_W^2 \sin\beta\cos\beta \\ B_\mu + m_W^2 \sin\beta\cos\beta & B_\mu \tan\beta + m_W^2 \sin^2\beta \end{pmatrix} \\
&= (B_\mu + m_W^2 \sin\beta\cos\beta) \begin{pmatrix} \cot\beta & 1 \\ 1 & \tan\beta \end{pmatrix},
\end{aligned}
\tag{1.2.102}
$$

yielding

$$
\lambda_1 \equiv m_{G^\pm}^2 = 0
\tag{1.2.103}
$$
$$
\lambda_2 \equiv m_{H^\pm}^2 = B_\mu(\cot\beta + \tan\beta) + m_W^2 = m_A^2 + m_W^2.
\tag{1.2.104}
$$

Finally one arrives at the mass matrix for the CP-even Higgs bosons,

$$
\left.\frac{\partial^2 V_H}{\partial H_u^0 \partial H_u^0}\right|_{\min} = m_{H_u}^2 + |\mu|^2 + \frac{1}{8}(g_Y^2 + g_2^2)(3v_u^2 - v_d^2)
\tag{1.2.105}
$$

$$
\left.\frac{\partial^2 V_H}{\partial H_d^0 \partial H_d^0}\right|_{\min} = m_{H_d}^2 + |\mu|^2 + \frac{1}{8}(g_Y^2 + g_2^2)(3v_d^2 - v_u^2)
\tag{1.2.106}
$$

$$
\left.\frac{\partial^2 V_H}{\partial H_u^0 \partial H_d^0}\right|_{\min} = -B_\mu - m_Z^2 \sin\beta\cos\beta,
\tag{1.2.107}
$$

which, in the basis $(H_{u_R}^0, H_{d_R}^0)$, is given by

$$
\begin{aligned}
\mathcal{M}_H^2 &= \begin{pmatrix} B_\mu \cot\beta + m_Z^2 \sin^2\beta & -B_\mu - m_Z^2 \sin\beta\cos\beta \\ -B_\mu - m_Z^2 \sin\beta\cos\beta & B_\mu \tan\beta + m_Z^2 \cos^2\beta \end{pmatrix} \\
&= \begin{pmatrix} m_A^2 \cos^2\beta + m_Z^2 \sin^2\beta & -(m_A^2 + m_Z^2)\sin\beta\cos\beta \\ -(m_A^2 + m_Z^2)\sin\beta\cos\beta & m_A^2 \sin^2\beta + m_Z^2 \cos^2\beta \end{pmatrix},
\end{aligned}
\tag{1.2.108}
$$

where B_μ has been swapped for m_A^2 using eq.(1.2.98), and whose eigenvalues are

$$
m_{h,H}^2 = \frac{1}{2}\left[m_A^2 + m_Z^2 \mp \sqrt{(m_A^2 + m_Z^2)^2 - 4m_A^2 m_Z^2 \cos^2 2\beta} \right].
\tag{1.2.109}
$$

Interestingly, while $m_{H^\pm}^2$ and m_H^2 grow with increasing $m_A^2 \leftrightarrow B_\mu/\sin 2\beta$ and can thus be arbitrarily large, m_h^2 is bounded by above [61, 62]: if one takes the limit $m_A^2 \gg m_Z^2$, then $m_h^2 \to m_Z^2 \cos^2 2\beta$. This means that, at tree level,

$$
m_h^2 \leq m_Z^2 \cos^2 2\beta,
\tag{1.2.110}
$$

and that therefore, in the MSSM, the loop corrections are sizeable. For an $m_h^2 \sim m_Z^2$, one requires $\sim (86\,\text{GeV})^2$ in contributions from loop corrections to m_h^2 to obtain the SM-Higgs value. The loop corrections in the MSSM are by and large dictated by the stop squarks via their top Yukawa coupling to the Higgs. These large stop contributions at loop-level arise from the residue of uncancelled stop and top loops that *would* have cancelled if SM masses and their superpartners truly had the same mass. As previously mentioned, the Higgs mass is controlled by the Higgs quartic coupling in the MSSM, but top-stop corrections to the Higgs quartic $\propto |y_t|^4 \log\left(m_{\tilde{t}_1} m_{\tilde{t}_2}/m_t^2\right)$ can have a powerful Higgs mass boosting effect. For that reason, many MSSM-like models require large stop masses and/or large stop mixing.

When one of the CP-even Higgs mass eigenstates is aligned in field space with the SM Higgs VEV, the lightest Higgs talks and walks like the SM-Higgs and it

$\cos(\beta - \alpha)$	$\sin(\beta - \alpha)$
$H W^{+\mu} W^{-\nu}$	$h W^{+\mu} W^{-\nu}$
$H Z^\mu Z^\nu$	$h Z^\mu Z^\nu$
$Z^\mu A h$	$Z^\mu A H$
$W^{\pm\mu} H^\mp h$	$W^{\pm\mu} H^\mp H$
$Z^\mu W^{\pm\nu} H^\mp h$	$Z^\mu W^{\pm\nu} H^\mp H$
$\gamma^\mu W^{\pm\nu} H^\mp h$	$\gamma^\mu W^{\pm\nu} H^\mp H$

Table 1.3: Proportionality of the Higgs couplings to the gauge bosons.

is said that there is *alignment* in the Higgs sector. This situation can occur when (1.2.110) is satisfied, by taking m_A^2, m_H^2 and $m_{H^\pm}^2$ as heavy: then there is *alignment with decoupling*. If the situation arises that m_h^2 is SM Higgs-like without needing to decouple the other Higgs states, then one says there is *alignment without decoupling*, and later it will be seen how this can come to life in Dirac gaugino extended SUSY models. The alignment scenario is equivalent to taking the mixing angle, α, defined in (1.2.91) as

$$\beta = \frac{\pi}{2} - \alpha \,. \tag{1.2.111}$$

At tree-level, α is related to β by

$$\frac{\sin 2\alpha}{\sin 2\beta} = -\left(\frac{m_H^2 + m_h^2}{m_H^2 - m_h^2}\right) \,, \qquad \frac{\tan 2\alpha}{\tan 2\beta} = \left(\frac{m_A^2 + m_Z^2}{m_A^2 - m_Z^2}\right) \,. \tag{1.2.112}$$

In the limit

$$\cos(\beta - \alpha) \simeq 0 \sin(\beta - \alpha) \simeq 1 \,, \tag{1.2.113}$$

h couples to the SM bosons, $W^\pm, Z$, while H decouples from them (see table 1.3). When alignment occurs, the Higgs sector of the SUSY model will appear synonymous with the SM one.

1.2.3.3   Sfermions and stop mixing in the MSSM

The Yukawa interactions between the Higgs bosons and the (s)fermions are derived, as was shown, from the second derivative of the superpotential. The Yukawa couplings relate to the tree-level fermion masses via

$$m_{u,c,t} = \frac{y_{u,c,t}}{\sqrt{2}} v \sin \beta \qquad m_{d,s,b} = \frac{y_{d,s,b}}{\sqrt{2}} v \cos \beta \,, \qquad m_{e,\mu,\tau} = \frac{y_{e,\mu,\tau}}{\sqrt{2}} v \cos \beta \,. \tag{1.2.114}$$

By requiring that the Yukawa couplings do not become non-perturbatively large, very rough limits can be placed on $\tan \beta$: for a $y_t \leq 1.4$, one requires $\tan \beta \geq 1$, and for a $y_b \leq 1.2$, one requires $\tan \beta \leq 50$. Contributions to the couplings between the sfermions and the MSSM Higgs come from multiple sources. Theoretically, any of the scalars in the model can mix with any other, providing that they both carry the same R-parity, electric charge and colour. For the most part, the mixing between most of the combinations is very small, but there can be substantial mixing, especially between left-right pairs such as $(\tilde{t}_R, \tilde{t}_L)$, $(\tilde{b}_R, \tilde{b}_L)$, $(\tilde{\tau}_R, \tilde{\tau}_L)$. The left and the right

handed squark and slepton pairs mix via the μ- and **a**- terms. In what follows inter-generational mixing is ignored. The purpose here is to derive the stop mass matrix, so the focus will only be on the up-type quarks, although the process is identical for the down-types. Obviously, to derive the mass matrix one starts with the potential. The first contribution comes from the F-terms of the superpotential, for which the relevant contributions are

$$
\begin{aligned}
W \supset{} & \mu \mathbf{H_u} \cdot \mathbf{H_d} + y_u \mathbf{Q} \cdot \mathbf{H_u \bar{u}} \\
={} & \mu(H_u^+ H_d^- - H_d^0 H_u^0) + y_u^{ij} \tilde{u}_{i,R}^c \left(\tilde{u}_{j,L} H_u^0 - \tilde{d}_{j,L} H_u^+ \right) \\
\supset{} & \mu(H_u^+ H_d^- - H_d^0 H_u^0) + y_t \tilde{t}_R^c \left(\tilde{t}_L H_u^0 - \tilde{b}_L H_u^+ \right) ,
\end{aligned}
\tag{1.2.115}
$$

where the conventions written in table 1.4 have been employed, and the second and third generation contributions in the 3rd line have been dropped: this is justified seeing as the Yukawa couplings are proportional to the fermion masses which, for the 1st and 2nd generations, are relatively negligible compared to those of the 3rd generation. The F-term (mass) contributions to the potential for the stops are then

$$
\begin{aligned}
V_F \supset{} & \left[\left| \frac{\partial W}{\partial H_u^0} \right|^2 + \left| \frac{\partial W}{\partial \tilde{t}_L} \right|^2 + \left| \frac{\partial W}{\partial \tilde{t}_R^c} \right|^2 \right]_{\min} \\
={} & \left[\left| y_t \tilde{t}_R^c \tilde{t}_L - \mu H_d^0 \right|^2 + \left| y_t \tilde{t}_R^c H_u^0 \right|^2 + \left| y_t (H_u^0 \tilde{t}_L - \tilde{b}_L H_u^+) \right|^2 \right]_{\min} \\
={} & \left| y_t \tilde{t}_R^c \tilde{t}_L - \frac{1}{\sqrt{2}} \mu v c_\beta \right|^2 + \frac{1}{2} v^2 s_\beta^2 \left[|y_t \tilde{t}_L|^2 + |y_t \tilde{t}_R^c|^2 \right] \\
\supset{} & -m_t \cot\beta \left[\mu \tilde{t}_R^c \tilde{t}_L + \mu^* (\tilde{t}_R^c)^* \tilde{t}_L^* \right] + m_t^2 \left[\tilde{t}_L^* \tilde{t}_L + (\tilde{t}_R^c)^* \tilde{t}_R^c \right] ,
\end{aligned}
\tag{1.2.116}
$$

where the first term will contribute an off-diagonal bilinear piece which mixes the left-handed and right-handed components, and the second term is a mass squared piece which will contribute to the diagonals.

The second set of contributions come from the D-term potential,

$$
\begin{aligned}
V_D \supset{} & \frac{1}{2} g_Y^2 \left(Y_{H_u} |H_u|^2 + Y_{H_d} |H_d|^2 + Y_{\tilde{u}_L} |\tilde{u}_L|^2 + Y_{\tilde{u}_R} |\tilde{u}_R^c|^2 \right)^2 \\
& + \frac{1}{2} g_2^2 \left(H_u^* \frac{\sigma^a}{2} H_u + H_d^* \frac{\sigma^a}{2} H_d + \tilde{u}_L^* \frac{\sigma^a}{2} \tilde{u}_L \right)^2 \\
\supset{} & \frac{1}{2} g_Y^2 \left(\frac{1}{2} |H_u^0|^2 - \frac{1}{2} |H_d^0|^2 + \frac{1}{6} |\tilde{t}_L|^2 - \frac{2}{3} |\tilde{t}_R^c|^2 \right)^2 \\
& + \frac{1}{8} g_2^2 \left(-|H_u^0|^2 + |H_d^0|^2 + |\tilde{t}_L|^2 \right)^2 ,
\end{aligned}
$$

such that

$$
\begin{aligned}
[V_D]_{\min} \supset{} & \frac{1}{2} g_Y^2 \left(-\frac{1}{4} v^2 c_{2\beta} + \frac{1}{6} |\tilde{t}_L|^2 - \frac{2}{3} |\tilde{t}_R^c|^2 \right)^2 + \frac{1}{8} g_2^2 \left(v^2 c_{2\beta} |\tilde{t}_L|^2 \right) \\
\supset{} & \frac{1}{4} v^2 c_{2\beta} \left[\frac{2}{3} g_Y^2 |\tilde{t}_R^c|^2 + |\tilde{t}_L|^2 \left(\frac{g_2^2}{2} - \frac{g_Y^2}{6} \right) \right] \\
={} & m_Z^2 c_{2\beta} \left[\left(\frac{1}{2} - \frac{2}{3} s_W^2 \right) |\tilde{t}_L|^2 + \frac{2}{3} s_W^2 |\tilde{t}_R^c|^2 \right] ,
\end{aligned}
\tag{1.2.117}
$$

having used that

$$
s_W^2 = \frac{g_Y^2}{g_Y^2 + g_2^2} .
\tag{1.2.118}
$$

Finally, there is also a contribution from the soft terms one saw in eq. (1.2.71). These are

$$V_{\text{soft}} \supset (\tilde{Q}^i)^\dagger (\mathbf{m_Q}^2)_i^j \tilde{Q}_j + \tilde{u}_R^{ci}(\mathbf{m_{\bar{u}}}^2)_i^j (\tilde{u}_{Rj}^c)^\dagger + \left(\mathbf{a_u}^{ij} \tilde{u}_{Ri}^c \tilde{Q}_j \cdot H_u + \text{c.c.} \right)$$

$$\supset (\tilde{Q}^3)^\dagger (\mathbf{m_Q}^2)_3^3 \tilde{Q}_3 + (\tilde{t}_R^c)(\mathbf{m_{\bar{u}}}^2)_3^3 (\tilde{t}_R^c)^\dagger + \left(y_t A_t \tilde{t}_R^c (\tilde{t}_L H_u^0 - \tilde{b}_L H_u^+) + \text{h.c.} \right) \, ,$$

such that

$$[V_{\text{soft}}]_{\min} \supset (\tilde{Q}^3)^\dagger (\mathbf{m_Q}^2)_3^3 \tilde{Q}_3 + (\tilde{t}_R^c)(\mathbf{m_{\bar{u}}}^2)_3^3 (\tilde{t}_R^c)^\dagger + m_t A_t \tilde{t}_R^c \tilde{t}_L + m_t A_t^* (\tilde{t}_R^c)^* \tilde{t}_L^* \, , \tag{1.2.119}$$

where it has been used that

$$\mathbf{m_Q}^2 \sim \begin{pmatrix} m_{Q_1}^2 & 0 & 0 \\ 0 & m_{Q_2}^2 & 0 \\ 0 & 0 & m_{Q_3}^2 \end{pmatrix} , \qquad \mathbf{m_{\bar{u}}}^2 \begin{pmatrix} m_{\bar{u}_1}^2 & 0 & 0 \\ 0 & m_{\bar{u}_2}^2 & 0 \\ 0 & 0 & m_{\bar{u}_3}^2 \end{pmatrix} , \tag{1.2.120}$$

and that the trilinear couplings $\mathbf{a_u}, \mathbf{a_d}, \mathbf{a_e}$ are related to the Yukawa couplings via the matrices $A_{,u,d,e}$ such that

$$(a_u)_{33} = y_t A_t, \qquad (a_d)_{33} = y_b A_b, \qquad (a_e)_{33} = y_\tau A_\tau \, . \tag{1.2.121}$$

Writing, for simplicity, $t_R \equiv (\tilde{t}_R^c)^*$, $t_R^c \equiv t_R^*$ and collecting all the $(\tilde{t}_L, \tilde{t}_R)$ contributions from the Lagranigan together, one sees that

$$-\mathcal{L}_{\text{stops}} = \tilde{t}_L^* m_{\tilde{t}_{11}}^2 \tilde{t}_L + \tilde{t}_R^* m_{\tilde{t}_{22}}^2 \tilde{t}_L \tilde{t}_R^* m_{\tilde{t}_{22}}^2 \tilde{t}_R + \tilde{t}_L^* m_{\tilde{t}_{12}}^2 \tilde{t}_R + \tilde{t}_R^* m_{\tilde{t}_{21}}^2 \tilde{t}_L$$

$$= \left(\tilde{t}_L^* \tilde{t}_R^* \right) \mathbf{m_{\tilde{t}}}^2 \begin{pmatrix} \tilde{t}_L \\ \tilde{t}_R \end{pmatrix} \, , \tag{1.2.122}$$

with

$$\mathbf{m_{\tilde{t}}}^2 = \begin{pmatrix} m_{\tilde{t}_{11}}^2 & m_{\tilde{t}_{12}}^2 \\ m_{\tilde{t}_{21}}^2 & m_{\tilde{t}_{22}}^2 \end{pmatrix} \, . \tag{1.2.123}$$

Then the stop mass matrix can be written:

$$\mathbf{m_{\tilde{t}}}^2 = \begin{pmatrix} m_t^2 + m_{Q_3}^2 + m_Z^2 c_{2\beta} \left(\frac{1}{2} - \frac{2}{3} s_W^2 \right) & m_t(A_t^* - \mu^* \cot\beta) \\ m_t(A_t - \mu \cot\beta) & m_t^2 + m_{\bar{u}_3}^2 + \frac{2}{3} m_Z^2 s_W^2 c_{2\beta} \end{pmatrix} \, . \tag{1.2.124}$$

Evidently, the off-diagonal contributions determine the stop-mixing. For reasons that will be discussed in section 1.2.3.5, the μ-term cannot completely vanish in the MSSM, which means that even if the trilinear couplings are small, for a $\tan\beta$ not too large, there will always be some amount of stop-mixing in the MSSM. On the other hand, in the limit of large $\tan\beta$, to have large stop-mixing one requires large A-terms.

1.2.3.4   The electroweakinos

A brief word should be mentioned on the electroweakinos in the MSSM, the charginos and the neutralinos, which form from the higgsinos and electroweak gauginos after EWSB. The neutralinos, $\tilde{\chi}_{1...4}$, are the 4 mass eigenstates that result from the mixing

between the bino, $\tilde{B}$; neutral wino, $\tilde{W}^0$; and two higgsinos $(\tilde{H}_u^0, \tilde{H}_d^0)$, and whose mass matrix is given by

$$\mathcal{M}_N = \begin{pmatrix} M_1 & 0 & -c_\beta s_W m_Z & s_\beta s_W m_Z \\ 0 & M_2 & c_\beta c_W m_Z & -s_\beta c_W m_Z \\ -c_\beta s_W m_Z & c_\beta c_W m_Z & 0 & -\mu \\ s_\beta s_W m_Z & -s_\beta c_W m_Z & -\mu & 0 \end{pmatrix} , \qquad (1.2.125)$$

where s_W is the weak mixing angle defined in eq.(1.2.118). As can be seen, in the MSSM neutralino mass matrix the Majorana masses, M_1, M_2, are on the diagonals: this will not be the case in the R-symmetry preserving Dirac gaugino scenarios considered later where these terms can be chosen to vanish. After diagonalisation, one ends up with 1 bino-like, 1 wino-like and 2 higgsino-like neutralinos in the MSSM spectrum. The charginos, $\chi_{1,2}^\pm$, are the result of mixing between the charged winos $(\tilde{W}^+, \tilde{W}^-)$ and charged higgsinos $(\tilde{H}_u^+, \tilde{H}_d^-)$, and have the mass matrix

$$\mathcal{M}_C = \begin{pmatrix} M_2 & \sqrt{2}M_W s_\beta \\ \sqrt{2}M_W c_\beta & \mu \end{pmatrix} . \qquad (1.2.126)$$

After diagonalisation, one gets 1 higgsino-like and 1 wino-like chargino. By convention it is chosen that the masses obey the hierarchical order $m_{\tilde{\chi}_1} < m_{\tilde{\chi}_2} < m_{\tilde{\chi}_3} < m_{\tilde{\chi}_4}$ and $m_{\tilde{\chi}_1^\pm} < m_{\tilde{\chi}_2^\pm}$. This convention will also be employed when looking at the electroweakino sector of the MDGSSM in chapter 3.

1.2.3.5   MSSM drawbacks

For all the problems that the MSSM holds solutions to, it is not without its mysteries. One such puzzle arises in the form of the "μ-problem" [11,63]. The MSSM contains the SUSY mass term $\mu \mathbf{H_u} \cdot \mathbf{H_d}$ in its superpotential, where μ is a dimensionful parameter: the only new parameter that arises in the MSSM that is *not* a consequence of SUSY being necessarily broken. As can be seen from the MSSM potential (1.2.75), the mass terms for the scalar Higgs fields are typical bosonic (scalar) mass terms, with a positive mass parametrization, $|\mu|^2(m_{H_u}^2 + m_{H_d}^2)$. This is already contrary to what is desired: a negative mass term which induces EWSB. As the μ-term preserves SUSY, there is no reason to believe that it is associated with the SUSY breaking scale, m_{soft}, and one would be well justified to think instead that it should either vanish, or be of the order of the Plank or unification scales (*i.e.* the assumed cutoff scale). However, as the complex Higgs scalars lie in chiral multiplets with their fermionic Higgsino superpartners, not only is the μ-term involved in the Higgs scalar masses,

$$-\mathcal{L}_{\text{SUSY Higgs mass}} = |\mu|^2 \left(|H_u^0|^2 + |H_u^+|^2 + |H_d^0|^2 + |H_d^-|^2 \right) , \qquad (1.2.127)$$

but also those of the Higgsinos,

$$-\mathcal{L}_{\text{Higgsino mass}} = \mu \left(\tilde{H}_u^+ \cdot \tilde{H}_d^- - \tilde{H}_u^0 \cdot \tilde{H}_d^0 \right) . \qquad (1.2.128)$$

The charged Higgsinos mix with the charged winos to form the charginos $\tilde{\chi}_{1,2}^\pm$ of the electroweakino sector. The lack of chargino-like particle at LEP implies a lower limit of ~ 103 GeV [64] on the charginos, which in turn corresponds to a limit on the dimensional $|\mu|$ parameter yielding $|\mu| \geq 100$ GeV [65]. So from experimental constraints, μ cannot be a vanishing parameter. What about $\mathcal{O}(\mu) \sim \mathcal{O}(M_{\text{plank}})$? If μ

is very large, then it is not possible to verify the EWSB condition (1.2.79): recall that one needs the potential to be a saddle point when $H_u = H_d = 0$. It turns out that to satisfy the conditions for EWSB, one requires $\mathcal{O}(\mu) \sim \mathcal{O}(m_{\text{soft}})$, which is exactly the same energy scale as the other parameters in the Higgs potential which are all SUSY breaking $(B_\mu, m_{H_u}^2, m_{H_d}^2)$. This is the μ-problem: why should a parameter that respects SUSY live at an energy scale the same as those that do not? Many models have been proposed that "solve" the μ-problem, such as excluding it altogether, or generating it as a consequence of SUSY breaking or from a common origin as the SUSY breaking parameters $e.g.$ [65–68].

Another pressing concern for the MSSM is that of *naturalness*. In essence, if a theory's prediction for electroweak scale physics is correct, then it is said to be *natural*. So far, no sign of SUSY has been discovered by collider experiments to the point that, in simplified MSSM scenarios, limits can already be set around 1-2 TeV on the squarks and gluinos [69–71]. Of course, simplified model scenarios are not a true representation of the complexity of a model such as the MSSM, but they are indicative of the scales we will need to probe to find new supersymmetric physics. As the sparticle masses get larger, so does the fine-tuning of the model. Fine-tuning in the MSSM is dominated by the necessity to obtain the correct Higgs mass, and how to generate large enough radiative corrections to get there - generically enabled via large stop masses or stop mixing. But this does not necessarily mean the end for the MSSM. The fine-tuning in the MSSM is of the order of a few percent [72], and arises because of two conflicting requirements: that (1) the Higgs receives large loop-corrections from heavy stops in order to pull up its tree-level mass from ~ 91 GeV to 125 GeV, and (2) that the stops can't be too heavy so as to avoid generating large lograrithmic corrections to the Higgs soft mass parameter, which would then in turn require that other parameters be fine-tuned in order to regain the correct EWSB scale (*i.e.* to re-obtain a Higgs VEV generating the correct values fo m_W, m_Z). This latter point ties in with the issue that the sparticle masses are continually being driven higher by experimental constraints. This is the *little hierarchy problem* [73]. However, this amount of fine-tuning is minimal in comparison to what the SM suffers, *i.e.* from the fact that the Higgs mass needs to be stabilised at the electroweak scale despite it receiving large radiative corrections from UV physics: this is the *hierarchy problem*. We recall that this is one of the reasons SUSY is so attractive in the first place - that it *can* stabilise the electroweak scale! So this brings us back round to where we started: is supersymmetry a satisfactory solution to the big hierarchy problem if it ends up reintroducing a little hierarchy between the electroweak and SUSY scale?

But supersymmetry, like the platypus, should not be considered endangered but merely vulnerable. Now will be discussed a branch of supersymmetric model, *Dirac gaugino models*, that can alleviate some of the troubles the MSSM suffers. Specifically in the case of the MDGSSM, one can generate a tree-level boost from new Higgs couplings, and require no stop mixing to get a good Higgs mass at tree-level, hence increasing naturalness in the model.

1.2.4   Minimal Dirac gaugino models

1.2.4.1   A brief overview

With the current bounds on colourful supersymmetric particles at the LHC, and the consequent implications for naturalness of the Minimal Supersymmetric Standard Model (MSSM), it is timely to consider *non-minimal* scenarios. A particularly well-motivated extension of the MSSM is to allow Dirac masses for the gauginos, ei-

ther instead of, or in addition to, Majorana ones. Dirac gaugino models have been well studied, for example in refs. [66, 67, 74–132]. Indeed the fermions of the standard model generated via the Higgs mechanism are of Dirac type[10], and there is no reason to believe that supplementary fermions could not be. Dirac gaugino models hold many interesting properties, including an enhanced tree-level Higgs mass owing to new quartic couplings; R-symmetry preservation leading to simpler SUSY breaking models, and the relaxing of LHC bounds due to the suppression of gluino direct production (which will be discussed in detail in section 3).

While it is possible to write the masses through hard breaking operators [124], in spontaneously broken SUSY, Dirac masses should only appear through the above *supersoft* terms which have the remarkable property that they do not appear in the renormalisation group (RG) equations for any other operators [77, 133, 134].

A Dirac term was in fact the original method proposed to allow the gluino to be massive [74], because the simplest models of global supersymmetry breaking preserve R-symmetry [135] and thus forbid Majorana (but not Dirac) masses; this remains an important motivation today. As opposed to the Majorana masses described in eq. (1.2.73), Dirac masses are four-component spinors and can be written in terms of two Weyl spinors,

$$\Psi = \begin{pmatrix} \psi_\alpha \\ \bar{\chi}^{\dot\alpha} \end{pmatrix}, \qquad \bar{\Psi} = (\chi^\alpha, \bar{\psi}_{\dot\alpha}), \tag{1.2.129}$$

giving rise to the supersoft SUSY breaking mass terms

$$\mathcal{L}_{\text{supersoft}} \supset -m_D \bar{\Psi}\Psi = -m_D \left(\chi^\alpha \psi_\alpha + \bar{\psi}_{\dot\alpha} \bar{\chi}^{\dot\alpha} \right). \tag{1.2.130}$$

As is known, the Lagrangian carries no R-charge, and the superpotential needs to carry an R-charge of 2 in order to be invariant under R-symmetry. Therefore in order to have R-symmetry conserving kinetic terms for the gauge fields, the supersymmetric gauge field strength superfields $\mathcal{W}^a$ must carry an R-charge of 1. It follows that the gaugino, the lowest component of $\mathcal{W}^a$, also has an R-charge of 1, and therefore the mass terms of eq. (1.2.73) are R-symmetry violating. On the contrary, Dirac gaugino masses are R-symmetry conserving, as an R-charge of -1 can be given to the new adjoint fermions. Each additional Weyl fermion contributes a further two fermionic degrees of freedom. As SUSY requires an equal number of degrees of freedom in both the scalar and fermionic sectors, this implies that, after EWSB, there will be four new neutral scalar degrees of freedom as compared to the MSSM. The phenomenology of the electroweakino spectrum will be discussed in detail in section sec. 3.1.2.

To endow gauginos with a Dirac mass, at a minimum, one needs to add chiral fermions $(\chi_S, \chi_T^a, \chi_O^a)$ in the adjoint representation of each gauge group: these are embedded in chiral superfields $\mathbf{S}, \mathbf{T^a}, \mathbf{O^a}$ which are respectively a $U(1)_Y$ singlet, $SU(2)_L$ triplet and $SU(3)_c$ octet and which carry no R-charge. Of course, this means that in addition to the chiral fermions necessary to form Dirac gauginos, one gets a set of complex scalar fields (S, T^a, O^a) thrown in for free. If just these fields are added, then one has the simplest Dirac-gaugino extension of the MSSM whose Higgs sector has been well studied [67, 83, 88, 105, 130]. These adjoint-superfields are defined by

$$\begin{aligned} \mathbf{S} = &\ S + \sqrt{2}\theta\chi_S + \theta\theta F_S \\ \mathbf{T^a} = &\ T^a + \sqrt{2}\theta\chi_T^a + \theta\theta F_T^a, \\ \mathbf{O^a} = &\ O^a + \sqrt{2}\theta\chi_O^a + \theta\theta F_O^a, \end{aligned} \tag{1.2.131}$$

---

[10]Potentially excepting the neutrino whose status - in the absence of detection of the expected right-handed neutrino - is unconfirmed.

Superfield		Scalars	Fermions	Vectors	$(SU(3), SU(2), U(1)_Y)$	R-charge
Matter Sector						
MSSM chiral superfields						
(S)quarks	$\mathbf{Q}_i$	$\tilde{Q}_i = (\tilde{u}_{i,L}, \tilde{d}_{i,L})$	(u_L, d_L)	-	$(\mathbf{3}, \mathbf{2}, 1/6)$	R_Q
	$\bar{\mathbf{u}}_i$	$\tilde{u}^c_{i,R}$	$u^c_{i,R}$	-	$(\bar{\mathbf{3}}, \mathbf{1}, \text{-}2/3)$	$2\text{–}R_Q\text{–}R_H$
	$\bar{\mathbf{d}}_i$	$\tilde{d}^c_{i,R}$	$d^c_{i,R}$	-	$(\bar{\mathbf{3}}, \mathbf{1}, 1/3)$	$R_H - R_Q$
(S)leptons	$\mathbf{L}_i$	$(\tilde{\nu}_{i,L}, \tilde{e}_{i,L})$	$(\nu_{i,L}, e_{i,L})$	-	$(\mathbf{1}, \mathbf{2}, \text{-}1/2)$	R_L
	$\bar{\mathbf{e}}_i$	$\tilde{e}^c_{i,R}$	$e^c_{i,R}$	-	$(\mathbf{1}, \mathbf{1}, 1)$	$R_H - R_L$
Higgs/	$\mathbf{H_u}$	(H_u^+, H_u^0)	$(\tilde{H}_u^+, \tilde{H}_u^0)$	-	$(\mathbf{1}, \mathbf{2}, 1/2)$	R_H
Higgsinos	$\mathbf{H_d}$	(H_d^0, H_d^-)	$(\tilde{H}_d^0, \tilde{H}_d^-)$	-	$(\mathbf{1}, \mathbf{2}, \text{-}1/2)$	$2 - R_H$
MSSM chiral superfields						
Gauge Sector						
MSSM gauge superfields						
Gluons/gluinos	$\mathbf{W_{3,\alpha}}$	-	$\lambda_{3,\alpha}$ $[\equiv \tilde{g}_\alpha]$	G_μ	$(\mathbf{8}, \mathbf{1}, 0)$	1
W/ Winos	$\mathbf{W_{2,\alpha}}$	-	$\lambda_{2,\alpha}$ $\left[\equiv \tilde{W}^0, \tilde{W}^\pm\right]$	$W_\mu^\pm, W_\mu^0$	$(\mathbf{1}, \mathbf{3}, 0)$	1
B/ Binos	$\mathbf{W_{Y,\alpha}}$	-	$\lambda_{1,\alpha}$ $\left[\equiv \tilde{B}\right]$	B_μ	$(\mathbf{1}, \mathbf{1}, 0)$	1

Dirac gaugino adjoint chiral superfields				
Superfield		Scalars ($R=0$)	Fermions ($R=-1$)	$(SU(3), SU(2), U(1)_Y)$
Adjoint octet	$\mathbf{O^a}$	$O^a = \frac{1}{\sqrt{2}}(O_1^a + iO_2^a)$	χ_O^a	$(\mathbf{8},\mathbf{1},0)$
Adjoint triplet	$\mathbf{T^a}$	$T^0 = \frac{1}{\sqrt{2}}(T_R^0 + iT_I^0), T^\pm$	$\tilde{W}'^0, \tilde{W}'^\pm [\equiv \chi_T^a]$	$(\mathbf{1},\mathbf{3},0)$
Adjoint singlet	$\mathbf{S}$	$S = \frac{1}{\sqrt{2}}(S_R + iS_I)$	$\tilde{B}'^0 [\equiv \chi_S]$	$(\mathbf{1},\mathbf{1},0)$

Table 1.4: Field content in the minimal Dirac gaugino case. Top panel: chiral and gauge multiplet fields of the MSSM; bottom panel: chiral and gauge multiplet fields added to those of the MSSM to allow Dirac masses for the gauginos. Note that the expansion $T^\pm$ is identical to that of T^0 but for the superscript $0 \leftrightarrow \pm$.

and the resulting field content is summarised in table 1.4.

It is from the extended gauge sector that additional supersymmetry breaking terms can emerge, and consequently Dirac masses for gauginos. As previously mentioned, these SUSY breaking terms are supersoft, and can be written as [77]

$$\mathcal{L}_{\text{supersoft}} = \int d^2\theta \sqrt{2} \frac{\mathcal{W}'^\alpha \mathcal{W}_{j\alpha}^a \mathbf{\Sigma}_j^a}{M} + \text{h.c}, \qquad (1.2.132)$$

where $\mathcal{W}_j^a = \lambda_j^a + \theta D_j^a + ...$ are the supersymmetric gauge field strengths associated to the $U(1)$, $SU(2)$ and $SU(3)$ gauge groups for $j = 1, 2, 3$ respectively; $\mathbf{\Sigma}_j^a = \Sigma_j^a + \sqrt{2}\theta D_j^a + ...$ are the Dirac gaugino multiplets with scalar components $\Sigma^a = S, T^a, O^a$ (for $j = 1, 2, 3$) with expansions as in (1.2.131); $\mathcal{W}' = \lambda' + \theta D' + ...$ is the field strength of some vector superfield in the hidden sector (such as a hidden sector $U(1)'$) and M is the mass scale at which the Dirac gaugino masses are generated. The (hidden) auxillary field D' then acquires a VEV, breaking SUSY spontaneously in the hidden

sector, leading to supersoft mass terms that break SUSY explicitly in the visible sector:

$$
\begin{aligned}
\mathcal{L}_{\text{supersoft}} &= \int d^2\theta \, \sqrt{2} \, \frac{\langle D' \rangle \theta^\alpha \mathcal{W}^a_\alpha \boldsymbol{\Sigma}^a}{M} + \text{h.c} \\
&= \int d^2\theta \sqrt{2} m_D \theta^\alpha \left(\lambda^a + \theta_\alpha D^a + ... \right) \left(\Sigma^a + \sqrt{2}\theta_\alpha \chi^a_\Sigma + ... \right) \\
&\supset -m_D \lambda^a \chi^a_\Sigma + \sqrt{2} m_D D^a \Sigma^a + \text{h.c.} \,, \qquad\qquad (1.2.133)
\end{aligned}
$$

where $m_D = \langle D' \rangle / M$ has been substitued, and $(\theta\lambda)(\theta\chi) = -\frac{1}{2}\theta\theta\lambda\chi$ has been used. As can be seen, the Dirac gaugino masses are suppressed by an order of the messenger scale, M. The first term in eq. (1.2.133) takes the same form as that in eq. (1.2.130), and is the Dirac mass term for the gaugino, λ^a, and the new adjoint fermion, χ^a_Σ. Once the auxilliary field D^a is integrated out, the second term in (1.2.133) generates a mass term for the adjoint scalars.

Supersoft terms for the gauginos means that Dirac gauginos can, in principle, be taken much heavier than their Majorana counterparts since, instead of inducing a logarithmically divergent corrections to the sfermion masses, they only induce a finite shift: when this hierarchy is maximally large (i.e. one starts with zero soft masses for sfermions) it is known as the *supersoft scenario*, which would be realised e.g. in models of goldstone gauginos [121, 122]. Therefore, unlike the *soft* scenario which still reintroduces logarithmic (but not quadratic) divergences in scalar masses, Dirac gaugino masses and the subsequent supersoft scenario allows for increased naturalness as the only corrections to scalar masses are given by finite contributions. This means that a larger hierarchy between the gaugino (of particular interest, the gluino) and squark masses can be accommodated in Dirac gaugino models than in more minimal models such as the MSSM, without ruining the naturalness of the model.

The supersoft property when applied to the Higgs masses means that Dirac gaugino (DG) models are much more *natural* than Majorana ones, although they do not completely alleviate the little hierarchy problem by themselves [107]. On the other hand, the singlet and triplet fields can have new superpotential couplings with the Higgs,

$$
W \supset \lambda_S \mathbf{S} \, \mathbf{H_u} \cdot \mathbf{H_d} + 2\lambda_T \, \mathbf{H_d} \cdot \mathbf{T} \mathbf{H_u} \,, \qquad\qquad (1.2.134)
$$

which naturally enhance the Higgs mass at tree level — and can also be associated with an $\mathcal{N} = 2$ supersymmetry in the gauge-Higgs sector [78,136]. An $\mathcal{N} = 2$ SUSY in turn leads automatically to alignment [137] due to the $SU(2)$ R-symmetry of the two Higgs doublets (which form an $\mathcal{N} = 2$ hypermultiplet) [138]. As will be shown in chapter 2, this alignment is surprisingly robust under quantum corrections, where there is an accidental cancellation of $\mathcal{N} = 2$ breaking effects [137]. Moreover, it has been found that the R-symmetry also prevents chirality-flip diagrams, which significantly relaxes flavour constraints [79,87,106] and suppresses squark production at the LHC, rendering DG models "supersafe" [139–142].

The above motivations led to many studies, and realisations being developed [66, 67, 75–78, 80, 82, 84, 86, 88, 90–92, 95, 98–100, 102–105, 108–112, 114, 115, 117–124, 126, 127, 131, 143]. The models fall either into the class of those that preserve an exact R-symmetry, or allow a small amount of R-breaking. On the former side, the principal example is the Minimal R-Symmetric Supersymmetric Standard Model (MRSSM) [79]: this requires the addition of supplementary R-Higgs fields (in the same gauge representation as the MSSM Higgs doublets but with different R-charges) which do not obtain expectation values after electroweak symmetry breaking. However, the

couplings in eq. (1.2.134) are forbidden, and the equivalent couplings between the Higgs and R-Higgs fields do not give any tree-level enhancement to the Higgs mass, making the Higgs sector rather like the MSSM — except that stop mixing is forbidden by the R-symmetry, so that in order to obtain the correct value of the Higgs mass either the new superpotential couplings must be very large [126, 127, 131] or the stops should be in the $\mathcal{O}(10\text{--}100)$ TeV range [137].

It will be seen momentarily how the triplet and singlet scalar fields contribute to an extended Higgs sector in more detail, but a brief word should be mentioned of the superpartners of the gluinos - the colour-octet scalar fields O^a often referred to as the *sgluon* -which is a singlet under the electroweak gauge groups. Multiple studies have been performed on the decays of the sgluons, for which the reader is referred to [81, 117, 144, 145] for more details. If CP is conserved, then the sgluon can be further distinguished by a real scalar (O_1^a in table 1.4) and a real pseudoscalar field (O_2^a in table 1.4). Typically after supersymmetry breaking, the slguon gets 3 types of mass term from $\mathcal{L}_{\text{standardsoft}}$ and $\mathcal{L}_{\text{supersoft}}$ above:

$$-\mathcal{L}_O \supset m_O^2 O^{a*} O^a + \frac{1}{2}\left(B_O O^a O^a + \text{h.c.}\right) + (m_{D3} O^a + \text{h.c.})^2 \,. \tag{1.2.135}$$

A rotation of the adjoint-octet chiral superfield $\mathbf{O^a}$ dictates that it is always possible to take the Dirac mass m_{D3} as real. However, without imposing CP invariance, it is not possible to require that both m_{D3} and B_O are real simultaneously. It follows that, if B_O is complex, then the real and imaginary parts of the scalar octet will mix. The scalar octet mass matrix can be diagonalised by a rotation of angle ϕ_O,

$$\phi_O = -\frac{1}{2}\text{Arg}(B_O + 2m_{3D}^2) \,, \tag{1.2.136}$$

such that

$$O^a = \frac{e^{i\phi_O}}{\sqrt{2}}(O_1^a + iO_2^a) \,. \tag{1.2.137}$$

When CP is conserved, the rotation angle $\phi_O \to 0$, and

$$-\mathcal{L}_O \xrightarrow[\text{Invariance}]{\text{CP}} \supset \frac{1}{2}\left(m_O^2 + B_O + 4m_{D3}\right)O_1^{a2} + \frac{1}{2}(m_O^2 - B_O)O_2^{a2} \,. \tag{1.2.138}$$

In this scenario it can be seen that, as the octet pseudoscalar O_2^a is then unrelated to the Dirac gluino mass, it can lie at a sub-TeV scale while escaping current LHC constraints [129]. The octet scalar O_1^a is typically taken as one of the heaviest particles in the theory; the pseudoscalar O_2^a can also be taken as heavy, however if B_O is large then it can be light. At tree-level, sgluons can decay either into gluino or squark pairs, which further decay into quarks and missing energy in the form of electroweakinos $\tilde{\chi}$,

$$O^a \to \tilde{g}\tilde{g} \to q q \tilde{q} \tilde{q} \to q q q q + \tilde{\chi}\tilde{\chi} \,, \qquad O^a \to \tilde{q}\tilde{q} \to q q + \tilde{\chi}\tilde{\chi} \,. \tag{1.2.139}$$

The scalar octets possess tree-level trilinear couplings to the squarks via the D-term,

$$\mathcal{L}_O \supset \sqrt{2}m_{D3}(O^a + O^{a*})D^a \,, \tag{1.2.140}$$

which, after spontaneous SUSY breaking become

$$-\mathcal{L}_O \supset 2g_s m_{3D}(O_1^a \cos\phi_O - O_2^a \sin\phi_O)(\tilde{q}_{Li}^* T_{ij}^a \tilde{q}_{Lj} + \tilde{q}_{Ri}^* T_{ij}^a \tilde{t}_{Rj}) \,, \tag{1.2.141}$$

where colour indices have been suppressed and where T^a are of the generators of the fundamental representation of $SU(3)$. As the pseudoscalar contribution is parametrised

by $\sin \phi_O$, when CP conservation is enforced, only the scalar octet will decay via the squark-antisquark channel as the pseudoscalar coupling vanishes. If kinematically allowed, the scalar octets will decay into gluinos and squarks in roughly equal proportion, although high LHC mass limits on the gluinos and squarks ($\gtrsim$ 1.5 TeV) [146] indicate the need for very heavy scalar octets to observe these decay channels, and hence they are unlikely to be seen at the LHC. The same applies for pseudoscalar decays into gluinos, and generally for the sgluons in CP violating scenarios. However, if the parameter space were accessible, from tree-level processes the decay of a sgluon could therefore produce signatures including 2-4 jets and missing energy (from 2 LSPs). Although, even more interestingly, as sgluons can be pair-produced, this number could increase to 4-8 jets and missing energy (from 4 LSPs).

The pseudoscalars (scalar octets) can also decay into quark-antiquark pairs (and gluons), however these are both suppressed at 1-loop level. The decay mode arising from the coupling between the sgluons and quark-antiquark pairs is proportional to a factor of the quark-mass squared, meaning that the biggest contribution comes from sgluons to top-quarks [117]. As the pseudoscalar coupling to the gluons vanishes under CP conservation this means that, certainly for the pseudoscalars, this leads to decays predominantly into tops, lending the sgluon to 4-top decay channel as a promising avenue at hadron colliders [145]. The sgluon decay rates for O_1^a and O_2^a for the different decay channels can be found in [117]. It should be noted that, although these small corrections will not be considered in what follows, as was shown in [130], the sgluons make contributions to the Higgs mass via two-loop corrections to the effective potential (although if CP is conserved, the pseudoscalar corrections will vanish).

The properties and particle content of two variations of Dirac gaugino model will now be discussed.

1.2.4.2   The minimal model: MDGSSM

In this section, the minimal model, often referred to as the Minimal Dirac Gaugino Supersymmetric Standard Model (MDGSSM), is considered, being described by just the matter content of the MSSM and the adjoint chiral superfields. As it can be seen in the table, there is a freedom in assigning R-charges to the chiral superfields, and numerous choices have been used in literature (see *e.g.* [79, 92, 103, 104, 114, 147]). While R-symmetry is not fully conserved in the MDGSSM, in section 1.2.4.3 there will be examples of Dirac gaugino models where further field content can be added to preserve R-symmetry in the full Lagrangian. In these models, the R-charges will differ in the chiral sector to the ones above in table 1.4. In fact, the MDGSSM *requires* R-symmetry to be broken explicitly in the Higgs sector by a B_μ term, otherwise it would be spontaneously broken at the same time as electroweak symmetry and generate a massless R-axion in the Higgs sector. This is because the B_μ term essentially controls the mass of the Higgs pseudoscalar, and so its absence would yield a massless pseudoscalar, or R-axion, in the Higgs sector at the time of electroweak symmetry breaking. If B_μ becomes very heavy, the heavy Higgs will become decoupled. If, on the other hand, B_μ becomes very light (around the mass of the lightest squarks), then the heavy Higgs will become involved in squark and gluino decays which makes the low energy phenomenology more complicated. The phenomenology of squark and gluino decays will be discussed further in chapter 3. Keeping $B_\mu \in (10^4, 10^7)$ GeV^4 means that B_μ will not become involved in the decays of the electroweakinos, and thus the B_μ term should be small but non-zero. As in [66, 83, 105, 116, 125], it shall be assumed that this is the *only* source of R-symmetry breaking, and is motivated by minimality, naturalness (allowing the couplings $\lambda_{S,T}$) and the idea that the Higgs

sector couples to a different source of SUSY breaking than the other fields (in order e.g. to generate the μ/B_μ terms of similar order etc). This is perfectly consistent at the level of the RG equations: the B_μ term does not generate other R-breaking operators on RG evolution. This means that the superpotential is

$$
\begin{aligned}
W_{\text{Higgs}}^{\text{MDGSSM}} =& Y_u^{ij} \, \mathbf{U}_i \mathbf{Q}_j \cdot \mathbf{H_u} - Y_d^{ij} \, \mathbf{D}_i \mathbf{Q}_j \cdot \mathbf{H_d} - Y_e^{ij} \, \mathbf{E}_i \mathbf{L}_j \cdot \mathbf{H_d} \\
&+ \mu \mathbf{H_u} \cdot \mathbf{H_d} + \lambda_S \mathbf{S} \, \mathbf{H_u} \cdot \mathbf{H_d} + 2\lambda_T \, \mathbf{H_d} \cdot \mathbf{T} \mathbf{H_u} \,,
\end{aligned}
\tag{1.2.142}
$$

where $\mathbf{Q}_i, \mathbf{L}_j \mathbf{U}_i, \mathbf{D}_i, \mathbf{E}_i, , \mathbf{H_d}, \mathbf{H_u}$ are, respectively, the superfields for the left-handed (LH) squarks; LH sleptons; right-handed (RH) up-type squarks; RH down-type squarks; RH sleptons; down- and up-type Higgs fields as in the MSSM, and $Y_u^{ij}, Y_d^{ij}, Y_e^{ij}$ which are the standard Yukawa couplings of the MSSM. It would also be possible to include superpotential couplings,

$$
W_{\text{RV}}^{\text{MDGSSM}} = L\mathbf{S} + \frac{M_1}{2}\mathbf{S}^2 + \frac{\kappa}{3}\mathbf{S}^3 + M_2 \text{tr}(\mathbf{TT}) + M_3 \text{tr}(\mathbf{O}^a \mathbf{O}^a)
\tag{1.2.143}
$$

$$
+ \lambda_{ST} \mathbf{S} \text{tr}(\mathbf{TT}) + \lambda_{SO} \mathbf{S} \text{tr}(\mathbf{O}^a \mathbf{O}^a) + \frac{\kappa_O}{3} \text{tr}(\mathbf{O}^a \mathbf{O}^a \mathbf{O}^a) \,,
\tag{1.2.144}
$$

but it is preferable not to include them here as they violate R-symmetry (RV). The most general choice that can be made for the Higgs and adjoint scalar sector for the *standard* soft terms is

$$
\begin{aligned}
\mathcal{L}_{\text{standard soft}} =& \ \overline{Q}^i (m_Q^2)_i^j Q_j + \overline{U}^i (m_U^2)_i^j U_j + \overline{D}^i (m_D^2)_i^j D_j + \overline{L}^i (m_L^2)_i^j L_j + \overline{E}^i (m_E^2)_i^j E_j \\
&+ m_{H_u}^2 |H_u|^2 + m_{H_d}^2 |H_d|^2 + B_\mu (H_u \cdot H_d + \text{h.c.}) + \frac{1}{2} M_i \lambda_i \lambda_i \\
&+ m_S^2 |S|^2 + 2 m_T^2 \text{tr}(T^\dagger T) + \frac{1}{2} B_S \left(S^2 + \text{h.c}\right) + B_T \left(\text{tr}(TT) + \text{h.c.}\right) \\
&+ m_O^2 |O|^2 + B_O \left(\text{tr}(OO) + \text{h.c.}\right) + A_S \left(SH_u \cdot H_d + \text{h.c.}\right) + 2 A_T \left(H_d \cdot T H_u + \text{h.c}\right) \\
&+ \frac{A_\kappa}{3} \left(S^3 + \text{h.c.}\right) + A_{ST} \left(S \text{tr}(TT) + \text{h.c}\right) + A_{SO} \left(S \text{tr}(OO) + \text{h.c}\right),
\end{aligned}
\tag{1.2.145}
$$

where $\lambda_i = \{\lambda_Y, \lambda_2, \lambda_3\}$ are the gauginos of hypercharge, $SU(2)$ and $SU(3)$ respectively, with Majorana masses M_Y, M_2, M_3. The first two lines show the MSSM soft-SUSY breaking terms as described in (1.2.71); while the third, fourth and fifth lines show soft-terms associated with the adjoint scalars. Importantly, the above *contains no SUSY-breaking squark trilinears*; but there is still some small mixing in the stop/sbottom sector due to the μ-term.

To these, the supersymmetry-breaking *supersoft* operators $m_{Di} \theta^\alpha$ for Dirac masses (as described in section 1.2.4.1) are added,

$$
\begin{aligned}
\mathcal{L}_{\text{supersoft}} = \int d^2\theta \Big[& \sqrt{2}\, m_{DY} \theta^\alpha \mathcal{W}_{1\alpha} \mathbf{S} + 2\sqrt{2}\, m_{D2} \theta^\alpha \text{tr}\left(\mathcal{W}_{2\alpha} \mathbf{T}\right) \\
&+ 2\sqrt{2}\, m_{D3} \theta^\alpha \text{tr}\left(\mathcal{W}_{3\alpha} \mathbf{O}\right) \Big] + \text{h.c.}\,,
\end{aligned}
\tag{1.2.146}
$$

where it is recalled that $\mathcal{W}_{i\alpha}$ are the supersymmetric gauge field strengths defined in (1.2.39).

The electroweak sector

This section considers the electroweak sector of the model, which will be the focus of chapter 2 where Higgs alignment will be discussed. The condition for tree-level Higgs alignment can be seen easily from the mass matrix of the CP-even neutral scalars,

which will be derived here, starting with the (neutral) electroweak scalar potential, V_{EW}. A more detailed derivation can be found in [83], along with a discussion of the potential in various limits. For the neutral fields, the electroweak scalar potential is given by

$$
\begin{aligned}
V_{EW} = {} & (m_{H_u}^2 + \mu^2)|H_u^0|^2 + (m_{H_d}^2 + \mu^2)|H_d^0|^2 - B_\mu(H_u^0 H_d^0 + h.c.) + \frac{g_2^2 + g_Y^2}{8}\left(|H_u^0|^2 - |H_d^0|^2\right)^2 \\
& + \left(\lambda_S^2 + \lambda_T^2\right)|H_u^0 H_d^0|^2 \qquad\qquad\qquad\qquad\qquad\qquad\qquad\qquad\qquad (1.2.147) \\
& + \frac{1}{2}\left(M_S^2 + m_S^2 + 4m_{DY}^2 + B_S\right)S_R^2 + \frac{1}{2}\left(M_S^2 + m_S^2 - B_S\right)S_I^2 \\
& + \frac{1}{2}\left(M_T^2 + m_T^2 + 4m_{D2}^2 + B_T\right)T_R^2 + \frac{1}{2}\left(M_T^2 + m_T^2 - B_T\right)T_I^2 \\
& + \left[\frac{\lambda_S^2}{2}(S_R^2 + S_I^2) + \frac{\lambda_T^2}{2}(T_I^2 + T_R^2) + \lambda_S\lambda_T\left(S_I T_I + S_R T_R\right) + \sqrt{2}\mu\left(\lambda_S S_R + \lambda_T T_R\right)\right] \\
& \quad \times \left(|H_u^0|^2 + |H_d^0|^2\right) \\
& + g_Y m_{1D} S_R\left(|H_u^0|^2 - |H_d^0|^2\right) + g_2 m_{2D} T_R\left(|H_d^0|^2 - |H_u^0|^2\right) \\
& - \frac{\lambda_S}{\sqrt{2}}(M_S + A_S)S_R(H_{dR}^0 H_{uR}^0 - H_{dI}^0 H_{uI}^0) - \frac{\lambda_S}{\sqrt{2}}(M_S - A_S)S_I(H_{dR}^0 H_{uI}^0 + H_{dI}^0 H_{uR}^0) \\
& - \frac{\lambda_T}{\sqrt{2}}(M_T + A_T)T_R(H_{dR}^0 H_{uR}^0 - H_{dI}^0 H_{uI}^0) - \frac{\lambda_T}{\sqrt{2}}(M_T - A_T)T_I(H_{dR}^0 H_{uI}^0 + H_{dI}^0 H_{uR}^0),
\end{aligned}
$$

with the Higgs scalar potential for the neutral components on line 1; a quartic contribution from the DG-adjoints on line 2; effective mass terms for the real and imaginary singlet a neutral triplet fields on lines 3 and 4, with $B_{S,T}$ soft-SUSY breaking bilinear terms; interaction terms from the superpotential on lines 5 and 6; D-term contributions on line 7 giving rise to masses for the adjoint scalars; and soft-SUSY breaking terms on lines 8 and 9 (these are often set to zero). All the parameters are chosen to be real, and thus CP-conserving. In this scenario, the imaginary components in the potential can be elimintated. While the choice has been made to neglect terms cubic in the singlet, an analysis involving a $\mathbf{S}^3$ term can be found in [67]. Compared to the MSSM potential, it can be seen that the D-flat direction $H_u = H_d$ is lifted by a supplementary quartic term (line 2). Reference [83] also discusses the different forms of the potential under various assumptions for the masses: in this work, it will be assumed that m_S and m_T are large, that the Majorana masses vanish, and that the Dirac masses are sub-TeV.

At the minimum of the scalar potential, the singlet and neutral triplet fields acquire VEVs:

$$
\langle S_R \rangle = v_S\,, \qquad\qquad \langle T_R \rangle = v_T\,. \qquad\qquad\qquad (1.2.148)
$$

Under the assumptions of a CP-neutral vacuum, and employing the abbreviations and relations stated in section 1.2.3.1, then the minimisation of the electroweak scalar potential yields the relations[11]

$$
\frac{M_Z^2}{2} = -\tilde{\mu}^2 + \frac{m_{H_d}^2 - m_{H_u}^2 t_\beta^2}{t_\beta^2 - 1} + \left[\frac{t_\beta^2 + 1}{t_\beta^2 - 1}\right](g_2 m_{2D} v_T - g_Y m_{1D} v_S), \quad (1.2.149)
$$

$$
m_A^2 \equiv \frac{2\tilde{B}_\mu}{s_{2\beta}} = m_{H_u}^2 + m_{H_d}^2 + 2\tilde{\mu}^2 + v^2 \frac{\left(\lambda_T^2 + \lambda_S^2\right)}{2}, \qquad\qquad (1.2.150)
$$

_____

[11]Equations (1.2.149, 1.2.150) can also be found in [67], where a mistype of $-c_\beta^2$ is noted in the last term of (3.10).

and

$$v_S = \frac{v^2}{2\tilde{m}_{SR}^2 + \lambda_S^2 v^2}\left[g_Y m_{DY} c_{2\beta} - \sqrt{2}\mu\lambda_S + \frac{\lambda_S}{\sqrt{2}}(M_S + A_S)s_{2\beta} - \lambda_S\lambda_T v_T\right] \quad (1.2.151)$$

$$v_T = \frac{-v^2}{2\tilde{m}_{TP}^2 + \lambda_T^2 v^2}\left[g_2 m_{D2} c_{2\beta} + \sqrt{2}\mu\lambda_T - \frac{\lambda_T}{\sqrt{2}}(M_T + A_T)s_{2\beta} + \lambda_S\lambda_T v_S\right] \quad (1.2.152)$$

where

$$\tilde{\mu} \equiv \mu + \frac{1}{\sqrt{2}}(\lambda_S v_S + \lambda_T v_T), \quad (1.2.153)$$

$$\tilde{B}_\mu \equiv B_\mu + \frac{\lambda_S}{\sqrt{2}}(M_S + A_S)v_S + \frac{\lambda_T}{\sqrt{2}}(M_T + A_T)v_T, \quad (1.2.154)$$

and

$$\tilde{m}_{SR}^2 = M_S^2 + m_S^2 + 4m_{DY}^2 + B_S, \quad (1.2.155)$$

$$\tilde{m}_{TP}^2 = M_T^2 + m_T^2 + 4m_{D2}^2 + B_T. \quad (1.2.156)$$

Masses of the CP even neutral scalars

The mass matrix for the CP even scalars in the basis (h, H, S_R, T_R^0) takes the form

$$\begin{pmatrix} M_Z^2 + \Delta_h s_{2\beta}^2 & \Delta_h s_{2\beta} c_{2\beta} & \Delta_{hs} & \Delta_{ht} \\ \Delta_h s_{2\beta} c_{2\beta} & M_A^2 - \Delta_h s_{2\beta}^2 & \Delta_{Hs} & \Delta_{Ht} \\ \Delta_{hs} & \Delta_{Hs} & \tilde{m}_{SR}^2 + \lambda_S^2\frac{v^2}{2} & \lambda_S\lambda_T\frac{v^2}{2} \\ \Delta_{ht} & \Delta_{Ht} & \lambda_S\lambda_T\frac{v^2}{2} & \tilde{m}_{TP}^2 + \lambda_T^2\frac{v^2}{2} \end{pmatrix}, \quad (1.2.157)$$

where the following have been defined:

$$\Delta_h = \frac{v^2}{2}(\lambda_S^2 + \lambda_T^2) - M_Z^2. \quad (1.2.158)$$

It is interesting to observe is that, when λ_S and λ_T take their $N = 2$, Δ_h vanishes (as it was observed in [78]): in this scenario, as will be discussed in detail in section 2, the off-diagonal contributions vanish and there is no mixing between the two CP-even neutral Higgs bosons, leaving the lightest of the two to behave like an SM-like Higgs. Off-diagonal elements describing the mixing of S_R and T_R^0 states with the light Higgs h are denoted by

$$\Delta_{hs} = -2\frac{v_S}{v}\tilde{m}_{SR}^2, \qquad \Delta_{ht} = -2\frac{v_T}{v}\tilde{m}_{TP}^2, \quad (1.2.159)$$

while

$$\Delta_{Hs} = g' m_{1D} v s_{2\beta} - \lambda_S \frac{v(A_s + M_s)}{\sqrt{2}} c_{2\beta}, \quad (1.2.160)$$

$$\Delta_{Ht} = -g m_{2D} v s_{2\beta} - \lambda_T \frac{v(A_T + M_T)}{\sqrt{2}} c_{2\beta}, \quad (1.2.161)$$

stand for the corresponding mixing with the heavier Higgs, H. However, the picture of the Higgs sector changes when an R-symmetry is implemented in the Lagrangian.

Superfield		Scalars	Fermions	$(SU(3), SU(2), U(1)_Y)$	R-charge
Extra MRSSM + unification chiral superfields					
R-Higgs/	$\mathbf{R_u}$	(R_u^+, R_u^0)	$(\tilde{R}_u^+, \tilde{R}_u^0)$	$(\mathbf{1}, \mathbf{2}, \text{-1/2})$	2
R-Higgsinos	$\mathbf{R_d}$	(R_d^0, R_d^-)	$(\tilde{R}_d^0, \tilde{R}_d^-)$	$(\mathbf{1}, \mathbf{2}, 1/2)$	2
Extra unification chiral superfields					
Fake electrons	$\hat{\mathbf{E}}(\times 2)$	$\hat{E}$	$\hat{\tilde{E}}$	$(\mathbf{1}, \mathbf{1}, 1)$	0
	$\hat{\mathbf{E}}'(\times 2)$	$\hat{E}$	$\hat{\tilde{E}}$	$(\mathbf{1}, \mathbf{1}, -1)$	0

Table 1.5: Additional field content in the MRSSM (first box) and CMDGSSM (first and second boxes) to prompt gauge-field unification in Dirac gaugino extended models.

1.2.4.3   R-symmetry preserving Dirac gaugino extensions

Another very popular realisation of Dirac gaugino models is the minimal R-symmetric supersymmetric standard model (MRSSM) [79, 115, 126, 127, 131], where one can extend the field content even further than table 1.4 to enable a Lagrangian that is fully invariant under R-symmetry. The R-charge assignments in the MRSSM differ slightly from those in table 1.4: in this model, an exact continuous R-symmetry is preserved by including some R-Higgs doublet superfields, $\mathbf{R}_u$ and $\mathbf{R}_d$, which couple to the Higgs bosons but do not obtain an expectation value. The Higgs-like leptons have the same gauge quantum numbers as the Higgs doublet fields, and allow the Higgs doublets H_u, H_d to have zero R-charge. The (s)quark and (s)lepton multiplets typically have an R-charge of 1, the R-Higgs an R-charge of 2, while the R-charges in the gauge sector and for the DG-adjoint fields do not change. In table 1.5 the reader will also see a set of unification fields: these can be added to the Dirac gaugino models to restore the property of gauge-coupling unification which is lost with the addidion of the new Dirac-adjoint fields to the MSSM field content. This additional content includes the two R-Higgs fields present in the MRSSM, as well as vector-like lepton fields. This MDGSSM-unified scenario was studied in [116, 125, 129], and is often referred to as the constrained minimal Dirac gaugino supersymmetric standard model (CMDGSSM).

In addition to the Yukawa interactions of the MSSM, the MRSSM allows the interactions[12]

$$
\begin{aligned}
W_{\text{Higgs}}^{\text{MRSSM}} \supset{} & \mu_u \, \mathbf{R_u} \cdot \mathbf{H_u} + \mu_d \, \mathbf{R_d} \cdot \mathbf{H_d} + \lambda_{S_u} \mathbf{S} \, \mathbf{R_u} \cdot \mathbf{H_u} + \lambda_{S_d} \mathbf{S} \, \mathbf{R_d} \cdot \mathbf{H_d} \\
& + 2\lambda_{T_u} \, \mathbf{R_u} \cdot \mathbf{TH_u} + 2\lambda_{T_d} \, \mathbf{R_d} \cdot \mathbf{TH_d} \, .
\end{aligned} \tag{1.2.162}
$$

One can see that, as required by R-symmetry, any couplings between two Higgs superfields; two R-Higgs superfields; multiple adjoint superfields, or scalar adjoint-Higgs superfields are forbidden. The most general MRSSM Lagrangian contains the standard soft terms of the MDGSSM in eq. 1.2.145 (except for the R-symmetry breaking Majorana mass terms), but also holomorphic scalar adjoint - Higgs couplings and new soft-mass terms for the Higgs-like leptons;

$$
\mathcal{L}_{\text{standard soft}}^{\text{MRSSM}} = m_{H_u}^2 |H_u|^2 + m_{H_d}^2 |H_d|^2 + B_\mu (H_u \cdot H_d + \text{h.c}) + m_{R_u}^2 |R_u|^2 + m_{R_d}^2 |R_d|^2
$$

$$
+ m_S^2 |S|^2 + 2m_T^2 \text{tr}(T^\dagger T) + \frac{1}{2} B_S (S^2 + h.c) + B_T (\text{tr}(TT) + h.c.) + B_O (\text{tr}(OO) + h.c.)
$$

---

[12]We note the discrepancy in coefficient 2 for the triplet coupling terms compared to [114, 115], which arises due to a difference in definition of T and the choice for the neutral components to take the same pre-factor as the singlet neutral components.

$$+ m_O^2 |O|^2 + A_S \left(S H_u \cdot H_d + h.c\right) + 2 A_T \left(H_d \cdot T H_u + h.c\right) + \frac{A_\kappa}{3} \left(S^3 + h.c.\right)$$
$$+ A_{ST} \left(Str(TT) + h.c\right) + A_{SO} \left(Str(OO) + h.c\right). \tag{1.2.163}$$

The trillinear terms A_i are usually neglected, but there is no symmetry that forbids them (even if they are expected to be small e.g. in gauge mediation models). A detailed description of the MRSSM Higgs sector is given in [115, 126, 127].

The expanded Higgs sector has the obvious impact of increasing the number electroweakinos in the MRSSM compared to the MDGSSM, giving rise to neutralinos (charginos) composed of 8 neutral (charged) Weyl fermions. The mass matrices are then subdivided according to R-charge, and the result is four physical 4-component neutralinos and two sets of two physical 4-component charginos: owing to R-symmetry conservation, these two sets of charginos do not mix with one another. As such, the MRSSM possesses a distinct and interesting phenomenology from the MDGSSM, however a study of the electroweakino sector is out of the scope of this text, and the reader is referred to [148, 149].

In the next section a preliminary study will be made into the behaviour of the Higgs sector in the MRSSM under the assumptions of high energy alignment, and the results will be compared to the findings of those within the context of the MDGSSM.

1.3 New physics and statistics

One important question, which branches across the paths of experimental and theoretical physics, concerns how it is possible to test for new theories. While hypotheses cannot be proved right, when one considers enough statistical distributions of data, it can become clear that some hypotheses are more correct than others. Colliders are ultimately counting experiments where the number of events, n, passing a given set of criteria will be predicted uniquely by different models. One example could be the number of particles in a given transverse momentum bin as the result of a proton-proton collision: probability theory quantifies and models the uncertainty in data concerned with the incidence of random events such as these.

When searching for new physics processes, one wants to count the number of events in a region where the new signal may be present. Given a number of predicted events within a given interval, under the assumption of a particular hypothesis, the observed number can be modelled as a probability distribution. Frequently in particle physics one needs to handle small event counts and account for the Possionian nature of the data. As such, for a discrete distribution of statistically independent events, *i.e.* in a sample space where the rate of the measurement range is known, occurrences can be modelled by a Poisson distribution,

$$\mathcal{P}(n|s+b) = \frac{(s+b)^n}{n!}e^{-(s+b)}\,, \tag{1.3.1}$$

for which the expectation value is

$$E(n) = s + b\,, \tag{1.3.2}$$

where n is the observed number of events, s is the expected number of signal events (or the *mean* number) and b is the predicted number of background events.

For large values of $s+b$ the Poisson distribution tends to a Gaussian distribution. It is possible to introduce a parameter μ which multiplies the number of events predicted for a given model *i.e.* such that $s + b \rightarrow \mu s + b$. This parameter is a rescaling of the signal prediction, deemed the signal strength, and putting a limit on μ from the data provides information about the exclusion of a model. If $\mu = 0$, it means that there is no signal present in the sample space and the model is therefore excluded. When $\mu = 1$, then the model is excluded at the given confidence limit that the value of μ is calculated at; the range $0 \leq \mu \leq 1$ indicates to what degree the model is excluded. If $\mu > 1$ then the amount of signal is greater than that predicted by the model and, in this instance, the model point cannot be excluded. For example, if a model predicted 50 events in a certain momentum bin, determining a value of $\mu = 1.5$ would mean that the model was viable unless it predicted 75 or more events there. The use of the signal strength as a measure of parameter space exclusion is explored in section 4.

Background predictions can also be modelled as Poisson distributions, with the background hypothesis H_0 corresponding to the case $s = 0$. Here, the events are counted in a region where little or no signal is expected. The background hypothesis implies that the observed data can be inferred from explanations of existing physics. Ideally, background predictions in searches for new processes are based on actual control sets of measured data, but frequently the data is not available and it is necessary to rely on Monte Carlo generated predictions.

Variables that can be ranked on a scale of more signal-like to more backgroundlike are called *test statistics*, and these permit the discrimination between proposed hypotheses. Test statistics are a function of the chosen observables, and can be simple

values like event count, or more complex quantities like likelihood functions. The distribution of the test statistic is known under the individual hypotheses: these should be predicted separately assuming (1) the background hypothesis ($= H_0$) is correct (typically taken as the Standard Model prediction), and (2) that the new hypothesis of signal and background ($= H_1$) is.

The plausibility of H can be identified by the likelihood ratio,

$$q = 2 \log \left[\frac{\mathcal{L}(n|\mu s + b)}{\mathcal{L}(n|b)} \right] \tag{1.3.3}$$

where

$$\mathcal{L}(n|s + b) = \prod_i \mathcal{P}(n_i|\mu s_i + b_i), \tag{1.3.4}$$

is the likelihood function of $\mu s + b$ (associated with the hypothesis H) given the outcome n. The observed number of events are measured in bins i: the probability for each bin is calculated, and the product of the probabilities for each bin gives the likelihood of the model to be true. For example, if $\mathcal{L}(n|s + b) > \mathcal{L}(n|s + b)$ then the data observed is more likely to have happened if the hypothesis were H_1 than if it were H_0. By nature of its definition, q increases as it becomes more signal-like, and decreases as it becomes more background-like.

How credible it is that the data is associated to one hypothesis or another can also be generated by a *confidence level* (CL). Specifically, the level of viability in a signal hypothesis is described by the CL_s procedure [150,151]. Such types of confidence level are determined from the expression

$$CL_H = \mathcal{P}_H(q \leq q_{\text{obs}}) = \int_{-\infty}^{q_{\text{obs}}} \frac{d\mathcal{P}(n|H)}{dq} dq, \tag{1.3.5}$$

where $d\mathcal{P}/dq$ is the probability distribution function (PDF) of the test-statistic q for $H = (b, s+b)$ experiments, denoting background and signal + background experiments respectively. When the value of CL_H is very close to 1, it indicates that the data shows poor agreement with the hypothesis, H, and favours the alternate theory.

It is not possible to write CL_s in this same way, as signal is always accompanied by background. Instead, the CL_s limit is defined by the normalisation of the confidence in the signal + background hypothesis to that in the background only,

$$CL_s \equiv \frac{CL_{s+b}}{CL_b} = \frac{\mathcal{P}_{s+b}(q_{s+b} \leq q_{obs})}{\mathcal{P}_b(q_b \leq q_{obs})}, \tag{1.3.6}$$

where

$$1 - CL_s \leq CL. \tag{1.3.7}$$

Interpreting CL_s statistics should be approached with caution: when $1 - CL_s \sim 0.95$, one cannot affirm that there is a 95% confidence level in the result, but rather that any point that lies in the excluded region where $1 - CL_s \geq 0.95$ has a probability less than 5% of having been falsely excluded. Exclusion limits in the squark v. gluino mass plane for both the MSSM and MDGSSM will be derived using the CL_s method in chapter 3.

There are many in depth resources out there on the subject of statistics in particle physics, to which the reader is referred to *e.g.* [152–155], among others, for more information.

2 – Higgs alignment from extended supersymmetry

2.1 Introduction

In the absence of signals of strongly-coupled particles at the LHC, it has become important to study the possibility of new particles that couple to Standard Model (SM) states only via couplings of electroweak strength. The bounds on such particles are still relatively weak but with much luminosity to arrive there is still a substantial parameter space to explore, and such theories perhaps represent now the best chance for discoveries. Among such theories, one that has received significant and now increasing attention is the Two Higgs Doublet Model (THDM); see e.g. [156–159] and references therein. It is important to ask the question: "does the Higgs sector just consist of one doublet?" because the answer will give profound information about nature. If there are indeed additional fundamental scalars that mix with the Higgs boson, then this dramatically worsens the Hierarchy problem and would necessitate a rethinking of our ideas of naturalness. On the other hand, such sectors naturally appear in the context of supersymmetry (SUSY) and it is conceivable that a second Higgs doublet could be the harbinger of a full SUSY theory.

However, the measurements of the Higgs boson's *couplings* already place significant constraints on the amount of mixing that it can suffer. It is for this reason that there has been much interest in the idea of *alignment* in the Higgs sector, i.e. that the mass eigenstates align with the vacuum expectation value, because in this case the couplings would be exactly SM-like.

To quantify this, consider two Higgs doublets Φ_1, Φ_2 which mix, and then rotate their neutral components as follows:

$$\begin{pmatrix} \mathrm{Re}(\Phi_1^0) \\ \mathrm{Re}(\Phi_2^0) \end{pmatrix} = \frac{1}{\sqrt{2}} \begin{pmatrix} c_\beta & -s_\beta \\ s_\beta & c_\beta \end{pmatrix} \begin{pmatrix} v + \tilde{h} \\ \tilde{H} \end{pmatrix} \qquad (2.1.1)$$

where the notation,

$$c_\beta \equiv \cos\beta, \qquad s_\beta \equiv \sin\beta, \qquad t_\beta \equiv \tan\beta,$$

shall be used throughout. In this basis, the mass matrix can be written as

$$\mathcal{M}_h^2 = \begin{pmatrix} Z_1 v^2 & Z_6 v^2 \\ Z_6 v^2 & m_A^2 + Z_5 v^2 \end{pmatrix}. \qquad (2.1.2)$$

Clearly the mass eigenstates are only $\tilde{h}, \tilde{H}$ if

$$Z_6 = 0,$$

and this is the condition for alignment, because the fields *align* with the electroweak vacuum expectation value. On the other hand, if $Z_6 \neq 0$, one must make a further rotation which is conventionally parameterised by an angle α as

$$\begin{pmatrix} \tilde{h} \\ \tilde{H} \end{pmatrix} = \begin{pmatrix} s_{\beta-\alpha} & c_{\beta-\alpha} \\ c_{\beta-\alpha} & -s_{\beta-\alpha} \end{pmatrix} \begin{pmatrix} h \\ H \end{pmatrix} \tag{2.1.3}$$

where now h, H are the two mass eigenstates. It shall be assumed throughout that h is the lightest eigenstate. In terms of the masses of the physical bosons $m_{h,H}$ this gives

$$Z_6 v^2 = s_{\beta-\alpha} c_{\beta-\alpha} (m_h^2 - m_H^2). \tag{2.1.4}$$

In both the type-I and type-II THDM, there is a Higgs eigenstate that couples to the up-type quarks, and this eigenstate shall be defined to be Φ_2. This means that the ratio of the h coupling to all up-type quarks compared to the SM Higgs' value is

$$\kappa_u = \frac{\cos\alpha}{\sin\beta},$$

while the ratio of the coupling to vector bosons to the SM value is also determined entirely by the mixing (neglecting loop effects from the rest of the extended Higgs sector):

$$\kappa_V = \sin(\beta - \alpha). \tag{2.1.5}$$

However, there is a combined ATLAS+CMS bound [160] on the ratio of these:

$$\lambda_{Vu} \equiv \frac{\kappa_V}{\kappa_u} = 1^{+0.13}_{-0.12} = \frac{1}{1 + \frac{1}{t_\beta t_{\beta-\alpha}}}. \tag{2.1.6}$$

This is enough to constrain

$$t_\beta t_{\beta-\alpha} \gtrsim 7.3 \Rightarrow |Z_6| \lesssim \left| -\frac{7.3 t_\beta}{53 + t_\beta^2} \frac{m_H^2 - m_h^2}{v^2} \right| \lesssim \left| -0.5 \frac{m_H^2 - m_h^2}{v^2} \right|, \tag{2.1.7}$$

where the latter bound comes from the value $t_\beta = 7.3$, and the bound is much more stringent for large or small t_β. For m_H somewhat above m_h this is a rather weak constraint, only becoming relevant when the two states approach degeneracy. However, in the type-II THDM, there is another constraint from the ratio of the ratio of the neutral Higgs coupling to all down-type quarks compared to its SM value

$$\kappa_d = -\frac{\sin\alpha}{\cos\beta}$$

via

$$\lambda_{du} \equiv \frac{\kappa_d}{\kappa_u} = 0.92 \pm 0.12 = \frac{1 - \frac{t_\beta}{t_{\beta-\alpha}}}{1 + \frac{1}{t_\beta t_{\beta-\alpha}}} \tag{2.1.8}$$

and, since from the previous constraint it is known that the denominator is nearly equal to one, one has

$$-0.04 \lesssim \frac{t_\beta}{t_{\beta-\alpha}} \lesssim 0.2 \tag{2.1.9}$$

which in turn implies $t_{\beta-\alpha} \gg t_\beta$ and so $s_{\beta-\alpha}c_{\beta-\alpha} \simeq \frac{1}{t_{\beta-\alpha}}$ and

$$-0.04\frac{m_H^2 - m_h^2}{t_\beta v^2} \lesssim Z_6 \lesssim 0.2\frac{m_H^2 - m_h^2}{t_\beta v^2}. \tag{2.1.10}$$

This leads to a sensible constraint; for example, for $m_H = 600$ GeV and $t_\beta = 5$ it leads to $Z_6 \lesssim 0.2$. So one sees that either the mass m_H should be taken to be large, in which case one has *decoupling*, or it is kept light in order to possibly detect it at the LHC, in which case one needs *alignment without decoupling*. However, this is non-trivial; as the LHC measurements become more precise, the constraints will tighten further, and it is in this spirit that it is important to consider models where the alignment is *natural* rather than *ad hoc*.

The problem for the different types of THDM is that alignment without decoupling is not generic when the masses are chosen – or equivalently quartic couplings – from the bottom up. Hence it is logical to derive the couplings of the THDM from some higher-energy theory and look for cases where alignment arises naturally. For example, [161, 162] proposed a model which leads to a natural alignment condition, based on additional bosonic symmetries. Here, on the other hand, it shall be shown how alignment arises automatically in a class of supersymmetric models, with the additional benefits of (greatly) increasing the naturalness of the model and being able to predict the scale of new superpartners. Moreover, it will be shown that quantum corrections actually *improve* the alignment!

The class of models that will be considered have a gauge sector which is enhanced to $\mathcal{N} = 2$ supersymmetry at a (potentially high) scale $M_{N=2}$. This fits into the framework of Dirac gaugino models that have been discussed in sec. 1.2.4.1. In particular, the idea of $\mathcal{N} = 2$ supersymmetry in the gauge sector only and the consequences for the Higgs sector were first explored in [78] and recently studied in [136, 139]; in general, though, this was either taken to be at the same scale as the other superpartners [136], or only a rough estimate of the main contribution of the chiral sector was included [78], while this work shall show that increasing $M_{N=2}$ improves alignment and increases naturalness!

Section 2.2 will describe the theory central to this work and how it leads to natural alignment at tree level. In section 2.3 the effect of radiative corrections will be outlined. In section 2.4 a precision study of the model will be performed using an EFT approach to obtain the parameters at low energies, the scale of new physics will be predicted from the value of the Higgs mass, and the consequences for alignment will be explored. In section 2.5 all of the relevant constraints on the model space will be considered, including the latest LHC search for decays to τ pairs, $B \to s\gamma$ searches and electroweak precision constraints, and it will be shown how this affects the model. In the appendix all of the one-loop threshold corrections will be given for the model at the scale of supersymmetry. Finally, in section 2.6 the case of the MRSSM will be briefly considered.

2.2 Alignment from extended supersymmety

2.2.1 The Higgs sector of Dirac gaugino models

2.2.1.1 The minimal model

As described in section 1.2.4.1, to endow gauginos with a Dirac mass one needs, at a minimum, to add chiral fermions in the adjoint representation of each gauge group,

which means adding adjoint chiral superfields: a singlet $\mathbf{S}$, an $SU(2)$ triplet $\mathbf{T}$, and an $SU(3)$ octet $\mathbf{O}$. However, one can then choose the superpotential according to the symmetries that one wants to preserve. One motivation for the adjoint fields is as the additional degrees of freedom from an $\mathcal{N} = 2$ supersymmetric gauge multiplet, and then the H_u, H_d fields become an $\mathcal{N} = 2$ hypermultiplet; in this work it shall be assumed that $\mathcal{N} = 2$ supersymmetry *in the gauge/Higgs sector only* is valid above some scale $M_{N=2}$. In this case, it is immediately possible to write down the superpotential (as in eq. (1.2.142))

$$W_{\mathrm{Higgs}} = \mu \, \mathbf{H_u} \cdot \mathbf{H_d} + \lambda_S \mathbf{S} \, \mathbf{H_u} \cdot \mathbf{H_d} + 2\lambda_T \, \mathbf{H_d} \cdot \mathbf{T} \mathbf{H_u} \qquad (2.2.1)$$

which contains the only interactions compatible with $\mathcal{N} = 2$ SUSY and includes a central role for the R-symmetry. Indeed, under the R-symmetry of the $\mathcal{N} = 1$ theory the adjoint scalars must have zero charge, and this prevents couplings of the form S^2, S^3 etc which would otherwise be permitted by the gauge symmetry. It was explained in section 1.2.1.6 that all interactions in an $\mathcal{N} = 2$ theory are gauge interactions. The condition of $\mathcal{N} = 2$ supersymmetry then imposes

$$\lambda_S = \frac{1}{\sqrt{2}}g_Y, \qquad \lambda_T = \frac{1}{\sqrt{2}}g_2 \qquad (2.2.2)$$

(where g_Y, g_2 are the hypercharge and $SU(2)$ gauge couplings) *at the scale $M_{N=2}$*, which shall in general be taken to be greater than the $\mathcal{N} = 1$ SUSY scale. The relevant soft and supersoft terms are given in eqs. (1.2.145), (1.2.146). For simplicity, the choice $A_\kappa = A_{ST} = A_{SO} = 0$ (eq. (1.2.145)) will also be implemented in the following, which is well justified in gauge mediation models [129], but it is not expected that these parameters would affect the bounds deduced in any significant way.

One must also add supersymmetry-breaking terms, and these do not necessarily need to respect the same symmetries as supersymmetric terms. The most general choice that one can make for the Higgs and adjoint scalar sector for the *standard* soft terms is the same as in eq. 1.2.145.

Since the interest here is in *Dirac* gaugino masses and their attractive theoretical and phenomenological properties, one should expect that the terms that violate R-symmetry should be small: this includes the Majorana gaugino masses; A_S, A_T; but also B_μ. However, it is required that the R-symmetry *is* broken at some scale, since it is believed that global symmetries cannot be exact; but also, in this model, the Higgs must carry R-charge and so the absence of an R-axion requires it. Indeed, the R-axion is essentially the Higgs pseudoscalar, whose mass is controlled by the B_μ term; therefore, as in earlier works, it is taken to have a small but non-zero value. One can also take motivation from models of gauge mediation of supersymmetry [82, 129], where the trilinears are all small, and these shall mostly be neglected in the following (although they do not significantly affect the analysis).

On the other hand, in gauge-mediated models the adjoint scalars are typically the heaviest states. Taking large m_S, m_T, m_O then motivates integrating them out of the light spectrum; but interestingly, since B_μ should remain small due to the approximate R-symmetry, if the Higgs masses were to be tuned such that only one remains light, then one would have very large $\tan\beta$, and would have trouble obtaining the correct Yukawa couplings for the down-type quarks and leptons – this implies that a second Higgs should be taken to be somewhat light, and motivates studying the two-Higgs doublet limit of the model.

As mentioned in section 1.2.4.3, If one wishes to naturally restore gauge coupling unification, additional vector-like lepton fields as shown in table 1.5 can be added.

Since they are vector-like, they could also form hypermultiplets of $\mathcal{N} = 2$ at $M_{N=2}$, but their inclusion will little change the discussion in this paper so for sake of generality they shall be neglected.

2.2.1.2   The MRSSM

The other Dirac gaugino extension investigated in this work is the MRSSM, as detailed in sec. 1.2.4.3. For convenience, the Higgs superpotential of eq. (1.2.162) is restated here:

$$
\begin{aligned}
W_{\text{Higgs}}^{\text{MRSSM}} \;=\;& \mu_u\,\mathbf{R_u}\cdot\mathbf{H_u} + \mu_d\,\mathbf{R_d}\cdot\mathbf{H_d} + \lambda_{S_u}\mathbf{S}\,\mathbf{R_u}\cdot\mathbf{H_u} + \lambda_{S_d}\mathbf{S}\,\mathbf{R_d}\cdot\mathbf{H_d} \\
&+ 2\lambda_{T_u}\,\mathbf{R_u}\cdot\mathbf{TH_u} + 2\lambda_{T_d}\,\mathbf{R_d}\cdot\mathbf{TH_d}\,.
\end{aligned} \tag{2.2.3}
$$

If $\mathcal{N} = 2$ supersymmetry is then imposed at some scale, one can treat (R_u, H_u) and (R_d, H_d) as hypermultiplets and then one would have

$$
\lambda_{S_u} = \frac{g_Y}{\sqrt{2}}, \qquad \lambda_{S_d} = -\frac{g_Y}{\sqrt{2}}, \qquad \lambda_{T_u} = \lambda_{T_d} = \frac{g_2}{\sqrt{2}}, \tag{2.2.4}
$$

where the difference in sign is explained by the different charges of the hypermultiplets. R-symmetry then limits the possible soft-supersymmetry breaking terms to consist of only the supersoft operator, squark/slepton masses and the standard soft terms of eq. 1.2.163

2.2.2   Two-Higgs doublet model limit

The Higgs sectors of the models in the previous subsection have been comprehensively studied. However, here it is desirable to map them onto the two Higgs doublet model once the adjoint scalars have been integrated out. The standard parametrisation of the Two-Higgs doublet model is

$$
\begin{aligned}
V_{EW} \;=\;& m_{11}^2\Phi_1^\dagger\Phi_1 + m_{22}^2\Phi_2^\dagger\Phi_2 - [m_{12}^2\Phi_1^\dagger\Phi_2 + \text{h.c}] + \frac{1}{2}\lambda_1(\Phi_1^\dagger\Phi_1)^2 + \frac{1}{2}\lambda_2(\Phi_2^\dagger\Phi_2)^2 \\
&+ \lambda_3(\Phi_1^\dagger\Phi_1)(\Phi_2^\dagger\Phi_2) + \lambda_4(\Phi_1^\dagger\Phi_2)(\Phi_2^\dagger\Phi_1) \\
&+ \left[\frac{1}{2}\lambda_5(\Phi_1^\dagger\Phi_2)^2 + [\lambda_6(\Phi_1^\dagger\Phi_1) + \lambda_7(\Phi_2^\dagger\Phi_2)]\Phi_1^\dagger\Phi_2 + \text{h.c}\right],
\end{aligned} \tag{2.2.5}
$$

To map our supersymmetric model onto this, the following identification can be made,

$$
\Phi_2 = H_u, \qquad \Phi_1^i = -\epsilon_{ij}(H_d^j)^* \leftrightarrow \begin{pmatrix} H_d^0 \\ H_d^- \end{pmatrix} = \begin{pmatrix} \Phi_1^0 \\ -(\Phi_1^+)^* \end{pmatrix}, \tag{2.2.6}
$$

from which the potential can be written down:

$$
\begin{aligned}
V_{EW} =\;& \left(m_{H_d}^2 + \mu^2\right)|H_d|^2 + \left(m_{H_u}^2 + \mu^2\right)|H_u|^2 + B_\mu[H_u\cdot H_d + \text{h.c}] \\
&+ \frac{1}{2}\lambda_1\left(|H_d|^2\right)^2 + \frac{1}{2}\lambda_2\left(|H_u|^2\right)^2 + \lambda_3|H_u|^2|H_d|^2 + \lambda_4|H_u\cdot H_d|^2
\end{aligned} \tag{2.2.7}
$$

with

$$
m_{11}^2 \;=\; m_{H_d}^2 + \mu^2, \qquad m_{22}^2 = m_{H_u}^2 + \mu^2, \qquad m_{12}^2 = B_\mu. \tag{2.2.8}
$$

The parameters λ_i were given at tree-level and with some loop corrections in [83,105] in the limit of neglecting μ and m_{DY}, m_{D2}. However, when the adjoint scalars are integrated out and these terms are retained, there are corrections due to the presence

of trilinear couplings; setting the parameters A_S, A_T to zero, one finds for the minimal model:

$$\lambda_1 = \frac{1}{4}(g_2^2 + g_Y^2) - \frac{\left(g_Y m_{DY} - \sqrt{2}\lambda_S\mu\right)^2}{m_{SR}^2} - \frac{\left(gm_{D2} + \sqrt{2}\lambda_T\mu\right)^2}{m_{TP}^2}$$

$$\lambda_2 = \frac{1}{4}(g_2^2 + g_Y^2) - \frac{\left(g_Y m_{DY} + \sqrt{2}\lambda_S\mu\right)^2}{m_{SR}^2} - \frac{\left(gm_{D2} - \sqrt{2}\lambda_T\mu\right)^2}{m_{TP}^2}$$

$$\lambda_3 = \frac{1}{4}(g_2^2 - g_Y^2) + 2\lambda_T^2 + \frac{g_Y^2 m_{DY}^2 - 2\lambda_S^2\mu^2}{m_{SR}^2} - \frac{g^2 m_{D2}^2 - 2\lambda_T^2\mu^2}{m_{TP}^2}$$

$$\lambda_4 = -\frac{1}{2}g_2^2 + \lambda_S^2 - \lambda_T^2 + \frac{2g_2^2 m_{D2}^2 - 4\lambda_T^2\mu^2}{m_{TP}^2},$$

$$\lambda_5 = \lambda_6 = \lambda_7 = 0. \tag{2.2.9}$$

Here the following definitions have been used:

$$m_{SR}^2 \equiv m_S^2 + B_S + 4m_{DY}^2, \qquad m_{TP}^2 \equiv m_T^2 + B_T + 4m_{D2}^2. \tag{2.2.10}$$

In fact, the terms suppressed by m_{SR}, m_{TP} all have the effect of suppressing the Higgs quartic coupling: in the limit of large Dirac gaugino masses so that m_S^2, B_S, m_T^2, B_T can be neglected, one finds

$$\lambda_1, \lambda_2 \to 0, \qquad \lambda_3 \to 2\lambda_T^2, \qquad \lambda_4 \to \lambda_S^2 - \lambda_T^2. \tag{2.2.11}$$

This simply corresponds to the well-known fact (see e.g. [77]) that the adjoint scalars eliminate the D-term potential of the Higgs, because they couple via the D-term; writing ϕ_i for (anti)fundamental scalars and Σ for adjoint scalars, one has

$$\mathcal{L} \supset \sqrt{2}m_{D\Sigma}\Sigma^a D^a + gD^a\phi_i^* T^a\phi_i \to V_D = \frac{1}{2}\left(\sqrt{2}m_{D\Sigma}\Sigma^a + g\phi_i^* T^a\phi_i\right)^2 \tag{2.2.12}$$

where T^a are the generators of the gauge group with coupling g, and one sees that the above will always be zero when Σ is integrated out.

For the MRSSM, for simplicity again neglecting A_S, A_T – for completeness the full corrections are given in appendix B.4.1 – one finds

$$\lambda_1^{\text{MRSSM}} = \frac{1}{4}(g_2^2 + g_Y^2) - \frac{(g_Y m_{DY} - \sqrt{2}\lambda_{S_d}\mu_d)^2}{m_{SR}^2} - \frac{(g_2 m_{D2} + \sqrt{2}\lambda_{T_d}\mu_d)^2}{m_{TP}^2}$$

$$\lambda_2^{\text{MRSSM}} = \frac{1}{4}(g_2^2 + g_Y^2) - \frac{(g_Y m_{DY} + \sqrt{2}\lambda_{S_u}\mu_u)^2}{m_{SR}^2} - \frac{(g_2 m_{D2} + \sqrt{2}\lambda_{T_u}\mu_u)^2}{m_{TP}^2}$$

$$\lambda_3^{\text{MRSSM}} = \frac{1}{4}(g_2^2 - g_Y^2)$$

$$+ \frac{(g_Y m_{DY} - \sqrt{2}\lambda_{S_d}\mu_d)(g_Y m_{DY} + \sqrt{2}\lambda_{S_u}\mu_u)}{m_{SR}^2} - \frac{(g_2 m_{D2} + \sqrt{2}\lambda_{T_d}\mu_d)(g_2 m_{D2} + \sqrt{2}\lambda_{T_u}\mu_u)}{m_{TP}^2}$$

$$\lambda_4^{\text{MRSSM}} = -\frac{1}{2}g_2^2 + 2\frac{(g_2 m_{D2} + \sqrt{2}\lambda_{T_d}\mu_d)(g_2 m_{D2} + \sqrt{2}\lambda_{T_u}\mu_u)}{m_{TP}^2}$$

$$\lambda_5^{\text{MRSSM}} = \lambda_6^{\text{MRSSM}} = \lambda_7^{\text{MRSSM}} = 0. \tag{2.2.13}$$

In this case, the supersoft limit is even worse, because in that limit *all* of the λ_i vanish. However, even with the additions of λ_S and λ_T in the minimal model, the potential is not stable in this limit – for example if H_d or H_u are set to zero the quartic terms vanish – and so one would require loop corrections to prevent runaway vacua. An

investigation of whether this is even viable is beyond the scope of this paper: instead, since one does not want to substantially reduce the Higgs quartic coupling at low scales instead it shall be considered that $|m_{DY}| \ll m_S, |m_{D2}| \ll m_T$. As is also well known (see e.g. [67, 105]) and shall later be discussed, this limit is also imposed by electroweak precision tests. In this limit one has instead at tree-level

$$\lambda_1, \lambda_2 \to \frac{1}{4}(g_2^2 + g_Y^2), \qquad \lambda_3 \to \frac{1}{4}(g_2^2 - g_Y^2) + 2\lambda_T^2, \qquad \lambda_4 \to -\frac{1}{2}g_Y^2 + \lambda_S^2 - \lambda_T^2,$$
(2.2.14)

and $\lambda_i^{\mathrm{MRSSM}} \to \lambda_i^{MSSM}$:

$$\lambda_i^{\mathrm{MSSM}}, \lambda_2^{\mathrm{MSSM}} \to \frac{1}{4}(g_2^2 + g_Y^2), \qquad \lambda_3^{\mathrm{MSSM}} \to \frac{1}{4}(g_2^2 - g_Y^2), \qquad \lambda_4^{\mathrm{MSSM}} \to -\frac{1}{2}g_Y^2.$$
(2.2.15)

Hence for the rest of the paper the low-energy theory is considered to be a type-II two Higgs doublet model with an additional (Dirac) bino and wino (the gluino must remain heavy due to LHC constraints – currently of the order of 2 TeV). The boundary conditions shall be fixed at high energies and some interesting conclusions.

2.2.3   Tree-level alignment

In [78, 136] the Higgs sector of Dirac gaugino models was investigated in the limit that the couplings λ_S, λ_T took their $\mathcal{N} = 2$ supersymmetric values at the low energy scale. However, they also pointed out that alignment in the Higgs sector would be broken by quantum corrections to the $(2, 2)$ element of the Higgs mass matrix. In this section the potential will be considered just at tree-level, with section 2.4 considering loop corrections, contrasting the results here with theirs.

To begin with, the mass-matrices for the CP-even neutral scalars in the two-Higgs doublet model can be parametrised in the *alignment basis* where

$$\begin{pmatrix} \mathrm{Re}(\Phi_1) \\ \mathrm{Re}(\Phi_2) \end{pmatrix} = \frac{1}{\sqrt{2}} \begin{pmatrix} c_\beta & -s_\beta \\ s_\beta & c_\beta \end{pmatrix} \begin{pmatrix} v + h \\ H \end{pmatrix}$$
(2.2.16)

is (see e.g. [156–158])

$$\mathcal{M}_h^2 = \begin{pmatrix} Z_1 v^2 & Z_6 v^2 \\ Z_6 v^2 & m_A^2 + Z_5 v^2 \end{pmatrix},$$
(2.2.17)

where, using $\lambda_{345} \equiv \lambda_3 + \lambda_4 + \lambda_5$ one has

$$Z_1 \equiv \lambda_1 c_\beta^4 + \lambda_2 s_\beta^4 + \frac{1}{2}\lambda_{345} s_{2\beta}^2, \qquad Z_5 \equiv \frac{1}{4} s_{2\beta}^2 [\lambda_1 + \lambda_2 - 2\lambda_{345}] + \lambda_5$$

$$Z_6 \equiv -\frac{1}{2} s_{2\beta} [\lambda_1 c_\beta^2 - \lambda_2 s_\beta^2 - \lambda_{345} c_{2\beta}].$$
(2.2.18)

The parameter m_A is the pseudoscalar mass, given by

$$m_A^2 = -\frac{m_{12}^2}{s_\beta c_\beta} - \lambda_5 v^2,$$
(2.2.19)

while the charged Higgs mass is

$$m_{H^+}^2 = \frac{1}{2}(\lambda_5 - \lambda_4)v^2 + m_A^2.$$
(2.2.20)

The neutral Higgs masses are

$$m_{H,h}^2 = \frac{1}{2}\left[m_A^2 + (Z_1 + Z_5)v^2 \pm \sqrt{\left(m_A^2 + (Z_5 - Z_1)v^2\right)^2 + 4Z_6^2 v^4} \right]. \quad (2.2.21)$$

For the *minimal* model one has

$$Z_1 = \frac{1}{4}(g_2^2 + g_Y^2)(1 - s_{2\beta}^2) + \frac{s_{2\beta}^2}{2}(\lambda_S^2 + \lambda_T^2) \qquad (2.2.22)$$

$$Z_5 = \frac{1}{2}s_{2\beta}^2\left[\frac{(g_2^2 + g_Y^2)}{2} - (\lambda_S^2 + \lambda_T^2)\right] \qquad (2.2.23)$$

$$Z_6 = -\frac{1}{2}s_{2\beta}c_{2\beta}\left[\frac{(g_2^2 + g_Y^2)}{2} - (\lambda_S^2 + \lambda_T^2)\right] \qquad (2.2.24)$$

and

$$m_{H,h}^2 = \frac{1}{2}\left[m_A^2 + \frac{v^2}{4}(g_2^2 + g_Y^2) \pm v^2\left[\left(\frac{1}{4}(g_2^2 + g_Y^2)(2s_{2\beta}^2 - 1) - s_{2\beta}^2(\lambda_S^2 + \lambda_T^2) + \frac{m_A^2}{v^2}\right)^2\right.\right.$$
$$\left.\left. + s_{2\beta}^2 c_{2\beta}^2\left(\frac{(g_2^2 + g_Y^2)}{2} - (\lambda_S^2 + \lambda_T^2)\right)^2\right]^{1/2}\right]. \qquad (2.2.25)$$

The Higgs mass matrix is diagonalised to find the physical Higgs masses and the mixing angle α. From the identification of the 2HDM parameters in (2.2.8) one obtains

$$s_{2(\beta-\alpha)} = \frac{v^2}{m_H^2 - m_h^2}s_{2\beta}c_{2\beta}\left[\frac{(g_2^2 + g_Y^2)}{2} - (\lambda_S^2 + \lambda_T^2)\right],$$

$$c_{\beta-\alpha} = \frac{s_{2\beta}c_{2\beta}\,v^2\left(g_Y^2 + g_2^2 - 2(\lambda_S^2 + \lambda_T^2)\right)}{4\sqrt{\left(m_H^2 - m_h^2\right)\left(m_H^2 - \frac{v^2}{2}\left\{(g_Y^2 + g_2^2)\frac{c_{2\beta}^2}{2} + (\lambda_S^2 + \lambda_T^2)s_{2\beta}^2\right\}\right)}}. \qquad (2.2.26)$$

The condition for alignment is the diagonalisation of $\mathcal{M}^2$ i.e. $Z_6 \to 0$. From equation (2.2.24) one sees this amounts at tree-level to having

$$\lambda_S^2 + \lambda_T^2 = \frac{g_Y^2 + g_2^2}{2}. \qquad (2.2.27)$$

In other words, when the couplings respect their $\mathcal{N} = 2$ values, the Higgs doublets are *automatically aligned*! From equations (2.2.26, 2.2.27) one finds that in this alignment limit, $c_{\beta-\alpha} \to 0$ and $s_{\beta-\alpha} \to 1$, therefore the heavy CP-even neutral scalar doest not take part in electroweak symmetry breaking while h is a Standard Model Higgs-like boson. The tree-level masses of the two neutral CP-even Higgs bosons are

$$m_h^{N=2} = m_Z, \qquad m_H^{N=2} = m_A, \qquad (2.2.28)$$

while the charged Higgs boson mass is given by

$$m_{H^\pm}^{2,N=2} = m_A^2 + 3m_W^2 - m_Z^2, \qquad (2.2.29)$$

correcting the expression given in [78, 136]. Hence, at tree-level, the model exhibits alignment *for any value of* $\tan\beta$ and the tree-level Higgs mass is independent of $\tan\beta$ (which was already noted in [78, 136]).

On the other hand, for the MRSSM there is no automatic alignment, because the Higgs sector at tree-level closely resembles that of the MSSM once the adjoint scalars and R-Higgs fields are decoupled; this can be seen just by putting $\lambda_S = \lambda_T = 0$ in the above equations. In the following the main focus will therefore be on the minimal Dirac gaugino model (with some further comments about the MRSSM).

2.3 Radiative corrections to alignment

2.3.1 Loop level alignment from $\mathcal{N} = 2$.

To preserve $\mathcal{N} = 2$ supersymmetry, one requires that the relations in eq. (2.2.2) hold at all loop orders. How the Yukawa couplings vary at loop level will depend on the expressions for the anomalous dimensions of the fields involved in the interaction (see appendix A). In other words, if the anomalous dimensions vanish or cancel, then the Yukawa coupling will not run and its tree level value will be unchanged (up to that order). To understand how $\mathcal{N} = 2$ plays a role at loop level, it is convenient to look at the runnings of $\lambda_{S,T}$, defined through the beta functions $\beta_{\lambda_{S,T}}$, at one-loop:

$$\beta_{\lambda_{S,T}}^{(1)} = \frac{\lambda_{S,T}}{16\pi^2}\left(\gamma_{S,T}^{(1)} + \gamma_{H_u}^{(1)} + \gamma_{H_d}^{(1)}\right). \tag{2.3.1}$$

The anomalous dimensions for the $\mathbf{H_{u,d}}$ hypermultiplets can be shown to vanish altogether (in a strictly vector-like theory): using (A.0.3) and looking at the anomalous dimension for $\mathbf{H_u}$,

$$
\begin{aligned}
\gamma_{\mathbf{H_u}}^{(1)\mathbf{H_u}} &= \frac{1}{2}Y_{\mathbf{H_u S\bar{H}_d}}Y^{\mathbf{H_u S\bar{H}_d}} + \frac{1}{2}Y_{\mathbf{H_u \bar{H}_d S}}Y^{\mathbf{H_u \bar{H}_d S}} \\
&\quad + \frac{1}{2}Y_{\mathbf{H_u T\bar{H}_d}}Y^{\mathbf{H_u T\bar{H}_d}} + \frac{1}{2}Y_{\mathbf{H_u \bar{H}_d T}}Y^{\mathbf{H_u \bar{H}_d T}} - 2g_Y^2 C_1(\mathbf{H_u}) - 2g_2^2 C_2(\mathbf{H_u}) \\
&= |\lambda_S|^2 + 3|\lambda_T|^2 - 2g_Y^2\left(\frac{1}{4}\right) - 2g_2^2\left(\frac{3}{4}\right) \\
&= \frac{1}{2}g_Y^2 + \frac{3}{2}g_2^2 - \frac{1}{2}g_Y^2 - \frac{3}{2}g_2^2 \\
&= 0!
\end{aligned}
\tag{2.3.2}
$$

Equivalently then, if $\gamma_{\mathbf{H_u}}^{(1)\mathbf{H_u}} = 0$, owing to the R-symmetry relating the scalars in the hypermultiplet, $R[\mathbf{H_u}] = R[\bar{\mathbf{H}}_{\mathbf{d}}]$, then $\gamma_{\bar{\mathbf{H}}_{\mathbf{d}}}^{(1)\bar{\mathbf{H}}_{\mathbf{d}}} = 0$ also. In a purely $\mathcal{N} = 2$ theory, the chiral matter fields would also sit in hypermultiplets and their anomalous dimensions would also vanish.

The classical definition of an anomalous dimension is given by

$$\gamma_\Phi^{(1)} = -\frac{1}{2}\frac{d\log Z_\Phi}{d\log\mu}, \tag{2.3.3}$$

where Z_Φ is the wavefunction renormalisation of the field Φ and can be read off as the coefficient of the kinetic term for the field. As the adjoint-fields, $\mathbf{S}, \mathbf{T}$, are related to the gauge fields within the $\mathcal{N} = 2$ vector multiplet, their anomalous dimensions are the same as those of the corresponding gauge fields. The kinetic terms for the latter are given by (1.2.41), which means that

$$\gamma_{S,T}^{(1)} = -\frac{1}{2}\frac{d\log Z_{S,T}}{d\log\mu} = -\frac{1}{2}\frac{d\log\frac{1}{2}g_{Y,2}^{-2}}{d\log\mu} = \frac{1}{g_{Y,2}}\frac{dg_{Y,2}}{d\log\mu}, \tag{2.3.4}$$

up to a constant factor. Therefore at one-loop order, putting this all together,

$$\frac{d\lambda_{S,T}}{\lambda_{S,T}} \equiv \beta_{\lambda_{S,T}}d\log\mu = \left[\frac{1}{16\pi^2}\gamma_{S,T}^{(1)S,T} + \frac{1}{16\pi^2}\gamma_{\mathbf{H_u}}^{(1)\mathbf{H_u}} + \frac{1}{16\pi^2}\gamma_{\bar{\mathbf{H}}_{\mathbf{d}}}^{(1)\bar{\mathbf{H}}_{\mathbf{d}}}\right]d\log\mu = \frac{dg_{Y,2}}{g_{Y,2}}, \tag{2.3.5}$$

with

$$\beta_\Phi = \frac{1}{16\pi^2}\beta_\Phi^{(1)}, \tag{2.3.6}$$

which means that the $\mathcal{N} = 2$ conditions hold for all energies and the Higgs sector is always aligned: this is expected, as in an $\mathcal{N} = 2$ theory, the interaction terms are purely governed by the gauge couplings.

However, in reality, the presence of chiral fields breaks the $\mathcal{N} = 2$ supersymmetry, and there must be a mass splitting between the fermionic and bosonic partners in the superfields, leading to the deviation of the Yukawa couplings from their $\mathcal{N} = 2$ values and the consequent re-emergence of energy dependent couplings. This is not to mention also that, while $\mathcal{N} = 2$ can be preserved in the electroweak sector, there is no similar symmetry between the strong gauge coupling and an octet Yukawa, which means that the running couplings will always deviate from the $\mathcal{N} = 2$ relations when the fields involved are charged under $SU(3)$.

As mentioned above, the perfect alignment obtained at tree-level is not preserved when the radiative corrections to the scalar effective potential are taken into account. In addition to the corrections already present in the MSSM, there are two new sources for this misalignment. The first is due to the appearance of chiral fields, quarks and leptons, at a scale $M_{N=2}$. This scale can be identified with the fundamental scale of the theory, or an intermediate scale where a partial breaking $N = 2 \to N = 1$ is achieved (while an explicit realisation of this partial supersymmetry breaking remains unknown for a chiral theory, there is not a no-go theorem showing it to be impossible). The second large contribution comes from the mass splitting between fermonic and bosonic components of all of the superfields, i.e. coming from the $\mathcal{N} = 2 \to \mathcal{N} = 0$ (or $\mathcal{N} = 1 \to \mathcal{N} = 0$) breaking. After a quick demonstration of how $\mathcal{N} = 2$ SUSY works to achieve alignment, both misalignment contributions will be discussed in turn.

2.3.2 Misalignment from $\mathcal{N} = 2 \to \mathcal{N} = 1$ (chiral matter)

Owing to the presence of MSSM chiral matter at the scale $\mathcal{N} = 2$ scale, when the couplings are run from $M_{N=2}$ to the scale of the $\mathcal{N} = 1$ supersymmetric superparticles (denoted M_{SUSY}) there will be a splitting induced of λ_S and λ_T relative to the $\mathcal{N} = 2$ SUSY relations. This in turn will lead to misalignment at M_{SUSY} via a non-zero Z_6:

$$Z_6(M_{\text{SUSY}}) = \frac{1}{4} s_{2\beta} c_{2\beta} \left[(2\lambda_S^2 - g_Y^2) + (2\lambda_T^2 - g_2^2) \right] + \text{threshold corrections}. \quad (2.3.7)$$

To obtain an estimate of the magnitude of this splitting, one can integrate over the difference in the beta functions for λ_S and λ_T,

$$\frac{\partial}{\partial \log \mu} \left(2\lambda_{S,T}^2 - g_{Y,2}^2 \right) = \mu^2 \left(4\lambda_{S,T} \frac{\partial \lambda_{S,T}}{\partial \mu^2} - 2g_{Y,2} \frac{\partial g_{Y,2}}{\partial \mu^2} \right)$$
$$= 4\lambda_{S,T} \beta_{\lambda_{S,T}} - 2g_{Y,2} \beta_{g_{Y,2}}$$

giving

$$\int_{M_{\text{SUSY}}}^{M_{N=2}} \partial \left(2\lambda_{S,T}^2 - g_{Y,2}^2 \right) \simeq \left(4\lambda_{S,T} \beta_{\lambda_{S,T}} - 2g_{Y,2} \beta_{g_{Y,2}} \right) \log \left(\frac{M_{N=2}}{M_{\text{SUSY}}} \right).$$

The one-loop beta functions for the trilinear and gauge couplings in the MDGSSM are given in Appendix B.3.2. To leading order, one finds

$$\left[2\lambda_S^2 - g_Y^2 \right]_{M_{\text{SUSY}}} \simeq -\frac{2g_Y^2}{16\pi^2} \left[3|y_t|^2 + 3|y_b|^2 + |y_\tau|^2 - 10g_Y^2 \right] \log \left(\frac{M_{N=2}}{M_{\text{SUSY}}} \right), (2.3.8)$$

$$\left[2\lambda_T^2 - g_2^2 \right]_{M_{\text{SUSY}}} \simeq -\frac{2g_2^2}{16\pi^2} \left[3|y_t|^2 + 3|y_b|^2 + |y_\tau|^2 - 6g_2^2 \right] \log \left(\frac{M_{N=2}}{M_{\text{SUSY}}} \right). (2.3.9)$$

These equations are only useful for small $M_{N=2}/M_{\text{SUSY}}$, because for large ratios the top Yukawa coupling can change by a factor of two or more, but it gives an indication of the amount of misalignment: even for $\log\left(\frac{M_{N=2}}{M_{\text{SUSY}}}\right) \sim \mathcal{O}(10)$ one finds

$$Z_6(M_{\text{SUSY}}) \sim -\mathcal{O}(0.1)\frac{t_\beta}{1+t_\beta^2}\left(\frac{t_\beta^2-1}{t_\beta^2+1}\right)\left(\frac{\log M_{N=2}/M_{\text{SUSY}}}{10}\right). \qquad (2.3.10)$$

This is a small deviation from alignment indeed, and very encouraging. This shall be investigated quantitatively in section 2.4, and it will be shown that due to the diminishing Yukawa couplings at high energies[1], the actual splitting is smaller than this naive estimate. As an aside, a similar conclusion is reached if the Dirac Gaugino theory is extended by including additional fields to the Minimal Dirac Gaugino Supersymmetric standard Model (MDGSSM) to restore gauge coupling unification.

2.3.3   Misalignment from $N = 1 \to N = 0$ (mass splitting)

More significantly, there is the potential misalignment induced from the threshold corrections at M_{SUSY} and then the running between M_{SUSY} and the scale of the THDM. Taking the matching scale (as is commonly done) to be the electroweak vev v, these can both be approximated at one loop by corrections to the $\delta\lambda_i$. Then, in the approximation that the singlet and triplet scalars are degenerate with mass M_Σ; the stop squarks are degenerate with mass $m_{\tilde{t}}$ and neglecting the splitting between the couplings $\lambda_{S,T}$ and their $\mathcal{N}=2$ values one finds, matching at a scale μ:

$$\delta\lambda_1 = \frac{1}{16\pi^2}\log\frac{M_\Sigma^2}{\mu^2}\left[\lambda_S^4 + 3\lambda_T^4 + 2\lambda_S^2\lambda_T^2\right]$$

$$\delta\lambda_2 = \delta\lambda_1 + \frac{3y_t^4}{8\pi^2}\log\frac{m_{\tilde{t}}^2}{\mu^2}$$

$$\delta\lambda_3 = \frac{1}{16\pi^2}\log\frac{M_\Sigma^2}{\mu^2}\left[\lambda_S^4 + 3\lambda_T^4 - 2\lambda_S^2\lambda_T^2\right]$$

$$\delta\lambda_4 = \frac{1}{16\pi^2}4\lambda_S^2\lambda_T^2\log\frac{M_\Sigma^2}{\mu^2}, \qquad (2.3.11)$$

using y_t, y_b, y_τ to denote the top, bottom and τ Yukawa couplings. Full (updated) expressions are given in the limit $m_{DY}, m_{D2} \ll m_S, m_T$ in appendix B.2.

One then finds the remarkable result that the singlet/triplet scalar contributions to Z_6 *exactly cancel out*! The dominant contribution to Z_6 is then that coming from the stops:

$$Z_6(v) \simeq Z_6(M_{\text{SUSY}}) + s_\beta^3 c_\beta \times \frac{3y_t^4}{8\pi^2}\log\frac{m_{\tilde{t}}^2}{m_t^2}, \qquad (2.3.12)$$

where m_t is the top quark mass. Although the magnitude of this is the same as the loop contribution to Z_6 in the MSSM, the misalignment thus induced is much smaller, because (a) there is no tree-level contribution, and (b) it is also proportional to the stop correction to the Higgs mass, which is smaller than in the MSSM due to the tree-level boost to the Higgs mass. To investigate the misalignment in this model further, however, in the next section a precision study using numerical tools will be performed, using the logic of the hMSSM [163]/h2MSSM [136] to show that the misalignment in the model is even smaller than the above naive estimate.

---

[1]This is true for reasonable values of $\tan\beta \gtrsim 1.5$. For values of $\tan\beta$ near unity the Yukawa couplings diverge at high energies so it is not possible to consistently place the $\mathcal{N}=2$ scale there.

2.4 Precision study

To precisely study the quantum corrections to alignment in the minimal model, the low-energy model consisting of the THDM supplemented by a Dirac bino and a Dirac Wino was implemented into the package `SARAH`. The couplings of the model are described in detail in appendix B.1. The code was then modified to implement the boundary at a supersymmetry scale M_{SUSY} and the two-loop supersymmetric RGEs used for the minimal Dirac gaugino extension of the MSSM [107, 134] as generated by `SARAH` [164–166]. While this theory does not fit into a GUT and has no gauge coupling unification, an $\mathcal{N} = 2$ supersymmetry scale was implemented where the couplings λ_S, λ_T take their $\mathcal{N} = 2$ supersymmetric values. By running all the way from a low-scale Q (which has been taken to be the scale of the Dirac gauginos and Heavy Higgses, but could equally be m_{top}) up to M_{SUSY} and then $M_{N=2}$ and back down, iterating until the results converge, it was possible to find consistent values of the parameters. At the scale Q, the threshold corrections are those that are included in `SARAH` by default:

- One-loop matching of Yukawa couplings to the Standard Model values, plus two-loop strong corrections to the top Yukawa.

- One-loop gauge threshold corrections.

- Two-loop corrections to the Higgs masses [167–169] (which implement the generic expressions of [168,170,171] and the solution to the Goldstone Boson catastrophe of [169,172]).

Two-loop RGEs for this model were employed up to M_{SUSY}, and then at the scale M_{SUSY}, the following thresholds were implemented:

- Tree-level correction to the λ_i from Dirac gaugino masses given in (2.2.9), even if Dirac gaugino masses are otherwise neglected.

- One-loop corrections to the λ_i given in B.2.3.

- Conversion of $\overline{\text{MS}}$ to $\overline{\text{DR}}$ gauge couplings given in B.2.1.

- Conversion of $\overline{\text{MS}}$ to $\overline{\text{DR}}$ Yukawa couplings proportional to the strong gauge coupling, given in B.2.1.

M_{SUSY} is taken to be a common mass of left- and right-handed stops, and it is assumed that other MSSM particles have masses at this scale; the singlet at triplet scalars are allowed to be heavier at a scale M_Σ. All R-symmetry-violating terms (such as squark trilinear couplings) are eliminated, and it is assumed that

$$m_{DY}, m_{D2}, \mu \ll M_{\text{SUSY}}.$$

This means that squark mixing is neglected, and this greatly simplifies the thresholds. The thresholds for supersymmetric particles that are included are then *nearly* complete in this limit; the gauge and Yukawa threshold corrections vanish for the MSSM couplings, and only the corrections to the gauge/Yukawas induced by the adjoint scalars are neglected – since their effect is in general very small; this work leaves the calculation and implementation of these for future work. However, it is preferable to include their contribution to the Higgs quartic couplings. Furthermore, in the limit of zero squark mixing the two-loop corrections to the Higgs quartic couplings are also small or even vanishing [173], and so this work is justified in neglecting them.
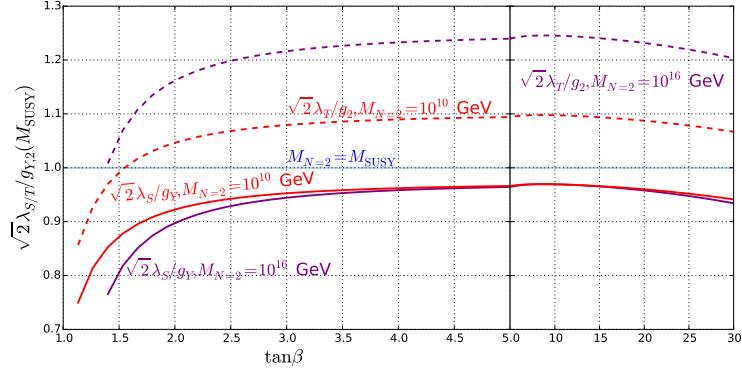
Figure 2.1: Variation of the ratios $\sqrt{2}\lambda_S/g_Y$ and $\sqrt{2}\lambda_T/g_2$ at the scale M_{SUSY} with $\tan\beta$, for $M_{N=2} = M_{\text{SUSY}}, 10^{10}$ GeV and 10^{16} GeV.

To perform a more general scan over the parameter space including trilinear scalar couplings, general masses and allowing μ, m_{DY}, m_{D2} to be of the order of M_{SUSY} one would need to compute the additional threshold corrections; while it is expected that the effect of μ, m_{DY}, m_{D2} on the results will be very small, it would nonetheless be interesting to compute these in the future.

Scans were performed over the values of $\tan\beta$ and M_{SUSY} was varied to obtain a light Higgs mass of 125.15 GeV. The other values are taken as

$$M_\Sigma = 5 \text{ TeV}, \qquad (m_{DY}, m_{D2}, \mu) = (400, 600, 500) \text{ GeV}, \qquad m_A^{\text{tree}} = 600 \text{ GeV} \tag{2.4.1}$$

by imposing

$$m_{12}^2 = -(m_A^{\text{tree}})^2 s_\beta c_\beta. \tag{2.4.2}$$

As shall be seen later, these are compatible with all current experimental constraints. Note, on the other hand, that collider limits on the electroweakinos shall not be discussed because the effect of changing their masses is tiny.

In the scans one sees little deviation between m_A^{tree} and the mass of the heavy/charged Higgses because the mixing is small; indeed the results are not especially sensitive to m_A^{tree} as a result.

2.4.1   Running from the $\mathcal{N} = 2$ scale

At the scale $Q = 400$ GeV, one finds $g_Y = 0.37, g_2 = 0.64 \pm 0.01$; these are barely different at the SUSY scale and vary little with $M_{N=2}$, but one does find some dependence of the ratios $\sqrt{2}\lambda_S/g_Y, \sqrt{2}\lambda_T/g_2$ on this scale, which are given in figure 2.1. The values in the plot were taken with a common supersymmetric scale of 3 TeV and have essentially no dependence on m_A.

An alternative way of visualising this information is in the quantity Z_1 evaluated at the SUSY scale; since our model is always very near alignment, this gives the "tree-level" Higgs mass and so in figure 2.2 $v\sqrt{Z_1(M_{\text{SUSY}})}$ is plotted. One sees that for $M_{N=2} = M_{\text{SUSY}}$ this is always essentially M_Z, while as $M_{N=2}$ is increased one obtains a *further* enhancement to the Higgs mass at small $\tan\beta \gtrsim 1.5$.

If no further corrections were to be included, then the value of Z_6 at M_{SUSY} would be given by

$$Z_6(M_{\text{SUSY}}) = \frac{1}{4} s_{2\beta} c_{2\beta} \left[g_Y^2 (2\lambda_S^2/g_Y^2 - 1) + g_2^2 (2\lambda_T^2/g_2^2 - 1) \right]. \tag{2.4.3}$$
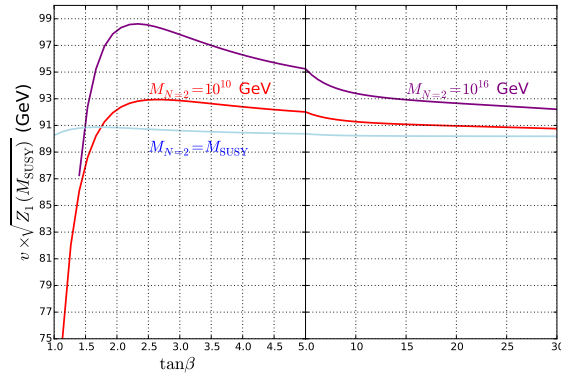
Figure 2.2: $v \times \sqrt{Z_1(M_{\mathrm{SUSY}})}$ against $\tan\beta$ for $M_{N=2} = M_{\mathrm{SUSY}}, 10^{10}$ GeV and 10^{16} GeV, which corresponds to the "tree-level" value of the Higgs mass before running from M_{SUSY} is taken (or equivalently the SUSY corrections at M_Z) into account (we take $v = 246$ GeV in the figure). One sees that increasing $M_{N=2}$ *increases* the Higgs mass, particularly for small $\tan\beta > 1.5$.

Crucially then it is seen that for $M_{N=2} > M_{\mathrm{SUSY}}$ this is dominated by the relative positive shift in λ_T, which in turn yields a negative contribution to Z_6. The results from our scans for the value of Z_6 at the SUSY scale almost exactly correspond to the above equation, which are plotted in figure 2.3. The differences (particularly the tiny difference from zero for the $\mathcal{N} = 2$ scale equal to M_{SUSY}) come from the tree-level and loop-level shifts.

2.4.2 Running below M_{SUSY}

Once two-loop running below M_{SUSY} is included, the picture changes substantially. This is dominated by the effects of the stops via their absence from the RGEs; the
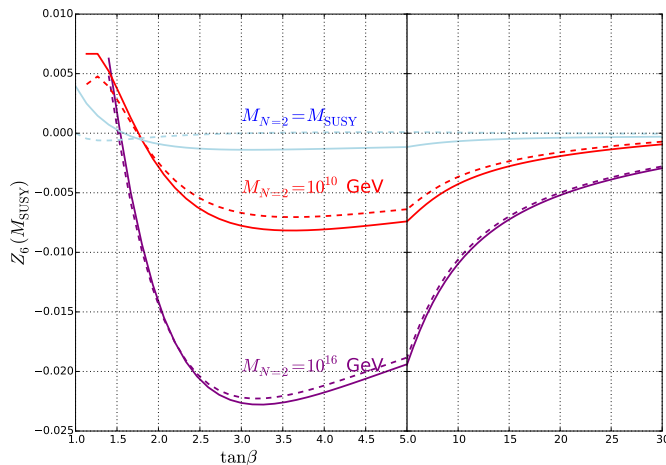
Figure 2.3: $Z_6(M_{\mathrm{SUSY}})$ against $\tan\beta$ for $M_{N=2} = M_{\mathrm{SUSY}}, 10^{10}$ GeV and 10^{16} GeV, which corresponds to just the contributions to Z_6 from the running of $\lambda_{S,T}$ and the threshold corrections. The solid lines show the full value of Z_6, while the dashed lines are just those given by equation (2.4.3), i.e. without threshold corrections.
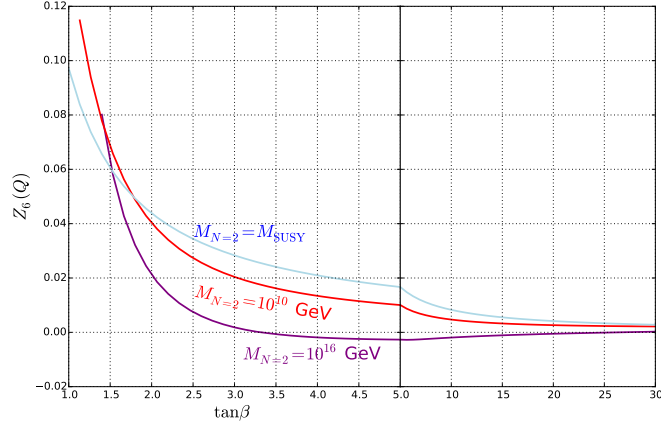
Figure 2.4: $Z_6(Q)$ against $\tan\beta$, where $Q = 400$ GeV is our low-energy matching scale. One finds that the model shows good alignment for all values of $\tan\beta > 1.5$, with the surprising conclusion that raising the $\mathcal{N} = 2$ scale *improves* the alignment.

results of Z_6 are plotted for the same scan as in figure 2.3 at the scale of our low-energy theory in figure 2.4.

Interestingly, the results can be understood by following the reasoning of the hMSSM [163]/h2MSSM [136] treatment. In that framework, the quantum corrections to the Higgs mass are assumed to be dominated by the $(2,2)$ component – and further that one can neglect the contributions to the other components compared to the tree-level ones; first a quick review will be made of what happens in the hMSSM and then the analysis will be applied to our case.

2.4.2.1   (Lack of) alignment in the hMSSM

In the hMSSM [163], one has $\lambda_2 = \frac{M_Z^2}{v^2} + \epsilon$ and all other terms are assumed to have their tree-level values as shown in eq.(2.2.15), giving the neutral Higgs mass matrix in the alignment basis (2.2.17, 2.2.18) of

$$m_{h,H}^2 = \begin{pmatrix} M_Z^2 c_{2\beta}^2 + \epsilon s_\beta^4 & -M_Z^2 s_{2\beta} c_{2\beta} + s_\beta^3 c_\beta \epsilon \\ -M_Z^2 s_{2\beta} c_{2\beta} + s_\beta^3 c_\beta \epsilon & m_A^2 + M_Z^2 s_{2\beta}^2 + s_\beta^2 c_\beta^2 \epsilon \end{pmatrix}. \tag{2.4.4}$$

Now supposing that the values are tuned to obtain alignment, one then has

$$\begin{aligned} -M_Z^2 s_{2\beta} c_{2\beta} + s_\beta^3 c_\beta \epsilon &= 0\,, \\ M_Z^2 c_{2\beta}^2 + \epsilon s_\beta^4 &= m_h^2\,, \end{aligned} \tag{2.4.5}$$

which leads to

$$c_{2\beta} = \frac{m_h^2}{M_Z^2} > 1 \qquad \text{or} \qquad c_\beta = 0, \tag{2.4.6}$$

i.e. it is impossible to achieve alignment without decoupling or going to the large $\tan\beta$ limit with these approximations. If one does not neglect the other contributions to Z_6, in the case of exact alignment one then has

$$0 = Z_6 = \frac{1}{v^2 t_\beta}(m_h^2 - M_Z^2 c_{2\beta}) - s_\beta c_\beta (c_\beta^2 \delta\lambda_1 - c_{2\beta}\delta\lambda_{345})$$

$$0 = (m_h^2 - M_Z^2 c_{2\beta}) - v^2 s_\beta^2 (c_\beta^2 \delta\lambda_1 - c_{2\beta}\delta\lambda_{345}) \tag{2.4.7}$$

Since one expects $\lambda_1, \lambda_{345} \ll \lambda_2$, and for $t_\beta > 1$ one has $s_\beta^2 > c_\beta^2, s_\beta^2 > |c_{2\beta}|$, this is still impossible to satisfy. However, it will be found that for the scenario considered here things are somewhat better.

2.4.2.2   Alignment in the Dirac-gaugino model

Using the expressions (2.2.14) for the quartic couplings, one can rewrite

$$\lambda_1 \equiv \frac{M_Z^2}{v^2} + \delta\lambda_1, \qquad \lambda_2 \equiv \frac{M_Z^2}{v^2} + \frac{\epsilon}{v^2},$$

$$\lambda_{345} \equiv \frac{M_Z^2}{v^2} + \frac{1}{2}(2\lambda_S^2 - g_Y^2) + \frac{1}{2}(2\lambda_T^2 - g_2^2) + \delta\lambda_{345}. \tag{2.4.8}$$

This leads to

$$Z_1 v^2 = M_Z^2 + \epsilon s_\beta^4 + \delta\lambda_1 c_\beta^4 + \frac{1}{2}\delta\lambda_{345} s_{2\beta}^2 + v^2\left[(2\lambda_S^2 - g_Y^2) + (2\lambda_T^2 - g_2^2)\right] s_\beta^2 c_\beta^2$$

$$Z_6 v^2 = s_\beta^3 c_\beta \epsilon - v^2 s_\beta c_\beta (c_\beta^2 \delta\lambda_1 - c_{2\beta}\delta\lambda_{345}) + \frac{1}{2}c_{2\beta}s_\beta c_\beta v^2\left[(2\lambda_S^2 - g_Y^2) + (2\lambda_T^2 - g_2^2)\right]. \tag{2.4.9}$$

The corrections $\delta\lambda_i$ can be interpreted as either coming from running the couplings between the scale M_{SUSY} and Q, or alternatively from integrating out the supersymmetric particles at the scale Q; in the latter case one can obtain an estimate of their values from the expressions (2.3.11) and see that they are typically suppressed relative to ϵ/v^2 by a numerical factor and also the ratio of the electroweak gauge coupling to the strong top Yukawa, and therefore is is possible to continue with the hMSSM approximation and neglect them. However, the effect from the running of λ_S, λ_T is non-negligible: eliminating ϵ in exchange for the Higgs mass and defining

$$\hat{\delta}\lambda_{345} \equiv \frac{1}{2}(2\lambda_S^2 - g_Y^2) + \frac{1}{2}(2\lambda_T^2 - g_2^2) \tag{2.4.10}$$

one has

$$Z_6 = \frac{s_\beta c_\beta}{v^2(m_A^2 s_\beta^2 + M_Z^2 c_\beta^2 - m_h^2)}\left[(m_A^2 - m_h^2)(m_h^2 - M_Z^2) - v^2\hat{\delta}\lambda_{345}\left(m_A^2 s_\beta^2 - M_Z^2 c_\beta^2 + m_h^2 c_{2\beta}\right)\right.$$

$$\left. + v^4 c_\beta^2 s_\beta^2(\hat{\delta}\lambda_{345})^2\right]$$

$$\approx \frac{0.12}{t_\beta} - \frac{1}{2}\frac{t_\beta}{1+t_\beta^2}\left[(2\lambda_S^2 - g_Y^2) + (2\lambda_T^2 - g_2^2)\right]. \tag{2.4.11}$$

Later, expressions shall be given for eliminating λ_2 and calculating Z_6 in any THDM with general $\lambda_i, i = 1...4$ in equations (2.6.3) and (2.6.5).

A comparison of the above formula with the curves in figure 2.4 shows that this gives a reasonable fit; in the case of $M_{N=2} = M_{\mathrm{SUSY}}$ the expression is particularly simple, but in the other cases one needs to take account of the varation of $\sqrt{2}\lambda_S(M_{\mathrm{SUSY}}), \sqrt{2}\lambda_T(M_{\mathrm{SUSY}})$ with $\tan\beta$ that can be seen in figure 2.1.

The main conclusion that can be drawn from the above formula is that the misalignment coming from the squark corrections required to enhance the Higgs mass can be compensated by the effect of running λ_S, λ_T. Indeed, one sees from figure 2.4 that for $M_{N=2} = 10^{16}$ GeV, Z_6 is essentially vanishing for $\tan\beta \gtrsim 3$. From the curves in

the figure, one sees that increasing the $\mathcal{N} = 2$ scale causes a partial or total cancellation of the misalignment contributions, meaning that the Higgs boson is accidentally very Standard-Model-like, independent of the mass of the heavy Higgs! This is the main result of the paper.

2.4.3 Higgs mass bounds on the SUSY scale

Finally the effect of the loop corrections in the low-energy theory on the Higgs mass (i.e. those coming from the Higgs sector itself, the top and the electroweakinos) will be considered. Figure 2.5 shows the tree-level and one-loop values for the Higgs mass as $\tan\beta$ is varied (with M_{SUSY} fixed to ensure $m_h = 125.15$ GeV at two-loops). A significant upward shift of about 7 GeV is found at one-loop, and then a downward shift of about 1 or 2 GeV from one to two loops. Note that it is possible to interpret the "tree-level" Higgs mass as the loop-level Higgs mass in the full Dirac gaugino model including the effects of the stops and gluinos.

Figure 2.6 shows the final curve of $\tan\beta$ against M_{SUSY}, for different values of the $\mathcal{N} = 2$ scale between M_{SUSY} and 10^{16} GeV.

The plot shows that there is a minimum for M_{SUSY} around $\tan\beta \simeq 2$ or 3, particularly for larger values of $M_{N=2}$, which can be understood in terms of the splitting of λ_T from its $\mathcal{N} = 2$ value and the consequent boost to the Higgs mass, which can be clearly seen in figure 2.2.

The results in figure 2.6 contrast starkly with the MSSM case matched onto the 2HDM as shown in e.g. [174]; due to the enhancement to the Higgs mass from the new couplings already seen in figure 2.2 one has a *much* lower SUSY scale. On the other hand, there are significant differences from the values quoted in [136] which are most closely related to the case $M_{N=2} = M_{\mathrm{SUSY}}$; here of course one has light electroweakinos, although the largest difference is the significantly more accurate EFT calculation employed here.
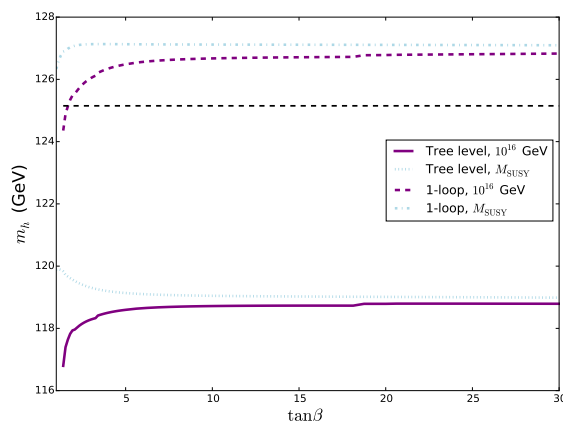
Figure 2.5: Effect of loop corrections in the low-energy theory on the Higgs mass. The tree-level and one-loop values for the Higgs mass are show against $\tan\beta$ for $\mathcal{N} = 2$ scales of the stop scale (M_{SUSY}) and 10^{16} GeV; the two-loop value of the Higgs mass is fixed to the black dotted line.
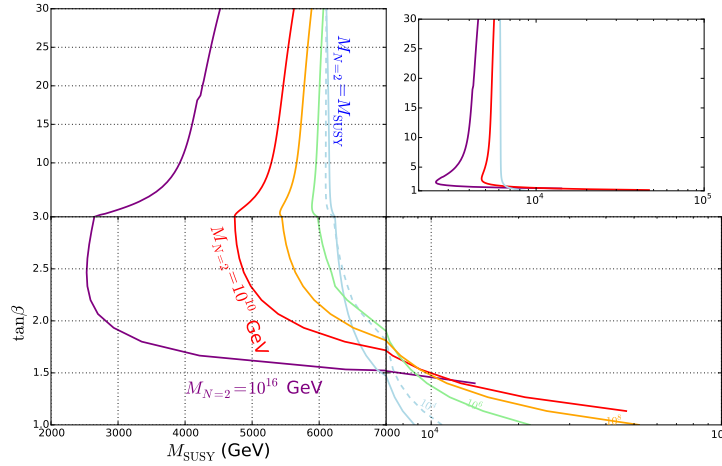
Figure 2.6: SUSY scale that fits $m_h = 125.2$ GeV against $\tan\beta$. The cases $M_{N=2} = \{M_{\text{SUSY}}, 10^{10}$ GeV, 10^{16} GeV$\}$ are the solid lines in blue, red and purple respectively and are labelled in full; the cases $M_{N=2} = \{10^4, 10^6, 10^8\}$ GeV are respectively shown in blue dashed, solid green and solid orange curves and only labelled with $\{10^4, 10^6, 10^8\}$. Due to the large range of scales M_{SUSY} values for small $\tan\beta$ and the little change for large $\tan\beta$ the plot has been split into three quadrants to show the values more clearly, but for comparison an inset graph is given showing the three curves $M_{N=2} = \{M_{\text{SUSY}}, 10^{10}$ GeV, 10^{16} GeV$\}$ with M_{SUSY} (GeV) on a logarithmic scale on the abscissa and $\tan\beta$ on a linear scale on the ordinate.

2.5 Experimental constraints

Since our model realises excellent alignment, the light Higgs couplings are very nearly Standard-Model-like across the whole parameter space, and so there is no significant constraint from those – this is in contrast to e.g. the hMSSM scenario, where for low $\tan\beta$ the Higgs couplings provided until recently the most important lower bound on the Heavy Higgs mass. However, there are still significant constraints on the parameter space coming from electroweak precision tests, flavour and direct searches, as shall be detailed below.

2.5.1 Electroweak precision corrections

There are two contributions to the electroweak precision parameters: those coming from the high-energy theory, and those coming from the low-energy theory. In the high-energy theory there will be contributions at tree-level from the triplet scalars: they should obtain a vacuum expectation value, and in our EFT this manifests itself as generating effective operators.

In the limit of zero CP violation, and neglecting the terms A_S, A_T the effective operator arising from integrating out the triplet can be written quite simply as

$$\mathcal{L} \supset \frac{1}{4m_{TP}^4} \text{tr} \left[D_\mu \left(\sigma^a \left[(\sqrt{2}\lambda_T \mu + g_2 m_{D2}) H_d^\dagger \sigma^a H_d + (g_2 m_{D2} - \sqrt{2}\lambda_T \mu) H_u^\dagger \sigma^a H_u \right] \right) \right]^2 \tag{2.5.1}$$

where summation is understood on the index a and

$$D_\mu \sigma^a = \sigma^a \partial_\mu - i g_2 [W_\mu, \sigma^a]. \tag{2.5.2}$$
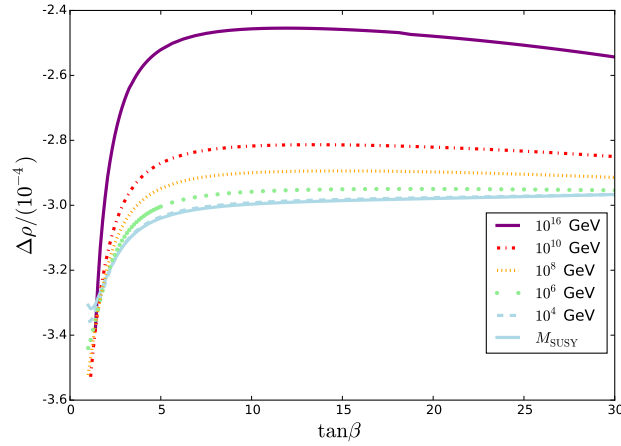
Figure 2.7: $\Delta\rho$ calculated at one-loop in the low-energy theory, for different values of $M_{N=2}$ given in the legend. One sees that the magnitude is roughly equal to the experimental error, and the model value is always well within 3σ of the experimental central value (which is anyway above the Standard Model value by 1.6σ).

When a vacuum expectation value is given to the Higgs, this translates into the constraint from the expectation value of the triplet:

$$\Delta\rho = \frac{\Delta m_W^2}{m_W^2} = \frac{v^2}{m_{TP}^4}\left(\sqrt{2}\lambda_T\mu + g_2 m_{D2}c_{2\beta}\right)^2, \tag{2.5.3}$$

while the experimental best-fit value is [175]

$$\Delta\rho = (3.7 \pm 2.3) \times 10^{-4}. \tag{2.5.4}$$

For $\mu = 500$ GeV and an approximately $\mathcal{N} = 2$ value for λ_T, with small $\tan\beta$ insisting that this contribution does not exceed the experimental bound by 3σ gives

$$m_{TP} > 1500 \text{ GeV} \tag{2.5.5}$$

while simply saturating without exceeding the central best-fit value would limit instead $m_{TP} > 2$ TeV.

On the other hand, one also has a contribution from the electroweakinos at loop level, which increases as the Dirac mass/μ-term become smaller. Hence they cannot be arbitrarily light. In figure 2.7 the value of $\Delta\rho$ is plotted, calculated in the low-energy theory for the scan values (2.4.1), and one finds that they are below the experimental limit across the whole parameter space.

2.5.2   Bounds on $\tan\beta$ and m_A

The most stringent constraints on the parameter space of our model come from the searches for $pp \to H/A \to \tau\tau$ at the LHC; and the decay $B \to s\gamma$ determined in [176], which bounds the charged Higgs mass to be heavier than 580 GeV independent of the value of $\tan\beta$ (which in turn bounds the mass of the pseudoscalar Higgs to be above around 568 GeV).

The bounds from run 1 of the LHC were rather mild on the hMSSM: they restricted $\tan\beta < 8$ for low m_A. In [136] it was claimed that in the h2MSSM these bounds would apply unaltered; while it is true that the couplings to the pseudoscalar are the same
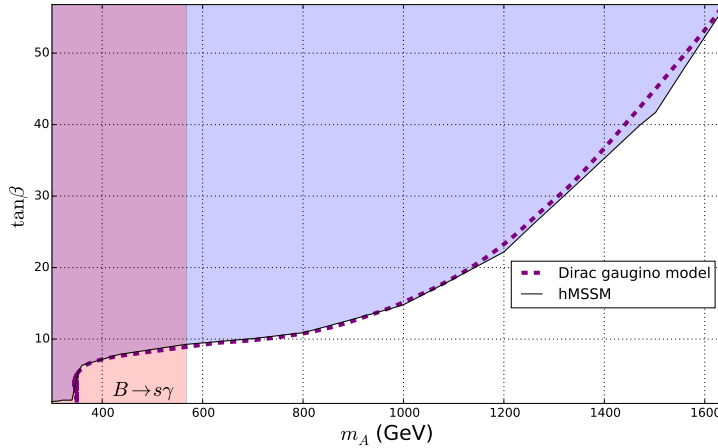
Figure 2.8: Bounds from $pp \to H/A \to \tau^+\tau^-$ (blue region) and $B \to s\gamma$ (red region, $m_A \lesssim 568$ GeV) interpreted in the $m_A/\tan\beta$ plane for the hMSSM (taken from [177]) and our model.

in the h2MSSM and hMSSM, the "heavy" Higgs does have altered couplings at small m_A and $\tan\beta$ – since it is more aligned. Since the production of the Heavy Higgs is dominated at small $\tan\beta$ by gluon fusion, and at large $\tan\beta$ by the bbH process, then one would expect some differences at small $\tan\beta$. However, recently, ATLAS produced a much enhanced bound [177] on gluon fusion and bbH production and then decay to τ pairs; they also interpreted this in terms of the hMSSM. To compare to the model here, Higgs production was computed using SusHi [178–184] and the production cross-sections were rescaled according to b-quark and gluon couplings computed in the SARAH/SPheno code, then multiplied by the tau decay branching fraction, and the bound combined assuming that the signals from H/A production overlap for small mass differences. The results are shown in figure 2.8, where the bound from [177] on the hMSSM is also shown. One finds almost no difference, except that the bound on the model here is very slightly weaker once decays to the electroweakinos are permitted. However, the branching ratio to electroweakinos in that region is never significant enough to reduce the τ decay fraction.

2.6 Alignment in the MRSSM

For completeness a brief discussion will be made of the MRSSM in the same limit as for the DG-MSSM. Since the tree-level THDM parameters are the same as those of the MSSM in the limit of large adjoint scalar and R-Higgs masses, there is no contribution to Z_6 from the running of the parameters $\lambda_{S_{u,d}}, \lambda_{T_{u,d}}$. One can first write the neutral Higgs mass matrix as

$$m_{h,H}^2 = \begin{pmatrix} M_Z^2 c_{2\beta}^2 + v^2 \Delta Z_1 & -M_Z^2 s_{2\beta} c_{2\beta} + v^2 \Delta Z_6 \\ -M_Z^2 s_{2\beta} c_{2\beta} + v^2 \Delta Z_6 & m_A^2 + M_Z^2 s_{2\beta}^2 + v^2 \Delta Z_5 \end{pmatrix}. \tag{2.6.1}$$

If one considers the loop corrections due to $\lambda_{S_{u,d}}, \lambda_{T_{u,d}}$ to be small, then the analysis of alignment is identical to the MSSM case, and the hMSSM logic can be applied. However, if instead they are taken to be non-negligible – such as in [114,115,126,127] – then the contributions to λ_2 no longer dominate, and the hMSSM reasoning may

no longer apply. On the other hand, the largest contribution from the other particles will still be to λ_2, and so one can assume that

$$\lambda_2 = \frac{M_Z^2 + \epsilon}{v^2}, \qquad \lambda_1 = \frac{M_Z^2}{v^2} + \delta\lambda_1$$

$$\lambda_5 = 0, \qquad \lambda_{345} = \lambda_{34} = -\frac{M_Z^2}{v^2} + \delta\lambda_{34}. \tag{2.6.2}$$

To eliminate ϵ, one writes λ_2 in terms of the Higgs mass, which for general $\lambda_i, i = 1...4$ (and $\lambda_5 = \lambda_6 = \lambda_7 = 0$):

$$\lambda_2 v^2 s_\beta^2 + m_A^2 c_\beta^2 = m_h^2 + \frac{s_\beta^2 c_\beta^2 (m_A^2 - \lambda_{34} v^2)^2}{\lambda_1 v^2 c_\beta^2 + m_A^2 s_\beta^2 - m_h^2}; \tag{2.6.3}$$

this can then be substituted into the expression for Z_6:

$$Z_6 = -\frac{s_\beta c_\beta}{\lambda_1 v^4 c_\beta^2 + m_A^2 v^2 s_\beta^2 - m_h^2 v^2} \times \tag{2.6.4}$$

$$\left[(\lambda_1 v^2 c_\beta^2 - m_h^2)(\lambda_1 v^2 c_\beta^2 - m_h^2 + m_A^2 - \lambda_{34} v^2 c_{2\beta}) + \lambda_{34} s_\beta^2 v^2 (m_A^2 - \lambda_{34} c_\beta^2 v^2) \right].$$

The loop corrections to the λ_i from the adjoint scalars are given in appendix B.4, but in the simplified case of $m_{T^+} = m_{T^-} = m_{SR} = m_{SI} = M_\Sigma$ and $g_Y = g_2 = 0$ one has, for matching at a scale μ:

$$\delta\lambda_1 = \frac{1}{16\pi^2} \log\frac{M_\Sigma^2}{\mu^2} \left(5\lambda_{T_d}^4 + 2\lambda_{S_d}^2 \lambda_{T_d}^2 + \lambda_{S_d}^4 \right)$$

$$\delta\lambda_2 = \frac{1}{16\pi^2} \log\frac{M_\Sigma^2}{\mu^2} \left(5\lambda_{T_u}^4 + 2\lambda_{S_u}^2 \lambda_{T_u}^2 + \lambda_{S_u}^4 \right)$$

$$\delta\lambda_3 = \frac{1}{16\pi^2} \log\frac{M_\Sigma^2}{\mu^2} \left(5\lambda_{T_d}^2 \lambda_{T_u}^2 + \lambda_{S_d}\lambda_{S_u}\lambda_{T_d}\lambda_{T_u} + \lambda_{S_d}^2 \lambda_{S_u}^2 \right)$$

$$\delta\lambda_4 = \frac{1}{16\pi^2} \log\frac{M_\Sigma^2}{\mu^2} \left(-4\lambda_{T_d}^2 \lambda_{T_u}^2 - 4\lambda_{T_d}\lambda_{T_u}\lambda_{S_d}\lambda_{S_u} \right). \tag{2.6.5}$$

If one then takes (as in [115, 126, 127]) $\lambda_{S_u} = -\lambda_{S_d} \equiv \lambda$, $\lambda_{T_u} = \lambda_{T_d} \equiv \Lambda$, and allows an additional contribution ϵ/v^2 to λ_2 from the stops, one then has

$$Z_6 = -\frac{1}{2}s_{2\beta}c_{2\beta}\left(\frac{2M_Z^2}{v^2} + \frac{2\Lambda^4}{16\pi^2} \log\frac{M_\Sigma^2}{\mu^2} \right) + \frac{\epsilon}{v^2} s_\beta^3 c_\beta$$

$$\Delta Z_1 = \frac{1}{16\pi^2} \log\frac{M_\Sigma^2}{\mu^2} \left[\lambda^4 + 2\lambda^2\Lambda^2 + 3\Lambda^4 + 2\Lambda^4 c_{2\beta}^2 \right] + \frac{\epsilon}{v^2} s_\beta^4. \tag{2.6.6}$$

When the couplings λ, Λ are large enough, the alignment will always be improved compared to the MSSM, because the enhancement to Z_1 is always greater than that to Z_6. Three cases of particular interest are noted:

1. If the contributions from the adjoint scalars are increased to the point that those from the stops can be neglected, then for small $\tan\beta$ one will easily have alignment (in contrast to the MSSM case).

2. Alternatively, one could enhance the contributions from λ rather than Λ, since the former coupling does not contribute to Z_6.

3. On the other hand, if one takes the $\mathcal{N} = 2$ supersymmetric limit

$$\lambda_{T_u} = \lambda_{T_d} = \frac{g_2}{\sqrt{2}}, \quad \lambda_{S_u} = \frac{g_Y}{\sqrt{2}}, \quad \lambda_{S_d} = -\frac{g_Y}{\sqrt{2}}, \tag{2.6.7}$$

one finds, using the expressions in appendix B.4 (and no longer neglecting the gauge couplings):

$$\delta\lambda_1 = \frac{1}{16\pi^2} \log \frac{M_\Sigma^2}{\mu^2} \frac{1}{4} \left(3g_2^4 + 2g_2^2 g_Y^2 + g_Y^4 \right)$$

$$\delta\lambda_2 = \delta\lambda_1$$

$$\delta\lambda_3 = \frac{1}{16\pi^2} \log \frac{M_\Sigma^2}{\mu^2} \frac{1}{4} \left(3g_2^4 - 2g_2^2 g_Y^2 + g_Y^4 \right)$$

$$\delta\lambda_4 = \frac{1}{16\pi^2} \log \frac{M_\Sigma^2}{\mu^2} \left(g_2^2 g_Y^2 \right) \tag{2.6.8}$$

giving

$$\delta\lambda_{345} = \delta\lambda_1 \equiv \delta\lambda, \tag{2.6.9}$$

so there is no shift to Z_6 from the adjoint scalars, but one does have a shift to Z_1, i.e

$$\Delta Z_1 = \delta\lambda, \qquad \Delta Z_6 = 0. \tag{2.6.10}$$

If the mass of the adjoint scalars is comparable to the mass of the stops, then this will however never be significant; on the other hand, if one takes the adjoint scalars to be very heavy, then this indicates that an improved alignment relative to the MSSM is possible. To quantify this, the above expression for Z_6 (2.6.5) can be used:

$$Z_6 = -\frac{s_\beta c_\beta}{(M_Z^2 v^2 + \delta\lambda v^4) c_\beta^2 + m_A^2 v^2 s_\beta^2 - m_h^2 v^2} \left[\Delta_0 + \delta\lambda v^2 (m_A^2 - m_h^2 + 2c_\beta^2 M_Z^2) \right] \tag{2.6.11}$$

where

$$\Delta_0 = m_h^2 (m_h^2 - m_A^2 - M_Z^2(4c_\beta^2 - 1)) + M_Z^2 c_{2\beta}(m_A^2 + 2M_Z^2 c_\beta^2) \tag{2.6.12}$$

which is the numerator for the MSSM case. In the case that $m_A^2 \gg m_h^2$ (which corresponds to the case of interest – even though one would like m_A small enough to not entirely be in the decoupling limit), one therefore finds

$$Z_6 \simeq \frac{1}{t_\beta} \left[\frac{m_h^2 - M_Z^2 c_{2\beta}}{v^2} - \delta\lambda \right]. \tag{2.6.13}$$

For $M_\Sigma = 100 M_{SUSY}$ (a rather extreme value) and matching at M_{SUSY} one finds

$$\delta\lambda \simeq 0.04 \frac{m_h^2}{v^2}, \tag{2.6.14}$$

and so the deviation of Z_6 from the MSSM value due to the adjoint scalars should be less than 4%. On the other hand, as shall be seen below, they can still have a significant effect on the SUSY scale.

Therefore, from the analysis above, in all three cases of interest, the alignment will never be as good as for the minimal Dirac gaugino model, because of the tree-level contribution to misalignment: this shall be illustrated for the $\mathcal{N} = 2$ case in the next subsection.

2.6.1   Numerical analysis of an $\mathcal{N} = 2$ MRSSM

To compare with our previous analysis of the DG-MSSM, here shall be presented a simplified numerical analysis for an $\mathcal{N} = 2$ MRSSM, as defined in point 3 above and equation (2.6.7). From our estimations above, the alignment should only differ from the MSSM when relatively extreme values are taken for the adjoint scalar masses, and so to perform a precise analysis one would need to have a tower of effective field theories and the appropriate threshold corrections. Instead it is decided to neglect all loop-level threshold corrections other than those from the adjoint scalars (although 2-loop RGEs are used throughout) and a simple analysis is performed where the low energy model is approximated by the Standard Model and type-II two-Higgs doublet model. In this way one should obtain an idea of how the adjoint scalar masses cause the SUSY scale and alignment to vary from the predictions of the MSSM.

2.6.1.1   Procedure

Two-loop Standard Model matching values were implemented at m_t for the standard model gauge, Yukawa, and Higgs quartic couplings from [19] and a two-loop Standard Model running was performed up to an intermediate scale $Q = 600$ GeV, where the $\lambda_i(Q)$ couplings were given approximate values to be determined through future iterations between the scales Q and $M_{N=2}$. The two-Higgs doublet model 2-loop running was implemented up to the supersymmetry breaking scale defining the leading squark masses, M_{SUSY}, where guesses were made for the inputs of the parameters $\lambda_{S,T_{u,d}}$. The MRSSM was then run to 2-loops to some high scale $M_{N=2}$ where the $\mathcal{N} = 2$ boundary conditions (2.6.7) were implemented. All two-loop beta functions were generated in SARAH, and the value of $m_A^{tree} = 600$ GeV was taken as in the minimal Dirac gaugino case. In this simplified model, as the electroweakinos are not taken to be light, the intermediate scale Q is taken to match the choice of heavy Higgs mass. Indeed, with these choices one should understand the Dirac gaugino masses m_{DY}, m_{D2}, m_{D3} and the higgsino mass to be at M_{SUSY}, and also the masses of the R-Higgs fields $R_{u,d}$ should be at that scale, because no threshold corrections are implemented from those fields (leaving these to future work).

On the run down, $\lambda_i(M_{SUSY})$ were matched to the 1-loop threshold corrections coming from the heavy S, T scalars as given in appendix B.4, taking the adjoint scalars to be degenerate with mass M_Σ. This process was iterated, re-matching the gauge and Yukawa couplings onto their 2-loop Standard Model running values at the scale Q, while the λ_i and $\lambda_{S,T_{u,d}}$ couplings were matched to the outputs from the previous running until their values converged. Finally, the λ_i parameters were mapped back onto the Higgs quartic coupling using $\lambda(Q) = Z_1(Q)$ and the Standard Model couplings were run back down to m_t. The correct Higgs mass was selected from the criterion $\lambda(m_t) = 0.252 \pm 0.002$, corresponding to a pole Higgs mass of $m_h = 125 \pm 0.5$ GeV.

This process was executed for scans over the values $\tan\beta \in [2, 20]$; $M_{SUSY} \in [0.5, 10]$ TeV; $M_\Sigma = \{5, 10, 100\} M_{SUSY}$ and $M_{N=2} = \{10^6, 10^{10}, 10^{16}\}$ GeV.

2.6.1.2   Running from the N=2 scale to M_{SUSY}
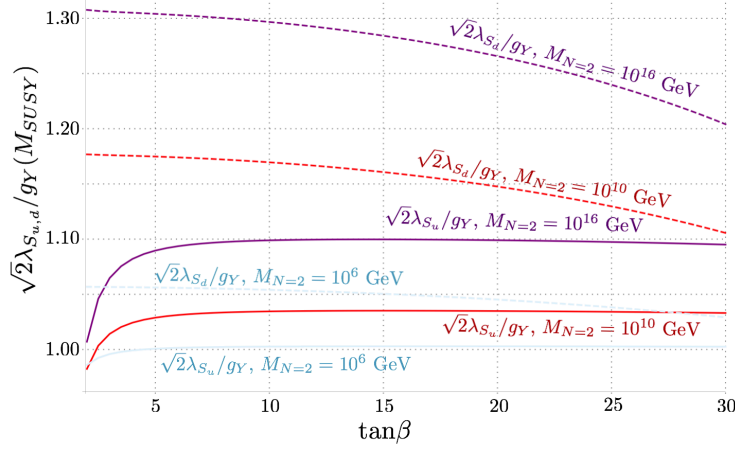
Figure 2.9: Variations in the ratio $\sqrt{2}\lambda_{S_{u,d}}/g_Y$ against $\tan\beta$ at the M_{SUSY} scale for $\mathcal{N}=2$ scales $10^6, 10^{10}$ and 10^{16} GeV.
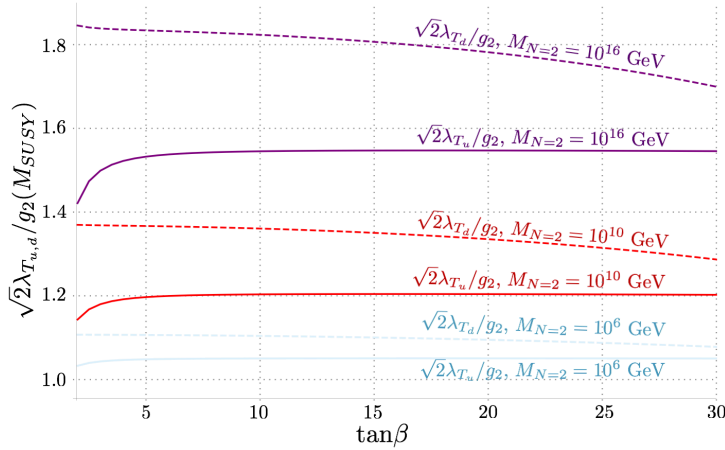
Figure 2.10: Variations in the ratio $\sqrt{2}\lambda_{T_{u,d}}/g$ against $\tan\beta$ at the M_{SUSY} scale for $\mathcal{N}=2$ scales $10^6, 10^{10}$ and 10^{16} GeV.

The ratios in figures (2.9, 2.10) are taken with a common M_{SUSY} scale of 10 TeV, while the associated value of m_h is unconstrained. M_Σ is kept fixed - in figures (2.9, 2.10) chosen as $M_\Sigma = 10\,M_{SUSY}$. Here the modulus of the ratio is plotted, since the λ_{S_d} ratio is negative to respect the $\mathcal{N}=2$ supersymmetry relations. As expected, the model is closest to the alignment limit when the $\mathcal{N}=2$ scale is closer to the M_{SUSY} scale. It can be seen that the Higgs mass is boosted to a greater extent by the down-type couplings than the up-type, where the ratio $\sqrt{2}\lambda_{T_d}/g$ has the largest effect, especially for higher values of $\mathcal{N}=2$ scale.
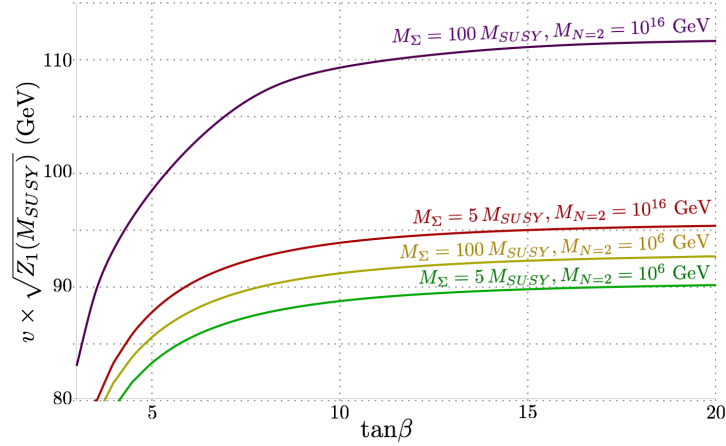
Figure 2.11: $v\sqrt{Z_1(M_{SUSY})}$ against $\tan\beta$ for $\mathcal{N} = 2$ scales 10^6 and 10^{16} GeV, corresponding to the "tree-level" value of m_h before running down in low-energy effective theory.

Figure 2.11 shows the "tree-level" Higgs mass against $\tan\beta$ before running down from M_{SUSY} (where the value of the Higgs mass calculated at m_t matches the experimental value). For the lowest values of $M_{N=2}$ and M_Σ plotted, $v\sqrt{Z_1(M_{SUSY})}$ is approximately M_Z, and where the former increase, so does the boost to the Higgs mass. This boost grows substantially for the simultaneously highest values of $M_{N=2}$ and M_Σ, owing to the large (almost non-perturbative) λ_T couplings. While not shown here, it should be noted that even for $M_{N=2} = 10^{10}$ GeV and $M_\Sigma = 100\, M_{SUSY}$, $v\sqrt{Z_1(M_{SUSY})}$ replicates almost identical behaviour to the red curve for $M_{N=2} = 10^{16}$ GeV and $M_\Sigma = 5\, M_{SUSY}$ shown here.

2.6.1.3 Running from $M_{SUSY} \to Q \to m_t$
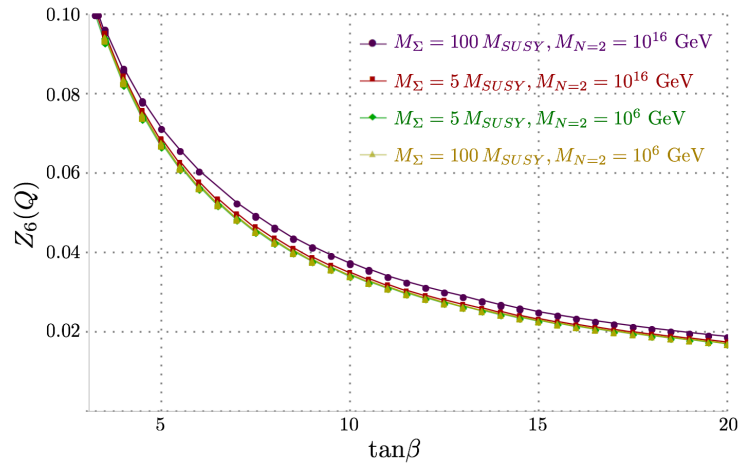
Figure 2.12: $Z_6(Q)$ against $\tan\beta$ for a Higgs mass of 125 GeV at m_t, for values of M_Σ = 5, 100 M_{SUSY} and $M_{N=2} = 10^6$ and 10^{16} GeV.

Figure 2.12 shows little deviation in the results for $Z_6(Q)$, regardless of M_Σ and $M_{N=2}$. Indeed, as anticipated above, the results are almost indistinguishable from the MSSM case, since the adjoint scalars in the MRSSM never give a large boost to the quartic couplings even for the extreme cases that have been taken. Exceptionally, the couplings in the case of very heavy scalars and very high $M_{N=2}$ are considerably enhanced and deviate from the $\mathcal{N} = 2$ relations, making the alignment in this case just marginally worse. While the adjoint scalars give only a very small boost to the Higgs mass, on the other hand it is enough to cause noticeable effects in the predicted M_{SUSY} scale, shown in figure 2.13, because of the logarithmic nature of the contributions from other SUSY states.
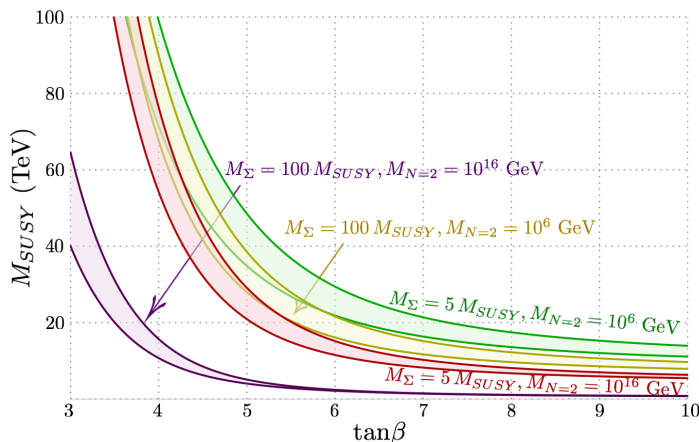
Figure 2.13: M_{SUSY} against $\tan\beta$ for a Higgs mass of 125 GeV at m_t and where $Q = 600$ GeV, plotted for values of $M_\Sigma = 5, 100\ M_{SUSY}$ and $M_{N=2} = 10^6$ and 10^{16} GeV.

Figure 2.13 shows the values of M_{SUSY} against $\tan\beta$ over the parameter scan producing a Higgs mass corresponding to $m_h = 125\pm0.5$ GeV: this margin is reflected in the enclosed transparent area[2]. For $\tan\beta < 4$, M_{SUSY} is required to be, at the very least, 20 TeV for the highest values of $M_{N=2}$ and very heavy M_Σ, and is closer to ~ 100 TeV for lower values. M_{SUSY} stabilises around $\tan\beta = 10$ for all values of M_Σ and $M_{N=2}$, where at this point M_{SUSY} can be as low as several hundred GeV for $M_{N=2} = 10^{16}$ and very heavy scalars. In this final extreme case (which is of course excluded experimentally, but gives an indication of the possible effects) the logarithms being resummed in the RGEs become smaller, it is possible that any neglected threshold effects could make a significant difference and the results become unreliable, but this is left as an additional analysis for future work.

2.7 Conclusions

This work has considered the consequences for the simplest realisation of Dirac gaugino models when $\mathcal{N} = 2$ supersymmetric boundary conditions are imposed for the

---

[2]The variation of 0.5 GeV is, however, not to imply the total error (which is hard to estimate, but should be comparable to this value although it may be smaller for large values of M_{SUSY}) but to give an indication of the sensitivity of the results on the final Higgs mass value.

Higgs/gauge sector at some energy scale. It was found that the model naturally re-alises alignment in the Higgs mass matrix, and that surprisingly this is preserved even by quantum corrections. Even more interestingly, the departure from $\mathcal{N} = 2$ relations due to running of the couplings actually leads to both an enhanced Higgs mass (and thus lower SUSY scale/more natural model) and also *improved* alignment when the effects of the squarks were taken into account.

The most accurate calculation to date has been provided for the SUSY scale in a Dirac gaugino model by employing the effective field theory approach, with one-loop boundary conditions at the high scale and two loops at the THDM scale. This leads to the prediction that the scale of coloured superpartners should be above 3 TeV (when one allows a very high scale for the breaking of the approximate $\mathcal{N} = 2$ SUSY) but across most of the parameter space it is below 10 TeV. While this is not encouraging for the detection of stops/gluinos at the LHC, this is well within the reach of a future 100 TeV collider. On the other hand, the LHC or a future e^+e^- collider should be able to explore the electroweak sector of the model, including the Higgs sector and the electroweakinos (if they are light).

There are many possible avenues for future work: improving the accuracy of the matching at M_{SUSY} (as noted recently, matching at two-loop order is often necessary for accuracy of the loop expansion to include all non-logarithmic corrections [185], although in this class of models as has been discussed all of the missing corrections are believed to be small) and including the effects of the electroweakinos in the matching at one loop, so that one can consider the model with $m_{DY} \sim m_{D2} \sim M_{\mathrm{SUSY}}$; also with the full set of thresholds an estimate of the error in the calculation could be performed (which, again, should already be small – see e.g. the estimates for the MSSM case in [186]); or including the effects of possible R-symmetry violating terms. On the other hand, it would also be interesting to more fully explore the consequences for different Dirac gaugino models, such as the MRSSM, where we have only performed a preliminary analysis.

3 – LHC constraints on the minimal Dirac gaugino model

The Higgs sector of the MDGSSM has now been well discussed, and the purpose of this section to derive recent limits on the gluinos and squarks in the same model. At the LHC, gluino-pair production is enhanced while squark production is suppressed as compared to the MSSM, and the decay signatures are altered by a more complex chargino and neutralino spectrum. The aim here is to investigate how this impacts current gluino and squark mass limits from Run 2 of the LHC. Concretely, four benchmark scenarios have been chosen to highlight different features of electroweakino spectrum, paying particular attention to the effect of the trilinear λ_S coupling, which induces a mass splitting between the mostly bino/U(1) adjoint states. Among other results, it will be shown that for large λ_S the additional $\tilde{\chi}_2^0 \to f\bar{f}\tilde{\chi}_1^0$ decays somewhat weaken the limits on gluinos (squarks) in case of heavy squarks (gluinos). Finally, the limits set in the gluino vs. squark mass plane in the MDGSSM will be compared to those obtained in equivalent MSSM scenarios.

In this chapter work will be presented re-examining the LHC bounds on squarks and gluinos in the MDGSSM, which have so far been studied only for Run 1 data [139–141]. For the MRSSM there was a study of collider bounds on sleptons and electroweakinos in the MRSSM using Run 1 data [187], and a recent examination of bounds on charginos in a gauge-mediation scenario [148]. The scalar octet partners of the gluons, or "sgluons", have received more attention in the literature: Dirac gaugino models predict *two* real sgluons, a scalar and pseudoscalar, since they come from a (complex) chiral superfield. These have very interesting collider phenomenology [81, 85, 89, 117, 128, 144, 188–191]; in particular, if CP is preserved then the pseudoscalar is likely to be relatively light and decay predominantly to tops, so they can be searched for in four-top events [129, 145].

As previously mentioned, the MDGSSM can be embedded in a GUT by adding additional electroweak-charged fields [116], the constrained scenario being the CMDGSSM. For simplicity and generality, these extra fields will not be included which, in any case, should not significantly affect the bounds on squarks and gluinos. Instead this work takes a phenomenological approach, choosing masses and couplings at the scale of the colourful superpartners. While the parameter space of such models is large, it shall be argued that the constraints found should be quite general for this class of models. In section 3.1 an overview is given of the phenomenological considerations that shall determine the benchmark scenarios, which are presented in section 3.2. Then, limits on gluino and squark masses will be derived, first using a simplified models approach in section 3.3, before undertaking a full recasting of the fully-hadronic gluino and squark search from ATLAS in section 3.4. A summary and conclusions are given in section 4.6.
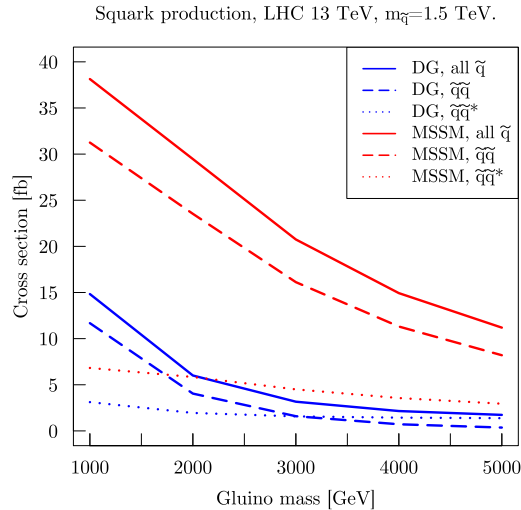
Figure 3.1:   Squark production cross-sections at leading order (LO) for the 13 TeV LHC as a function of the gluino mass in the MSSM (in red) and in the DG case (in blue), for $m_{\tilde{q}} = 1.5$ TeV, assuming an 8-fold squark degeneracy ($\tilde{q} = \tilde{u},\ \tilde{d},\ \tilde{c},\ \tilde{s}$). The dashed, dotted and full lines show the squark-squark, squark-antisquark and total squark production cross-sections, respectively.

3.1 Phenomenological considerations

3.1.1 Squark and gluino production at the LHC

As mentioned above, previous studies of Dirac vs. Majorana gauginos highlighted a weakening of collider limits on squarks due to the absence of a chirality flip in the DG case [139–142]. In the MSSM, squark–anti-squark production at the LHC ($pp \rightarrow \tilde{q}_L \tilde{q}_L^*,\ q_R \tilde{q}_R^*$) proceeds via s-channel gluon and t-channel gluino exchange; squark–squark production ($pp \rightarrow \tilde{q}\tilde{q},\ q^*\tilde{q}^*$) of same ($LL$, RR) and mixed (LR) chirality via t-channel gluino exchange is another important contribution to the total squark production. Squark–squark production of same chirality however requires a chirality flip, so it is absent in the DG case. Moreover, the other t-channel gluino exchange processes are suppressed by $|p|/m_{\tilde{g}}^2$ in the amplitude, where $|p|$ is the momentum in the propagator. This has a huge impact on the total squark production in the presence of a heavy Dirac gluino as illustrated in Fig. 3.1. This suppression of light-flavour squark production at the LHC is the perhaps best known consequence of Dirac gauginos.

There are also other interesting consequences, which may impact collider phenomenology. For one, the cross-section of gluino-pair production is enhanced in the DG case because of the larger number of degrees of freedom than in the MSSM (see [192] for a detailed discussion). Another important aspect is the more complex electroweakino spectrum. Concretely, while in the MSSM the neutralinos are a linear combination of the four neutral fermions, the bino $\tilde{B}$, wino $\tilde{W}^0$ and higgsinos $\tilde{H}_u^0$ and $\tilde{H}_d^0$, in the DG model this is supplemented by two adjoint fermions: a bino $\tilde{B}'$ and wino $\tilde{W}'^0$. In the chargino sector, the charged winos $\tilde{W}^{\pm}$ and higgsinos $\tilde{H}_u^+$, $\tilde{H}_d^-$ are supplemented by the triplet $\tilde{W}'^{\pm}$. Thus there are six neutralino and three chargino mass eigenstates, which may appear in gluino and squark cascade decays.

One may therefore expect that LHC phenomenology, and constraints from current searches, are different in DG models as compared to the MSSM. The purpose of this

paper is to investigate what are the concrete LHC limits on gluinos and squarks in the DG case.

3.1.2 Electroweak-ino spectrum

The neutralino mass matrix $\mathcal{M}_N$ in the basis $(\tilde{B}', \tilde{B}, \tilde{W}'^0, \tilde{W}^0, \tilde{H}_d^0, \tilde{H}_u^0)$ is given by

$$\mathcal{M}_N = \tag{3.1.1}$$

$$\begin{pmatrix} 0 & m_{DY} & 0 & 0 & -\frac{\sqrt{2}\lambda_S}{g_Y}m_Z s_W s_\beta & -\frac{\sqrt{2}\lambda_S}{g_Y}m_Z s_W c_\beta \\ m_{DY} & 0 & 0 & 0 & -m_Z s_W c_\beta & m_Z s_W s_\beta \\ 0 & 0 & 0 & m_{D2} & -\frac{\sqrt{2}\lambda_T}{g_2}m_Z c_W s_\beta & -\frac{\sqrt{2}\lambda_T}{g_2}m_Z c_W c_\beta \\ 0 & 0 & m_{D2} & 0 & m_Z c_W c_\beta & -m_Z c_W s_\beta \\ -\frac{\sqrt{2}\lambda_S}{g_Y}m_Z s_W s_\beta & -m_Z s_W c_\beta & -\frac{\sqrt{2}\lambda_T}{g_2}m_Z c_W s_\beta & m_Z c_W c_\beta & 0 & -\mu \\ -\frac{\sqrt{2}\lambda_S}{g_Y}m_Z s_W c_\beta & m_Z s_W s_\beta & -\frac{\sqrt{2}\lambda_T}{g_2}m_Z c_W c_\beta & -m_Z c_W s_\beta & -\mu & 0 \end{pmatrix},$$

where it has been used that $s_W = \sin\theta_W$, $s_\beta = \sin\beta$, $c_\beta = \cos\beta$ and $\tan\beta = v_u/v_d$ the ratio of the Higgs vevs; m_{DY} and m_{D2} the bino and wino Dirac masses; μ the conventional higgsino mass term, and λ_S and λ_T the couplings between the singlet and triplet fermions with the Higgs and higgsino fields. The various origins of these mass terms as well as the rotation matrices and eigenvalues are explained in detail in [83].

Diagonalising the neutralino mass matrix above, one ends up with pairs of bino-like, wino-like and higgsino-like neutralinos, with small mass splittings *within* the bino or wino pairs induced by λ_S or λ_T.[1] Taking, for instance, m_{DY} sufficiently smaller than m_{D2} and μ, one finds a mostly bino/U(1) adjoint lightest SUSY particle (LSP) with a mass splitting of

$$\Delta m_{\text{LSP}} \equiv m_{\tilde{\chi}_2^0} - m_{\tilde{\chi}_1^0} = \left| 2\frac{M_Z^2 s_W^2}{\mu}\frac{(2\lambda_S^2 - g_Y^2)}{g_Y^2}c_\beta s_\beta \right|. \tag{3.1.2}$$

For the models that shall be considered here, this can go up to tens of GeV.

Turning to the charged fermions, there are three charginos $\tilde{\chi}_{1...3}^\pm$ from a linear combination of the charged higgsinos, $\tilde{H}_u^+$, $\tilde{H}_d^-$, charged gauginos $\tilde{W}^\pm$ and adjoint $\tilde{W}'^\pm$. In the basis $v^+ = (\tilde{W}'^+, \tilde{W}^+, \tilde{H}_u^+)$, $v^- = (\tilde{W}'^-, \tilde{W}^-, \tilde{H}_d^-)$, the chargino mass matrix is

$$\mathcal{M}_C = \begin{pmatrix} 0 & m_{2D} & \frac{2\lambda_T}{g}m_W c_\beta \\ m_{2D} & 0 & \sqrt{2}m_W s_\beta \\ -\frac{2\lambda_T}{g}m_W s_\beta & \sqrt{2}m_W c_\beta & \mu \end{pmatrix}, \tag{3.1.3}$$

where again it is assumed that Majorana mass terms are absent. This gives one higgsino-like $\tilde{\chi}^\pm$ and two wino-like $\tilde{\chi}^\pm$ – the latter ones again with a small splitting driven by λ_T.

The possible impact on collider phenomenology becomes apparent when considering that gluino and squark decays will be shared out over the different neutralino and chargino states with small mass splittings. For instance, for a mostly bino/U(1) adjoint LSP, $\tilde{q}_R \to q\tilde{\chi}_1^0$ or $q\tilde{\chi}_2^0$ with roughly equal branching ratios. If $\Delta m_{\text{LSP}} < m_Z$, the $\tilde{\chi}_2^0$ then decays to $f\bar{f}\tilde{\chi}_1^0$ via an off-shell Z-boson. Therefore, while in the MSSM with a bino-like LSP $pp \to \tilde{q}_R\tilde{q}_R$ leads to events with 2 jets + E_T^{miss}, in the DG model with somewhat split binos, one may get a mix of events with 2, 4 or 6 jets + E_T^{miss}, and with a small rate also jets + $\ell^+\ell^-$ + E_T^{miss}. It should also be noted that, due to

---

[1]At least assuming a somewhat hierarchical pattern in m_{DY}, m_{D2} and μ; if two or all three mass parameters are close to each other there will be additional effects from sizeable bino, wino and/or higgsino mixing like in the MSSM.

$Z^* \to \nu\bar{\nu}$, some of the $\tilde{\chi}_2^0$ decays will be invisible. Similar considerations apply to all SUSY cascade decays.

Finally, the mass splitting between the two lightest neutralinos determines the $\tilde{\chi}_2^0$ lifetime. If the splitting is very small, the $\tilde{\chi}_2^0$ can live long enough to effectively be a co-LSP on collider scales and appear only as E_T^{miss}. For larger mass splittings, the $\tilde{\chi}_2^0$ can decay promptly, leading to the complex signatures discussed in the paragraphs above. In between, the $\tilde{\chi}_2^0$ is a long-lived neutral particle, whose decays can give signatures with displaced vertices.

3.1.3 Effect of R-symmetry breaking

The mass-splittings in the neutralinos are due to the R-symmetry breaking effect of both the H_u and H_d fields obtaining an expectation value – hence they are proportional to $c_\beta s_\beta$ which vanishes for large and small $\tan\beta$. In addition, when $\lambda_S = g_Y/\sqrt{2}, \lambda_T = g_2/\sqrt{2}$, there is an effective global symmetry among the gauginos and higgsinos which allows the neutralinos and charginos to remain of Dirac type at tree-level – this is not actually the $SU(2)$ R-symmetry, of which the higgsinos are actually singlets.

This means that any Majorana masses for the neutralinos and charginos (which are neglected here) should be smaller than the above splittings in order for the analysis in this paper to be valid: this makes a difference to the softness of the decays from $\tilde{\chi}_2^0$ to $\tilde{\chi}_1^0$, for example.

Turning to the gluinos, at tree level $\tilde{g}_{1,2}$ are exactly Dirac in our model; the two states are only split by a tiny difference at one loop from the small amount of mixing between the left- and right-handed squarks proportional to μ. Here, however, a modest Majorana mass could be tolerated, since the only effect would be to split the eigenstates and so be distinguishable in a detector as separate particles: in our benchmarks they shall be indistinguishable. Interestingly, in our model the octet fermion χ_O only couples to the scalar octets, gluino and gluons. Hence the two gluino mass eigenstates, $\tilde{g}_1, \tilde{g}_2 = \frac{1}{\sqrt{2}}(\lambda_3 + \chi_O), \frac{i}{\sqrt{2}}(\lambda_3 - \chi_O)$, couple only to the squarks and quarks through the component λ_3, and their couplings are the same up to a factor of i. This means that over the parameter space, their decays are *almost* identical, meaning that together they behave like a purely Dirac gluino—except for when the decay is highly non-relativistic.

In the model presented, the only relevant non-relativistic two-body decays of a gluino are when a squark becomes nearly degenerate with it; and so to obtain differences between $\tilde{g}_1$ and $\tilde{g}_2$ decays one would furthermore need a sizeable source of R-symmetry breaking, which means squark mixing. One can therefore expect a sizeable difference between the two gluino decays into stops or sbottoms only near the kinematic limit. This can be seen as follows: for a two-body decay $\tilde{g}_i \to q\tilde{q}$ for $i = 1, 2$ the couplings can be written (suppressing the gauge and Lorentz indices) as

$$\mathcal{L} \supset -\sqrt{2}g_3\tilde{q}_L^* q_L \lambda_3 + \sqrt{2}g_3\bar{q}_R\tilde{q}_R\bar{\lambda}_3 \qquad (3.1.4)$$

and so if $\tilde{q}_L = \cos\theta_q\tilde{q}_1 + \sin\theta_q\tilde{q}_2$, $\tilde{q}_R^* = -\sin\theta_q\tilde{q}_1 + \cos\theta_q\tilde{q}_2$, then the coupling to say $\tilde{q}_1$ is

$$\mathcal{L} \supset -\tilde{q}_1^*\Big[c_L^i(q\tilde{g}_i) + c_R^i(\bar{q}\bar{\tilde{g}}_i)\Big], \qquad c_L^1 = \sqrt{2}g_3\cos\theta_q, \quad c_R^1 = -\sqrt{2}g_3\sin\theta_q, \qquad (3.1.5)$$

while $c_L^2 = -ic_L^1, (c_R^2)^* = -ic_R^1$. The width for the gluino decays is then

$$\Gamma(\tilde{g}_i \to q\tilde{q}_i) = \frac{K}{32\pi m_{\tilde{g}_i}^3}\Big[(m_{\tilde{g}_i}^2 + m_q^2 - m_{\tilde{q}_i}^2)(|c_L|^2 + |c_R|^2) + 2m_q m_{\tilde{q}_i}(c_L^* c_R + c_R^* c_L)\Big],$$

$$K \equiv \sqrt{(m_{\tilde{g}}^2 - m_q^2 - m_{\tilde{q}_i}^2)^2 - 4m_q^2 m_{\tilde{q}_i}^2}. \tag{3.1.6}$$

So then when $m_{\tilde{g}_i} \sim m_q + m_{\tilde{q}_i}, m_{\tilde{q}_i} \gg m_q$, one has $(m_{\tilde{g}_i}^2 + m_q^2 - m_{\tilde{q}_i}^2) \simeq 2m_q m_{\tilde{q}_i}$ and

$$\Gamma(\tilde{g}_i \rightarrow q\tilde{q}_i) \simeq \frac{K m_q g_3^2}{16\pi m_{\tilde{g}_i}^2} \left[1 \pm 2\cos\theta_q \sin\theta_q \right]. \tag{3.1.7}$$

Hence for maximal squark (stop or sbottom) mixing there is a complete suppression of one of the decays in this limit.

For three-body decays of a gluino to neutralinos and quarks, it shall be argued below that in this model the neutralinos should be light, and so even though the neutralinos themselves significantly break the R-symmetry through their mixings, the quarks/neutralinos should be relativistic and one should not see a significant difference between the two gluino components.

3.1.4 Model constraints

The model constraints in the MDGSSM have largely been covered in previous sections, but the most important will be summarised below. As mentioned above, the limits on gluino and (first/second generation) squark masses depend on the other parameters in the model, in particular the mass of the lightest supersymmetric partner, but also on the details of the decay chains. In the (phenomenological) MSSM, it is reasonable to consider the bino/wino/higgsino masses as free parameters. However, in the MDGSSM (and in DG models generally) these have a large effect on the Higgs mass at tree level. Indeed, it is well known that in the supersoft limit the Higgs D-term potential is erased [77]; and a large μ-term has a similar effect. Moreover, the singlet and triplet scalars obtain tree-level masses m_{SR}, m_{TP} proportional to the Dirac mass terms:

$$m_{SR}^2 = m_S^2 + 4|m_{DY}|^2 + B_S, \qquad m_{TP}^2 = m_T^2 + 4|m_{D2}|^2 + B_T,$$

and so if m_{DY} or m_{D2} are large then the scalar singlet/triplet should be heavy. If then they are integrated out, then the correction to the Higgs quartic coupling is

$$\delta\lambda \sim \mathcal{O}\left(\frac{g_Y m_{DY}}{m_{SR}}\right)^2 + \mathcal{O}\left(\frac{\sqrt{2}\lambda_S m_{DY}}{m_{SR}}\right)^2 + \mathcal{O}\left(\frac{g_2 m_{D2}}{m_{TP}}\right)^2 + \mathcal{O}\left(\frac{\sqrt{2}\lambda_T m_{D2}}{m_{TP}}\right)^2, \tag{3.1.8}$$

with the exact expressions for the Two-Higgs Doublet model parameters are given in (2.3.11) and appendix B. This means that the singlet and triplet scalars need to be made heavy *relative to the gauginos and higgsinos* in order to not suppress the Higgs mass or even render the potential unstable. Without removing the scalars from the spectrum entirely and losing all trace of naturalness, this means keeping the gauginos/higgsinos well below a TeV.

The scalar triplet fields are well-known to generate a shift to the electroweak ρ-parameter at tree-level, with the electroweak precision constraints on the model stipulated in section 2.5. The experimental best fit value for ρ (2.5.4) is satisfied by taking $m_{TP} \gtrsim 2$ TeV for typical values of $\mu, m_{D2} \sim 500$ GeV. Numerically it is found hard to find satisfactory parameter points for gaugino/higgsino masses of $\mathcal{O}(\text{TeV})$ and so in the benchmark points here they shall be taken to be only a few hundred GeV.

On the other hand, in the decoupling limit, the light Higgs mass is given by

$$m_{h_1}^2 \simeq M_Z^2 c_{2\beta}^2 + \frac{(\lambda_S^2 + \lambda_T^2)}{2} v^2 s_{2\beta}^2 + ..., \tag{3.1.9}$$
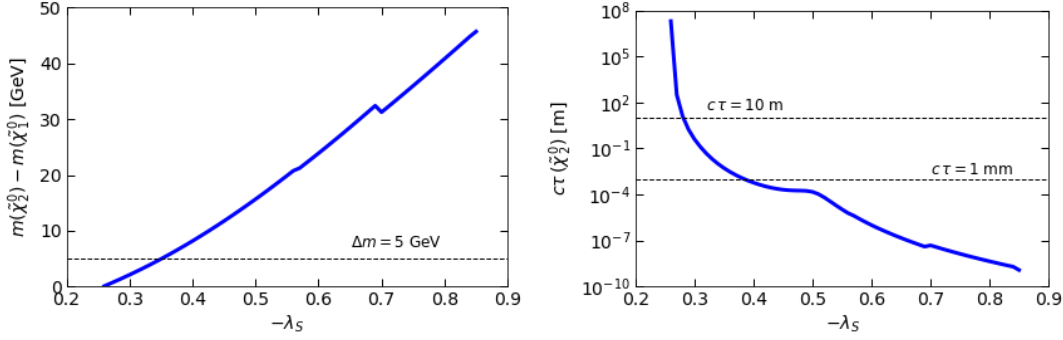
Figure 3.2: Influence of λ_S on the mass splitting between the two bino-like mass eigenstates $\tilde{\chi}^0_{1,2}$ (left) and on the lifetime of the $\tilde{\chi}^0_2$ (right) for the parameters of eq. (3.2.1) and $\tan\beta = 2$.

with the full expression for the tree-level Higgs mass given in (2.2.25), and so taking small $\tan\beta$ and moderate values of λ_S, λ_T the Higgs mass can be enhanced at tree-level without having exceptionally heavy stops (given that the stop mixing will be small in the absence of SUSY-breaking trilinear couplings).

3.2   Benchmark scenarios

It has been argued that a typical MDGSSM scenario should have electroweakinos of $\mathcal{O}(500)$ GeV, a triplet scalar heavier than 2 TeV, and if one wants to enhance naturalness of the model (avoiding stop masses larger than $\mathcal{O}(10)$ TeV), small $\tan\beta$ and $2(\lambda_S^2 + \lambda_T^2) > g_Y^2 + g_2^2$. For the sake of simplicity, and since there is no reason to suspect a large splitting of left- and right-chiral squarks, the equivalencies $m_{Q_i}^2 = m_{U_i}^2 = m_{D_i}^2$ are taken, as well as a common value for the first two generations, while allowing the third generation squark masses to vary so as to obtain the correct Higgs mass (some stop contribution is necessary unless large values of λ_S, λ_T are chosen).

To quantitatively investigate how this influences the LHC limits, four benchmark scenarios are chosen with different values of λ_S, λ_T. Concretely the limit $m_{DY} < \mu < m_{2D}$ is taken with, for the first three benchmarks,

$$m_{DY} = 200 \text{ GeV}, \quad \mu = 400 \text{ GeV}, \quad m_{D2} = 500 \text{ GeV}. \qquad (3.2.1)$$

Moreover, to favour a large tree-level boost to m_{h_1}, $\tan\beta = 2$ is taken. This gives a hierarchical spectrum of bino-, higgsino- and wino-like states with masses of about 200, 400 and 500 GeV, respectively. Finally, $\lambda_T = 0.2$ is set and two values of λ_S, $\lambda_S = -0.27$ and -0.74 are chosen, to have cases with small and sizeable $\tilde{\chi}^0_{1,2}$ mass splittings. The dependence of the $\tilde{\chi}^0_{1,2}$ mass splitting and the $\tilde{\chi}^0_2$ lifetime on λ_S is shown in Fig. 3.2.

With this setup, the masses of gluinos and squarks are treated as free parameters (m_{3D} and a scalar soft mass-squared parameter), while the masses of the 3rd generation squarks are adjusted such that $m_{h_1} \in [123, 127]$ GeV. The calculation of the mass spectrum and decay branching ratios is done with SARAH [165, 165, 166, 193–195] and SPheno [196], including Higgs mass calculation at the 2-loop level [167–169]. Three distinct cases are considered:[2]

$$\text{DG1}: \quad \lambda_S = -0.27; \; m_{\tilde{t}} \sim m_{\tilde{b}} \sim 3.6 \text{ TeV}, \qquad (3.2.2)$$

---

[2]It should be noted that no dark matter constraints are considered here. This is justified as this work is interested in unequivocal collider constraints on the coloured sector without assumptions

Parameters				
	DG1	DG2	DG3	DG4
m_{1D}	200	200	200	200
m_{2D}	500	500	500	1175
μ	400	400	400	400
$\tan\beta$	2	2	2	2
$-\lambda_S$	0.27	0.74	0.74	0.79
$\sqrt{2}\,\lambda_T$	0.14	0.14	0.14	-0.26
$m_{\tilde{Q}_3}^2$	1.25e7	6.5e6	2.26e6	8.26e6
$m_{\tilde{Q}_1}^2$	6.25e6	6.25e6	6.25e6	6.25e6
m_{3D}	1750	1750	1750	1750

Masses				
	DG1	DG2	DG3	DG4
$\tilde{\chi}_1^0$	201.35	182.1	181.8	182.4
$\tilde{\chi}_2^0$	201.72	218.0	216.6	213.2
$\tilde{\chi}_3^0$	403	400	396	408
$\tilde{\chi}_4^0$	419	445	441	437
$\tilde{\chi}_5^0$	537	536	535	1226
$\tilde{\chi}_6^0$	548	548	546	1227
$\tilde{\chi}_1^\pm$	400	395	391	398
$\tilde{\chi}_2^\pm$	536	536	534	1224
$\tilde{\chi}_3^\pm$	549	548	547	1229
$\tilde{t}_1$	3604	2607	1590	2894
$\tilde{t}_2$	3613	2637	1613	2927
h_1	124.0	125.0	125.3	125.2

Table 3.1: Parameters and masses (in GeV) of the four benchmark scenarios; m_{1D}, m_{2D}, μ, $\tan\beta$, λ_S, λ_T and the soft masses of the third generation ($m_{\tilde{Q}_3}^2 = m_{\tilde{U}_3}^2 = m_{\tilde{D}_3}^2$) are fixed for each benchmark, while m_{3D} and $m_{\tilde{Q}_1}^2 = m_{\tilde{U}_1}^2 = m_{\tilde{Q}_1}^2$ will be varied to scan over gluino and squark masses. The sgluons have masses of about 1.6 and 3.9 TeV and play no role for the phenomenology discussed here.

$$\text{DG2}: \quad \lambda_S = -0.74; \; m_{\tilde{t}} \sim m_{\tilde{b}} \sim 2.6\,\text{TeV}, \tag{3.2.3}$$

$$\text{DG3}: \quad \lambda_S = -0.74; \; m_{\tilde{t}} \sim m_{\tilde{b}} \sim 1.6\,\text{TeV}. \tag{3.2.4}$$

For DG1 with $\lambda_S = -0.27$, the two bino-like mass eigenstates $\tilde{\chi}_{1,2}^0$ are quasi-degenerate with sub-GeV mass splitting, and the $\tilde{\chi}_2^0$ has a mean decay length of nearly 3 km, so that it will appear as a co-LSP. For $\lambda_S = -0.74$ (DG2 and DG3), the two bino-like mass eigenstates $\tilde{\chi}_{1,2}^0$ have masses of about 182 GeV and 216–218 GeV, respectively, and the $\tilde{\chi}_2^0$ decays promptly into $\tilde{\chi}_1^0 f\bar{f}$ via an off-shell Z.

Since the main interest is in gluino and squark cascade decays, a fourth benchmark is also considered with heavy winos by moving m_{2D} above 1 TeV, thus on the one hand somewhat suppressing decays into wino-like states, and on the other hand changing the kinematic distributions of such cascades. Concretely,

$$\text{DG4}: \quad m_{1D} = 200 \text{ GeV}, \; \mu = 400 \text{ GeV}, \; m_{2D} = 1175 \text{ GeV},$$
$$\lambda_S = -0.79, \; \lambda_T = -0.37, \; m_{\tilde{t}} \sim m_{\tilde{b}} \sim 3\,\text{TeV}. \tag{3.2.5}$$

The main parameters and resulting masses for the four benchmark scenarios are summarised in Table 3.1. Examples of gluino and squark decay branching ratios are given in Table 3.2 and compared to the branching ratios in the MSSM with an equivalent bino/wino/higgsino spectrum.

The complete SLHA spectrum files produced with `SARAH/SPheno` are available at [197].[3] Note here, that these conventions differ (as usual) from the `SARAH DiracGauginos`

---

on the cosmological history of the universe. For a discussion of DG dark matter within standard cosmology, see [83].

[3]For the sake of reproducibility of these results, the `SPheno` model and input files are provided, as well as the UFO model and two helpful scripts for modifying the `SPheno` .spc files so they can be used for event generation with `MadGraph/Pythia`.

	DG1	DG2	DG3	DG4	MSSM1	MSSM4
Gluino decays, $m_{\tilde{g}} \approx 2$ TeV, $m_{\tilde{q}} \approx 2.6$ TeV						
$\tilde{g} \to q\bar{q} + \text{binos}$	12%	6%	–	18%	10%	15%
$\tilde{g} \to b\bar{b} + \text{binos}$	–	1%	–	6%	–	1%
$\tilde{g} \to t\bar{t} + \text{binos}$	1%	4%	–	6%	1%	3%
$\tilde{g} \to (q\bar{q}^{(')}, b\bar{b}) + \text{heavy EW-inos}$	66%	36%	–	13%	66%	19%
$\tilde{g} \to (t\bar{t}, t\bar{b}, b\bar{t}) + \text{heavy EW-inos}$	20%	53%	–	61%	23%	62%
$\tilde{g} \to t + \tilde{t}_{1,2}$	–	–	48%	–	–	–
$\tilde{g} \to b + \tilde{b}_{1,2}$	–	–	52%	–	–	–
Squark decays, $m_{\tilde{q}} \approx 2$ TeV, $m_{\tilde{g}} \approx 2.6$ TeV						
$\tilde{q}_R \to q + \text{binos}$	99%	99%	98%	99%	92%	92%
$\tilde{q}_L \to q + \text{heavy EW-inos}$	99%	99%	99%	97%	98%	97%

Table 3.2: Branching ratios of gluino and squark decays for DG1–DG4. For gluino decays the mass hierarchy $m_{\tilde{q}} < m_{\tilde{g}_{1,2}}$ is considered, and for squark decays the mass hierarchy $m_{\tilde{g}_{1,2}} > m_{\tilde{q}}$. The columns MSSM1 and MSSM4 give the comparison to the equivalent MSSM case with $M_1 = 200$ GeV, $\mu = 400$ GeV and $M_2 = 500$ GeV (MSSM1) or 1200 GeV (MSSM4); third generation squark masses are about 3.6 TeV for MSSM1 and 3 TeV for MSSM4, while $\tan\beta = 10$ and $A_t = -4$ TeV to achieve $m_{h_1} \approx 125$ GeV.

implementation. Used here are

Parameter	SARAH convention
λ_S	$-\texttt{lam}$
λ_T	$\texttt{LT}/\sqrt{2}$

$$. \tag{3.2.6}$$

Scenarios DG1, DG2 and DG3 have heavy stops and sbottoms, so the gluino branching ratios in Table 3.2 will not change significantly with the gluino mass in the region accessible with current LHC data, as long as $m_{\tilde{g}} < m_{\tilde{q}}$ (if $m_{\tilde{g}} > m_{\tilde{q}}$, then of course $\tilde{g} \to q\tilde{q}$ decays dominate). This is different for DG3 which has stops and sbottoms at about 1.6 TeV. Here the gluino branching ratios vary a lot with $m_{\tilde{g}}$ up to 2 TeV, as shown in Fig. 3.3. Note that in this figure the $\text{BR}(\tilde{g}_1)$ and $\text{BR}(\tilde{g}_2)$ are averaged over because R-symmetry breaking effects lead to differences in $\tilde{g}_1$ and $\tilde{g}_2$ decays near the threshold where 2-body decays into sbottoms/stops become kinematically allowed. These differences are however experimentally not observable.

3.3   Simplified model limits

Within the MSSM, ATLAS and CMS have excluded gluino (light-flavor squark) masses up to about 1800–2025 (1550) GeV assuming decoupled squarks (gluinos) and a single decay channel into the neutralino LSP with 100% branching ratio [69, 70]. In the DG case, the twice as large gluino production cross-section should increase the gluino mass limit by about 150–200 GeV; the bound on squark masses remains the same, since the quoted MSSM limit is already for decoupled gluinos.

The constraints which can be derived in the context of such "simplified models" considerably weaken in realistic scenarios where the gluinos (squarks) share out their
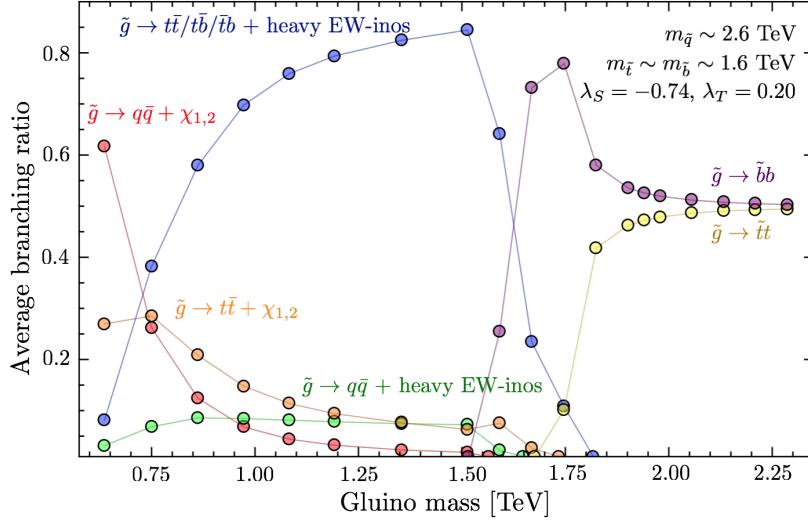
Figure 3.3: Branching ratios of gluino decays (averaged over $\tilde{g}_1$ and $\tilde{g}_2$) for DG3 as function of the gluino mass, for $m_{\tilde{q}} \approx 2.6$ TeV.

branching ratios over several decay channels [198].[4] For instance, if $\mathrm{BR}(\tilde{g} \to q\bar{q}\tilde{\chi}_1^0) = 0.1$, only 1% of the total gluino-pair production is constrained by the $pp \to \tilde{g}\tilde{g}$, $\tilde{g} \to q\bar{q}\tilde{\chi}_1^0$ simplified model upper limits. Likewise, if $\tilde{q}_L$ decay via heavy EW-inos, only $\tilde{q}_R^* \tilde{q}_R$ production is effectively constrained by the $pp \to \bar{\tilde{q}}\tilde{q}$, $\tilde{q} \to q\tilde{\chi}_1^0$ simplified model limits. On the other hand, the production cross-sections themselves can be [much] larger than in the simplified model picture, if gluino (squark) contributions to squark (gluino) production are not decoupled in the parameter space one is interested in.

To illustrate explicitly the consequences for our benchmark scenarios, gluino and squark masses are scanned over for two cases, DG1 and DG3, and evaluate the simplified model constraints with SModelS [199, 200]. Here the v1.1.2 database of SModelS is used, which includes the Run 2 SUSY search results for 36 fb^{-1} from CMS as detailed in [201]. The decay branching ratios are again computed with SARAH/SPheno. Cross-sections are computed at leading order with MadGraph5_aMC@NLO [202] using the Dirac gaugino UFO model of [165]. (The effect of higher-order corrections will be commented on in the next section.)

The result is shown in Fig. 3.4. For DG1, when $m_{\tilde{g}} < m_{\tilde{q}}$ the strongest constraint comes from the $pp \to \tilde{g}\tilde{g}$, $\tilde{g} \to q\bar{q}\tilde{\chi}_1^0$ simplified model (denoted as T1) and excludes gluino masses up to about 1250 GeV for LO cross-sections. When $m_{\tilde{q}} < m_{\tilde{g}}$, the strongest constraint mostly comes from the $pp \to \tilde{q}\tilde{q}^{(*)}$, $\tilde{q} \to q\tilde{\chi}_1^0$ simplified model (denoted as T2), excluding squark masses up to roughly 1300 GeV as long as the gluino is not too heavy. In the equivalent MSSM case (MSSM1 scenario in Table 3.2), the gluino mass limit would be only 1 TeV due to the smaller gluino pair-production cross-section while, conversely, the squark mass limit would be about 2 TeV for 2.6 TeV gluinos.

For DG3, which has stops around 1600 GeV and a $\tilde{\chi}_2^0$–$\tilde{\chi}_1^0$ mass splitting of about 35 GeV, the picture changes. On the one hand, over a large part of the region with $m_{\tilde{g}} < m_{\tilde{q}}$, the strongest constraint now comes from the $pp \to \tilde{g}\tilde{g}$, $\tilde{g} \to t\bar{t}\tilde{\chi}_1^0$ simplified model (denoted as T1tttt). Moreover, and more importantly, gluino and squark decays via the bino-like $\tilde{\chi}_2^0$ are followed by $\tilde{\chi}_2^0 \to \tilde{\chi}_1^0 f\bar{f}$ via an off-shell Z, which is a different

---

[4]This is in particular the case if only cross-section upper limits are available for simplified model spectra. Efficiency maps for all signal regions for a large enough set of simplified models would allow us to combine the contributions from different signal topologies in the simplified model approach [199].
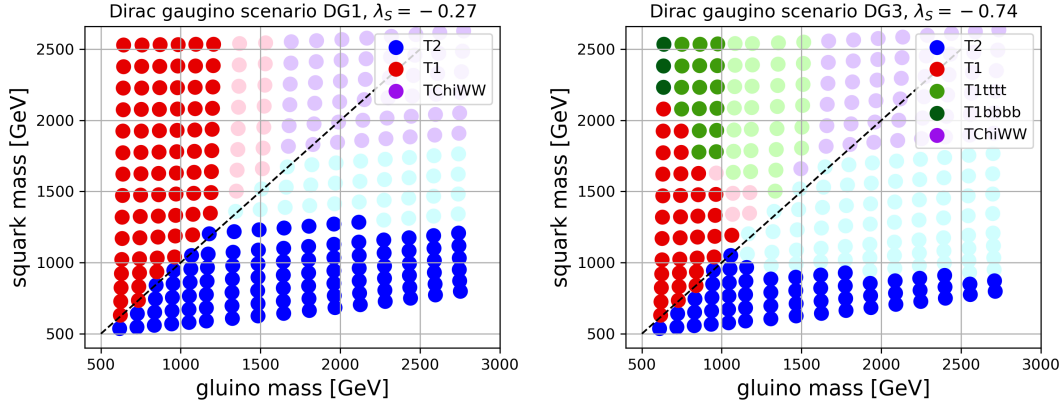
Figure 3.4: `SModelS` constraints in the gluino versus squark mass plane, on the left for DG1, on the right DG3. The colour code denotes the simplified model which gives the strongest constraint (T1: $pp \to \tilde{g}\tilde{g}$, $\tilde{g} \to q\bar{q}\tilde{\chi}_1^0$; T1tttt: $pp \to \tilde{g}\tilde{g}$, $\tilde{g} \to t\bar{t}\tilde{\chi}_1^0$; T2: $pp \to \tilde{q}\tilde{q}^{(*)}$, $\tilde{q} \to q\tilde{\chi}_1^0$; TChiWW: $pp \to \tilde{\chi}_i^\pm \tilde{\chi}_i^\pm$, $\tilde{\chi}_i^\pm \to W^\pm \tilde{\chi}_1^0$). Full-colour (non-transparent) points are excluded by `SModelS`, while light-shaded points escape the simplified model limits.

topology in the simplified model picture.[5] This drastically reduces the effective cross-section ($\sigma \times$ BRs) that goes into the T1, T1tttt or T2 topologies. Consequently, the excluded region is noticeably smaller for DG3 than for DG1, with a gluino mass limit of only 1 TeV (corresponding to the factor 2 reduction of the T1 cross-section which is also seen in the comparison between DG1 and MSSM1 above), and a squark mass limit below 1 TeV.

It is also worth pointing out that for heavy gluinos and squarks, the effective T1(tttt) or T2 cross-sections become too small and electroweak production of charginos followed by $\tilde{\chi}_i^\pm \to W^\pm \tilde{\chi}_1^0$ decays (denoted as TChiWW) takes over as the most constraining simplified model signature. Note however that TChiWW upper limit maps are available for 8 TeV only—neither ATLAS nor CMS have provided them for the 13 TeV data—and do not exclude any of the scan points.

3.4   Recast of the ATLAS multi-jet plus E_T^{miss} analysis

From the above discussion it is clear that the simplified model limits are not sufficient for constraining complex scenarios as the ones considered here. Instead, a full recasting of the experimental search(es) is necessary to derive the true exclusion limit. To this end, the ATLAS multijet search [69] was implemented in `MadAnalysis 5` [203–205]. This is a generic search for squarks and gluinos in final states with jets and large missing transverse momentum, E_T^{miss}, using 36 fb^{-1} of $\sqrt{s} = 13$ TeV pp collision data. It employs two approaches: one referred to as Meff-based search and a second, complementary search using the recursive jigsaw reconstruction technique.

Here only the Meff-based analysis is used, which comprises 24 inclusive signal regions characterised by a minimum required jet multiplicity of two, four, five or six jets with transverse momenta $p_T > 50$ GeV. The missing energy of the event must be larger than 250 GeV, and events with a baseline electron or muon with $p_T > 7$ GeV are vetoed. Signal regions requiring the same jet multiplicity are distinguished by

---

[5]In `SModelS` txname notation, these would be constrained by, e.g., T5ZZoff or T6ZZoff results, which are however not available.
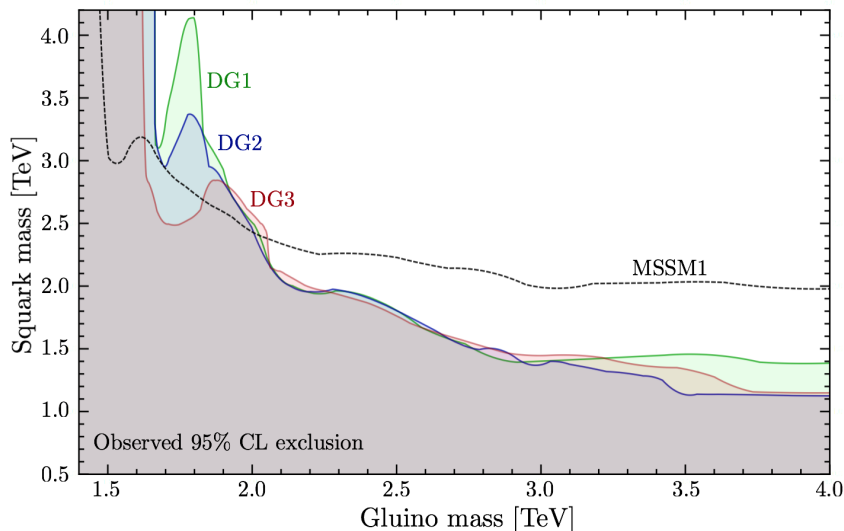
Figure 3.5: 95% CL exclusion limits in the gluino vs. squark mass plane for DG1 (green), DG2 (blue) and DG3 (red) contrasted with MSSM1 (black dashed line), derived from the recasting of the ATLAS 2–6 jets + E_T^{miss} analysis for 36 fb^{-1} at $\sqrt{s} = 13$ TeV. Only the most sensitive (=best expected) signal region is used for the limit setting.

increasing background rejection through cuts in variables like the p_T of the leading jets, $\Delta\Phi$ between jets and E_T^{miss}, and the effective mass variable M_{eff} [206] (defined as the scalar sum of the p_T of the leading jets and the E_T^{miss}), among others. Of these 24 signal regions, 22 are implemented in the `MadAnalysis 5` recast code, which is publicly available as [207] and part of the `MadAnalysis 5` Public Analysis Database [205]. Two additional signal regions using larger-radius jets (dubbed 2jB-1600 and 2jB-2400 in the ATLAS paper) are not included as a good enough agreement with the validation material provided by ATLAS could not be reached.

To evaluate the sensitivity of this search to gluinos and squarks in the Dirac gaugino model, a scan is performed over gluino and light-flavor squark masses for the four benchmark scenarios of section 3.2. For each scan point, 30K events are simulated with `MadGraph5_aMC@NLO` [202], including all $2 \rightarrow 2$ SUSY production processes in pp collisions at 13 TeV using `nn23lo1` PDFs. Decays, parton shower and hadronization are done in `Pythia 8.2` [208] and the simulation of the ATLAS detector with `Delphes 3` [209]. Finally the events are analysed with `MadAnalysis 5` and an exclusion confidence level (CL) is computed with the CL$_s$ technique [150]. See [210] for a comprehensive introduction to recasting with `MadAnalysis 5`, explaining the full procedure. Note that in each scan point only the "best" (i.e. the statistically most sensitive) signal region is used for limit setting.[6]

Let us start with the light wino scenarios. Figure 3.5 shows the resulting 95% CL exclusion lines in the gluino vs. squark mass plane for DG1, DG2, DG3 and MSSM1. As can be seen, for $m_{\tilde{g}} \approx m_{\tilde{q}}$, the limit is about 2.1 TeV for both gluino and squark masses in all DG benchmark scenarios. For 4 TeV gluinos, the squark mass limit is about 1.4 TeV in the least favourable DG case (DG1), decreasing to about 1.1– 1.15 TeV for DG2 and DG3, where $\tilde{\chi}_2^0 \rightarrow Z^* \tilde{\chi}_1^0$ decays appear in the squark decay chains. (The comparison with the MSSM will be done at the end of this section.)

The gluino mass limit in the region $m_{\tilde{q}} > m_{\tilde{g}}$ depends more sensitively on the

---

[6]Since the signal regions are inclusive (= overlapping) they actually cannot be combined.

assumed DG scenario. While a robust limit of $m_{\tilde{g}} \gtrsim 1.65$ TeV is found for very heavy squarks in all cases, one also observes different "dips" in the exclusion contours for the different benchmark scenarios. To understand the shape of the exclusion contour, it is instructive to consider which signal regions are used for the limit setting and how the various production modes contribute to the final CLs value. To this end, Fig. 3.6 shows the CLs values in the best signal region from various proton-proton processes as a function of gluino mass, for medium heavy squarks of $m_{\tilde{q}} \sim 2.6$ TeV.

One sees that the best signal region switches from 6j-Meff-1800 (6 jets, $M_{\text{eff}} > 1800$ GeV) to 6j-Meff-2600 (6 jets, $M_{\text{eff}} > 2600$ GeV) at different values of gluino mass for the three benchmark scenarios. In particular for DG3 this leads to the exclusion CL dropping below 0.95 for $m_{\tilde{g}} \sim 1.7$ TeV, where gluino decays into 3rd generation squarks become dominant, and getting back above 0.95 for $m_{\tilde{g}} \sim 1.8$–2 TeV. Moreover, one observes that taking into account gluino-pair production would only give a bound of $m_{\tilde{g}} \gtrsim 1.65$–1.7 TeV, as is also found in the limit of heavy squarks in Fig. 3.5. The inclusion of both gluino-pair and gluino-squark production is essential for a correct limit setting.[7]

Next, a comparison in Fig. 3.7 shows the CLs values in different signal regions for DG1 and DG3. In order to cut across the dip-peak features in the exclusion contours, chosen here are $m_{\tilde{q}} \sim 3.6$ TeV for DG1 and $m_{\tilde{q}} \sim 2.6$ TeV for DG3. One sees again that for relatively light gluinos the best signal region is 6j-Meff-1800 and the observed CL value drops below 0.95 for gluino masses around 1.65 TeV. The 6j-Meff-2600 signal region, on the other hand, excludes higher gluino masses, up to about 1.8 TeV in DG1 with $m_{\tilde{q}} \sim 3.5$ TeV, and up to about 2 TeV in DG3 with $m_{\tilde{q}} \sim 2.6$ TeV. However, 6j-Meff-2600 becomes the "best" signal region (used for the limit setting in Fig. 3.5) only for gluino masses of 1.8 TeV onwards. This is responsible for the dip-peak structure in the exclusion curve in Fig. 3.5; using only the 6j-Meff-2600 signal region, the gluino mass limit would be stronger.

Turning to the squark exclusion limits, Fig. 3.8 shows the CLs values in the best signal regions as a function of squark mass, for fixed gluino mass. Again only DG1 and DG3 are compared, as DG2 is very similar to the latter. For $m_{\tilde{g}} \sim 2.4$ TeV, signal regions with 4 jets (first 4j-Meff-2600 and then 4j-Meff-3000) exclude squark masses up to 1.9 (1.8) TeV for DG1 (DG3). This is partly due to a substantial contribution from gluino-squark production. As the gluino mass is increased to ~ 4 TeV, both squark-pair and gluino-squark production cross-sections are suppressed, and the best signal region is typically one with only 2 jets. The exception is DG3 with squark masses around 1 TeV, where a 5-jet signal region with rather low M_{eff} cut (5j-Meff-1600) becomes the best one. This is again a consequence of the $\tilde{\chi}_2^0 \to Z^* \tilde{\chi}_1^0$ decays, which are present in DG3 (and DG2) but not in DG1.

---

[7]This was also pointed out in [198] in the context of simplified model limits.
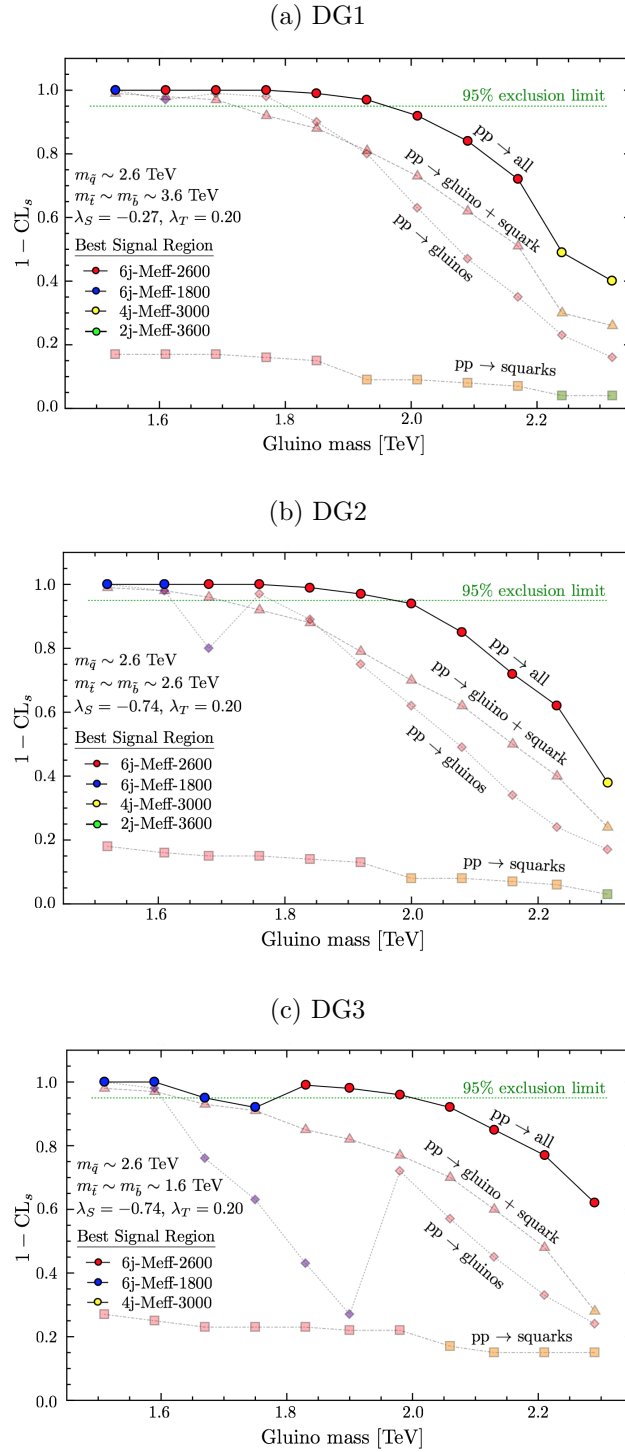
Figure 3.6: 1-CLs values in the best signal regions from all proton-proton processes as a function of gluino mass for (a) DG1, (b) DG2, (c) DG3; $m_{\tilde{q}} \sim 2.6$ TeV in all three cases. Individual contributions to the total CLs (denoted by the solid black line labelled $pp \rightarrow$ all) are given by the faint dashed lines, namely gluino-pair production (diamonds); squark-pair production (triangles) and gluino-squark production (squares). The best signal region at each gluino mass value is identified by the colour code as indicated in the plot legends.
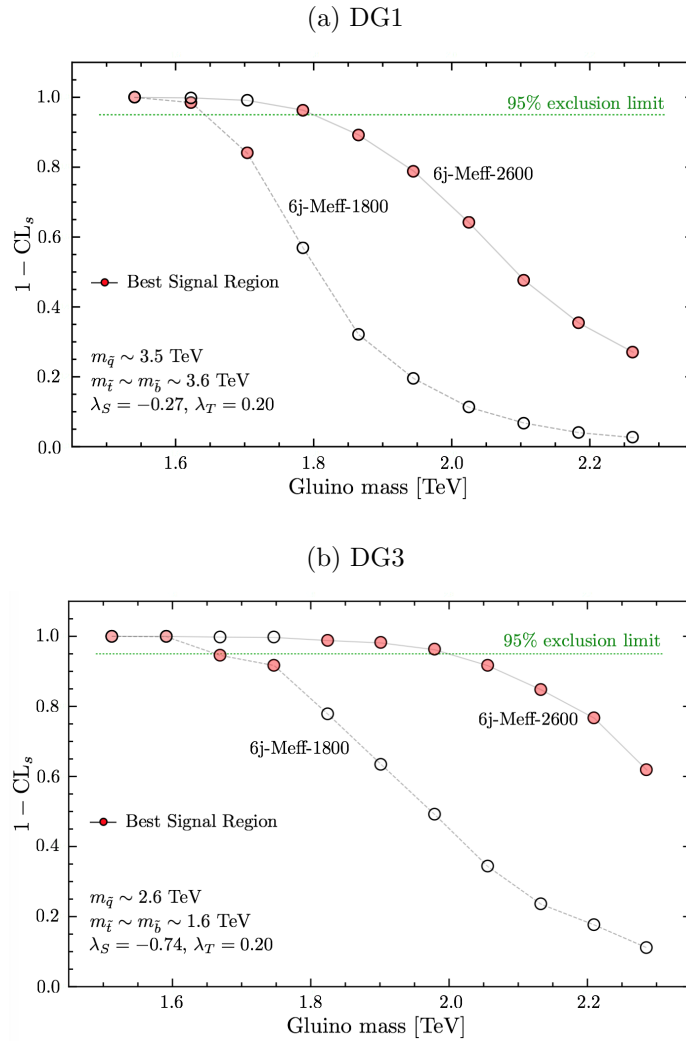
(a) DG1

(b) DG3

Figure 3.7: Comparison of 1-CLs values in the 6j-Meff-1800 and 6j-Meff-2600 signal regions as a function of gluino mass, for (a) DG1 with $m_{\tilde{q}} \sim 3.6$ TeV and (b) DG3 with $m_{\tilde{q}} \sim 2.6$ TeV. The best signal region is identified by full red circles.
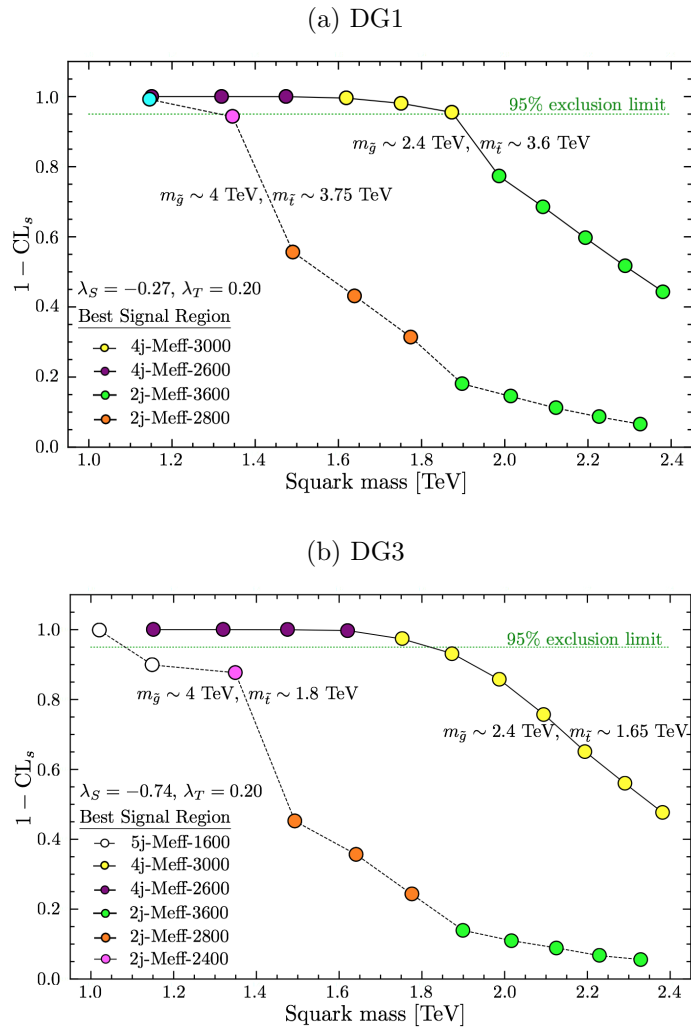
Figure 3.8: 1-CLs values in the best signal regions from all proton-proton processes as a function of squark mass for (a) DG1 and (b) DG3. The solid lines are for $m_{\tilde{g}} \sim 2.4$ TeV, while the dashed lines are for $m_{\tilde{g}} \sim 4$ TeV. (Since the input parameters are the soft masses, $m_{\tilde{t}}$ and $m_{\tilde{b}}$ vary slightly in the two cases.)
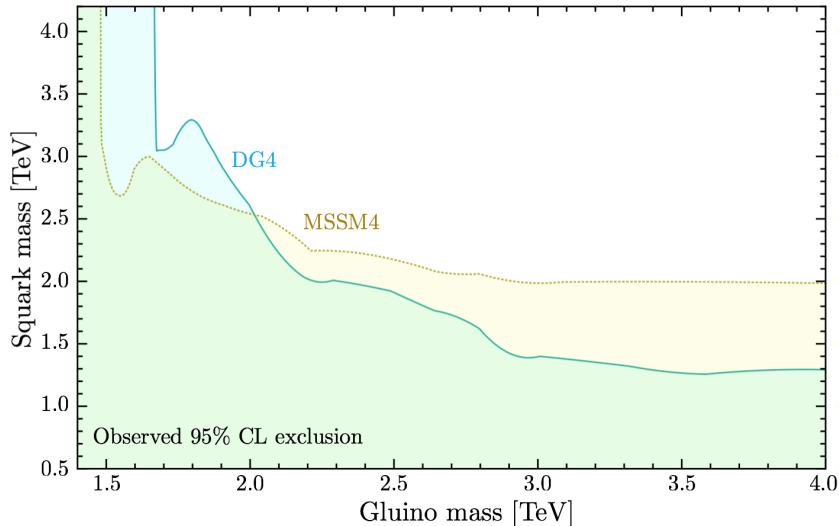
Figure 3.9: 95% CL exclusion limits in the gluino vs. squark mass plane for DG4, and comparison to MSSM4.

Comparing all this to the equivalent MSSM1 scenario, one sees the expected ~ 200 GeV lower gluino mass limit; the squark mass limit is however considerably stronger when gluinos are heavy, still reaching $m_{\tilde{q}} \gtrsim 2$ TeV for 4 TeV gluinos, as Majorana gluinos decouple very slowly.

Last but not least let us explore the role of light or heavy winos appearing in the decay chains. To this end, Fig. 3.9 shows the 95% CL exclusion limits in the gluino vs. squark mass plane for the DG4 and MSSM4 scenarios, to be compared with the exclusion lines for DG2 and MSSM1 in Fig. 3.5. Interestingly, the results are very similar for heavy and light winos; the main difference is an increase in the squark mass limit by about 100–200 GeV (for fixed gluino mass) when winos are heavy. In particular, $m_{\tilde{q}} \gtrsim 1.3$ TeV at $m_{\tilde{g}} \gtrsim 4$ TeV for DG4, which lies in between the values for DG1 and DG2,3.

Before concluding, a comment is in order on the effect of higher-order corrections. It is well known from the MSSM [211, 212] that K-factors for gluino-pair and gluino-squark production can be very large, of the order of a factor 2–3, depending on the PDF set used; K-factors for squark production are somewhat smaller but still sizeable. For the DG case, the next-to-leading order (NLO) corrections to squark production in the R-symmetric model were computed in [131], with the conclusion that NLO K-factors are generally larger than in the MSSM by the order of 10–20%. Since the cross-section of squark production falls off very steeply with increasing squark mass, K ≈ 2 has only little impact, pushing the gluino mass limit about 100 GeV higher. The higher-order corrections for Dirac gluino final states have not been computed explicitly, but one may assume they are not vastly different from the MSSM. Taking a K-factor of 2–3 as the reference, the gluino mass limit increases by roughly 200 GeV to $m_{\tilde{g}} \gtrsim 2$ TeV for heavy squarks, while for $m_{\tilde{g}} \approx m_{\tilde{q}}$ the limit is pushed to roughly 2.3–2.4 TeV. This is illustrated explicitly for the scenario DG4 in Fig. 3.10.

3.5 Conclusions

Most SUSY searches at the LHC are optimised for the MSSM, where gauginos are Majorana particles. Dirac gauginos are, however, an interesting and theoretically
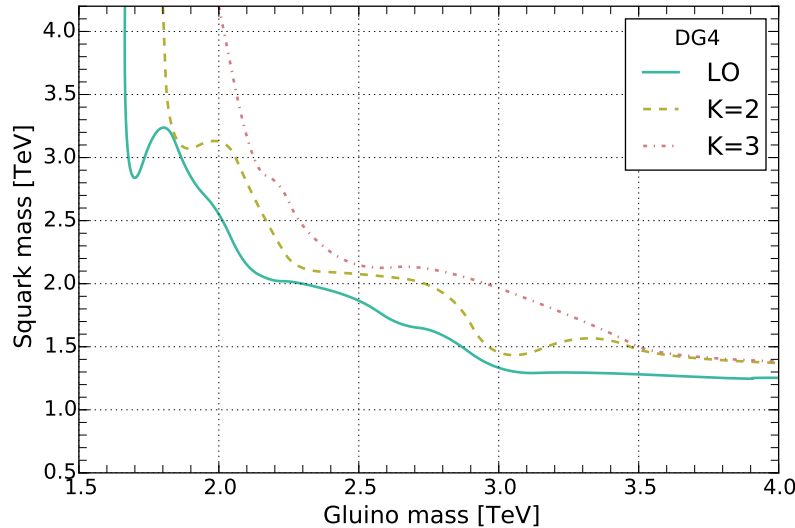
Figure 3.10: 95% CL exclusion limits in the gluino vs. squark mass plane for benchmark DG4 with K-factors 1 (LO), 2 and 3.

well-motivated alternative. Their phenomenological consequences at the LHC include that gluino-pair production is enhanced by a factor 2 as compared to the MSSM, while squark production is strongly suppressed due to a much faster decoupling of the gluino t-channel exchange. Moreover, the extended chargino and neutralino sector present in DG models can have important effects on the collider signatures.

In this paper, bounds from LHC searches on squarks and gluinos have been investigated in the Minimal Dirac Gaugino Supersymmetric Standard Model for several representative benchmark scenarios. Since a typical MDGSSM scenario should have electroweakinos not too far above the electroweak scale, as a primary test case, scenarios with a bino-like LSP around 200 GeV, higgsinos around 400 GeV and winos around 500 GeV were chosen. Thus all charginos and neutralinos may appear in gluino and squark cascade decays. Also considered was a scenario with heavier winos of about 1200 GeV, and these were all compared to the nearest equivalent models in the MSSM.

In the context of simplified model constraints, derived with `SModelS`, the large variety of possible decay modes in our benchmark scenarios led to very weak limits. The reason is, that in complex scenarios like the ones considered here, only a small fraction of the total SUSY production leads to simple signal topologies which are constrained by the available simplified model results.

The benchmark scenarios were then confronted with a full recasting of the ATLAS multi-jet E_T^{miss} search [69] with `MadAnalysis 5`. By comparing the bounds in the DG benchmark scenarios to those in the MSSM, it was confirmed and quantified by how much supersoft models are supersafe: for large gluino masses, the bounds on squarks are very significantly (by several hundred GeV) suppressed compared to the MSSM, and this should have consequences for the naturalness of allowed models. It was shown that this statement is robust even including loop corrections to the production. On the other hand, for smaller gluino masses, the extra degrees of freedom lead to larger production cross-sections, and so the lower limit on the gluino mass in these models is somewhat higher than in the MSSM.

An important feature of the DG case, which was discussed in some detail in this paper, is that the trilinear λ_S and λ_T couplings, which give a tree-level boost to the

light Higgs mass, lead to small mass splittings within the bino and wino states. This is important for LHC phenomenology because, if the mass splitting between the two lightest states (in our benchmark scenarios the two binos) is very small, then the $\tilde{\chi}_2^0$ can live long enough to effectively be a co-LSP on collider scales and appear only as E_T^{miss}. For larger mass splittings, however, the $\tilde{\chi}_2^0$ may decay promptly into $f\bar{f}\tilde{\chi}_1^0$ via an off-shell Z-boson, leading to an additional step in part of the gluino and squark cascade decays. For $m_{\tilde{g}} \approx m_{\tilde{q}}$ this has no noticeable influence on the mass limits. For heavy gluinos or squarks, however, it was shown that the mass limits slightly weaken when λ_S is large. Last but not least, there exists a range of λ_S where the $\tilde{\chi}_2^0$ is a long-lived neutral particle, whose decays can give signatures with displaced vertices. A detailed study of this case is left for future work.

For the sake of reproducibility of our study, ample material is provided on Zenodo [197, 213].

4 – Sleptons without hadrons

4.1 Introduction

Weak-scale supersymmetry, if realised in nature, presents an attractive solution to several longstanding theoretical and observational shortcomings of the Standard Model of particle physics (SM). For example, supersymmetry can protect the Higgs boson mass from large quantum corrections, ensure gauge coupling unification at high scales, and provide a viable weakly interacting dark matter candidate [214,215]. While light, sub-TeV superpartners of quarks and gluons have largely been excluded by direct searches at the CERN Large Hadron Collider (LHC) [69–71, 216], the situation is far less conclusive for electroweak (EW) boson and lepton superpartners due to their smaller production cross sections [217,218]. Current constraints only exclude slepton masses up to a few hundreds of GeV [219,220]. For electroweak boson partners [221–223], the case is slightly more interesting due to several small excesses, which reveal a local significance of 3.5σ and favor $100 - 300$ GeV neutralino and chargino masses in the Minimal Supersymmetric Standard Model (MSSM) [224]. Hence, studies into new analysis strategies that can improve searches for electroweakinos and sleptons are highly motivated.

Among the several promising lines of such investigations are those that consider the impact of jet vetoes (*i.e.*, the rejection of events featuring jets with a transverse momentum greater than some threshold p_T^{Veto} [225–229]) in measurements of and searches for heavy, colorless SM [230–244] and beyond the SM [245–252] states. Interestingly, recent studies of multilepton searches for heavy, colourless exotic particles have demonstrated that dynamic jet vetoes can significantly improve discovery potential [251,252]. More specifically, a proposed analysis premised on setting p_T^{Veto} on an event-by-event basis to the hardness (p_T) of the event's leading lepton was found to improve sensitivity by roughly an order of magnitude. The improvement followed from an increase (relative to a static jet veto) in signal rate passing the jet veto, an ability to veto top quark events without heavy quark flavour-tagging, and a sensitivity to jets misidentified as charged leptons [251].

While serving a similar goal, such a veto functions in a qualitatively different manner than rapidity-dependent vetoes [237, 239, 240] by associating p_T^{Veto} with a measure of the hard process scale Q. A key point is that the improvement, which was demonstrated for both the Drell-Yan (DY) and electroweak boson fusion processes, followed from the veto effectively discriminating local leptonic activity against local hadronic activity [252].

In light of this, this report explores the impact of dynamic jet vetoes on the discovery potential of dimuon plus missing energy searches for right-handed smuon pairs ($\tilde{\mu}_R^+\tilde{\mu}_R^-$) decaying to neutralinos ($\tilde{\chi}_1$) via the DY mode,

$$q\bar{q} \to \gamma^*/Z^{(*)} \to \tilde{\mu}_R^+\tilde{\mu}_R^- \to \mu^+\mu^-\tilde{\chi}_1\tilde{\chi}_1 \ , \tag{4.1.1}$$
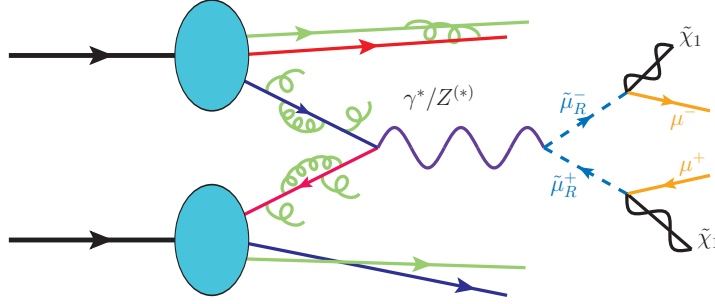
Figure 4.1: Drell-Yan production of a pair of right-handed smuons $(\tilde{\mu}_R^+ \tilde{\mu}_R^-)$ decaying into a pair of muons $(\mu^\pm)$ and lightest neutralinos $(\tilde{\chi}_1)$. Generated with JAXO-DRAW [253].

as illustrated in fig. 4.1. Going beyond refs. [251, 252], which determined only the improved sensitivity of setting p_T^{Veto} to the leading lepton p_T, several complementary measures of local and global leptonic and hadronic activity will be considered, including the scalar sum of the lepton transverse momenta (S_T) as well as the (inclusive) scalar sum of the transverse momenta of hadronic objects (H_T). As a benchmark, a CMS-inspired analysis [219] that features a standard (flavour-independent), static, central jet veto of $p_T^{\text{Veto}} = 25\text{GeV}$ will be used. As will be shown below, a dynamic veto can improve the discovery potential of the analysis in most cases.

The remainder of this report continues in the following manner: in sec. 4.2, a simplified model describing right-handed smuon production and decay in hadron collisions will be introduced, and the present constraints on the model discussed. Section 4.3 will summarise the computational setup, which includes state-of-the-art event generation up to NLO in QCD matched to parton showers (PS). Slepton pair production at the LHC and the qualitative impact of different dynamic jet vetoes for the signal and background processes will then be discussed in sec. 4.4. There the proposed dynamic veto and benchmark collider analyses will also be defined. The results and outlook will be presented in sec. 4.5, before summarising and concluding in sec. 4.6.

4.2   Model

In order to investigate smuon production in a model-independent way, a benchmark simplified model inspired by the MSSM is chosen. An MSSM limit is considered in which all superpartners are decoupled, with the exception of the right-handed smuon $\tilde{\mu}_R$ (of mass $m_{\tilde{\mu}_R}$) and the lightest neutralino $\tilde{\chi}_1$ (of mass $m_{\tilde{\chi}_1}$) that is taken as bino-like. The Lagrangian describing the new physics dynamics of our model is given, using four-component fermion notations, by

$$
\begin{aligned}
\mathcal{L} = {} & \left[\partial_\mu \tilde{\mu}_R^\dagger\right]\left[\partial^\mu \tilde{\mu}_R\right] + \frac{i}{2}\overline{\tilde{\chi}_1}\slashed{\partial}\tilde{\chi}_1 - m_{\tilde{\mu}_R}^2 \tilde{\mu}_R^\dagger \tilde{\mu}_R - \frac{1}{2}m_{\tilde{\chi}_1}\overline{\tilde{\chi}_1}\tilde{\chi}_1 \\
& + \left[\partial^\mu \tilde{\mu}_R^\dagger \tilde{\mu}_R - \tilde{\mu}_R^\dagger \partial^\mu \tilde{\mu}_R\right]\left[ieA_\mu - \frac{ies_W}{c_W}Z_\mu\right] \\
& - \frac{\sqrt{2}e}{c_W}\left[\left(\overline{\tilde{\chi}_1}P_R\mu\right)\tilde{\mu}_R^\dagger + \text{H.c.}\right]
\end{aligned}
\tag{4.2.1}
$$

Here, the smuon gauge interactions with the photon A_μ and Z boson field Z_μ (second line) have been explicitly indicated, as well as the supersymmetric gauge interactions

of the muon μ, the smuon $\tilde{\mu}_R$, and the bino $\tilde{\chi}_1$ (last line). As irrelevant for the purposes of this paper, D-term contributions are neglected. It should also be noted that s_W and c_W are the sine and cosine of the electroweak mixing angle, e is the electromagnetic coupling constant, and P_R the right-handed chirality projector.

Despite its simplicity, the model is only weakly constrained by LHC searches for smuon pair production in the dimuon plus missing transverse energy channel [219]. This is due to large backgrounds, consisting mainly of W boson and top quark pair production, as well as being an electroweak signal production mode, as illustrated by eq. (4.1.1). For a massless neutralino, the smuon mass is constrained with $\mathcal{L} = 39.5$ fb^{-1} of $\sqrt{s} = 13$TeV data to satisfy, at the 95% confidence level (CL), $m_{\tilde{\mu}_R} > 220$GeV. There is almost no constraint when the neutralino is heavier than 100GeV.

As the neutralino is stable, it is a viable candidate for a dark matter particle. Bino dark matter with light sleptons can be accommodated provided that the slepton-neutralino mass splitting is of at most 10% of the neutralino mass. Under this condition, there are sufficient co-annihilations so that the universe is not overclosed [254]. However, in the aim of using simplified models as tools for characterising given phenomena, this latter constraint is ignored.

4.3 Computational Setup

To conduct the study, signal and background events in pp collisions at a center-of-mass energy $\sqrt{s} = 14$TeV are simulated and analysed. The simplified model Lagrangian of eq. (4.2.1) is implemented into FEYNRULES [255], that is jointly used with the NLOCT [256] and FEYNARTS [257] packages to generate a UFO library [258] that includes tree-level vertices as well as ultraviolet and R_2 counterterms. This enables numerical computations up to one-loop in the strong coupling constant α_s. Event generation for signal and background processes is performed with MADGRAPH5_AMC@NLO v2.6.3.2 [202], allowing the matching of NLO QCD fixed-order calculations with parton showers with the MC@NLO prescription [259].

For background samples, the totally inclusive process at NLO in QCD is matched to its first jet multiplicity at NLO according to the FxFx method [260]. This has the effect of promoting the first and second QCD emissions in the inclusive sample, which, respectively, are only described at LO+LL and LL precision, to NLO+LL and LO+LL quantities. In these instances, the generator-level cuts $p_T^j > 30$GeV and $|\eta^j| < 5$ are applied with a merging scale $Q_{\text{cut}} = 60$GeV. Background processes are dressed with multiple particle interactions (MPI) using PYTHIA 8's underlying event model [208, 261, 262].

The programs MADSPIN [263] and MADWIDTH [264] are used to handle the smuon decays into a muon–neutralino system. The use of PYTHIA v8.230 [208], steered by the CUETP8M1 "Monash*" tune [265], is employed to handle parton showering (including QED radiation), the hadronization of all final-state partons, as well as the decays of hadrons and tau leptons.

Particle-level reconstruction is handled with MADANALYSIS5 v1.7.10 [203, 210], in which jet clustering is enforced using the anti-k_T algorithm [266], as implemented in FASTJET v3.3.0 [267]. A jet radius of $R = 1$ is chosen, following the jet veto analysis of ref. [250]. During the clustering procedure, ideal b-jet, light-jet, and hadronic tau (τ_h) tagging is assumed; potential misidentification of one particle species as another is implemented at the analysis level as done in ref. [252]. Computations use the NNPDF 3.1 NLO+LUXQED parton distribution function (PDF) set [268], while both PDF and $\alpha_s(\mu)$ evolutions are managed by using LHAPDF 6 v1.7 [269].

In addition to event generation, totally inclusive cross section normalisations at NLO and with next-to-leading logarithmic (NLL) threshold corrections are obtained with RESUMMINO v2.0.1 [270]. Again the NNPDF 3.1 NLO+LUXQED PDF set is used, despite the availability of PDFs extracted using threshold-corrected matrix elements [271]. This choice is motivated by the much larger statistical uncertainty associated with the resummed PDF, which obfuscates their improved perturbative precision / systematic uncertainty. The reader is referred to ref. [272] for a study of their impact on the hadroproduction of slepton pairs.

For total signal rates up to NLO+NLL, the collinear factorisation (μ_f) and QCD renormalisation (μ_r) scales are set to the smuon mass. For signal and background event generation, an event-by-event scale set to half the scalar sum of the transverse energy of all final-state particles is used,

$$\mu_{f,r} = \xi \times \mu_0 \quad \text{with} \quad \mu_0 = \frac{1}{2} \sum_{k \in \{\text{final state}\}} \sqrt{|p_T^k|^2 + m_k^2}, \qquad (4.3.1)$$

where by default, $\xi = 1$. The residual perturbative scale dependency is then quantified by varying μ_r and μ_f independently over the discrete range $\xi \in \{0.5, 1.0, 2.0\}$.

4.4 Smuon Pairs at the LHC

4.4.1 Smuon Pair Production

Like electroweakinos, sleptons can be produced through a variety of mechanisms in proton-proton collisions. For simplicity, this study is restricted to the production of right-handed smuon pairs through the inclusive, Drell-Yan process,

$$pp \rightarrow \gamma^*/Z^* + X \rightarrow \tilde{\mu}_R^+ \tilde{\mu}_R^- + X, \qquad (4.4.1)$$

as illustrated in fig. 4.1. At the hadronic level X above denotes an arbitrary number of (predominantly forward) QCD jets. If vector boson fusion becomes a relevant production mode of TeV-scale smuons [273–275], as for example at higher collider energies and integrated luminosities beyond the LHC, then one can expect much of the same dynamic jet veto behavior as presented below [252].

In the upper panel of fig. 4.2, the totally inclusive NLO+NLL cross section for neutral-current DY smuon production at a center-of-mass energy $\sqrt{s} = 14\text{TeV}$ is shown. The results are given as a function of the smuon mass, and the uncertainties stemming from perturbative scale variation (black band) and PDF fitting (light band) are indicated. In the lower panel of the figure, QCD K-factors are presented, with their uncertainties, defined relative to the Born process,

$$K^{\text{NLO}+\text{N}^k\text{LL}} = \frac{\sigma^{\text{NLO}+\text{N}^k\text{LL}}(pp \rightarrow \tilde{\mu}_R^+ \tilde{\mu}_R^- + X)}{\sigma^{\text{LO}}(pp \rightarrow \tilde{\mu}_R^+ \tilde{\mu}_R^- + X)}. \qquad (4.4.2)$$

The cases $k < 0$ and $k = 1$, respectively, correspond to computations at NLO and NLO+NLL.

For smuon masses $m_{\tilde{\mu}_R} \in [200, 900]\text{GeV}$ (*i.e.*, the range of interest for the LHC), the NLO+NLL production cross section varies from approximately 10 fb to 10 ab, with the corresponding scale uncertainties reaching the $\pm 2 - 3\%$ level. In this mass regime, NLO+NLL predictions sit well within the NLO perturbative uncertainty band that has a width of about $\pm 4\%$. Furthermore, the QCD K-factors for both the NLO and NLO+NLL computations are of about $K \approx 1.15$ and largely independently of the
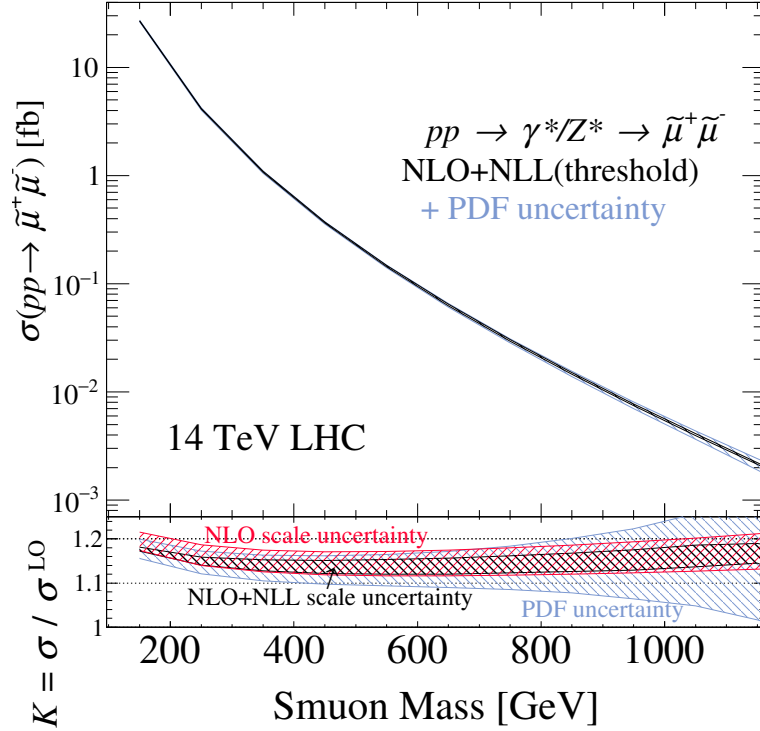
Figure 4.2: Upper: totally inclusive neutral-current DY production cross section of $\tilde{\mu}_R^+\tilde{\mu}_R^-$ pairs at NLO+NLL, and at a center-of-mass energy $\sqrt{s} = 14\text{TeV}$ with scale uncertainty (black band) and PDF uncertainty (lightest band). Lower: NLO+NLL (black band) and NLO (lighter band) QCD K-factor, with PDF uncertainty (lightest band).

smuon mass. On different grounds and still in this mass range, PDF uncertainties are only marginally larger than the NLO scale uncertainties, before growing significantly for $m_{\tilde{\mu}_R} \gtrsim 800\text{GeV}$ (due to the absence of data in the PDF fits). As the same PDF set is used for both the NLO and NLO+NLL computations, the size of their uncertainties is essentially identical.

For the parameter space consistent with the simplified model assumptions, the gluon fusion contribution to inclusive $\tilde{\mu}_R^+\tilde{\mu}_R^-$ production, which formally arises at $\mathcal{O}(\alpha_s^2)$, is small compared with the neutral-current DY component [276, 277]. Moreover, for DY-like processes that give rise to high-p_T charged leptons, QCD scale uncertainties in cross sections featuring a dynamic jet veto at NLO+PS (which are formally at the leading-logarithmic accuracy) are comparable with the total inclusive cross section uncertainty at NLO due to the absence of large jet veto logarithms [251, 252]. This holds independently of the jet radius for a dynamic veto [252]. For a static veto, choosing a jet radius of $R = 1$ significantly helps to minimise the perturbative uncertainties [250, 278–280], though worsens the universal, non-perturbative ones [238, 250, 281]. Thus, it may be concluded that cross sections for $\tilde{\mu}_R^+\tilde{\mu}_R^-$ production obtained from event generation at NLO+PS, either with or without a dynamic jet veto, are reliable estimates of the true rate. The reliability of NLO+PS predictions with static jet vetoes applied to SM diboson and weak boson scattering processes have similarly been reported elsewhere [235, 244]. Hence, for the purposes here and for discovery purposes, NNLO and NNLL (threshold) terms in fixed order and resummed signal predictions can be ignored.

4.4.2 Dynamic Jet Vetoes Beyond p_T

Jet vetoes have long been established as powerful tools to improve the discovery potential of sleptons and electroweakinos in multilepton searches at hadron colliders [245–248, 282]. In practice, LHC experiments rely on fixed/static veto thresholds of $p_T^{\text{Veto}} = 20-50\,\text{GeV}$ for central jets within a pseudorapidity $|\eta^j| \lesssim 2.5$ [220, 283–288]. Recently [251, 252], though, it was demonstrated that dynamic jet veto schemes, namely ones wherein p_T^{Veto} is set on an event-by-event basis to the p_T of an event's leading lepton, can improve the sensitivity of multilepton searches for exotic, colourless particles. In conjunction with selection cuts on leptonic observables, this type of jet veto ultimately discriminates against the relative amounts of hadronic and leptonic activity in each event.

In this sense, dynamic jet vetoes can be generalised by considering observables that measure an event's global hadronic and leptonic activities instead of just the p_T of an event's leading objects. For example: the inclusive scalar sum of p_T of all hadron clusters in an event ($H_T^{\text{Incl.}}$),

$$H_T^{\text{Incl.}} \equiv \sum_{k \in \{\text{clusters}\}} |\vec{p}_T^{\,k}|, \quad |\eta^k| \lesssim 4.5, \tag{4.4.3}$$

or the exclusive scalar sum of p_T of the two leading charged leptons (ℓ_1, ℓ_2) in an event ($S_T^{\text{Excl.}}$),

$$S_T^{\text{Excl.}} \equiv \sum_{k=1}^{2} |\vec{p}_T^{\,\ell_k}|, \tag{4.4.4}$$

are natural candidates. Here the usual particle ordering is adopted, where $p_T^{k_i} > p_T^{k_{i+1}}$ for particles k_i and k_{i+1} of species k. Henceforth the "Incl./Excl." labels will also be suppressed for brevity, but it is stressed that the results here should not be expected to uniformly carry over to exclusive H_T and inclusive S_T.

Explicitly, the summation over "hadron clusters" in Eq. (4.4.3) means the summation over the set of momentum vectors that are the output of a jet clustering algorithm applied to hadrons within a pseudorapidity of $|\eta^{\text{Had.}}| < \eta^{\text{max}} = 4.5$. Clusters that satisfy additional kinematic requirements, *e.g.*, a minimal p_T threshold, are further classified as jets.

Qualitatively, H_T differs from the p_T of the leading (or subleading) central jet $p_T^{j_1}$ (or $p_T^{j_2}$) in that H_T is much more sensitive to complicated colour topologies in a hard scattering processes. The simplest colour topologies, *e.g.*, eq. 4.4.1, have at most one or two colour dipoles / antennas, and hence less QCD radiation, resulting in H_T that is comparable to $p_T^{j_1}$. On the other hand, complex QCD processes, *e.g.*, $pp \to WW + nj$, have many color antennas, and hence more sources of QCD radiation, resulting in H_T significantly larger than $p_T^{j_1}$.

Due to its exclusive nature, S_T acts to exaggerate and accentuate the characteristic behavior of the leading charged leptons ℓ_1 and ℓ_2. If they stem from a resonant (continuum) process, then S_T will characteristically have a narrow (shallow) distribution. If the two are pair-produced, then one expects the scaling $S_T \sim 2p_T^{\ell_1}$. Likewise, any relative (in)dependence of $p_T^{\ell_k}$ on the hadronic activity is inherited by S_T. By virtue of the Collinear Factorisation Theorem, central, high-p_T charged leptons in hadron collisions stem from a hard underlying process. Hence, the S_T of leading leptons probes an event's hard-scattering core, and, up to possible kinematic decay factors, must scale like the hard scattering scale Q. This helps to protect against the emergence of large veto logarithms. It should briefly be remarked that exclusive S_T differs from inclusive
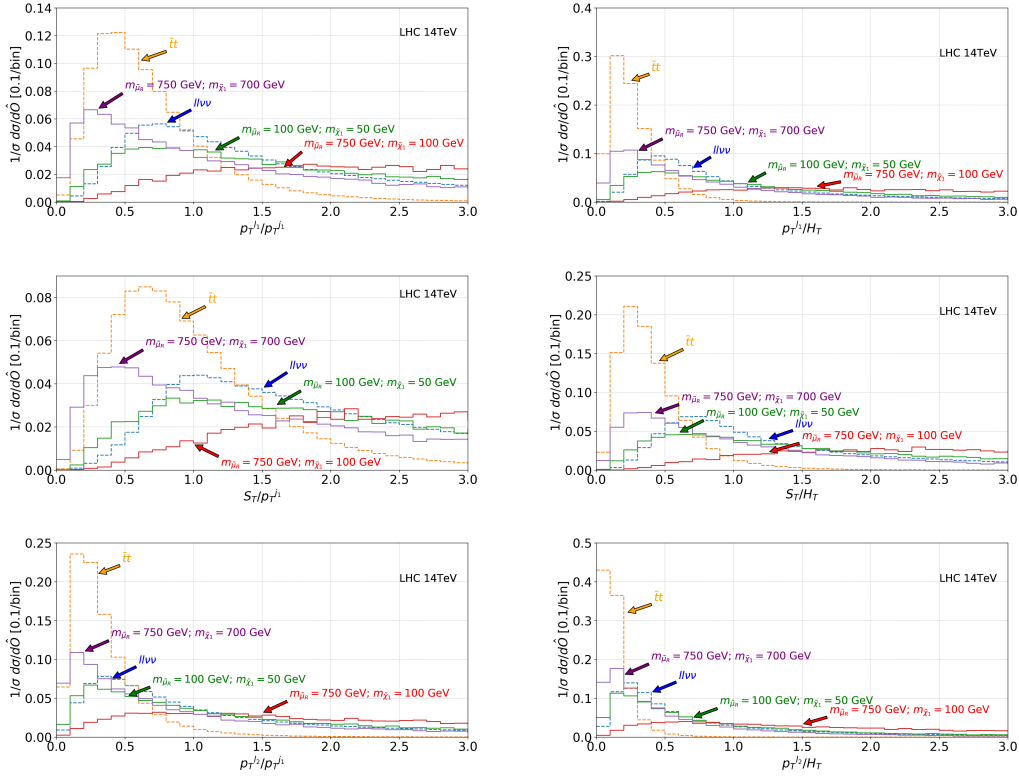
Figure 4.3: Ratios of measures of hadronic and leptonic activity for representative signal (solid) and background (dashed) samples used in the dynamic veto analysis, showing (a) $p_T^{l_1}/p_T^{j_1}$, (b) $p_T^{l_1}/H_T$, (c) $S_T/p_T^{j_1}$, (d) S_T/H_T, (e) $p_T^{\ell_2}/p_T^{j_1}$, (f) $p_T^{\ell_2}/H_T$.

S_T in that the latter sums over the trailing charged leptons and additionally probes universal, low-Q^2 physics, such as hadron decays and QED parton showering.

In application, a dynamic, H_T-based jet veto would work, for example, by rejecting events in which H_T exceeds $p_T^{\ell_1}$. Analogously, an S_T-based veto functions by requiring, for example, an event to satisfy $p_T^{j_1} < S_T$ for $|\eta^{j_1}| < \eta^{\mathrm{max}}$.

To explore these alternative dynamic veto schemes, presented in fig. 4.3 are the normalised distributions for the following ratios of leptonic and hadronic activities:

$$\text{(a) } p_T^{\ell_1}/p_T^{j_1}, \qquad \text{(b) } p_T^{\ell_1}/H_T, \qquad \text{(c) } S_T/p_T^{j_1},$$
$$\text{(d) } S_T/H_T, \qquad \text{(e) } p_T^{\ell_2}/p_T^{j_1}, \qquad \text{(f) } p_T^{\ell_2}/H_T.$$

These are considered for the signal process given in eq. 4.4.1, assuming three benchmark parameter space points,

$$\begin{aligned}
\text{Signal Category} \quad &: \quad (m_{\tilde{\mu}_R}, m_{\tilde{\chi}_1}), \\
\text{High-mass, Large mass splitting} \quad &: \quad (750\,\mathrm{GeV}, 100\,\mathrm{GeV}), \\
\text{High-mass, Small mass splitting} \quad &: \quad (750\,\mathrm{GeV}, 700\,\mathrm{GeV}), \\
\text{Low-mass, Small mass splitting} \quad &: \quad (100\,\mathrm{GeV}, 50\,\mathrm{GeV}),
\end{aligned}$$

with smuons decaying into an SM muon and a neutralino. The following representative backgrounds are also considered,

$$pp \to t\bar{t} \to \ell^+\ell^- + X, \qquad pp \to \ell^+\ell^-\nu\bar{\nu}, \qquad (4.4.5)$$

with $\ell \in \{e, \mu, \tau_h\}$. All signal and background processes are considered at NLO+PS, after jet clustering. At least two oppositely charged muons are required, with any number of clusters satisfying the truth-level kinematical requirements,

$$|\eta^{\text{clust.}}| < 4.5, \quad |\eta^\ell| < 2.4, \quad \text{and} \quad p_T^\ell > 10\text{GeV}. \qquad (4.4.6)$$

For reference, a brief discussion should be made of the first the kinematic ratio $r_{j_1}^{\ell_1} = p_T^{\ell_1}/p_T^{j_1}$, as studied by refs. [251,252] and shown in fig. 4.3(a). For the signal processes, one sees a difference in behaviour according to whether or not the smuon and neutralino are close in mass. Whereas the high-mass, large mass splitting configuration possesses a very broad distribution, with most of the phase space exceeding $r_{j_1}^{\ell_1} > 1$, the more compressed configurations possess relatively narrower distributions, with significantly more phase space below the $r_{j_1}^{\ell_1} = 1$ threshold. For the large mass splitting case, final-state muons carry $p_T^\ell \sim m_{\tilde{\mu}_R}(1 - m_{\tilde{\chi}_1}^2/m_{\tilde{\mu}_R}^2)/2 \sim m_{\tilde{\mu}_R}/2 \sim 375\text{GeV}$. This is significantly larger than the leading jet p_T, which is generally of the order of the Sudakov peak. For on-shell slepton pair production, the Sudakov peak is much lower than $2m_{\tilde{\mu}_R}$, indicating that characteristically $p_T^{j_1} \ll p_T^{\ell_1} \sim m_{\tilde{\mu}_R}/2$. For the compressed cases, the muons carry only $p_T^\ell \lesssim 40 - 50\text{GeV}$ and drive the relationship $r_{j_1}^{\ell_1}(\text{high-mass, small-splitting.}) \lesssim r_{j_1}^{\ell_1}(\text{low-mass, small-splitting.}) \lesssim 1$.

Considering the background processes, one observes that most events populate the region around $r_{j_1}^{\ell_1} \sim 0.25 - 0.75$. In both cases, the behavior follows from kinematic arguments [251]. For an at-rest top quark decaying into leptons, the characteristic momenta of the charged lepton and associated b-quark give rise to the scaling

$$r_{j_1}^{\ell_1} \sim \frac{p_T^\ell}{p_T^b} \sim \frac{m_t \left(1 + M_W^2/m_t^2\right)/4}{m_t \left(1 - M_W^2/m_t^2\right)/2} \sim 0.75. \qquad (4.4.7)$$

In a full simulation at NLO+PS with large-R jets, this is pushed significantly to smaller values due to a large $t\bar{t} + 1j$ sub-channel, boosts from large $(t\bar{t})$-invariant masses, and into-cone radiation. Each enhances p_T^j or p_T^b relatively to p_T^ℓ. Despite being a color-singlet process, the inclusive $pp \to \ell\ell\nu\nu + X$ channel has a relatively large $pp \to \ell\ell\nu\nu + 1j$ fraction. This is due to the Born-like $pp \to W\gamma^*/WZ + 0j$ processes being suppressed by radiation zeroes [289–296]. In turn, $r_{j_1}^{\ell_1}$ is inherently less than unity.

Figure 4.3(b) considers the impact of including secondary QCD radiation and shows the distribution for $r_{H_T}^{\ell_1} = p_T^{\ell_1}/H_T$. For the signal processes, some difference from $r_{j_1}^{\ell_1}$ is observed in the normalization and position of the distributions' maxima. Here, the maxima are marginally taller and pushed to slightly lower values of $r_{H_T}^{\ell_1}$. This is indicative of the low hadronic activity in DY-like processes, which is in fact why a jet veto is considered at all. On the other hand, for both background processes, values of $r_{H_T}^{\ell_1}$ much smaller than $r_{j_1}^{\ell_1}$ are observed. For $t\bar{t}$ specifically, the shift (and narrowing) from $r_{j_1}^{\ell_1} \lesssim 0.5$ to $r_{H_T}^{\ell_1} \lesssim 0.25$ is consistent with H_T, which sums over both bottom jets, being roughly $1/H_T \sim 1/(2 \times p_T^{j_1}) \sim 1/(2 \times p_T^{b_1})$. The low-mass, compressed signal distribution is in particular hardly distinguishable from the $\ell\ell\nu\nu$ distribution.

Considering now a more global measure of leptonic activity, presented in figs. 4.3(c) and (d) are the distributions for the ratios $r_{j_1}^{S_T} = S_T/p_T^{j_1}$ and $r_{H_T}^{S_T} = S_T/H_T$, respectively. For all cases one sees that the $r_{j_1}^{S_T}$ and $r_{H_T}^{S_T}$ curves are broader than their $r_{j_1}^{\ell_1}$ and $r_{j_1}^{S_T}$ counterparts, and that the distributions' maxima are shifted slightly rightward. As in the (a) and (b) panels, the compressed signal and both background processes have a significant fraction of their respective phase spaces below unity.

As an alternative measure of local leptonic activity, figs. 4.3(e) and (f) show the distributions for the ratios $r_{j_1}^{\ell_2} = p_T^{\ell_2}/p_T^{j_1}$ and $r_{H_T}^{\ell_2} = p_T^{\ell_2}/H_T$, respectively. Immediately, one sees a larger separation than in (a) and (c) of the high-mass, compressed signal process from all other processes. Notably, the $t\bar{t}$ distributions are much narrower, with almost all events falling below $r_{j_1}^{\ell_2} \lesssim 0.5$ and $r_{H_T}^{\ell_2} \lesssim 0.25$.

Taken together, a picture emerges for generalised definitions of dynamic jet vetoes. One finds that all of the proposed veto schemes exhibit uniform behaviour. For the signal process with the highest charged lepton momenta, *i.e.*, the high-mass, large mass splitting signal category, there is a clear signal-to-background separation against representative background processes. For signal processes with charged lepton momenta comparable to SM processes, one finds significantly less but nonetheless interesting discriminating power. In particular, for the low-mass, compressed category, one sees reasonable separation from $t\bar{t}$ but poor separation from $\ell\ell\nu\nu$, whereas for the high-mass, compressed category the opposite is observed. This suggests that it may be possible to salvage additional signal space with complementary selection cuts. Quantitatively, a larger signal-to-background separation is observed for dynamic veto schemes with more inclusive/global hadronic observables, *e.g.*, H_T, and more exclusive/local charged lepton observables, *e.g.*, $p_T^{\ell_2}$. The worst separation is given by $r_{j_1}^{S_T}$, which makes use of the multilepton activity of background processes but not the relatively low hadronic activity of the signal processes. The ratio $r_{H_T}^{\ell_2}$ appears to be exceptionally powerful in rejecting top quark background.

4.4.3 Jet Veto Collider Analyses

The static and dynamic jet veto analyses are now defined, to quantify how generalised dynamic jet vetoes may improve the discovery potential of smuon pairs at the LHC - if at all. For all analyses, analysis-quality charged leptons and jets are defined as those that satisfy the following kinematical, fiducial, and isolation requirements,

$$p_T^{e\ (\mu)\ [\tau_h]\ \{j\}} > 10\ (10)\ [20]\ \{25\}\text{GeV},$$
$$|\eta^{e\ (\mu)\ [\tau_h]\ \{j\}}| < 2.4, \quad \Delta R_{\ell_m,\ell_n} > 0.4, \quad \Delta R_{\ell j} > 0.4.$$

Electron and muon efficiencies as reported[1] in ref. [219] are used for leptons with $p_T \geq 20$ GeV, and those reported in ref. [297] for leptons with $p_T \in [10, 20[$ GeV. Hadronic decays of τ leptons (τ_h) with $p_T \geq 20$ GeV are tagged using the efficiencies reported in ref. [298]. All objects are smeared with a Gaussian profile as done in ref. [252], using publicly available resolution parameterizations as reported by the ATLAS and CMS collaborations [299–302]. The magnitude of the transverse momentum imbalance vector ($\not{E}_T$) is defined with respect to all visible momenta within $|\eta| < 4.5$,

$$\not{E}_T = |\ \vec{\not{p}}_T|, \quad \vec{\not{p}}_T = - \sum_{k \in \{\text{visible}\}} \vec{p}_T^{\ k}. \tag{4.4.8}$$

The following background processes

$$pp \to \ell\ell\ell\nu, \qquad pp \to \ell\ell\nu\nu,$$
$$pp \to t\bar{t} \to 2\ell X, \qquad pp \to WWW \to 3\ell X,$$

are simulated at NLO+PS with FxFx-merging for the first jet multiplicity. The additional background processes

$$pp \to \ell\ell\ell\ell, \qquad pp \to \ell^+\ell^-,$$

---

[1] https://twiki.cern.ch/twiki/bin/view/CMSPublic/SUSMoriond2017ObjectsEfficiency

Analysis Object Criteria at $\sqrt{s} = 14$ TeV:
$p_T^{e\ (\mu)\ [\tau_h]\ \{j\}} > 10\ (10)\ [20]\ \{25\}$GeV,
$|\eta^{e\ (\mu)\ [\tau_h]\ \{j\}}| < 2.4,\quad$ anti-k_T w./ $R = 1$
$\Delta R_{\ell_m,\ell_n} > 0.4,\quad \Delta R_{\ell j} > 0.4$
Common Analysis Requirements:
$N(\mu^+) = 1,\quad N(\mu^-) = 1,\quad N(\ell) = 2,$
$m_{\mu\mu} > 20$ GeV, $|m_{\mu\mu} - M_Z| > 15$GeV,
$M_{T2} > 90$GeV, $\not{E}_T > 100$GeV,
Binned signal region: $\not{E}_T \in\ (a)[100, 150[,$
$(b)[150, 225[,\ (c)[225, 300[,\ (d)[300, \infty[$GeV
Benchmark (Static) Jet Veto Analysis Requirements:
$p_T^{\mu_1\ (\mu_2)} > 50\ (20)$GeV,$\quad p_T^{\text{Veto}} = 25$GeV
Dynamic Jet Veto Analysis Requirements:
Overlapping Signal Categories:
(a) $p_T^{\text{Veto}} = p_T^{\ell_1}$ $\quad$ (b) $H_T^{\text{Veto}} = p_T^{\ell_1}$
(c) $p_T^{\text{Veto}} = S_T$ $\quad$ (d) $H_T^{\text{Veto}} = S_T$
(e) $p_T^{\text{Veto}} = p_T^{\ell_2}$ $\quad$ (f) $H_T^{\text{Veto}} = p_T^{\ell_2}$

Table 4.1: (Top) Analysis object / particle identification requirements at $\sqrt{s} = 14$TeV; (upper) common analysis requirements; (lower) benchmark static veto analysis requirements; and (bottom) dynamic jet veto analysis requirements.

$$pp \to t\bar{t}\ell\nu \to 3\ell X, \qquad pp \to WW\ell\ell \to 2\ell X,$$

simulated in contrast at the NLO+PS accuracy, were found to give a negligible background contribution after all selection cuts in all analyses, and therefore are ignored for the remainder of the report.

Shared Analysis Baseline

As a baseline for all analyses, the CMS search for slepton pair production in dilepton final states at $\sqrt{s} = 13$ TeV with $\mathcal{L} = 35.9$ fb^{-1} of data [219] is closely followed. Events featuring one pair of analysis quality, opposite-sign muons are pre-selected, and events with additional analysis-quality charged leptons are vetoed. The analysis is thus inclusive with respect to additional leptons outside these criteria. Low-mass hadronic resonances and Z-pole contributions are removed with the invariant mass cuts: $m_{\mu\mu} > 20$GeV and $|m_{\mu\mu} - M_Z| > 15$GeV. The SM DY continuum is further suppressed by requiring $\not{E}_T > 100$GeV, and diboson and top pair processes are reduced by requiring a "stransverse mass" cut of $M_{T2} > 90$GeV [303,304]. Section 4.5 describes the impact of relaxing this cut. Events are then binned according to $\not{E}_T$. Analysis object definitions and shared analysis requirements are summarised in the top two sections of table 4.1.

Benchmark, Static Jet Veto Analysis

At this point, our jet veto collider analyses diverge. Our benchmark, static jet veto analysis continues as prescribed in the baseline CMS analysis [219] and further requires
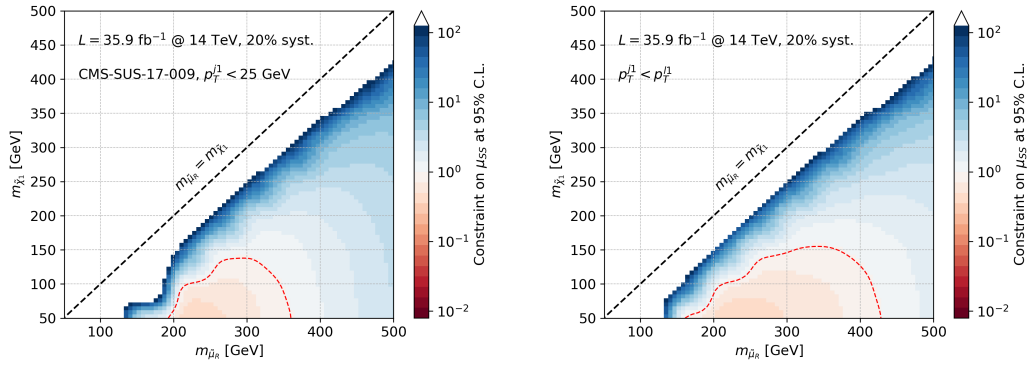
Figure 4.4: Exclusion contours on the signal strength μ_{SS} for smuon pair production in the $(m_{\tilde{\chi}_1}, m_{\tilde{\mu}_R})$ plane with $\mathcal{L} = 35.9$ fb^{-1}, for (a) the static jet veto analysis based on ref. [219], with $p_T^{\text{Veto}} = 25$GeV, and (b) the dynamic jet veto analysis with $p_T^{\text{Veto}} = p_T^{\ell_1}$.

that the p_T of the leading and subleading muons satisfy

$$p_T^{\ell_1\ (\ell_2)} > 50\ (20)\text{GeV}. \tag{4.4.9}$$

Lastly, a static jet veto of $p_T^{\text{Veto}} = 25$GeV is imposed on analysis-quality jets. As such objects must sit within $|\eta| < 2.4$, the veto is more specifically a static, central jet veto. Relaxing this pseudorapidity restriction will be briefly explored in the following section. Analysis requirements are summarised in the third section of table 4.1.

For background processes, comparable cross sections after selection cuts are found to those reported by CMS for all signal regions except the lowest $\not{E}_T$ bin.

There, the background rate is found to be about 50% lower and is driven by a difference in the normalisation of the "Flavour Symmetric" background, which is largely populated by the $t\bar{t}$ and diboson processes.

The difference in this bin is attributed to the background normalisations used here being accurate only up to NLO+PS, meaning that they are therefore missing numerically large $\mathcal{O}(\alpha_s^2)$ contributions. There are also potentially missing contributions from mismeasurements which are not captured by our detector fast simulation.

These effects can both introduce significant differences to CMS' data-driven predictions. The cutflows for the dominant backgrounds are summarised in table 4.2.

Dynamic Jet Veto Analysis

The goal of this study is to see to what extent, if at all, generalisations of dynamic jet vetoes can improve searches for multilepton final states over traditional, static, central jet vetoes. To do this, a class of analyses that simplifies the static veto analysis of the preceding subsection is proposed. This is executed by removing the stringent high-p_T selection cuts on charged leptons given in eq. (4.4.9) and by setting the central jet veto threshold on an event-by-event basis. More precisely, events are vetoed either (i) if there exists an analysis-quality jet with $p_T^j > p_T^{\text{Veto}}$ or (ii) if the event possess $H_T > H_T^{\text{Veto}}$. In no case are vetoes considered simultaneously on p_T^j and on H_T. The veto threshold are set dynamically according to the following permutations:

$$\text{(a)}\ p_T^{\text{Veto}} = p_T^{\ell_1}, \quad \text{(b)}\ H_T^{\text{Veto}} = p_T^{\ell_1}, \quad \text{(c)}\ p_T^{\text{Veto}} = S_T,$$
$$\text{(d)}\ H_T^{\text{Veto}} = S_T, \quad \text{(e)}\ p_T^{\text{Veto}} = p_T^{\ell_2}, \quad \text{(f)}\ H_T^{\text{Veto}} = p_T^{\ell_2}.$$

In principle, one can introduce a scaling factor r, *e.g.*, $H_T^{\text{Veto}} = r \times S_T$, with $r = 0.75$, and improve the signal-to-background ratio S/B according to fig. 4.3. However, this is beyond the proof-of-concept scope of our study. Needless to say, investigations into optimising a "smart jet veto" are encouraged.

4.5 Results and Outlook

To quantify the impact of dynamic jet vetoes on searches for smuon pairs, the CL_S technique [150] is used to first determine the 95% CL reach in terms of the event rate $N_{95} = \sigma_{95} \times \mathcal{L}$, for a luminosity $\mathcal{L}$. Monte Carlo uncertainties are taken into account for both the signal and the background, and use a flat systematic uncertainty of 20% on the background prediction derived from the FxFx + MPI samples. The combined likelihood ratio of the four signal regions is used as the test statistic. Sensitivity is then expressed in terms of the signal strength (μ_{SS}),

$$\mu_{SS} = \sigma_{95}/\sigma_p, \tag{4.5.1}$$

where σ_p is the predicted cross section in our simplified model. A signal strength of $\mu_{SS} < 1$ means that the signal hypothesis is excluded with at least 95% confidence.

As a check, shown in fig. 4.4 is μ_{SS} for (a) the static jet veto analysis based on ref. [219], where $p_T^{\text{Veto}} = 25\text{GeV}$, and (b) the dynamic jet veto $p_T^{\text{Veto}} = p_T^{\ell_1}$, assuming $\mathcal{L} = 35.9 \text{ fb}^{-1}$ at $\sqrt{s} = 14\text{TeV}$.

The derivation of these figures considers only the Monte Carlo uncertainty and a flat 20% additional systematic uncertainty (which is intended to approximate all additional theory and experimental systematic uncertainties) in the limit setting, to keep the comparison as clear as possible. One finds that the constraints derived using the reference analysis are stronger than those reported in ref. [219]. This is attributed to three reasons. First, in comparison with the 13 TeV results explored with data, $\sqrt{s} = 14\text{TeV}$ is taken here. Second, this study uses a highly simplified treatment of systematic uncertainties, and finally, a slightly smaller background prediction for the lowest $\not{E}_T$ signal region is recovered compared with the data-driven prediction of ref. [219] (see sec. 4.4.3).

With the dynamic jet veto analysis, an improvement in sensitivity is observed over the static veto analysis, with $m_{\tilde{\mu}_R} \lesssim 425\text{GeV}$ being accessible for $m_{\tilde{\mu}_R} \gg m_{\tilde{\chi}_1}$, to be confronted to $m_{\tilde{\mu}_R} \lesssim 360\text{GeV}$ in the static case. A comparable improvement is found at larger luminosities. However, as part of the improvement comes from higher signal acceptance rather than large improvements in S/B, the relative improvement diminishes somewhat. It should be stressed that while this improvement appears limited, it has been obtained by relaxing several selection cuts of the somewhat sophisticated analysis of ref. [219], and naïvely applying a dynamic jet veto that has not been optimised according to fig. 4.3. This "out-of-the-box" improvement even for relatively light smuon masses is encouraging.

To present the main results of this report, for a given jet veto scheme and luminosity, the ratio of signal strengths are considered:

$$\mathcal{R}_{\text{Dy. Veto}} = \frac{\mu_{SS}^{\text{CMS}}}{\mu_{SS}^{\text{Dy. Veto}}} = \frac{\sigma_{95}^{\text{CMS}}/\sigma_p^{\text{CMS}}}{\sigma_{95}^{\text{Dy. Veto}}/\sigma_p^{\text{Dy. Veto}}}, \tag{4.5.2}$$

where μ_{SS}^{CMS} is the signal strength as determined using the reference static jet veto analysis and $\mu_{SS}^{\text{Dy. Veto}}$ is the signal strength as determined with the dynamic jet veto analysis. The double ratio has the simple interpretation that a value of $\mathcal{R} > 1$ implies
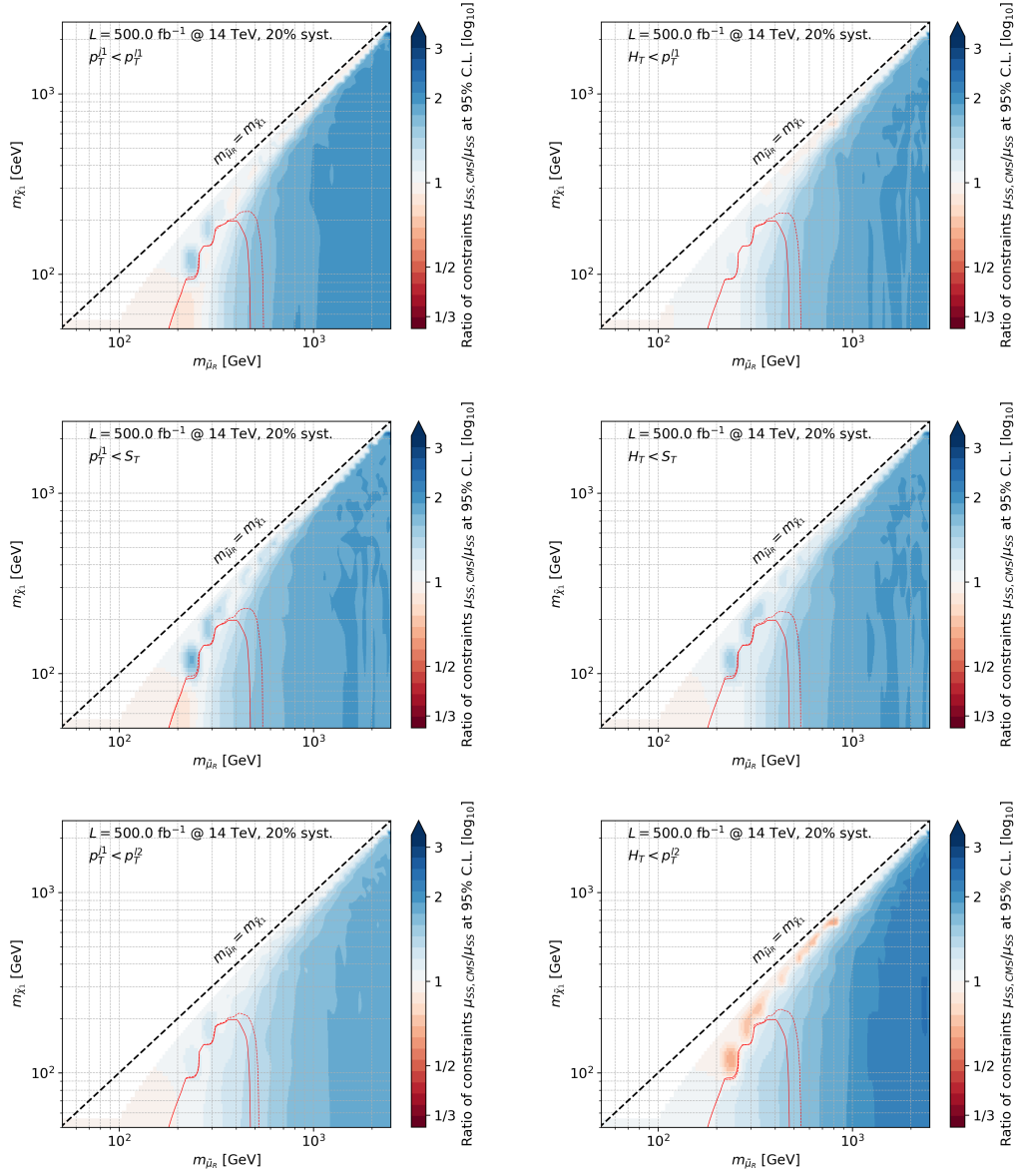
Figure 4.5: The ratio of signal strengths (μ_{SS}) for (a) $p_T^{\mathrm{Veto}} = p_T^{\ell_1}$, (b) $H_T^{\mathrm{Veto}} = p_T^{\ell_1}$, (c) $p_T^{\mathrm{Veto}} = S_T$, (d) $H_T^{\mathrm{Veto}} = S_T$, (e) $p_T^{\mathrm{Veto}} = p_T^{\ell_2}$, and (f) $H_T^{\mathrm{Veto}} = p_T^{\ell_2}$, compared with the CMS reference analysis using $\mathcal{L} = 500$ fb^{-1}. The solid red line shows the 95% exclusion for $\mu_{SS} = 1$ for the benchmark CMS analysis, and the dashed red line the same exclusion for the dynamic analysis.

that the dynamic veto analysis is more sensitive than the static veto analysis for a given input.

In fig. 4.5, assuming $\mathcal{L} = 500$ fb^{-1}, $\mathcal{R}$ is presented for

$$(a) p_T^{\mathrm{Veto}} = p_T^{\ell_1}, \quad (b) H_T^{\mathrm{Veto}} = p_T^{\ell_1}, \quad (c) p_T^{\mathrm{Veto}} = S_T,$$
$$(d) H_T^{\mathrm{Veto}} = S_T, \quad (e) p_T^{\mathrm{Veto}} = p_T^{\ell_2}, \quad (f) H_T^{\mathrm{Veto}} = p_T^{\ell_2}.$$

In the large mass splitting regime where $m_{\tilde{\mu}_R} \gg m_{\tilde{\chi}_1}$, one finds that the veto scheme (f) $H_T^{\mathrm{Veto}} = p_T^{\ell_2}$ outperforms the static veto analysis for $m_{\tilde{\mu}_R} \gtrsim 200\,\mathrm{GeV}$; this finding extends to (b) $H_T^{\mathrm{Veto}} = p_T^{\ell_1}$, (d) $H_T^{\mathrm{Veto}} = S_T$ and (e) $p_T^{\mathrm{Veto}} = p_T^{\ell_2}$ for $m_{\tilde{\mu}_R} \gtrsim 250\,\mathrm{GeV}$;
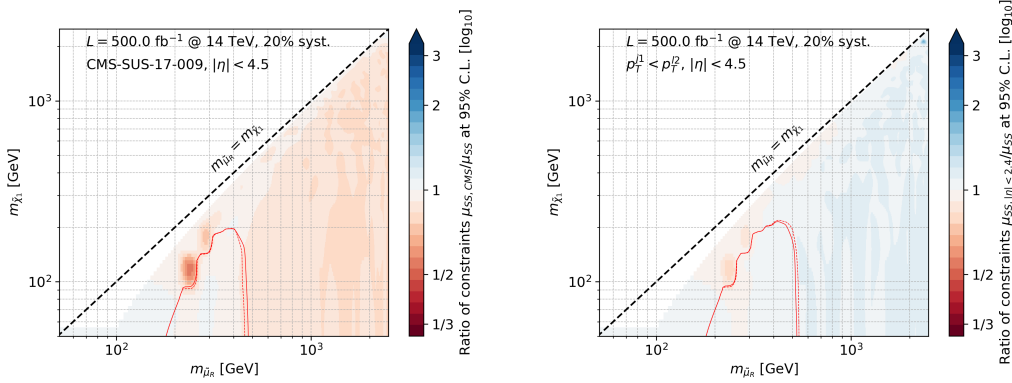
Figure 4.6: The ratio of constraints at $\mathcal{L} = 500$ fb^{-1} for (a) the default CMS analysis, and (b) the dynamic $p_T^{j1} < p_T^{l2}$, both with a jet pseudorapidity cut of $|\eta| < 4.5$, compared with their respective default analyses employing $|\eta| < 2.4$. The solid red line shows the 95% exclusion for $\mu_{SS} = 1$ for the standard $|\eta| < 2.4$ analysis, and the dashed red line the same exclusion for $|\eta| < 4.5$ analysis.

and reportedly, all dynamic jet veto schemes show improvement for $m_{\tilde{\mu}_R} \gtrsim 300$GeV. Of the schemes considered, the choice $(c)p_T^{\text{Veto}} = p_T^{\ell_2}$ arguably performs worst, with limited improvement over the static analysis for much of the phenomenologically relevant parameter space. For the compressed regime where $m_{\tilde{\mu}_R} \sim m_{\tilde{\chi}_1}$, the S_T schemes demonstrate some improvement, while (f) $H_T^{\text{Veto}} = p_T^{\ell_2}$ is considerably weaker than the static analysis.

For much of the parameter space of interest, one sees that the improvement is in excess of 25 to 50%. The relative improvement grows with increasing $m_{\tilde{\mu}_R}$ which allows for improvement in excess of 100% since the static veto reduces the signal efficiency for heavier mass scales (due to harder initial-state radiation) while the dynamic veto schemes generally remain efficient or become more efficient (due to harder, final-state charged leptons). At lower $m_{\tilde{\mu}_R}$ and close to the degenerate limit, final-state leptons are relatively soft. This leads to p_T^{Veto} and H_T^{Veto} thresholds that are as tight as, if not more stringent than, the static veto, thereby eliminating any improvement from relaxing other selection cuts.

Qualitatively, it is observed that H_T-based vetoes tend to perform better at high masses while p_T^{j1}-based vetoes are better at low masses, indicating the utility of veto schemes that employ more inclusive measures of the hadronic activity, e.g., H_T. S_T-based schemes are competitive. However $p_T^{\text{Veto}} = S_T$ is too inclusive for small $m_{\tilde{\mu}_R}$ where the static analysis gives better results. The inclusive nature of S_T is particularly useful in the compressed region, where individual lepton momenta are the smallest. In short, a whole class of dynamic jet vetoes can improve discovery potential of smuon pairs, but the difference in performance across the various limits of parameter space suggests that no single combination of hadronic and leptonic activity measures will be ideal in all cases. The appropriate leptonic measure should be investigated on an analysis-by-analysis basis in order to target specific kinematic regions.

Impact of Jet Veto Rapidity Window

Experimentally, jets can be reconstructed up to the maximal range of the detector, i.e. with a pseudorapidity of $\eta \leq 4.5$ for ATLAS and CMS. In practice though, jet vetoes are often only applied within the coverage of the tracker, typically for jets with

$|\eta| \lesssim 2.4$, to avoid the significant contribution of pile-up to the low-p_T jet rate by jets that would normally never exceed the veto threshold. This avoidance, however, is at the cost of an increased dependence on higher order QCD splittings, and hence an increased theoretical uncertainty [240]. It was, however, shown that these uncertainties can be alleviated if, instead, cuts are made on both η and p_T^j in a step-like fashion, in particular wherein p_T^{Veto} is relaxed for increasing jet pseudorapidity [240]. Indeed it has been shown that such jet vetoes are lready experimentally viable [305]. Moreover, extending dynamic jet vetoes to the forward region was found to be necessary to ensure a sufficient suppression of SM backgrounds in studies at higher $\sqrt{s}$ [252].

In this context, the impact of a dynamic jet veto when expanding the η range of the jet veto-window from $|\eta| < 2.4$ to $|\eta| < 4.5$ is briefly investigated. For a widened η range, fig. 4.6 shows the signal strength ratio,

$$\mathcal{R}_X = \mu_{SS}^{\mathrm{X}}(|\eta^{\mathrm{Veto}}| < 2.4)/\mu_{SS}^{\mathrm{X}}(|\eta^{\mathrm{Veto}}| < 4.5), \qquad (4.5.3)$$

for (a) the benchmark static jet veto analysis, where $p_T^{\mathrm{Veto}} = 25\mathrm{GeV}$, and (b) the dynamic analysis, with $p_T^{\mathrm{Veto}} = p_T^{\ell_2}$. As before, a ratio of $\mathcal{R}_X > 1$ indicates improved sensitivity. When a static veto is used and the pseudorapidity range increased, the vetoing of jets outside the central region reduces background rates while simultaneously reducing the signal rates, thereby maintaining a similar signal-to-background efficiency as in the reference analysis. For the dynamic veto, however, there is a uniform $\mathcal{O}(5-20)\%$ improvement for most of the parameter space due to slightly higher background rejection coupled with a smaller decrease in signal efficiency. It is anticipated that this behaviour to hold for all other dynamic veto schemes considered in this analysis.

Impact of Jet Vetoes When Lifting The M_{T2} Cut

As shown in Table 4.2, requiring the selection cut $M_{T2} > 90$ GeV greatly suppresses electroweak diboson and top quark pair production independently of a jet veto. However, the cut also reduces considerably the signal acceptance when sparticles are mass-degenerate. Notably, it is reported that choosing a more aggressive dynamic jet veto can control the top pair background sufficiently in the absence of the M_{T2} cut, leading to a significant improvement in sensitivity.

It has been checked that using $H_T < p_T^{l2}$ as a dynamic veto is stringent enough to control the top pair background when lifting the M_{T2} cut, independently of the signal region. When relaxing M_{T2}, total background rates grow by a factor of 5 for the lowest $\not{E}_T$ signal region up to a factor of 1.5 for the highest $\not{E}_T$ signal region, while there is a large, overall increase in signal efficiency. For the benchmark point $(m_{\tilde{\mu}_R}, m_{\tilde{\chi}_1}) = (750\mathrm{GeV}, 700\mathrm{GeV})$, this results in negligible changes in the signal (S) over background (B) ratio S/B for the two lower $\not{E}_T$ signal regions but significant increases in S/B for the two higher $\not{E}_T$ signal regions. Lifting the M_{T2} cut when using a stringent dynamic veto based on H_T therefore allows for improvements in sensitivity in the compressed region, independently of the integrated luminosity, due to the top pair background being sufficiently controlled by the dynamic veto itself.

One finds though that the improvement does not hold for all veto schemes considered. When requiring $p_T^{j1} < p_T^{l2}$ and no M_{T2} restriction, the top pair background comes to dominate the background rate in the two lower $\not{E}_T$ signal regions and increases the rates by factors of $20-30$, thereby reducing S/B, despite the increased signal efficiency. The two higher $\not{E}_T$ signal regions are less affected due to a much smaller the top pair contribution, with only a factor of 2 increase in the total background rate for the highest $\not{E}_T$ one. For $(m_{\tilde{\mu}_R}, m_{\tilde{\chi}_1}) = (750\mathrm{GeV}, 700\mathrm{GeV})$, one sees a

reduction in S/B in all signal regions, except for the highest $\not{E}_T$ one, suggesting that the simplest incarnations of dynamic jet vetoes are not sufficient in their own right. This was noted previously in refs. [251, 252].

4.6 Summary and Conclusion

In summary, this study has undergone an investigation into several measures of leptonic and hadronic activities in the process

$$pp \to \gamma^*/Z^* + X \to \tilde{\mu}_R^+ \tilde{\mu}_R^- + X \to \mu^+ \mu^- + \not{E}_T + X, \qquad (4.6.1)$$

and the associated SM background processes, to explore possible generalisations of dynamic jet vetoes. Using this information, it has been demonstrated that a general class of dynamic jet vetoes can be used to improve the sensitivity of searches for right-handed smuon pair production at the LHC. The improvement becomes more significant as mass scales further above the EW scales are probed, and in some instances hold even when the final-state particles are soft. Most choices of measures for hadronic and leptonic activities perform better than the CMS-inspired benchmark analysis, which features a static jet veto threshold of $p_T^{\text{Veto}} = 25\text{GeV}$ (see fig. 4.5). Differences suggest that no single dynamic veto scheme will always be ideal for all parameter space regions and rather should be investigated on an analysis-by-analysis basis. Qualitatively, one finds that dynamic jet vetoes using more inclusive measures of the hadronic activity, e.g., H_T, perform best, while the ideal choice of leptonic activity depends on the signal kinematics (see sec. 4.5). This study reports that the impact of including MPI/UE and NLO-accurate jet merging, *e.g.,* via the FxFx method, does not appreciably alter this picture; see table 4.2. The impact of enlarging the jet veto rapidity window and complementarity to other selection cuts were also addressed.

Due to the dynamic nature of these cuts, sensitivity can likely be considerably improved with machine learning techniques and such future investigations are encouraged. Our results should generalise to other searches for new, heavy, uncoloured physics that employ jet vetoes at the LHC.

Cut/Channel	$\sigma(\ell\ell\nu\nu)$ [fb]	$\sigma(\ell\ell\ell\nu)$ [fb]	$\sigma(t\bar{t})$ [fb]
Common Analysis Requirements			
Generator	$10\,300^{+4.5\%}_{-5.1\%}$	$1680^{+5.5\%}_{-6.2\%}$	$91\,000^{+11.9\%}_{-11.7\%}$
Dimuon Selection	$840^{+4.9\%}_{-5.3\%}$ (8.4%)	$140^{+6.1\%}_{-6.5\%}$ (8.6%)	$6800^{+12\%}_{-13\%}$ (7.5%)
$+m_{\ell\ell}$ Requirements	$580^{+5.3\%}_{-5.5\%}$ (69%)	$40^{+6.3\%}_{-6.8\%}$ (29%)	$5300^{+12\%}_{-13\%}$ (78%)
+Minimum M_{T2}	$2.4^{+9.0\%}_{-6.2\%}$ (0.42%)	$0.56^{+7.0\%}_{-8.2\%}$ (1.4%)	$8.6^{+12\%}_{-25\%}$ (0.16%)
Benchmark Static Jet Veto Analysis Requirements			
$+p_T^{\ell_1} > 50\mathrm{GeV}$, $p_T^{\ell_2} > 20\mathrm{GeV}$	$2.3^{+12\%}_{-7.2\%}$ (96%)	$0.53^{+7.8\%}_{-10\%}$ (95%)	$7.8^{+12\%}_{-33\%}$ (91%)
+Static Jet Veto	$1.6^{+13\%}_{-7.8\%}$ (70%)	$0.31^{+7.8\%}_{-13\%}$ (60%)	$0.15^{+68\%}_{-58\%}$ (1.9%)
Dynamic Jet Veto Analysis Requirements			
$p_T^{\mathrm{Veto}} = p_T^{\ell_1}$	$2.4^{+10\%}_{-7.4\%}$ ($> 99\%$)	$0.55^{+7.3\%}_{-8.6\%}$ (99%)	$4.5^{+32\%}_{-32\%}$ (57%)
$p_T^{\mathrm{Veto}} = p_T^{\ell_2}$	$2.2^{+11\%}_{-8.6\%}$ (91%)	$0.50^{+7.1\%}_{-7.5\%}$ (87%)	$0.98^{+57\%}_{-17\%}$ (12%)
$p_T^{\mathrm{Veto}} = S_T$	$2.4^{+8.9\%}_{-6.7\%}$ ($> 99\%$)	$0.56^{+6.9\%}_{-9.0\%}$ ($> 99\%$)	$6.6^{+23\%}_{-26\%}$ (89%)
$H_T^{\mathrm{Veto}} = p_T^{\ell_1}$	$2.2^{+9.2\%}_{-5.8\%}$ (87%)	$0.46^{+7.3\%}_{-13\%}$ (84%)	$0.54^{+22\%}_{-25\%}$ (7.1%)
$H_T^{\mathrm{Veto}} = p_T^{\ell_2}$	$1.5^{+7.7\%}_{-7.3\%}$ (60%)	$0.33^{+8.6\%}_{-8.9\%}$ (58%)	$0.12^{+62\%}_{-81\%}$ (1.5%)
$H_T^{\mathrm{Veto}} = S_T$	$2.3^{+9.6\%}_{-9.7\%}$ (97%)	$0.54^{+7.0\%}_{-8.5\%}$ (95%)	$1.9^{+31\%}_{-20\%}$ (23%)

Table 4.2: The cross section [fb] with uncertainties $[^{+\%}_{-\%}]$ and cut efficiency [(%)] of the selection cuts in table 4.1 for the dominant SM backgrounds, when modeled for FxFx-merging with MPI (FxFx+MPI). Uncertainties are obtained by adding the renormalisation and factorisation scale envelope with the shower scale envelope and statistical uncertainty in quadrature. At the generator-level, statistical confidence corresponds to 5-10 M events for each sample and shower variation.

Conclusion

The discovery of the Higgs boson in 2012 closed one chapter of modern particle physics and consequently shifted the limelight onto the half-open can of worms in the corner. The completed Standard Model on its own leaves too many questions unanswered for particle theorists to lock their office doors and head off for early retirement; the community as a whole is rather confident that this is not the end of the story. It may be that new physics has not yet been found at the LHC, but instead of throwing in the towel, the community creates more theories, refines their search analyses and recasts the ones already performed for their favourite models. The domain is as active as ever and for good reason; whoever went to study physics without seeking a challenge clearly enrolled in the wrong class.

The Higgs boson itself, or the "god" particle (said no particle physicist ever), is at the centre of the Venn diagram, and not only enables physicists to understand the origin of mass and massive particles, but also to discover new ones. The Higgs boson is uniquely placed to feel the effects of higher energy physics, and enables the particle physics community to entertain and constrain various SM extensions. This quality is central to chapter 2, which explored the idea of the Higgs boson as part of a type-II Higgs doublet model originating from a higher energy Dirac gaugino model which is automatically aligned in the minimal model. Indeed, it was shown that this attribute held robustly under quantum corrections and the alteration of the scale at which the extended supersymmetry is manifest. An effective field theory approach was employed, implementing the running of two-loop RGEs and including extensive threshold corrections at the THDM and SUSY energy scales, and the effects of the Higgs mass bounds and experimental constraints from run 2 of the LHC on the SUSY scale subsequently studied. This section was concluded by a quick comparison to the MRSSM case - a model in which alignment is not predicted.

With the numerous SM-extensions existing, it would be a tough feat indeed for experimental collaborations to produce exclusion limits for all theoretical proposals. As such, a large majority of supersymmetry searches are based on the MSSM and simplified variations. However not all SUSY models are created equal, and as discussed in chapter 3, SUSY extensions can open up new production mechanisms and decay channels, and the associated exclusion limits can considerably vary in comparison to the simplified models. Using resources provided by the experimental collaborations, it is possible instead for phenomenologists to determine indicative limits on their own BSM models. Chapter 3 sought to further this goal, by primarily using simplified model constraints to do a fast limit setting on 4 representative scenarios with the MDGSSM – introduced first in the introduction section 1.2.4 and which was the focus of chapter 2. This was followed up by a full recasting of the ATLAS-SUSY-2016-07 analysis to set constraints on the squarks and gluinos in the MDGSSM in the context of LHC run 2, and a comparison was performed for equivalent corresponding MSSM scenarios.

The final chapter complements the antecedent one, in looking to further ameliorate searches for weak-scale supersymmetry by modifying the way that hadronic activity is processed through the currently used search analyses. Large background sources, which are typically hadronic in proton-proton colliders such as the LHC, will always be a hurdle to overcome when trying to pick out a search signal. Traditionally, static central jet-vetoes are applied to cut out large hadronic background sources, but it has recently been proposed [251, 252] that dynamic jet vetoes can be applied in searches for colourless physics and the sensitivity of the search can be improved. Chapter 4 considered the Drell-Yann production of a pair of right-handed smuons with missing energy in a simplified MSSM model. Several global and local measures of hadronic and leptonic activity were scrutinised in order to increase the signal-to-background efficiency, and it was shown that, independent of the integrated luminosity, the search sensitivity was enhanced.

If and when new physics is detected it is without a doubt that the particle physics community will be waiting, escorting numerous tools with which to fully analyse and optimise the search results. Until then, it will simply continue to express mild concern towards where its next bit of funding might appear from.

A – Basic representation theory

The anomalous dimension of a general field can be defined by

$$\gamma_\phi \equiv -\frac{1}{2}\frac{\partial \log Z_\phi}{\partial \log \mu}\,, \tag{A.0.1}$$

where Z_ϕ is the wavefunction renormalisation coefficient responsible for the renormalisation of the kinetic term for the field ϕ. By definition, the dimension of ϕ changes when a dimensionful function is put in front of it, and thus the dimension of the field itself acquires an anomalous dimension. The energy-dependence of this dimensionful function is exactly what defines an anomalous dimension. At tree-level, the couplings are implicitly devoid of any energy dependence. In reality, as the energy scale at which the theory is defined changes, so do the values of the couplings. For this one needs to consider the renormalisation group equations.

Consider an arbitrary Yukawa coupling $Y_{ijk}\Phi^i\Phi^j\Phi^k$ between three superfields in a general supersymmetric superpotential. In a supersymmetric theory, to derive the beta-function for a Yukawa coupling,

$$\beta_{Y_{ijk}} \equiv \frac{d}{dt}Y^{ijk} = Y^{ijp}\left[\frac{1}{16\pi^2}\gamma_p^{(1)k} + \cdots\right] + \text{permutations}\,, \tag{A.0.2}$$

it suffices to know the expressions for the anomalous dimensions, γ_i^j, of the coupling. At one loop γ_i^j is defined by

$$\gamma_i^{(1)j} = \frac{1}{2}Y_{ipq}Y^{jpq} - 2\delta_i^j g_a^2 C_a(\Phi_i)\,, \tag{A.0.3}$$

where g_a are the gauge couplings and $C_a(\Phi_i)$ are the quadratic Casimir group theory invariants of the *representation* of a given chiral superfield Φ_i, with a denoting the appropriate gauge group.

Together, the quadratic Casimir and the Dynkin index, $S_a(i)$ (a normalisation coefficient for the generators), charactertise the group representation *via*

$$\text{Tr}\left(T_{(R)}^a T_{(R)}^b\right) = S_a(i)\delta^{ab} \tag{A.0.4}$$

$$\left(T_{(R)}^a T_{(R)}^a\right)_i^j = C_a(\Phi_i)\delta_i^j\,, \tag{A.0.5}$$

where $T_{(R)}^a$ are the generator matrices: a set of finite-dimensional traceless hermitian matrices defining the representation. More specifically, there are $D(R) \times D(R)$ generator matrices for each group, with $D(R)$ denoting the dimension of the representation. Generally speaking in literature, when the R subscript is dropped, T^a indicates the set of matrices defining the *fundamental*, or defining, representation. The generator matrices obey commutation relations of the form

$$[T_{(R)}^a, T_{(R)}^b] = if^{abc}T_{(R)}^c\,, \tag{A.0.6}$$

119

where f^{abc} are real numbers called the structure constants which, if non-vanishing, imply the group is non-abelian. The other important representation in this work is the *adjoint* representation, whose dimension is equal to the dimension of the *group*, and is defined by

$$\left(T_{(A)}^a\right)^{ce} = -if^{ace} \,. \tag{A.0.7}$$

Using the Jacobi identify,

$$f^{abd}f^{cde} + f^{bcd}f^{ade} + f^{cad}f^{bde} = 0 \,, \tag{A.0.8}$$

it is possible to show that the adjoint generators also satisfy the commutation relation (A.0.6):

$$\begin{aligned}
\left[T^a, T^b\right]^{ce} &= [T^a]^{cd}[T^b]^{de} - [T^b]^{cd}[T^a]^{de}\\
&= -f^{acd}f^{bde} + f^{bcd}f^{ade}\\
&= f^{cad}f^{bde} + f^{bcd}f^{ade}\\
&= -f^{abd}f^{cde}\\
&= f^{abd}f^{dce}\\
&= if^{abd}[T^d]^{ce} \,.
\end{aligned} \tag{A.0.9}$$

Setting $i = j$ and taking the trace of eq. (A.0.5) and using (A.0.4) one sees that

$$\begin{aligned}
(T^aT^a) = C_a(i)\mathbb{1} \to \mathrm{Tr}(T^aT^a) &= C_a(\Phi_i)N\\
&= S_a(i)\delta^{aa} \,,
\end{aligned}$$

with $\delta^{aa} = D(A)$ the dimensionality of the adjoint representation (equal to the number of group generators) and $N = D(R)$ the dimensionality of the representation of the generators. Therefore one has that

$$C_a(\Phi_i)D(R) = S_a(i)D(A) \,. \tag{A.0.10}$$

The value that each of the above elements takes varies depending on the group, be it $SU(N)$, $SO(N)$, $U(N)$ *etc.* Noteably, for an $\mathcal{N} = 2$ gauge multiplet, the gauge bosons and fermions are in the same representation, and in this instance one finds that $C_a(\Phi_i) = S_a(i)$. The total Dynkin index, $S_a(i)$ refers to the Dynkin index sum over all the chiral superfields Φ_i. For the groups relevant in the calculations presented here, the Dynkin index takes the values

$$S_a(\Phi_i) = \begin{cases} 1/2 & \text{for } \Phi_i \text{ in a (anti)fundamental representation of } SU(N)\\ N & \text{for } \Phi_i \text{ in the adjoint representation of } SU(N)\\ Q_Y^2 & \text{for } \Phi_i \text{ charged under } U(1) \,. \end{cases} \tag{A.0.11}$$

From this one can derive the quadratic Casimir, *e.g.*, for a field in the fundamental irreducible representation of $SU(3)$, such as $\bar{\mathbf{u}}, \bar{\mathbf{d}}, \mathbf{Q}$ *etc.* In this instance the generators are given by

$$T_a(3) = \frac{\lambda_a}{2} \,, \tag{A.0.12}$$

where λ_a are the eight $(N^2 - 1 = 9 - 1)$ Gell-Mann traceless Hermitian matrices for the $SU(3)$ group. Then from (A.0.10) one gets that $C(3) \cdot 3 = \frac{1}{2} \cdot 8$ so that $C(3) = \frac{4}{3}$. Following the same procedure, for the supermultiplets discussed in this text:

$$C_3(\Phi_i) = \begin{cases} 3 & \text{for } \Phi_i = O; \ SU(3) \text{ octets} \\ 4/3 & \text{for } \Phi_i = Q, \bar{u}, \bar{d}; \ SU(3) \text{ triplets} \\ 0 & \text{for } \Phi_i = L, \bar{e}, H_u, H_d; \ SU(3) \text{ singlets} \end{cases} \quad \text{(A.0.13)}$$

$$C_2(\Phi_i) = \begin{cases} 2 & \text{for } \Phi_i = T; \ SU(2) \text{ triplets} \\ 3/4 & \text{for } \Phi_i = Q, L, H_u, H_d; \ SU(2) \text{ doublets} \\ 0 & \text{for } \Phi_i = \bar{u}, \bar{d}, \bar{e}; \ SU(2) \text{ singlets} \end{cases}$$

$$C_1(\Phi_i) = Q_Y^2 \text{ for each } \Phi_i \text{ charged under } U(1) \text{ with hypercharge } Q_Y. \quad \text{(A.0.14)}$$

Gauge coupling renormalisation is instead given by

$$\frac{d}{dt} g_a \equiv \frac{1}{16\pi^2} \beta_{g_a}^{(1)} + \frac{1}{(16\pi^2)^2} \beta_{g_a}^{(2)} + \dots, \quad \text{(A.0.15)}$$

where, at one loop,

$$\beta_{g_a}^{(1)} = g_a^3 \left[\sum_R S_a(i) - 3 C_a(G) \right], \quad \text{(A.0.16)}$$

with $C_a(G)$ - not to be confused with $C_a(\Phi_i)$ - denoting the quadratic Casimir of the gauge *group* (rather than the representation),

$$C_a(G) = \begin{cases} 0 & \text{for U}(1) \\ N & \text{for } SU(N). \end{cases} \quad \text{(A.0.17)}$$

B – Alignment in DG models: more on corrections and matching scales

B.1 THDM with light electroweakinos

In the interesting limit, the electroweakinos are much lighter than the singlet and triplet scalars; in order to avoid washing out the tree-level Higgs quartic coupling and generating a large contribution to ρ they should be light. At energies below the stop/sbottom masses, then, there is an effective theory of the two-Higgs doublet model augmented by light electroweakinos. This looks a little like Split supersymmetry or the scenario of [306] (which considered a split scenario with both Higgs doublets light), except that our electroweakinos have Dirac masses and our gluino is heavy; here are therefore new Yukawa couplings between the Higgs doublets Φ_i, the left and right bino $\tilde{B}_i$ and wino $\tilde{W}_i^a$ for $i = 1, 2$, and the higgsinos $\tilde{h}_{u,d}$:

$$\mathcal{L} \supset -\frac{1}{\sqrt{2}}\left[\tilde{g}_{1u}^{ij}\Phi_i^*\tilde{B}_j\tilde{h}_u + \tilde{g}_{2u}^{ij}\Phi_i^*\tilde{W}_j^a\sigma^a\tilde{h}_u + \tilde{g}_{1d}^{ij}\Phi_i\tilde{B}_j\tilde{h}_d + \tilde{g}_{2d}^{ij}\Phi_i\tilde{W}_j^a\sigma^a\tilde{h}_d + h.c.\right]. \tag{B.1.1}$$

This gives neutral and charged fermion mass matrices

$$\mathcal{M}_{\chi^0} = \begin{pmatrix} M_B & 0 & -\frac{1}{2}v_k g_{1d}^{ki} & \frac{1}{2}v_k g_{1u}^{ki} \\ 0 & M_W & -\frac{1}{2}v_k g_{2d}^{ki} & -\frac{1}{2}v_k g_{2u}^{ki} \\ -\frac{1}{2}v_k g_{1d}^{ki} & -\frac{1}{2}v_k g_{2d}^{ki} & 0 & -\mu \\ \frac{1}{2}v_k g_{1u}^{ki} & -\frac{1}{2}v_k g_{2u}^{ki} & -\mu & 0 \end{pmatrix}, \tag{B.1.2}$$

$$\mathcal{M}_{\chi^\pm} = \begin{pmatrix} M_W & \frac{1}{\sqrt{2}}v_k g_{2u}^{ki} \\ -\frac{1}{\sqrt{2}}v_k g_{2d}^{ki} & \mu \end{pmatrix}, \tag{B.1.3}$$

where the bases are $\chi^0 = (\tilde{B}_1, \tilde{B}_2, \tilde{W}_1^0, \tilde{W}_2^0, \tilde{h}_d^0, \tilde{h}_u^0)$ and the charged mass terms are $\mathcal{L} \supset -(\tilde{W}_i^-, h_d^-)\mathcal{M}_{\chi^\pm}\begin{pmatrix} \tilde{W}_i^+ \\ h_u^+ \end{pmatrix}$. Note that M_B, M_W are 2×2 matrices.

At the SUSY scale, one matches the above to the corresponding couplings in the Dirac gaugino theory:

$$\mathcal{L}^{DG} \supset -\frac{g_Y}{\sqrt{2}}H_u^*\tilde{B}_1\tilde{h}_u - \frac{g_2}{\sqrt{2}}H_u^*\tilde{W}_1^a\sigma^a\tilde{h}_u + \frac{g_Y}{\sqrt{2}}H_d^*\tilde{B}_1\tilde{h}_d - \frac{g_2}{\sqrt{2}}H_d^*\tilde{W}_1^a\sigma^a\tilde{h}_d \tag{B.1.4}$$

$$ - \lambda_S H_u \cdot \tilde{B}_2\tilde{h}_d - \lambda_S\tilde{h}_u \cdot \tilde{B}_2 H_d - \lambda_T H_d \cdot \tilde{W}_2^a\sigma^a\tilde{h}_u - \lambda_T\tilde{h}_d \cdot \tilde{W}_2^a\sigma^a H_u + h.c.$$

The following definition is chosen:

$$\Phi_2 = H_u, \qquad \Phi_1^i = -\epsilon_{ij}(H_d^j)^* \leftrightarrow \begin{pmatrix} H_d^0 \\ H_d^- \end{pmatrix} = \begin{pmatrix} \Phi_1^0 \\ -(\Phi_1^+)^* \end{pmatrix} \tag{B.1.5}$$

meaning $H_u \cdot H_d \leftrightarrow -\Phi_1^\dagger \Phi_2$, which leads to the identifications

$$g_{1d}^{11} = 0, \qquad g_{1d}^{21} = \sqrt{2}\lambda_S, \qquad g_{1u}^{11} = -\sqrt{2}\lambda_S, \qquad g_{1u}^{21} = 0 \tag{B.1.6}$$

$$g_{1d}^{12} = g_Y, \qquad g_{1d}^{22} = 0, \qquad g_{1u}^{12} = 0, \qquad g_{1u}^{22} = g_Y \tag{B.1.7}$$

$$g_{2d}^{11} = 0, \qquad g_{2d}^{21} = \sqrt{2}\lambda_T, \qquad g_{2u}^{11} = \sqrt{2}\lambda_T, \qquad g_{2u}^{21} = 0 \tag{B.1.8}$$

$$g_{2d}^{12} = -g_2, \qquad g_{2d}^{22} = 0, \qquad g_{2u}^{12} = 0, \qquad g_{2u}^{22} = g_2. \tag{B.1.9}$$

These are, however, given in terms of the $\overline{\text{DR}}$ parameters: making the conversion to $\overline{\text{MS}}$ one finds

$$(\tilde{g}_{1u,d}^{ij})_{\overline{\text{MS}}} = (\tilde{g}_{1u,d}^{ij})_{\overline{\text{DR}}}\left[1 - \frac{1}{4}\frac{g_Y^2}{32\pi^2} - \frac{3}{4}\frac{g_2^2}{32\pi^2}\right]$$

$$(\tilde{g}_{2u,d}^{ij})_{\overline{\text{MS}}} = (\tilde{g}_{2u,d}^{ij})_{\overline{\text{DR}}}\left[1 - \frac{1}{4}\frac{g_Y^2}{32\pi^2} + \frac{5}{4}\frac{g_2^2}{32\pi^2}\right]. \tag{B.1.10}$$

B.2 Threshold corrections

In this section, the one-loop threshold corrections to the couplings in the theory will be given . Throughout the definitions

$$\kappa \equiv \frac{1}{16\pi^2}$$

$$\overline{\log} \, x \equiv \log\frac{x}{\mu^2}$$

$$P_{SS}(x,y) \equiv \frac{x\overline{\log}x - y\overline{\log}y}{x - y} - 1, \tag{B.2.1}$$

are used, where μ is the renormalisation scale at which the quantities are evaluated.

B.2.1 Conversion from $\overline{\text{MS}}$ to $\overline{\text{DR}}$

The conversion of the gauge couplings from the $\overline{\text{MS}}$ to $\overline{\text{DR}}$ renormalisation scheme is given by

$$(g_Y)_{\overline{\text{MS}}} = (g_Y)_{\overline{\text{DR}}}$$

$$(g_2)_{\overline{\text{MS}}} = (g_2)_{\overline{\text{DR}}}\left[1 - \frac{\kappa g_2^2}{3}\right]$$

$$(g_3)_{\overline{\text{MS}}} = (g_3)_{\overline{\text{DR}}}\left[1 - \frac{\kappa g_3^2}{2}\right]. \tag{B.2.2}$$

For the Yukawa couplings, only the strong gauge coupling dependence is retained:

$$y_{\overline{\text{MS}}}^{t,b} \simeq y_{\overline{\text{DR}}}^{t,b}\left(1 + \frac{4}{3}\kappa g_3^2\right). \tag{B.2.3}$$

For the Higgs quartic couplings, defining

$$\lambda_i^{\overline{\text{MS}}} = \lambda_i^{\overline{\text{DR}}} + \delta\lambda_i \, , \tag{B.2.4}$$

then

$$\delta\lambda_1 = \delta\lambda_2 = -\frac{\kappa}{4}\left(g_Y^4 + 3g_2^4 + g_Y^2 g_2^2\right)$$

$$\delta\lambda_3 = -\frac{\kappa}{4}\left(g_Y^4 + 3g_2^4 - 2g_Y^2 g_2^2\right)$$

$$\delta\lambda_4 = -\kappa g_Y^2 g_2^2. \tag{B.2.5}$$

If the quartic couplings are expressed in terms of the $\overline{\text{MS}}$ gauge couplings at tree level, then there is a further shift from the shift to g_2 of $+\frac{\kappa}{6}g_2^4$ for $\lambda_{1,2}$ and $-\frac{\kappa}{6}g_2^4$ for λ_3.

B.2.2 Squark contributions

B.2.2.1 Matching at the SUSY scale

In the limit that taken in the body of the paper, all of the threshold corrections coming from squarks vanish at the matching scale. However, to extend the results of [174,307] to our model, the corrections were computed coming from stops, sbottoms and staus to the quartic couplings allowing non-zero squark trilinears and μ. They are given by

$$\delta\lambda_i \equiv \delta_{\text{th}}^{(1)}\lambda_i + \delta_{\Phi}^{(1)}\lambda_i, \tag{B.2.6}$$

where the $\delta_{\text{th}}^{(1)}\lambda_i$ contributions are those from bubble, triangle and box diagrams and are unchanged from the MSSM case given in [174,307], while the $\delta_{\Phi}^{(1)}\lambda_i$ are the wave-function corrections that *are* modified for our model:

$$\kappa^{-1}\delta_{\Phi}^{(1)}\lambda_1 = -\frac{g_2^2 + g_Y^2}{12M_S^2}(3A_b^2 + 3y_t^2\mu^2 + A_\tau^2)$$

$$\kappa^{-1}\delta_{\Phi}^{(1)}\lambda_2 = -\frac{g_2^2 + g_Y^2}{12M_S^2}(3A_t^2 + 3y_b^2\mu^2 + \mu^2 y_\tau^2)$$

$$\kappa^{-1}\delta_{\Phi}^{(1)}\lambda_3 = -\frac{g_2^2 - g_Y^2 + 8\lambda_T^2}{24M_S^2}(3A_t^2 + 3A_b^2 + 3(y_b^2 + y_t^2)\mu^2 + A_\tau^2 + y_\tau^2\mu^2)$$

$$\kappa^{-1}\delta_{\Phi}^{(1)}\lambda_4 = \frac{g_2^2 - 2\lambda_S^2 + 2\lambda_T^2}{12M_S^2}(3A_t^2 + 3A_b^2 + 3(y_b^2 + y_t^2)\mu^2 + A_\tau^2 + y_\tau^2\mu^2)$$

$$\kappa^{-1}\delta_{\Phi}^{(1)}\lambda_5 = 0$$

$$\kappa^{-1}\delta_{\Phi}^{(1)}\lambda_6 = \frac{\lambda_S^2 + \lambda_T^2}{12M_S^2}\mu(3A_t y_t + 3A_b y_b + A_\tau y_\tau)$$

$$\kappa^{-1}\delta_{\Phi}^{(1)}\lambda_7 = \kappa^{-1}\delta_{\Phi}^{(1)}\lambda_6. \tag{B.2.7}$$

B.2.2.2 Matching at a general scale

If the squarks are not degenerate or are integrated out at a scale other than a common SUSY scale, then in our limit,

$$\kappa^{-1}\delta\lambda_1 = \frac{1}{24}\left[(9g_2^4 + g_Y^4 - 36g_2^2 y_b^2 - 12g_Y^2 y_b^2 + 72y_b^4)\overline{\log}m_Q^2 + 8g_Y^4\overline{\log}m_U^2 + 2(g_Y^2 - 6y_b^2)^2\overline{\log}m_D^2\right]$$

$$+ \frac{1}{8}\left[2(g_Y^2 - 2y_\tau^2)^2\overline{\log}m_E^2 + (g_2^4 + g_Y^4 - 4g_2^2 y_\tau^2 + 4g_Y^2 y_\tau^2 + 8y_\tau^4)\overline{\log}m_L^2\right]$$

$$\kappa^{-1}\delta\lambda_2 = \frac{1}{24}\left[(9g_2^4 + g_Y^4 - 36g_2^2 y_t^2 - 12g_Y^2 y_t^2 + 72y_t^4)\overline{\log}m_Q^2 + 2g_Y^4\overline{\log}m_D^2 + 8(g_Y^2 - 3y_t^2)^2\overline{\log}m_U^2\right]$$

$$+ \frac{1}{8}\left[2g_Y^4\overline{\log}m_E^2 + (g_2^4 + g_Y^4)\overline{\log}m_L^2\right]$$

$$\kappa^{-1}\delta\lambda_3 = 3y_b^2 y_t^2 P_{SS}(m_D^2, m_U^2)$$

$$+ \frac{1}{24}\bigg[(9g_2^4 - g_Y^4 + 72y_t^2 y_b^2 + 6g_Y^2(y_b^2 - y_t^2) - 18g_2^2(y_b^2 + y_t^2))\overline{\log}m_Q^2$$

$$- 2g_Y^2(g_Y^2 - 6y_b^2)\overline{\log}m_D^2 - 8g_Y^2(g_Y^2 - 3y_t^2)\overline{\log}m_U^2\bigg]$$

$$+ \frac{1}{8}\bigg[-2g_Y^2(g_Y^2 - 2y_\tau^2)\overline{\log}m_E^2 + (g_2^2 + g_Y^2)(g_2^2 - g_Y^2 - 2y_\tau^2)\overline{\log}m_L^2\bigg]$$

$$\kappa^{-1}\delta\lambda_4 = -3y_b^2 y_t^2 P_{SS}(m_D^2, m_U^2) - \frac{3}{4}\bigg[(g_2^2 - 2y_b^2)(g_2^2 - 2y_t^2)\bigg]\overline{\log}m_Q^2$$

$$- \frac{1}{4}g_2^2(g_2^2 - 2y_\tau^2)\overline{\log}m_L^2. \tag{B.2.8}$$

If all squarks are considered to be at a common SUSY scale M_S, then these simplify to

$$\kappa^{-1}\delta\lambda_1 = \frac{1}{6}\overline{\log}M_S^2\bigg[3g_2^4 + 5g_Y^4 - 3(g_2^2 + g_Y^2)(3y_b^2 + y_\tau^2) + 12(3y_b^4 + y_\tau^4)\bigg]$$

$$\kappa^{-1}\delta\lambda_2 = \frac{1}{6}\overline{\log}M_S^2\bigg[3g_2^4 + 5g_Y^4 - 9g_2^2 y_t^2 - 15g_Y^2 y_t^2 + 36y_t^4\bigg]$$

$$\kappa^{-1}\delta\lambda_3 = \frac{1}{12}\overline{\log}M_S^2\bigg[6g_2^4 - 10g_Y^4 + 72y_b^2 y_t^2 - 3(g_2^2 + g_Y^2)(3y_b^2 + 3y_t^2 + y_\tau^2))\bigg]$$

$$\kappa^{-1}\delta\lambda_4 = \frac{1}{2}\overline{\log}M_S^2\bigg[-2g_2^4 - 12y_b^2 y_t^2 + g_2^2(3y_b^2 + 3y_t^2 + y_\tau^2))\bigg]$$

$$\kappa^{-1}(\delta\lambda_3 + \delta\lambda_4) = \frac{1}{12}\overline{\log}M_S^2\bigg[-6g_2^4 - 10g_Y^4 + 3(g_2^2 - g_Y^2)(3y_b^2 + 3y_t^2 + y_\tau^2))\bigg]. \tag{B.2.9}$$

B.2.3 Contributions from the S, T scalars

The mass splitting between superpartners leads to important radiative corrections at one-loop that modify the scalar potential. At this order, the main contribution comes from the top quark Yukawa coupling, already present in the MSSM, and from the contribution of the splitting between scalar and fermionic modes in the **S** and **T** superfields. These lead to new contributions to the two-Higgs doublet model effective potential and consequently modify the alignment condition. The purpose of this section is to elaborate on the equations given in (2.3.11) on the contributions to the quartic couplings coming from the adjoint scalars S, T, in the limit $m_{DY}, m_{D2} \ll m_S, m_T, B_S, B_T$ and assuming no CP-violation. The scalars have (effective) masses

$$m_{SR}^2 = m_S^2 + B_S + 4m_{DY}^2 \simeq m_S^2 + B_S, \qquad m_{SI}^2 = m_S^2 - B_S \tag{B.2.10}$$

$$m_{TP}^2 = m_T^2 + B_T + 4m_{D2}^2 \simeq m_T^2 + B_T, \qquad m_{TM}^2 = m_T^2 - B_T. \tag{B.2.11}$$

When full one loop corrections to the quartic couplings are:

$$\delta\lambda_1 = \delta\lambda_2 = \frac{1}{16\pi^2}\frac{1}{2}\bigg[\lambda_S^4 \log\frac{m_{SR}^2 m_{SI}^2}{\mu^4} + 3\lambda_T^4 \log\frac{m_{TP}^2 m_{TM}^2}{\mu^4} + (g_2^2 - 2\lambda_T^2)^2 P_{SS}(m_{TM}^2, m_{TP}^2)$$

$$+ 2\lambda_S^2 \lambda_T^2\bigg(P_{SS}(m_{SR}^2, m_{TP}^2) + P_{SS}(m_{SI}^2, m_{TM}^2)\bigg)\bigg]$$

$$\delta\lambda_3 = \frac{1}{16\pi^2}\frac{1}{2}\bigg[\lambda_S^4 \log\frac{m_{SR}^2 m_{SI}^2}{\mu^4} + 3\lambda_T^4 \log\frac{m_{TP}^2 m_{TM}^2}{\mu^4} + (g_2^2 - 2\lambda_T^2)^2 P_{SS}(m_{TM}^2, m_{TP}^2)$$

$$- 2\lambda_S^2 \lambda_T^2\bigg(P_{SS}(m_{SR}^2, m_{TP}^2) + P_{SS}(m_{SI}^2, m_{TM}^2)\bigg)\bigg]$$

$$\delta\lambda_4 = \frac{1}{16\pi^2}\Bigg[-(g_2^2 - 2\lambda_T^2)^2 P_{SS}(m_{TM}^2, m_{TP}^2)$$

$$+ 2\lambda_S^2\lambda_T^2\Big(P_{SS}(m_{SR}^2, m_{TP}^2) + P_{SS}(m_{SI}^2, m_{TM}^2)\Big)\Bigg]. \qquad (B.2.12)$$

These results update those previously given in the literature by including the electroweak contributions.

A simple derivation of the leading contributions that come from quartic vertices will be presented in the case that there is no splitting between the imaginary and real components of the scalar masses, and additionally that there is no splitting of the Yukawa couplings and their $\mathcal{N} = 2$ relations. These can be found using the Coleman-Weinberg potential,

$$V_{CW} = \frac{1}{64\pi^2}\text{tr}\left[\mathcal{M}^4\left(\log\left(\frac{\mathcal{M}^2}{\Lambda^2}\right) - \frac{3}{2}\right)\right], \qquad (B.2.13)$$

from which one can find the mass matrix $\mathcal{M}^2$ of the S, T fields. Its eigenvalues can be written as the perturbative expansion,

$$m_i^{(D)2} = m_i^2 + a_i\epsilon + b_i\epsilon^2 + ..., \qquad (B.2.14)$$

giving

$$
\begin{aligned}
V_{CW} &= \frac{1}{64\pi^2}\sum_i (m_i^2 + a_i\epsilon + b_i\epsilon^2 + ...)^2\left[\log\left(\frac{m_i^2 + a_i\epsilon + b_i\epsilon^2 + ...}{\Lambda^2}\right) - \frac{3}{2}\right] \\
&= \frac{1}{64\pi^2}\sum_i \left[m_i^4 + \epsilon(2m_i^2 a_i) + \epsilon^2(a_i^2 + 2m_i^2 b_i) + ...\right] \\
&\quad \times \left[\log\left(\frac{m_i^2}{\Lambda^2}\right) - \frac{3}{2} + \epsilon\frac{a_i}{m_i^2} + \epsilon^2\left(\frac{b_i}{m_i^2} - \frac{a_i^2}{2m_i^2}\right) + ...\right]. \qquad (B.2.15)
\end{aligned}
$$

The terms quartic in the couplings are parametrised by ϵ^2,

$$V_{CW} \supset \epsilon^2\frac{1}{64\pi^2}\sum_{i=S,T}\left[a_i^2\log\frac{m_i^2}{\Lambda^2} + 2b_i m_i^2\left(\log\frac{m_i^2}{\Lambda^2} - 1\right)\right]. \qquad (B.2.16)$$

The pure couplings are mass diagonal, and so the contribution of the first order eigenvalues to the potential can be read off straight away:

$$
\begin{aligned}
V_{CW} \supset\ & \frac{\lambda_T^4}{64\pi^2}\log\frac{m_T^2}{\Lambda^2}\left[10|H_d|^2 + 10|H_u|^2 + 20|H_d|^2|H_u|^2 - 16|H_u \cdot H_d|^2\right] \\
+\ & \frac{\lambda_S^4}{64\pi^2}\log\frac{m_S^2}{\Lambda^2}\left[2|H_d|^2 + 2|H_u|^2 + 4|H_u|^2|H_d|^2\right], \qquad (B.2.17)
\end{aligned}
$$

giving the radiative corrections to the two-Higgs model parameters,

$$\frac{1}{2}\delta_{\lambda_1}^{(diag)} = \frac{1}{64\pi^2}\left[2\lambda_S^4\log\left(\frac{m_S^2}{\Lambda^2}\right) + 10\lambda_T^4\log\left(\frac{m_T^2}{\Lambda^2}\right)\right] = \frac{1}{2}\delta_{\lambda_2}^{(diag)} \quad (B.2.18)$$

$$\delta_{\lambda_3}^{(diag)} = \frac{1}{64\pi^2}\left[4\lambda_S^4\log\left(\frac{m_S^2}{\Lambda^2}\right) + 20\lambda_T^4\log\left(\frac{m_T^2}{\Lambda^2}\right)\right] \qquad (B.2.19)$$

$$\delta_{\lambda_4}^{(diag)} = \frac{1}{64\pi^2}\left[-16\lambda_T^4\log\left(\frac{m_T^2}{\Lambda^2}\right)\right]. \qquad (B.2.20)$$

To find the contributions to the second order eigenvalues, b_i, it is convenient to set the first order eigenvalues to zero. One can then diagonalise the mass matrix to have

the contributions from the mixed terms $\lambda_S \lambda_T$ restricted to one independent entry of the matrix. Given the superpotential,

$$W_{DG} \supset \lambda_S \mathbf{S} \epsilon_{ij} \mathbf{H_u}^i \mathbf{H_d}^j + \lambda_T \mathbf{T}^a \mathbf{H_u}^i \mathbf{H_d}^j \epsilon_{jk} \sigma_{ki}^a . \tag{B.2.21}$$

the mixed terms read

$$V \supset \lambda_S \lambda_T \left[S \bar{T}^a \left\{ H_d^\dagger \sigma^a H_d - H_u^\dagger \sigma^a H_u \right\} + h.c. \right] , \tag{B.2.22}$$

where it is used that $\epsilon_{ij} = i\sigma_{ij}^2$, $\sigma^2 \bar{\sigma}^i \sigma^2 = -(\bar{\sigma}^i)^T = -(\sigma^i)^\dagger = -\sigma^i$. Writing the mass matrix in the basis S, T^a, the two eigenvalues of the charged scalars will be given by m_T^2, while the remaining two eigenvalues can be embedded in a 2×2 complex matrix, with off-diagonals mixed terms,

$$\begin{pmatrix} m_T^2 & \lambda_S \lambda_T |H_d^\dagger \sigma^a H_d - H_u^\dagger \sigma^a H_u| \\ \lambda_S \lambda_T |H_d^\dagger \sigma^a H_d - H_u^\dagger \sigma^a H_u| & m_S^2 \end{pmatrix} . \tag{B.2.23}$$

The eigenvalues are found by the characteristic equation,

$$(m_T^2 - m_i^{(D)2})(m_S^2 - m_i^{(D)2}) - \lambda_S^2 \lambda_T^2 \sum_a |H_d^\dagger \sigma^a H_d - H_u^\dagger \sigma^a H_u|^2 = 0 , \tag{B.2.24}$$

such that

$$m_i^{(D)4} - m_i^{(D)2}(m_T^2 + m_S^2) - \left(\lambda_S^2 \lambda_T^2 \sum_a |H_d^\dagger \sigma^a H_d - H_u^\dagger \sigma^a H_u|^2 - m_T^2 m_S^2 \right) = 0, \tag{B.2.25}$$

yielding

$$m_S^{(D)2} \simeq m_S^2 + \lambda_S^2 \lambda_T^2 \sum_a \frac{|H_d^\dagger \sigma^a H_d - H_u^\dagger \sigma^a H_u|^2}{m_S^2 - m_T^2} , \tag{B.2.26}$$

$$m_T^{(D)2} \simeq m_T^2 - \lambda_S^2 \lambda_T^2 \sum_a \frac{|H_d^\dagger \sigma^a H_d - H_u^\dagger \sigma^a H_u|^2}{m_S^2 - m_T^2} . \tag{B.2.27}$$

Comparing these eigenvalue expressions to the expansion, and remembering that zeroth order eigenvalues have been ignored here, one sees that

$$b_S = \lambda_S^2 \lambda_T^2 \sum_a \frac{|H_d^\dagger \sigma^a H_d - H_u^\dagger \sigma^a H_u|^2}{m_S^2 - m_T^2} = -b_T , \tag{B.2.28}$$

and therefore

$$V_{CW} \supset \sum_{i,a} \frac{2\lambda_S^2 \lambda_T^2}{64\pi^2} \frac{|H_d^\dagger \sigma^a H_d - H_u^\dagger \sigma^a H_u|^2}{m_S^2 - m_T^2} \left\{ m_S^2 \left(\log \frac{m_S^2}{\Lambda^2} - 1 \right) - m_T^2 \left(\log \frac{m_S^2}{\Lambda^2} - 1 \right) \right\}$$

$$= \frac{1}{64\pi^2} \left[\frac{4\lambda_S^2 \lambda_T^2}{m_S^2 - m_T^2} \left(|H_u|^4 + |H_d|^4 - 2|H_u|^2 |H_d|^2 + 4|H_u \cdot H_d|^2 \right) \right.$$

$$\left. \times \left\{ m_S^2 \left(\log \frac{m_S^2}{\Lambda^2} - 1 \right) - m_T^2 \left(\log \frac{m_S^2}{\Lambda^2} - 1 \right) \right\} \right] , \tag{B.2.29}$$

where a factor of 2 comes from the complex nature of the fields S, T^as. From this the radiative corrections to the two-Higgs doublet model parameters coming from the mixed terms are given by

$$\frac{1}{2} \delta_{\lambda_1}^{(off)} = \frac{1}{16\pi^2} \frac{\lambda_S^2 \lambda_T^2}{m_S^2 - m_T^2} \left\{ m_S^2 \left(\log \frac{m_S^2}{\Lambda^2} - 1 \right) - m_T^2 \left(\log \frac{m_S^2}{\Lambda^2} - 1 \right) \right\} = \frac{1}{2} \delta_{\lambda_2}^{(off)}$$

$$
\delta_{\lambda_3}^{(off)} = -\frac{1}{8\pi^2}\frac{\lambda_S^2\lambda_T^2}{m_S^2 - m_T^2}\left\{ m_S^2\left(\log\frac{m_S^2}{\Lambda^2} - 1\right) - m_T^2\left(\log\frac{m_S^2}{\Lambda^2} - 1\right)\right\}
$$

$$
\delta_{\lambda_4}^{(off)} = \frac{1}{4\pi^2}\frac{\lambda_S^2\lambda_T^2}{m_S^2 - m_T^2}\left\{ m_S^2\left(\log\frac{m_S^2}{\Lambda^2} - 1\right) - m_T^2\left(\log\frac{m_S^2}{\Lambda^2} - 1\right)\right\}. \quad\text{(B.2.30)}
$$

The total leading order contribution from radiative corrections to the two-Higgs doublet model parameters is given by the sum

$$
\delta_{\lambda_i}^{(1)} = \delta_{\lambda_i}^{(top)} + \delta_{\lambda_i}^{(bot)} + \delta_{\lambda_i}^{(diag)} + \delta_{\lambda_i}^{(off)} \quad\text{(B.2.31)}
$$

of the contribution $\delta_{\lambda_i}^{(top)}$ of the top quark, $\delta_{\lambda_i}^{(bot)}$ of the bottom quark, $\delta_{\lambda_i}^{(diag)}$ from diagonal λ_i^4 terms and $\delta_{\lambda_i}^{(off)}$ from mixed $\lambda_S^2\lambda_T^2$ terms. This gives

$$
\begin{aligned}
\delta_{\lambda_1}^{(1)} = {}& \frac{3}{8\pi^2}y_b^4\log\left(\frac{m_{\tilde{b}_1}m_{\tilde{b}_2}}{v^2}\right) + \frac{5}{16\pi^2}\lambda_T^4\log\left(\frac{m_T^2}{v^2}\right) + \frac{1}{16\pi^2}\lambda_S^4\log\left(\frac{m_S^2}{v^2}\right) \\
& + \frac{1}{8\pi^2}\frac{\lambda_S^2\lambda_T^2}{m_T^2 - m_S^2}\left\{ m_T^2[\log\left(\frac{m_T^2}{v^2}\right) - 1] - m_S^2[\log\left(\frac{m_S^2}{v^2}\right) - 1]\right\},
\end{aligned} \quad\text{(B.2.32)}
$$

$$
\begin{aligned}
\delta_{\lambda_2}^{(1)} = {}& \frac{3}{8\pi^2}y_t^4\log\left(\frac{m_{\tilde{t}_1}m_{\tilde{t}_2}}{m_t^2}\right) + \frac{5}{16\pi^2}\lambda_T^4\log\left(\frac{m_T^2}{v^2}\right) + \frac{1}{16\pi^2}\lambda_S^4\log\left(\frac{m_S^2}{v^2}\right) \\
& + \frac{1}{8\pi^2}\frac{\lambda_S^2\lambda_T^2}{m_T^2 - m_S^2}\left\{ m_T^2[\log\left(\frac{m_T^2}{v^2}\right) - 1] - m_S^2[\log\left(\frac{m_S^2}{v^2}\right) - 1]\right\},
\end{aligned} \quad\text{(B.2.33)}
$$

$$
\begin{aligned}
\delta_{\lambda_3}^{(1)} = {}& \frac{5}{16\pi^2}\lambda_T^4\log\left(\frac{m_T^2}{v^2}\right) + \frac{1}{16\pi^2}\lambda_S^4\log\left(\frac{m_S^2}{v^2}\right) \\
& - \frac{1}{8\pi^2}\frac{\lambda_S^2\lambda_T^2}{m_T^2 - m_S^2}\left\{ m_T^2[\log\left(\frac{m_T^2}{v^2}\right) - 1] - m_S^2[\log\left(\frac{m_S^2}{v^2}\right) - 1]\right\},
\end{aligned} \quad\text{(B.2.34)}
$$

$$
\begin{aligned}
\delta_{\lambda_4}^{(1)} = {}& -\frac{1}{4\pi^2}\lambda_T^4\log\left(\frac{m_T^2}{v^2}\right) \\
& + \frac{1}{4\pi^2}\frac{\lambda_S^2\lambda_T^2}{m_T^2 - m_S^2}\left\{ m_T^2[\log\left(\frac{m_T^2}{v^2}\right) - 1] - m_S^2[\log\left(\frac{m_S^2}{v^2}\right) - 1]\right\},
\end{aligned} \quad\text{(B.2.35)}
$$

with no corrections to the other effective two-Higgs doublet model parameters.

The alignment limit in the effective two-Higgs model is governed by the relative value of the off-diagonal element Z_6 relative to the diagonal ones. The tree-level value is then modified at one-loop order (in the relevant limits stated above) to

$$
\begin{aligned}
Z_6^{(1)} = {}& -\frac{1}{2}s_{2\beta}\left[\left(\lambda_1 + \delta_{\lambda_1}^{(1)}\right)c_\beta^2 - \left(\lambda_2 + \delta_{\lambda_2}^{(1)}\right)s_\beta^2 - \left\{\left(\lambda_3 + \delta_{\lambda_3}^{(1)}\right)\right. \right. \\
& \left. \left. + \left(\lambda_4 + \delta_{\lambda_4}^{(1)}\right) + \left(\lambda_5 + \delta_{\lambda_5}^{(1)}\right)\right\}c_{2\beta}\right] \\
= {}& -\frac{1}{2}s_{2\beta}c_{2\beta}\left[\frac{1}{2}(g^2 + g'^2) - (\lambda_S^2 + \lambda_T^2) + \frac{\lambda_T^4}{4\pi^2}\log\left(\frac{m_T^2}{v^2}\right)\right] \\
& - \frac{3}{16\pi^2}s_{2\beta}\left[y_b^4\log\left(\frac{m_{\tilde{b}_1}m_{\tilde{b}_2}}{v^2}\right)c_\beta^2 - y_t^4\log\left(\frac{m_{\tilde{t}_1}m_{\tilde{t}_2}}{m_t^2}\right)s_\beta^2\right].
\end{aligned} \quad\text{(B.2.36)}
$$

Note that there is no explicit dependence on λ_S as the latter appears in the scalar potential as a coefficient of terms that are invariant under rotations towards the alignment limit in the plane of $\{H_u, H_d\}$.

B.3 One-loop RGEs

B.3.1 THDM with electroweakinos

For our numerical study two-loop RGEs are used throughout, as generated by `SARAH`. They are too long to put into print; however, for illustration provide here are the one-loop expressions for the low-energy theory of the THDM with electroweakinos, after making the simplification that:

- Only third generation Yukawa couplings are included.

- No CP-violation, hence all couplings real.

- Respecting the matching conditions (B.1.6-B.1.9), the beta functions for the couplings that are zero at the supersmmetry scale are zero along the flow, and hence the couplings g_{1d}^{11}, g_{1u}^{21}, g_{1d}^{22}, g_{1u}^{12}, g_{2d}^{11}, g_{2u}^{21}, g_{2d}^{22}, g_{2u}^{12} are set to zero.

Then defining

$$\frac{dx}{d\log\mu} \equiv \kappa\beta_x^{(1)} + \kappa^2\beta_x^{(2)} + ... \tag{B.3.1}$$

the RGEs for the dimensionless quantities in the theory are given below.

B.3.1.1 Gauge couplings

$$\beta_{g_Y}^{(1)} = \frac{23}{3}g_Y^3$$

$$\beta_{g_2}^{(1)} = \frac{1}{3}g_2^3 \tag{B.3.2}$$

$$\beta_{g_3}^{(1)} = -7g_3^3$$

B.3.1.2 Yukawa couplings

$$\beta_{y_b}^{(1)} = \frac{1}{12}y_b(-27g_2^2 - 96g_3^2 - 5g_Y^2 + 54y_b^2 + 6y_t^2 + 12y_\tau^2$$
$$+ 6(g_{1d}^{12})^2 + 6(g_{1u}^{11})^2 + 18(g_{2d}^{12})^2 + 18(g_{2u}^{11})^2)$$

$$\beta_{y_t}^{(1)} = \frac{1}{12}y_t(-27g_2^2 - 96g_3^2 - 17g_Y^2 + 6y_b^2 + 54y_t^2$$
$$+ 6(g_{1d}^{21})^2 + 6(g_{1u}^{22})^2 + 18(g_{2d}^{21})^2 + 18(g_{2u}^{22})^2)$$

$$\beta_{y_\tau}^{(1)} = \frac{1}{4}y_\tau(-9g_2^2 - 15g_Y^2 + 2(6y_b^2 + 5y_\tau^2 + (g_{1d}^{12})^2 + (g_{1u}^{11})^2 + 3(g_{2d}^{12})^2 + 3(g_{2u}^{11})^2))$$

$$\beta_{g_{1d}^{12}}^{(1)} = \frac{1}{20}(10g_{1u}^{22}(2g_{1u}^{11}g_{1d}^{21} + g_{1d}^{12}g_{1u}^{22} + 6g_{2u}^{11}g_{2d}^{21}) + +5g_{1d}^{12}(-9g_2^2 - 3g_Y^2 + 12y_b^2 + 4y_\tau^2$$
$$+ 5(g_{1d}^{12})^2 + 2(g_{1u}^{11})^2 + 9(g_{2d}^{12})^2 + 6(g_{2u}^{11})^2 + (g_{1d}^{21})^2 + 3(g_{2d}^{21})^2))$$

$$\beta_{g_{1u}^{11}}^{(1)} = \frac{1}{20}(10g_{1d}^{21}(g_{1u}^{11}g_{1d}^{21} + 2g_{1d}^{12}g_{1u}^{22} + 6g_{2d}^{12}g_{2u}^{22}) + 5g_{1u}^{11}(-9g_2^2 - 3g_Y^2 + 12y_b^2 + 4y_\tau^2$$
$$+ 2(g_{1d}^{12})^2 + 5(g_{1u}^{11})^2 + 6(g_{2d}^{12})^2 + 9(g_{2u}^{11})^2 + (g_{1u}^{22})^2 + 3(g_{2u}^{22})^2))$$

$$\beta_{g_{2d}^{12}}^{(1)} = \frac{1}{20}(5g_{2d}^{12}(-33g_2^2 - 3g_Y^2 + 12y_b^2 + 4y_\tau^2 + 3(g_{1d}^{12})^2 + 2(g_{1u}^{11})^2 + 11(g_{2d}^{12})^2 + 6(g_{2u}^{11})^2$$
$$+ (g_{1d}^{21})^2 + 3(g_{2d}^{21})^2) + 10g_{2u}^{22}(2g_{1u}^{11}g_{1d}^{21} - 2g_{2u}^{11}g_{2d}^{21} + g_{2d}^{12}g_{2u}^{22}))$$

$$\beta_{g_{2u}^{11}}^{(1)} = \frac{1}{20}(10g_{2d}^{21}(2g_{1d}^{12}g_{1u}^{22} + g_{2u}^{11}g_{2d}^{21} - 2g_{2d}^{12}g_{2u}^{22}) + 5g_{2u}^{11}(-33g_2^2 - 3g_Y^2 + 12y_b^2 + 4y_\tau^2$$
$$+ 2(g_{1d}^{12})^2 + 3(g_{1u}^{11})^2 + 6(g_{2d}^{12})^2 + 11(g_{2u}^{11})^2 + (g_{1u}^{22})^2 + 3(g_{2u}^{22})^2))$$

$$\beta_{g_{1d}^{21}}^{(1)} = \frac{1}{20}(10g_{1u}^{11}(g_{1u}^{11}g_{1d}^{21} + 2g_{1d}^{12}g_{1u}^{22} + 6g_{2d}^{12}g_{2u}^{22}) + 5g_{1d}^{21}(-9g_2^2 - 3g_Y^2 + 12y_t^2$$
$$+ (g_{1d}^{12})^2 + 3(g_{2d}^{12})^2 + 5(g_{1d}^{21})^2 + 2(g_{1u}^{22})^2 + 9(g_{2d}^{21})^2 + 6(g_{2u}^{22})^2))$$

$$\beta_{g_{1u}^{22}}^{(1)} = \frac{1}{4}(2(g_{1d}^{12})^2 g_{1u}^{22} + 4g_{1d}^{12}(g_{1u}^{11}g_{1d}^{21} + 3g_{2u}^{11}g_{2d}^{21}) + g_{1u}^{22}(-9g_2^2 - 3g_Y^2 + 12y_t^2$$
$$+ (g_{1u}^{11})^2 + 3(g_{2u}^{11})^2 + 2(g_{1d}^{21})^2 + 5(g_{1u}^{22})^2 + 6(g_{2d}^{21})^2 + 9(g_{2u}^{22})^2))$$

$$\beta_{g_{2d}^{21}}^{(1)} = \frac{1}{20}(10g_{2u}^{11}(2g_{1d}^{12}g_{1u}^{22} + g_{2u}^{11}g_{2d}^{21} - 2g_{2d}^{12}g_{2u}^{22}) + 5g_{2d}^{21}(-33g_2^2 - 3g_Y^2 + 12y_t^2$$
$$+ (g_{1d}^{12})^2 + 3(g_{2d}^{12})^2 + 3(g_{1d}^{21})^2 + 2(g_{1u}^{22})^2 + 11(g_{2d}^{21})^2 + 6(g_{2u}^{22})^2))$$

$$\beta_{g_{2u}^{22}}^{(1)} = \frac{1}{4}(4g_{1u}^{11}g_{2d}^{12}g_{1d}^{21} - 4g_{2d}^{12}g_{2u}^{11}g_{2d}^{21} + (g_{1u}^{11})^2 g_{2u}^{22} + 2(g_{2d}^{12})^2 g_{2u}^{22}$$
$$+ g_{2u}^{22}(-33g_2^2 - 3g_Y^2 + 12y_t^2 + 3(g_{2u}^{11})^2 + 2(g_{1d}^{21})^2 + 3(g_{1u}^{22})^2 + 6(g_{2d}^{21})^2 + 11(g_{2u}^{22})^2)).$$

$$(B.3.3)$$

B.3.1.3   Quartic scalar couplings

$$\beta_{\lambda_1}^{(1)} = \frac{1}{4}\left(9g_2^4 + 3g_Y^4 + 6g_2^2(g_Y^2 - 6\lambda_1) - 12g_Y^2\lambda_1\right) - \left(12y_b^4 + 4y_\tau^4 - 12y_b^2\lambda_1 - 4y_\tau^2\lambda_1 - 12\lambda_1^2\right.$$
$$- 4\lambda_3^2 - 4\lambda_3\lambda_4 - 2\lambda_4^2 - 2\lambda_5^2 - 2\lambda_1(g_{1d}^{12})^2 + (g_{1d}^{12})^4 - 2\lambda_1(g_{1u}^{11})^2 + (g_{1u}^{11})^4 - 6\lambda_1(g_{2d}^{12})^2$$
$$+ 2(g_{1d}^{12})^2(g_{2d}^{12})^2 + 5(g_{2d}^{12})^4 - 6\lambda_1(g_{2u}^{11})^2 + 2(g_{1u}^{11})^2(g_{2u}^{11})^2 + 5(g_{2u}^{11})^4\right)$$

$$\beta_{\lambda_2}^{(1)} = \frac{1}{4}\left(9g_2^4 + 3g_Y^4 + 6g_2^2(g_Y^2 - 6\lambda_2) - 12g_Y^2\lambda_2\right) - \left(12y_t^4 - 12y_t^2\lambda_2 - 12\lambda_2^2 - 4\lambda_3^2 - 4\lambda_3\lambda_4\right.$$
$$- 2\lambda_4^2 - 2\lambda_5^2 + (g_{1d}^{21})^4 + (g_{1u}^{22})^4 + 2(g_{1d}^{21})^2(g_{2d}^{21})^2 + 5(g_{2d}^{21})^4 + 2(g_{1u}^{22})^2(g_{2u}^{22})^2 + 5(g_{2u}^{22})^4$$
$$- 2\lambda_2\left[(g_{1d}^{21})^2 + (g_{1u}^{22})^2 + 3((g_{2d}^{21})^2 + (g_{2u}^{22})^2)\right]\right)$$

$$\beta_{\lambda_3}^{(1)} = \frac{9}{4}g_2^4 - \frac{3}{2}g_2^2 g_Y^2 + \frac{3}{4}g_Y^4 - 12y_b^2 y_t^2 - 9g_2^2\lambda_3 - 3g_Y^2\lambda_3 + 6y_b^2\lambda_3 + 6y_t^2\lambda_3 + 2y_\tau^2\lambda_3 + 6\lambda_1\lambda_3$$
$$+ 6\lambda_2\lambda_3 + 4\lambda_3^2 + 2\lambda_1\lambda_4 + 2\lambda_2\lambda_4 + 2\lambda_4^2 + 2\lambda_5^2 + 3\lambda_3(g_{2d}^{12})^2 + 3\lambda_3(g_{2u}^{11})^2 + \lambda_3(g_{1d}^{21})^2$$
$$- (g_{1u}^{11})^2(g_{1d}^{21})^2 - 2(g_{2d}^{12})^2(g_{1d}^{21})^2 + \lambda_3(g_{1u}^{22})^2 - (g_{1d}^{12})^2(g_{1u}^{22})^2 - 2(g_{2u}^{11})^2(g_{1u}^{22})^2$$
$$+ 2g_{1u}^{11}g_{2u}^{11}g_{1d}^{21}g_{2d}^{21} - 4g_{1d}^{12}g_{2u}^{11}g_{1u}^{22}g_{2d}^{21} + 3\lambda_3(g_{2d}^{21})^2 - 4(g_{2d}^{12})^2(g_{2d}^{21})^2 - 5(g_{2u}^{11})^2(g_{2d}^{21})^2$$
$$+ (g_{1d}^{12})^2(\lambda_3 - 2(g_{2d}^{21})^2) - 4g_{1u}^{11}g_{2d}^{12}g_{1d}^{21}g_{2u}^{22} + 2g_{1d}^{12}g_{2d}^{12}g_{1u}^{22}g_{2u}^{22} + 8g_{2d}^{12}g_{2u}^{11}g_{2d}^{21}g_{2u}^{22}$$
$$+ 3\lambda_3(g_{2u}^{22})^2 - 5(g_{2d}^{12})^2(g_{2u}^{22})^2 - 4(g_{2u}^{11})^2(g_{2u}^{22})^2 + (g_{1u}^{11})^2(\lambda_3 - 2(g_{2u}^{22})^2)$$

$$\beta_{\lambda_4}^{(1)} = 3g_2^2 g_Y^2 + 12y_b^2 y_t^2 - 9g_2^2\lambda_4 - 3g_Y^2\lambda_4 + 6y_b^2\lambda_4 + 6y_t^2\lambda_4 + 2y_\tau^2\lambda_4 + 2\lambda_1\lambda_4 + 2\lambda_2\lambda_4$$
$$+ 8\lambda_3\lambda_4 + 4\lambda_4^2 + 8\lambda_5^2 + 3\lambda_4(g_{2d}^{12})^2 + 3\lambda_4(g_{2u}^{11})^2$$
$$+ \lambda_4(g_{1d}^{21})^2 + (g_{2d}^{12})^2(g_{1d}^{21})^2 - 2g_{1d}^{12}g_{1u}^{11}g_{1d}^{21}g_{1u}^{22} + \lambda_4(g_{1u}^{22})^2 + (g_{2u}^{11})^2(g_{1u}^{22})^2$$
$$- 4g_{1u}^{11}g_{2u}^{11}g_{1d}^{21}g_{2d}^{21} + 2g_{1d}^{12}g_{2u}^{11}g_{1u}^{22}g_{2d}^{21} + 3\lambda_4(g_{2d}^{21})^2 - (g_{2d}^{12})^2(g_{2d}^{21})^2 + 4(g_{2u}^{11})^2(g_{2d}^{21})^2$$
$$+ (g_{1d}^{12})^2\lambda_4 - (g_{1d}^{21})^2 + (g_{2d}^{21})^2) + 2g_{1u}^{11}g_{2d}^{12}g_{1d}^{21}g_{2u}^{22} - 4g_{1d}^{12}g_{2d}^{12}g_{1u}^{22}g_{2u}^{22} - 10g_{2d}^{12}g_{2u}^{11}g_{2d}^{21}g_{2u}^{22}$$
$$+ 3\lambda_4(g_{2u}^{22})^2 + 4(g_{2d}^{12})^2(g_{2u}^{22})^2 - (g_{2u}^{11})^2(g_{2u}^{22})^2 + (g_{1u}^{11})^2(\lambda_4 - (g_{1u}^{22})^2 + (g_{2u}^{22})^2)$$

$$\beta_{\lambda_5}^{(1)} = \lambda_5\left(-9g_2^2 - 3g_Y^2 + 6y_b^2 + 6y_t^2 + 2y_\tau^2 + 2\lambda_1 + 2\lambda_2 + 8\lambda_3 + 12\lambda_4\right.$$

$$+ (g_{1d}^{12})^2 + (g_{1u}^{11})^2 + 3(g_{2d}^{12})^2 + 3(g_{2u}^{11})^2 + (g_{1d}^{21})^2 + (g_{1u}^{22})^2 + 3(g_{2d}^{21})^2 + 3(g_{2u}^{22})^2 \Big).$$

(B.3.4)

B.3.2 MDGSSM

Once again including only third generation Yukawa couplings, the beta functions for the dimensionless quantities of the MDGSSM are given by:

B.3.2.1 Yukawa couplings

$$\beta_{\lambda_S} = \frac{\lambda_S}{16\pi^2} \left[4|\lambda_S|^2 + 6|\lambda_T|^2 + 3|y_t|^2 + 3|y_b|^2 + |y_\tau|^2 - g_Y^2 - 3g_2^2 \right],$$

$$\beta_{\lambda_T} = \frac{\lambda_T}{16\pi^2} \left[2|\lambda_S|^2 + 8|\lambda_T|^2 + 3|y_t|^2 + 3|y_b|^2 + |y_\tau|^2 - g_Y^2 - 7g_2^2 \right],$$

$$\beta_{y_t} = \frac{y_t}{16\pi^2} \left[6|y_t|^2 + |y_b|^2 + |\lambda_S|^2 + 3|\lambda_T|^2 - \frac{13}{9}g_Y^2 - 3g_2^2 - \frac{16}{3}g_3^2 \right], \qquad \text{(B.3.5)}$$

$$\beta_{y_b} = \frac{y_b}{16\pi^2} \left[6|y_b|^2 + |y_t|^2 + |y_\tau|^2 + |\lambda_S|^2 + 3|\lambda_T|^2 - \frac{7}{9}g_Y^2 - 3g_2^2 - \frac{16}{3}g_3^2 \right],$$

$$\beta_{y_\tau} = \frac{y_\tau}{16\pi^2} \left[4|y_\tau|^2 + 3|y_b|^2 + |\lambda_S|^2 + 3|\lambda_T|^2 - 3g_Y^2 - 3g_2^2 \right],$$

B.3.2.2 Gauge couplings

$$\beta_{g_Y} = 11\frac{g_Y^3}{16\pi^2},$$

$$\beta_{g_2} = 3\frac{g_2^3}{16\pi^2}, \qquad \text{(B.3.6)}$$

$$\beta_{g_3} = 0.$$

B.4 MRSSM corrections

Collected here are the tree-level and leading one-loop threshold corrections to the THDM parameters in the MRSSM.

B.4.1 Tree-level

The tree-level λ_i are given by

$$\lambda_1 = \lambda_2 = \frac{1}{4}(g_2^2 + g_Y^2), \qquad \lambda_3 = \frac{1}{4}(g_2^2 - g_Y^2), \qquad \lambda_4 = -\frac{1}{2}g_2^2. \qquad \text{(B.4.1)}$$

The shifts from integrating out the adjoint scalars give

$$\delta\lambda_1 = -\frac{(g_Y m_{DY} - \sqrt{2}\lambda_{S_d}\mu_d)^2}{m_{SR}^2} - \frac{(g_2 m_{D2} + \sqrt{2}\lambda_{T_d}\mu_d)^2}{m_{TP}^2}$$

$$\delta\lambda_2 = -\frac{(g_Y m_{DY} + \sqrt{2}\lambda_{S_u}\mu_u)^2}{m_{SR}^2} - \frac{(g_2 m_{D2} + \sqrt{2}\lambda_{T_u}\mu_u)^2}{m_{TP}^2}$$

$$\delta\lambda_3 = -\frac{A_T^2}{m_{TM}^2} - \frac{A_T^2}{m_{TP}^2} + \frac{(g_Y m_{DY} - \sqrt{2}\lambda_{S_d}\mu_d)(g_Y m_{DY} + \sqrt{2}\lambda_{S_u}\mu_u)}{m_{SR}^2}$$

$$- \frac{(g_2 m_{D2} + \sqrt{2}\lambda_{T_d}\mu_d)(g_2 m_{D2} + \sqrt{2}\lambda_{T_u}\mu_u)}{m_{TP}^2}$$

$$\delta\lambda_4 = -\frac{A_S^2}{2m_{SI}^2} - \frac{A_S^2}{2m_{SR}^2} + \frac{A_T^2}{2m_{TM}^2} + \frac{A_T^2}{2m_{TP}^2}$$

$$+ 2\frac{(g_2 m_{D2} + \sqrt{2}\lambda_{T_d}\mu_d)(g_2 m_{D2} + \sqrt{2}\lambda_{T_u}\mu_u)}{m_{TP}^2}$$

$$\delta\lambda_5 = \frac{A_S^2}{2m_{SI}^2} - \frac{A_S^2}{2m_{SR}^2} + \frac{A_T^2}{2m_{TM}^2} - \frac{A_T^2}{2m_{TP}^2}$$

$$\delta\lambda_6 = \frac{A_S(-g_Y m_{DY} + \sqrt{2}\lambda_{S_d}\mu_d)}{\sqrt{2}m_{SR}^2} + \frac{A_T(g_2 m_{D2} + \sqrt{2}\lambda_{T_d}\mu_d)}{\sqrt{2}m_{TP}^2}$$

$$\delta\lambda_7 = \frac{A_S(g_Y m_{DY} + \sqrt{2}\lambda_{S_u}\mu_u)}{\sqrt{2}m_{SR}^2} - \frac{A_T(g_2 m_{D2} + \sqrt{2}\lambda_{T_u}\mu_u)}{\sqrt{2}m_{TP}^2} \tag{B.4.2}$$

B.4.2 One-loop

The one-loop corrections from the adjoint scalars in the limit that the Dirac gaugino masses can be neglected are given by:

$$\kappa^{-1}\delta\lambda_1 = \frac{1}{2}\left[3\lambda_{T_d}^4 \log\frac{(m_{TM}^2 m_{TP}^2)}{\mu^4} + \lambda_{S_d}^4 \log\frac{(m_{SR}^2 m_{SI}^2)}{\mu^4} + 2\lambda_{S_d}^2\lambda_{T_d}^2\left(P_{SS}(m_{SR}^2, m_{TP}^2)\right.\right.$$

$$\left.\left. + P_{SS}(m_{SI}^2, m_{TM}^2)\right) + (g_2^2 - 2\lambda_{T_d}^2)^2 P_{SS}(m_{TM}^2, m_{TP}^2)\right]$$

$$\kappa^{-1}\delta\lambda_2 = \frac{1}{2}\left[3\lambda_{T_u}^4 \log\frac{(m_{TM}^2 m_{TP}^2)}{\mu^4} + \lambda_{S_u}^4 \log\frac{(m_{SR}^2 m_{SI}^2)}{\mu^4} + 2\lambda_{S_u}^2\lambda_{T_u}^2\left(P_{SS}(m_{SR}^2, m_{TP}^2)\right)\right.$$

$$\left. + P_{SS}(m_{SI}^2, m_{TM}^2) + (g_2^2 - 2\lambda_{T_u}^2)^2 P_{SS}(m_{TM}^2, m_{TP}^2)\right]$$

$$\kappa^{-1}\delta\lambda_3 = \frac{1}{2}\left[3\lambda_{T_u}^2\lambda_{T_d}^2 \log\frac{(m_{TM}^2 m_{TP}^2)}{\mu^4} + \lambda_{S_u}^2\lambda_{S_d}^2 \log\frac{(m_{SR}^2 m_{SI}^2)}{\mu^4}\right.$$

$$+ 2\lambda_{S_u}\lambda_{T_u}\lambda_{S_d}\lambda_{T_d}\left(P_{SS}(m_{SR}^2, m_{TP}^2) + P_{SS}(m_{SI}^2, m_{TP}^2)\right)$$

$$\left. + (g_2^2 - 2\lambda_{T_u}^2)(g_2^2 - 2\lambda_{T_d}^2)P_{SS}(m_{TM}^2, m_{TP}^2)\right]$$

$$\kappa^{-1}\delta\lambda_4 = -\left[2\lambda_{S_u}\lambda_{T_u}\lambda_{S_d}\lambda_{T_d}\left(P_{SS}(m_{SR}^2, m_{TP}^2) + P_{SS}(m_{SI}^2, m_{TM}^2)\right)\right.$$

$$\left. + (g_2^2 - 2\lambda_{T_u}^2)(g_2^2 - 2\lambda_{T_d}^2)P_{SS}(m_{TM}^2, m_{TP}^2)\right] \tag{B.4.3}$$

List of Figures

Bibliography

[1] F. HALZEN & A. D. MARTIN; *QUARKS AND LEPTONS: AN INTRODUCTORY COURSE IN MODERN PARTICLE PHYSICS* (1984); ISBN 0471887412, 9780471887416. 1

[2] J. F. DONOGHUE, E. GOLOWICH & B. R. HOLSTEIN; «Dynamics of the standard model»; Camb. Monogr. Part. Phys. Nucl. Phys. Cosmol. **2**, p. 1–540 (1992). [Camb. Monogr. Part. Phys. Nucl. Phys. Cosmol.35(2014)]. 1

[3] M. ROBINSON; *Symmetry and the standard model: Mathematics and particle physics* (Springer, New York, USA) (2011); ISBN 9781441982667. 1

[4] M. D. SCHWARTZ; *Quantum Field Theory and the Standard Model* (Cambridge University Press) (2014); ISBN 1107034736, 9781107034730. http://www.cambridge.org/us/academic/subjects/physics/theoretical-physics-and-mathematical-physics/quantum-field-theory-and-standard-model. 1

[5] H. E. LOGAN; «TASI 2013 lectures on Higgs physics within and beyond the Standard Model»; (2014)1406.1786. 1

[6] P. PAL; *An introductory course of particle physics* (2014). 1

[7] J. GOLDSTONE; «Field Theories with Superconductor Solutions»; Nuovo Cim. **19**, p. 154–164 (1961). 2

[8] J. GOLDSTONE, A. SALAM & S. WEINBERG; «Broken Symmetries»; Phys. Rev. **127**, p. 965–970 (1962). 2

[9] Y. FUKUDA *et al.*; «Evidence for oscillation of atmospheric neutrinos»; Phys. Rev. Lett. **81**, p. 1562–1567 (1998). hep-ex/9807003. 8

[10] M. DINE, W. FISCHLER & M. SREDNICKI; «A Simple Solution to the Strong CP Problem with a Harmless Axion»; Phys. Lett. **104B**, p. 199–202 (1981). 8

[11] J. E. KIM & H. P. NILLES; «The mu Problem and the Strong CP Problem»; Phys. Lett. **138B**, p. 150–154 (1984). 8, 38

[12] J. E. KIM & G. CAROSI; «Axions and the Strong CP Problem»; Rev. Mod. Phys. **82**, p. 557–602 (2010). 0807.3125. 8

[13] R. D. PECCEI; «The Strong CP problem and axions»; Lect. Notes Phys. **741**, p. 3–17 (2008). [,3(2006)]; hep-ph/0607268. 8

[14] J. ELLIS; «Physics Beyond the Standard Model»; Nucl. Phys. **A827**, p. 187C–198C (2009). [,187(2009)]; 0902.0357. 8

[15] J. Ellis; «Outstanding questions: Physics beyond the Standard Model»; Phil. Trans. Roy. Soc. Lond. **A370**, p. 818–830 (2012). 8

[16] C. Csáki & P. Tanedo; «Beyond the Standard Model»; dans «Proceedings, 2013 European School of High-Energy Physics (ESHEP 2013): Paradfurdo, Hungary, June 5-18, 2013», p. 169–268 (2015); 1602.04228. 8

[17] B. C. Allanach; «Beyond the Standard Model Lectures for the 2016 European School of High-Energy Physics»; dans «Proceedings, 2016 European School of High-Energy Physics (ESHEP2016): Skeikampen, Norway, June 15-28 2016», p. 123–152 (2017); 1609.02015. 8

[18] G. Degrassi, S. Di Vita, J. Elias-Miro, J. R. Espinosa, G. F. Giudice, G. Isidori & A. Strumia; «Higgs mass and vacuum stability in the Standard Model at NNLO»; JHEP **08**, p. 098 (2012). 1205.6497. 9

[19] D. Buttazzo, G. Degrassi, P. P. Giardino, G. F. Giudice, F. Sala, A. Salvio & A. Strumia; «Investigating the near-criticality of the Higgs boson»; JHEP **12**, p. 089 (2013). 1307.3536. 9, 75

[20] H. Georgi & S. L. Glashow; «Unity of All Elementary Particle Forces»; Phys. Rev. Lett. **32**, p. 438–441 (1974). 9

[21] P. H. Frampton & S. L. Glashow; «Staying Alive With SU(5)»; Phys. Lett. **131B**, p. 340 (1983). [Erratum: Phys. Lett.135B,515(1984)]. 9

[22] G. Bertone, D. Hooper & J. Silk; «Particle dark matter: Evidence, candidates and constraints»; Phys. Rept. **405**, p. 279–390 (2005). hep-ph/0404175. 9

[23] J. C. Kapteyn; «First Attempt at a Theory of the Arrangement and Motion of the Sidereal System»; Astrophys. J. **55**, p. 302–328 (1922). 9

[24] K. G. Begeman, A. H. Broeils & R. H. Sanders; «Extended rotation curves of spiral galaxies: Dark haloes and modified dynamics»; Mon. Not. Roy. Astron. Soc. **249**, p. 523 (1991). 9

[25] C. J. Copi, D. N. Schramm & M. S. Turner; «Big bang nucleosynthesis and the baryon density of the universe»; Science **267**, p. 192–199 (1995). astro-ph/9407006. 10

[26] J. A. Bagger; «Weak scale supersymmetry: Theory and practice»; dans «QCD and beyond. Proceedings, Theoretical Advanced Study Institute in Elementary Particle Physics, TASI-95, Boulder, USA, June 4-30, 1995», p. 109–162 (1996); hep-ph/9604232. 11

[27] J. D. Lykken; «Introduction to supersymmetry»; dans «Fields, strings and duality. Proceedings, Summer School, Theoretical Advanced Study Institute in Elementary Particle Physics, TASI'96, Boulder, USA, June 2-28, 1996», p. 85–153 (1996). http://lss.fnal.gov/cgi-bin/find_paper.pl?pub-96-445-T; hep-th/9612114. 11

[28] S. P. Martin; «A Supersymmetry primer»; p. 1–98 (1997). [Adv. Ser. Direct. High Energy Phys.18,1(1998)]; hep-ph/9709356. 11

[29] J. F. GUNION; «A Simplified summary of supersymmetry»; AIP Conf. Proc. **397**, p. 41–64 (1997). `hep-ph/9704349`. 11

[30] M. DREES, R. GODBOLE & P. ROY; *Theory and phenomenology of sparticles: An account of four-dimensional N=1 supersymmetry in high energy physics* (2004). 11

[31] F. QUEVEDO, S. KRIPPENDORF & O. SCHLOTTERER; «Cambridge Lectures on Supersymmetry and Extra Dimensions»; (2010)`1011.1491`. 11, 23

[32] M. BERTOLINI; «Lectures on Supersymmetry (2016)»; `https://people.sissa.it/~bertmat/susycourse.pdf`; accessed: 2019-02-19. 11, 13, 23

[33] S. R. COLEMAN & J. MANDULA; «All Possible Symmetries of the S Matrix»; Phys. Rev. **159**, p. 1251–1256 (1967). 12, 23

[34] R. HAAG, J. T. LOPUSZANSKI & M. SOHNIUS; «All Possible Generators of Supersymmetries of the s Matrix»; Nucl. Phys. **B88**, p. 257 (1975). [,257(1974)]. 12, 23

[35] M. GOODSELL; «Lectures on Supersymmetry (2017)»; Accessed: 2019-03-20. 13

[36] R. RUFFINI & J. A. WHEELER; «Introducing the black hole»; Phys. Today **24**, p. 30 (1971). 21

[37] N. SEIBERG & E. WITTEN; «Electric - magnetic duality, monopole condensation, and confinement in N=2 supersymmetric Yang-Mills theory»; Nucl. Phys. **B426**, p. 19–52 (1994). [Erratum: Nucl. Phys.B430,485(1994)]; `hep-th/9407087`. 21

[38] N. SEIBERG & E. WITTEN; «Monopoles, duality and chiral symmetry breaking in N=2 supersymmetric QCD»; Nucl. Phys. **B431**, p. 484–550 (1994). `hep-th/9408099`. 21

[39] S. WEINBERG; «The Quantum Theory of Fields: Volume I Foundations»; Cambridge: Cambridge University Press. . 23

[40] X. BEKAERT, N. BOULANGER & P. SUNDELL; «How higher-spin gravity surpasses the spin two barrier: no-go theorems versus yes-go examples»; Rev. Mod. Phys. **84**, p. 987–1009 (2012). `1007.0435`. 23

[41] Y. TACHIKAWA; *N=2 supersymmetric dynamics for pedestrians*; tome 890 (2014); `1312.2684`. 23

[42] N. SEIBERG; «Naturalness versus supersymmetric nonrenormalization theorems»; Phys. Lett. **B318**, p. 469–475 (1993). `hep-ph/9309335`. 23

[43] S. WEINBERG; «Nonrenormalization theorems in nonrenormalizable theories»; Phys. Rev. Lett. **80**, p. 3702–3705 (1998). `hep-th/9803099`. 23

[44] D. AMATI, G. C. ROSSI & G. VENEZIANO; «Instanton Effects in Supersymmetric Gauge Theories»; Nucl. Phys. **B249**, p. 1–41 (1985). 25

[45] M. DINE, R. ROHM, N. SEIBERG & E. WITTEN; «Gluino Condensation in Superstring Models»; Phys. Lett. **156B**, p. 55–60 (1985). 25

[46] C. P. Burgess, J. P. Derendinger, F. Quevedo & M. Quiros; «On gaugino condensation with field dependent gauge couplings»; Annals Phys. **250**, p. 193–233 (1996). hep-th/9505171. 25

[47] E. Poppitz & S. P. Trivedi; «Dynamical supersymmetry breaking»; Ann. Rev. Nucl. Part. Sci. **48**, p. 307–350 (1998). hep-th/9803107. 25

[48] D. J. H. Chung, L. L. Everett, G. L. Kane, S. F. King, J. D. Lykken & L.-T. Wang; «The Soft supersymmetry breaking Lagrangian: Theory and applications»; Phys. Rept. **407**, p. 1–203 (2005). hep-ph/0312378. 25

[49] K. A. Intriligator & N. Seiberg; «Lectures on Supersymmetry Breaking»; Class. Quant. Grav. **24**, p. S741–S772 (2007). [Les Houches87,125(2008)]; hep-ph/0702069. 25

[50] M. Dine & J. D. Mason; «Supersymmetry and Its Dynamical Breaking»; Rept. Prog. Phys. **74**, p. 056 201 (2011). 1012.2836. 25

[51] L. Girardello & M. T. Grisaru; «Soft Breaking of Supersymmetry»; Nucl. Phys. **B194**, p. 65 (1982). 25

[52] M. Ibe, A. Rajaraman & Z. Surujon; «Does Supersymmetry Require Two Higgs Doublets?»; (2010)1012.5099. 26

[53] H. E. Haber & J. D. Mason; «Hard supersymmetry-breaking 'wrong-Higgs' couplings of the MSSM»; Phys. Rev. **D77**, p. 115 011 (2008). 0711.2890. 27

[54] S. Nandi & Z. Tavartkiladze; «A New Extensions of MSSM: FMSSM»; Phys. Lett. **B672**, p. 240–245 (2009). 0804.1996. 27

[55] B. A. Dobrescu & P. J. Fox; «Uplifted Supersymmetric Higgs Region»; Eur. Phys. J. **C70**, p. 263–270 (2010). 1001.3147. 27

[56] A. Bilal; «Lectures on Anomalies»; (2008)0802.0634. 27

[57] P. Fayet; «Supersymmetry and Weak, Electromagnetic and Strong Interactions»; Phys. Lett. **64B**, p. 159 (1976). 28

[58] P. Fayet; «Spontaneously Broken Supersymmetric Theories of Weak, Electromagnetic and Strong Interactions»; Phys. Lett. **69B**, p. 489 (1977). 28

[59] V. Takhistov; «Review of Nucleon Decay Searches at Super-Kamiokande»; dans «Proceedings, 51st Rencontres de Moriond on Electroweak Interactions and Unified Theories: La Thuile, Italy, March 12-19, 2016», p. 437–444 (2016); 1605.03235. 28

[60] S. Dimopoulos & D. W. Sutter; «The Supersymmetric flavor problem»; Nucl. Phys. **B452**, p. 496–512 (1995). hep-ph/9504415. 29

[61] K. Inoue, A. Kakuto, H. Komatsu & S. Takeshita; «Low-Energy Parameters and Particle Masses in a Supersymmetric Grand Unified Model»; Prog. Theor. Phys. **67**, p. 1889 (1982). 34

[62] R. A. Flores & M. Sher; «Higgs Masses in the Standard, Multi-Higgs and Supersymmetric Models»; Annals Phys. **148**, p. 95 (1983). 34

[63] N. POLONSKY; «The Mu parameter of supersymmetry»; dans «Supersymmetry, supergravity and superstring. Proceedings, KIAS-CTP International Symposium, Seoul, Korea, June 23-26, 1999», p. 100–124 (1999); `hep-ph/9911329`. 38

[64] D. L. LEPSUSYWG, ALEPH & L. S. W. G. OPAL COLLABORATIONS; «Charginos, Large m_0»; `http://lepsusy.web.cern.ch/lepsusy/Welcome.html`. 38

[65] U. ELLWANGER, C. HUGONIE & A. M. TEIXEIRA; «The Next-to-Minimal Supersymmetric Standard Model»; Phys. Rept. **496**, p. 1–77 (2010). `0910.1785`. 38, 39

[66] A. E. NELSON, N. RIUS, V. SANZ & M. UNSAL; «The Minimal supersymmetric model without a mu term»; JHEP **08**, p. 039 (2002). `hep-ph/0206102`. 39, 40, 42, 45

[67] K. BENAKLI, M. D. GOODSELL & A.-K. MAIER; «Generating mu and Bmu in models with Dirac Gauginos»; Nucl. Phys. **B851**, p. 445–461 (2011). `1104.2695`. 39, 40, 42, 46, 47, 59

[68] S. DIMOPOULOS, K. HOWE & J. MARCH-RUSSELL; «Maximally Natural Supersymmetry»; Phys. Rev. Lett. **113**, p. 111 802 (2014). `1404.7554`. 39

[69] M. AABOUD *et al.*; «Search for squarks and gluinos in final states with jets and missing transverse momentum using 36/fb of sqrt(s)=13 TeV pp collision data with the ATLAS detector»; Phys. Rev. **D97**, p. 112 001 (2018). `1712.02332`. 39, 88, 90, 97, 99

[70] A. M. SIRUNYAN *et al.*; «Search for new phenomena with the M_{T2} variable in the all-hadronic final state produced in protonproton collisions at $\sqrt{s} = 13$ TeV»; Eur. Phys. J. **C77**, p. 710 (2017). `1705.04650`. 39, 88, 99

[71] M. AABOUD *et al.*; «Search for squarks and gluinos in events with an isolated lepton, jets, and missing transverse momentum at $\sqrt{s} = 13$ TeV with the ATLAS detector»; Phys. Rev. **D96**, p. 112 010 (2017). `1708.08232`. 39, 99

[72] L. J. HALL, D. PINNER & J. T. RUDERMAN; «A Natural SUSY Higgs Near 126 GeV»; JHEP **04**, p. 131 (2012). `1112.2703`. 39

[73] H.-C. CHENG & I. LOW; «TeV symmetry and the little hierarchy problem»; JHEP **09**, p. 051 (2003). `hep-ph/0308199`. 39

[74] P. FAYET; «MASSIVE GLUINOS»; Phys. Lett. **78B**, p. 417–420 (1978). 40

[75] J. POLCHINSKI & L. SUSSKIND; «Breaking of Supersymmetry at Intermediate-Energy»; Phys. Rev. **D26**, p. 3661 (1982). 40, 42

[76] L. J. HALL & L. RANDALL; «U(1)-R symmetric supersymmetry»; Nucl. Phys. **B352**, p. 289–308 (1991). 40, 42

[77] P. J. FOX, A. E. NELSON & N. WEINER; «Dirac gaugino masses and supersoft supersymmetry breaking»; JHEP **08**, p. 035 (2002). `hep-ph/0206096`. 40, 41, 42, 58, 85

[78] I. Antoniadis, K. Benakli, A. Delgado & M. Quiros; «A New gauge medi-
ation theory»; Adv. Stud. Theor. Phys. **2**, p. 645–672 (2008)hep-ph/0610265.
40, 42, 47, 55, 59, 60

[79] G. D. Kribs, E. Poppitz & N. Weiner; «Flavor in supersymmetry with an
extended R-symmetry»; Phys. Rev. **D78**, p. 055 010 (2008). 0712.2039.   40,
42, 43, 44, 48

[80] S. D. L. Amigo, A. E. Blechman, P. J. Fox & E. Poppitz; «R-symmetric
gauge mediation»; JHEP **01**, p. 018 (2009). 0809.1112.   40, 42

[81] T. Plehn & T. M. P. Tait; «Seeking Sgluons»; J. Phys. **G36**, p. 075 001 (2009).
0810.3919.   40, 43, 81

[82] K. Benakli & M. D. Goodsell; «Dirac Gauginos in General Gauge
Mediation»; Nucl. Phys. **B816**, p. 185–203 (2009). 0811.4409.   40, 42, 56

[83] G. Belanger, K. Benakli, M. Goodsell, C. Moura & A. Pukhov; «Dark
Matter with Dirac and Majorana Gaugino Masses»; JCAP **0908**, p. 027 (2009).
0905.1043.   40, 45, 46, 57, 83, 87

[84] K. Benakli & M. D. Goodsell; «Dirac Gauginos and Kinetic Mixing»; Nucl.
Phys. **B830**, p. 315–329 (2010). 0909.0017.   40, 42

[85] S. Y. Choi, J. Kalinowski, J. M. Kim & E. Popenda; «Scalar gluons and
Dirac gluinos at the LHC»; Acta Phys. Polon. **B40**, p. 2913–2922 (2009)0911.
1951.   40, 81

[86] G. D. Kribs, T. Okui & T. S. Roy; «Viable Gravity-Mediated Supersymmetry
Breaking»; Phys. Rev. **D82**, p. 115 010 (2010). 1008.1798.   40, 42

[87] R. Fok & G. D. Kribs; «μ to e in R-symmetric Supersymmetry»; Phys. Rev.
D82, p. 035 010 (2010). 1004.0556.   40, 42

[88] K. Benakli & M. D. Goodsell; «Dirac Gauginos, Gauge Mediation and
Unification»; Nucl. Phys. **B840**, p. 1–28 (2010). 1003.4957.   40, 42

[89] S. Y. Choi, D. Choudhury, A. Freitas, J. Kalinowski, J. M. Kim & P. M.
Zerwas; «Dirac Neutralinos and Electroweak Scalar Bosons of N=1/N=2 Hy-
brid Supersymmetry at Colliders»; JHEP **08**, p. 025 (2010). 1005.0818.   40,
81

[90] L. M. Carpenter; «Dirac Gauginos, Negative Supertraces and Gauge
Mediation»; JHEP **09**, p. 102 (2012). 1007.0017.   40, 42

[91] S. Abel & M. Goodsell; «Easy Dirac Gauginos»; JHEP **06**, p. 064 (2011).
1102.0014.   40, 42

[92] R. Davies, J. March-Russell & M. McCullough; «A Supersymmetric One
Higgs Doublet Model»; JHEP **04**, p. 108 (2011). 1103.1647.   40, 42, 44

[93] K. Benakli; «Dirac Gauginos: A User Manual»; Fortsch. Phys. **59**, p. 1079–
1082 (2011). 1106.1649.   40

[94] J. Kalinowski; «Higgs bosons of R-symmetric supersymmetric theories»; PoS
EPS-HEP2011, p. 265 (2011).   40

[95] C. FRUGIUELE & T. GREGOIRE; «Making the Sneutrino a Higgs with a $U(1)_R$ Lepton Number»; Phys. Rev. **D85**, p. 015 016 (2012). 1107.4634. 40, 42

[96] H. ITOYAMA & N. MARU; «D-term Dynamical Supersymmetry Breaking Generating Split N=2 Gaugino Masses of Mixed Majorana-Dirac Type»; Int. J. Mod. Phys. **A27**, p. 1250 159 (2012). 1109.2276. 40

[97] K. REHERMANN & C. M. WELLS; «Weak Scale Leptogenesis, R-symmetry, and a Displaced Higgs»; (2011)1111.0008. 40

[98] E. BERTUZZO & C. FRUGIUELE; «Fitting Neutrino Physics with a $U(1)_R$ Lepton Number»; JHEP **05**, p. 100 (2012). 1203.5340. 40, 42

[99] R. DAVIES; «Dirac gauginos and unification in F-theory»; JHEP **10**, p. 010 (2012). 1205.1942. 40, 42

[100] R. ARGURIO, M. BERTOLINI, L. DI PIETRO, F. PORRI & D. REDIGOLO; «Holographic Correlators for General Gauge Mediation»; JHEP **08**, p. 086 (2012). 1205.4709. 40, 42

[101] R. FOK, G. D. KRIBS, A. MARTIN & Y. TSAI; «Electroweak Baryogenesis in R-symmetric Supersymmetry»; Phys. Rev. **D87**, p. 055 018 (2013). 1208.2784. 40

[102] R. ARGURIO, M. BERTOLINI, L. DI PIETRO, F. PORRI & D. REDIGOLO; «Exploring Holographic General Gauge Mediation»; JHEP **10**, p. 179 (2012). 1208.3615. 40, 42

[103] C. FRUGIUELE, T. GREGOIRE, P. KUMAR & E. PONTON; «'L=R' - $U(1)_R$ as the Origin of Leptonic 'RPV'»; JHEP **03**, p. 156 (2013). 1210.0541. 40, 42, 44

[104] C. FRUGIUELE, T. GREGOIRE, P. KUMAR & E. PONTON; «'L=R' – $U(1)_R$ Lepton Number at the LHC»; JHEP **05**, p. 012 (2013). 1210.5257. 40, 42, 44

[105] K. BENAKLI, M. D. GOODSELL & F. STAUB; «Dirac Gauginos and the 125 GeV Higgs»; JHEP **06**, p. 073 (2013). 1211.0552. 40, 42, 45, 57, 59

[106] E. DUDAS, M. GOODSELL, L. HEURTIER & P. TZIVELOGLOU; «Flavour models with Dirac and fake gluinos»; Nucl. Phys. **B884**, p. 632–671 (2014). 1312.2011. 40, 42

[107] A. ARVANITAKI, M. BARYAKHTAR, X. HUANG, K. VAN TILBURG & G. VILLADORO; «The Last Vestiges of Naturalness»; JHEP **03**, p. 022 (2014). 1309.3568. 40, 42, 64

[108] H. ITOYAMA & N. MARU; «D-term Triggered Dynamical Supersymmetry Breaking»; Phys. Rev. **D88**, p. 025 012 (2013). 1301.7548. 40, 42

[109] S. CHAKRABORTY & S. ROY; «Higgs boson mass, neutrino masses and mixing and keV dark matter in an $U(1)_R-$ lepton number model»; JHEP **01**, p. 101 (2014). 1309.6538. 40, 42

[110] C. CSAKI, J. GOODMAN, R. PAVESI & Y. SHIRMAN; «The $m_D - b_M$ problem of Dirac gauginos and its solutions»; Phys. Rev. **D89**, p. 055 005 (2014). 1310.4504. 40, 42

[111] H. Itoyama & N. Maru; «126 GeV Higgs Boson Associated with D-term Triggered Dynamical Supersymmetry Breaking»; Symmetry **7**, p. 193–205 (2015). 1312.4157. 40, 42

[112] H. Beauchesne & T. Gregoire; «Electroweak precision measurements in supersymmetric models with a U(1)$_R$ lepton number»; JHEP **05**, p. 051 (2014). 1402.5403. 40, 42

[113] K. Benakli; «(Pseudo)goldstinos, SUSY fluids, Dirac gravitino and gauginos»; EPJ Web Conf. **71**, p. 00 012 (2014). 1402.4286. 40

[114] E. Bertuzzo, C. Frugiuele, T. Gregoire & E. Ponton; «Dirac gauginos, R symmetry and the 125 GeV Higgs»; JHEP **04**, p. 089 (2015). 1402.5432. 40, 42, 44, 48, 72

[115] P. Diessner, J. Kalinowski, W. Kotlarski & D. Stöckinger; «Higgs boson mass and electroweak observables in the MRSSM»; JHEP **12**, p. 124 (2014). 1410.4791. 40, 42, 48, 49, 72, 73

[116] K. Benakli, M. Goodsell, F. Staub & W. Porod; «Constrained minimal Dirac gaugino supersymmetric standard model»; Phys. Rev. **D90**, p. 045 017 (2014). 1403.5122. 40, 45, 48, 81

[117] M. D. Goodsell & P. Tziveloglou; «Dirac Gauginos in Low Scale Supersymmetry Breaking»; Nucl. Phys. **B889**, p. 650–675 (2014). 1407.5076. 40, 42, 43, 44, 81

[118] D. Busbridge; «Constrained Dirac gluino mediation»; (2014)1408.4605. 40, 42

[119] S. Chakraborty, A. Datta & S. Roy; «h → γγ in U(1)$_R$ -lepton number model with a right-handed neutrino»; JHEP **02**, p. 124 (2015). [Erratum: JHEP09,077(2015)]; 1411.1525. 40, 42

[120] R. Ding, T. Li, F. Staub, C. Tian & B. Zhu; «Supersymmetric standard models with a pseudo-Dirac gluino from hybrid F - and D -term supersymmetry breaking»; Phys. Rev. **D92**, p. 015 008 (2015). 1502.03614. 40, 42

[121] D. S. M. Alves, J. Galloway, M. McCullough & N. Weiner; «Goldstone Gauginos»; Phys. Rev. Lett. **115**, p. 161 801 (2015). 1502.03819. 40, 42

[122] D. S. M. Alves, J. Galloway, M. McCullough & N. Weiner; «Models of Goldstone Gauginos»; Phys. Rev. **D93**, p. 075 021 (2016). 1502.05055. 40, 42

[123] L. M. Carpenter & J. Goodman; «New Calculations in Dirac Gaugino Models: Operators, Expansions, and Effects»; JHEP **07**, p. 107 (2015). 1501.05653. 40, 42

[124] S. P. Martin; «Nonstandard supersymmetry breaking and Dirac gaugino masses without supersoftness»; Phys. Rev. **D92**, p. 035 004 (2015). 1506.02105. 40, 42

[125] M. D. Goodsell, M. E. Krauss, T. Müller, W. Porod & F. Staub; «Dark matter scenarios in a constrained model with Dirac gauginos»; JHEP **10**, p. 132 (2015). 1507.01010. 40, 45, 48

[126] P. DIESSNER, J. KALINOWSKI, W. KOTLARSKI & D. STÖCKINGER; «Two-loop correction to the Higgs boson mass in the MRSSM»; Adv. High Energy Phys. **2015**, p. 760 729 (2015). 1504.05386. 40, 42, 43, 48, 49, 72, 73

[127] P. DIESSNER, J. KALINOWSKI, W. KOTLARSKI & D. STÖCKINGER; «Exploring the Higgs sector of the MRSSM with a light scalar»; JHEP **03**, p. 007 (2016). 1511.09334. 40, 42, 43, 48, 49, 72, 73

[128] W. KOTLARSKI; «Sgluons in the same-sign lepton searches»; JHEP **02**, p. 027 (2017). 1608.00915. 40, 81

[129] K. BENAKLI, L. DARMÉ, M. D. GOODSELL & J. HARZ; «The Di-Photon Excess in a Perturbative SUSY Model»; Nucl. Phys. **B911**, p. 127–162 (2016). 1605. 05313. 40, 43, 48, 56, 81

[130] J. BRAATHEN, M. D. GOODSELL & P. SLAVICH; «Leading two-loop corrections to the Higgs boson masses in SUSY models with Dirac gauginos»; JHEP **09**, p. 045 (2016). 1606.09213. 40, 44

[131] P. DIESSNER, W. KOTLARSKI, S. LIEBSCHNER & D. STÖCKINGER; «Squark production in R-symmetric SUSY with Dirac gluinos: NLO corrections»; JHEP **10**, p. 142 (2017). 1707.04557. 40, 42, 43, 48, 96

[132] S. CHAKRABORTY & J. CHAKRABORTTY; «Natural emergence of neutrino masses and dark matter from R-symmetry»; JHEP **10**, p. 012 (2017). 1701. 04566. 40

[133] I. JACK & D. R. T. JONES; «Quasiinfrared fixed points and renormalization group invariant trajectories for nonholomorphic soft supersymmetry breaking»; Phys. Rev. **D61**, p. 095 002 (2000). hep-ph/9909570. 40

[134] M. D. GOODSELL; «Two-loop RGEs with Dirac gaugino masses»; JHEP **01**, p. 066 (2013). 1206.6697. 40, 64

[135] A. E. NELSON & N. SEIBERG; «R symmetry breaking versus supersymmetry breaking»; Nucl. Phys. **B416**, p. 46–62 (1994). hep-ph/9309299. 40

[136] J. ELLIS, J. QUEVILLON & V. SANZ; «Doubling Up on Supersymmetry in the Higgs Sector»; JHEP **10**, p. 086 (2016). 1607.05541. 42, 55, 59, 60, 63, 67, 69, 71

[137] K. BENAKLI, M. D. GOODSELL & S. L. WILLIAMSON; «Higgs alignment from extended supersymmetry»; Eur. Phys. J. **C78**, p. 658 (2018). 1801.08849. 42, 43

[138] K. BENAKLI, Y. CHEN & G. LAFFORGUE-MARMET; «R-symmetry for Higgs alignment without decoupling»; (2018)1811.08435. 42

[139] M. HEIKINHEIMO, M. KELLERSTEIN & V. SANZ; «How Many Supersymmetries?»; JHEP **04**, p. 043 (2012). 1111.4322. 42, 55, 81, 82

[140] G. D. KRIBS & A. MARTIN; «Supersoft Supersymmetry is Super-Safe»; Phys. Rev. **D85**, p. 115 014 (2012). 1203.4821. 42, 81, 82

[141] G. D. KRIBS & A. MARTIN; «Dirac Gauginos in Supersymmetry – Suppressed Jets + MET Signals: A Snowmass Whitepaper»; (2013)1308.3468. 42, 81, 82

[142] G. Grilli di Cortona, E. Hardy & A. J. Powell; «Dirac vs Majorana gauginos at a 100 TeV collider»; JHEP **08**, p. 014 (2016). 1606.07090. 42, 82

[143] J. Kalinowski; «Phenomenology of R-symmetric supersymmetry»; Acta Phys. Polon. **B42**, p. 2425–2432 (2011). 42

[144] S. Y. Choi, M. Drees, J. Kalinowski, J. M. Kim, E. Popenda & P. M. Zerwas; «Color-Octet Scalars of N=2 Supersymmetry at the LHC»; Phys. Lett. **B672**, p. 246–252 (2009). 0812.3586. 43, 81

[145] L. Darm, B. Fuks & M. Goodsell; «Cornering sgluons with four-top-quark events»; Phys. Lett. **B784**, p. 223–228 (2018). 1805.10835. 43, 44, 81

[146] G. Chalons, M. D. Goodsell, S. Kraml, H. Reyes-González & S. L. Williamson; «LHC limits on gluinos and squarks in the minimal Dirac gaugino model»; JHEP **04**, p. 113 (2019). 1812.09293. 44

[147] F. Riva, C. Biggio & A. Pomarol; «Is the 125 GeV Higgs the superpartner of a neutrino?»; JHEP **02**, p. 081 (2013). 1211.4526. 44

[148] C. Alvarado, A. Delgado & A. Martin; «Constraining the *R*-symmetric chargino NLSP at the LHC»; Phys. Rev. **D97**, p. 115 044 (2018). 1803.00624. 49, 81

[149] G. D. Kribs, A. Martin & T. S. Roy; «Squark Flavor Violation at the LHC»; JHEP **06**, p. 042 (2009). 0901.4105. 49

[150] A. L. Read; «Presentation of search results: The CL(s) technique»; J. Phys. **G28**, p. 2693–2704 (2002). [,11(2002)]. 51, 91, 110

[151] A. L. Read; «Modified frequentist analysis of search results (The CL(s) method)»; dans «Workshop on confidence limits, CERN, Geneva, Switzerland, 17-18 Jan 2000: Proceedings», p. 81–101 (2000). http://weblib.cern.ch/abstract?CERN-OPEN-2000-205. 51

[152] E. Gross; «LHC statistics for pedestrians»; dans «Statistical issues for LHC physics. Proceedings, Workshop, PHYSTAT-LHC, Geneva, Switzerland, June 27-29, 2007», p. 205–212 (2007). http://cds.cern.ch/record/1099994/files/p205.pdf. 51

[153] G. Cowan; «Statistical tests with weighted Monte Carlo events»; (2012). https://www.pp.rhul.ac.uk/~cowan/stat/notes/weights.pdf. 51

[154] L. Lista; «Practical Statistics for Particle Physicists»; dans «Proceedings, 2016 European School of High-Energy Physics (ESHEP2016): Skeikampen, Norway, June 15-28 2016», p. 213–258 (2017); 1609.04150. 51

[155] H. B. Prosper; «Practical Statistics for Particle Physicists»; dans «Proceedings, 2013 European School of High-Energy Physics (ESHEP 2013): Paradfurdo, Hungary, June 5-18, 2013», p. 301–328 (2016); 1608.03201. 51

[156] J. F. Gunion, H. E. Haber, G. L. Kane & S. Dawson; «The Higgs Hunter's Guide»; Front. Phys. **80**, p. 1–404 (2000). 53, 59

[157] S. Davidson & H. E. Haber; «Basis-independent methods for the two-Higgs-doublet model»; Phys. Rev. **D72**, p. 035 004 (2005). [Erratum: Phys. Rev.D72,099902(2005)]; hep-ph/0504050. 53, 59

[158] J. Bernon, J. F. Gunion, H. E. Haber, Y. Jiang & S. Kraml; «Scrutinizing the alignment limit in two-Higgs-doublet models: m_h=125 GeV»; Phys. Rev. **D92**, p. 075 004 (2015). 1507.00933. 53, 59

[159] J. Bernon, J. F. Gunion, H. E. Haber, Y. Jiang & S. Kraml; «Scrutinizing the alignment limit in two-Higgs-doublet models. II. m_H=125GeV»; Phys. Rev. **D93**, p. 035 027 (2016). 1511.03682. 53

[160] G. Aad *et al.*; «Measurements of the Higgs boson production and decay rates and constraints on its couplings from a combined ATLAS and CMS analysis of the LHC pp collision data at $\sqrt{s}$ = 7 and 8 TeV»; JHEP **08**, p. 045 (2016). 1606.02266. 54

[161] P. S. Bhupal Dev & A. Pilaftsis; «Maximally Symmetric Two Higgs Doublet Model with Natural Standard Model Alignment»; JHEP **12**, p. 024 (2014). [Erratum: JHEP11,147(2015)]; 1408.3405. 55

[162] A. Pilaftsis; «Symmetries for standard model alignment in multi-Higgs doublet models»; Phys. Rev. **D93**, p. 075 012 (2016). 1602.02017. 55

[163] A. Djouadi, L. Maiani, G. Moreau, A. Polosa, J. Quevillon & V. Riquer; «The post-Higgs MSSM scenario: Habemus MSSM?»; Eur. Phys. J. **C73**, p. 2650 (2013). 1307.5205. 63, 67

[164] F. Staub; «SARAH»; (2008)0806.0538. 64

[165] F. Staub; «SARAH 3.2: Dirac Gauginos, UFO output, and more»; Comput. Phys. Commun. **184**, p. 1792–1809 (2013). 1207.0906. 64, 86, 89

[166] F. Staub; «SARAH 4 : A tool for (not only SUSY) model builders»; Comput. Phys. Commun. **185**, p. 1773–1790 (2014). 1309.7223. 64, 86

[167] M. D. Goodsell, K. Nickel & F. Staub; «Two-Loop Higgs mass calculations in supersymmetric models beyond the MSSM with SARAH and SPheno»; Eur. Phys. J. **C75**, p. 32 (2015). 1411.0675. 64, 86

[168] M. Goodsell, K. Nickel & F. Staub; «Generic two-loop Higgs mass calculation from a diagrammatic approach»; Eur. Phys. J. **C75**, p. 290 (2015). 1503.03098. 64, 86

[169] J. Braathen, M. D. Goodsell & F. Staub; «Supersymmetric and non-supersymmetric models without catastrophic Goldstone bosons»; Eur. Phys. J. **C77**, p. 757 (2017). 1706.05372. 64, 86

[170] S. P. Martin; «Two loop effective potential for a general renormalizable theory and softly broken supersymmetry»; Phys. Rev. **D65**, p. 116 003 (2002). hep-ph/0111209. 64

[171] S. P. Martin; «Two loop scalar self energies in a general renormalizable theory at leading order in gauge couplings»; Phys. Rev. **D70**, p. 016 005 (2004). hep-ph/0312092. 64

[172] J. Braathen & M. D. Goodsell; «Avoiding the Goldstone Boson Catastrophe in general renormalisable field theories at two loops»; JHEP **12**, p. 056 (2016). 1609.06977. 64

[173] E. Bagnaschi, G. F. Giudice, P. Slavich & A. Strumia; «Higgs Mass and Unnatural Supersymmetry»; JHEP **09**, p. 092 (2014). 1407.4081. 64

[174] G. Lee & C. E. M. Wagner; «Higgs bosons in heavy supersymmetry with an intermediate m_A»; Phys. Rev. **D92**, p. 075 032 (2015). 1508.00576. 69, 125

[175] C. Patrignani *et al.*; «Review of Particle Physics»; Chin. Phys. **C40**, p. 100 001 (2016). 71

[176] M. Misiak & M. Steinhauser; «Weak radiative decays of the B meson and bounds on $M_{H^\pm}$ in the Two-Higgs-Doublet Model»; Eur. Phys. J. **C77**, p. 201 (2017). 1702.04571. 71

[177] M. Aaboud *et al.*; «Search for additional heavy neutral Higgs and gauge bosons in the ditau final state produced in 36 fb^{-1} of pp collisions at $\sqrt{s} = 13$ TeV with the ATLAS detector»; (2017)1709.07242. 72

[178] R. V. Harlander, S. Liebler & H. Mantler; «SusHi: A program for the calculation of Higgs production in gluon fusion and bottom-quark annihilation in the Standard Model and the MSSM»; Comput. Phys. Commun. **184**, p. 1605–1617 (2013). 1212.3249. 72

[179] R. V. Harlander, S. Liebler & H. Mantler; «SusHi Bento: Beyond NNLO and the heavy-top limit»; Comput. Phys. Commun. **212**, p. 239–257 (2017). 1605.03190. 72

[180] R. V. Harlander & W. B. Kilgore; «Next-to-next-to-leading order Higgs production at hadron colliders»; Phys. Rev. Lett. **88**, p. 201 801 (2002). hep-ph/0201206. 72

[181] R. V. Harlander & W. B. Kilgore; «Higgs boson production in bottom quark fusion at next-to-next-to leading order»; Phys. Rev. **D68**, p. 013 001 (2003). hep-ph/0304035. 72

[182] S. Actis, G. Passarino, C. Sturm & S. Uccirati; «NLO Electroweak Corrections to Higgs Boson Production at Hadron Colliders»; Phys. Lett. **B670**, p. 12–17 (2008). 0809.1301. 72

[183] R. Harlander & P. Kant; «Higgs production and decay: Analytic results at next-to-leading order QCD»; JHEP **12**, p. 015 (2005). hep-ph/0509189. 72

[184] K. G. Chetyrkin, J. H. Kuhn & M. Steinhauser; «RunDec: A Mathematica package for running and decoupling of the strong coupling and quark masses»; Comput. Phys. Commun. **133**, p. 43–65 (2000). hep-ph/0004189. 72

[185] J. Braathen, M. D. Goodsell, M. E. Krauss, T. Opferkuch & F. Staub; «N-loop running should be combined with N-loop matching»; Phys. Rev. **D97**, p. 015 011 (2018). 1711.08460. 79

[186] . 79

[187] P. Diessner; *Phenomenological Study of the Minimal R-symmetric Supersymmetric Standard Sodel*; Thèse de doctorat; Dresden, Tech. U. (2016). https://iktp.tu-dresden.de/IKTP/pub/16/Disseration_Philip_Diessner.pdf. 81

[188] D. Goncalves-Netto, D. Lopez-Val, K. Mawatari, T. Plehn & I. Wigmore; «Sgluon Pair Production to Next-to-Leading Order»; Phys. Rev. **D85**, p. 114 024 (2012). 1203.6358. 81

[189] C.-Y. Chen, A. Freitas, T. Han & K. S. M. Lee; «Heavy Color-Octet Particles at the LHC»; JHEP **05**, p. 135 (2015). 1410.8113. 81

[190] L. Beck, F. Blekman, D. Dobur, B. Fuks, J. Keaveney & K. Mawatari; «Probing top-philic sgluons with LHC Run I data»; Phys. Lett. **B746**, p. 48–52 (2015). 1501.07580. 81

[191] W. Kotlarski; «Scalar color octets and triplets in the SUSY with R-symmetry»; J. Phys. Conf. Ser. **873**, p. 012 043 (2017). 1703.09548. 81

[192] S. Y. Choi, M. Drees, A. Freitas & P. M. Zerwas; «Testing the Majorana Nature of Gluinos and Neutralinos»; Phys. Rev. **D78**, p. 095 007 (2008). 0808.2410. 82

[193] F. Staub; «From Superpotential to Model Files for FeynArts and CalcHep/CompHep»; Comput.Phys.Commun. **181**, p. 1077–1086 (2010). 0909.2863. 86

[194] F. Staub; «Automatic Calculation of supersymmetric Renormalization Group Equations and Self Energies»; Comput.Phys.Commun. **182**, p. 808–833 (2011). 1002.0840. 86

[195] M. D. Goodsell, S. Liebler & F. Staub; «Generic calculation of two-body partial decay widths at the full one-loop level»; Eur. Phys. J. **C77**, p. 758 (2017). 1703.09237. 86

[196] W. Porod & F. Staub; «SPheno 3.1: Extensions including flavour, CP-phases and models beyond the MSSM»; Comput. Phys. Commun. **183**, p. 2458–2469 (2012). 1104.1573. 86

[197] Zenodo dataset, "Dirac gaugino benchmark points from arXiv:1812.09293", https://doi.org/10.5281/zenodo.2422746. 87, 98

[198] F. Ambrogi, S. Kraml, S. Kulkarni, U. Laa, A. Lessa & W. Waltenberger; «On the coverage of the pMSSM by simplified model results»; Eur. Phys. J. **C78**, p. 215 (2018). 1707.09036. 89, 92

[199] F. Ambrogi, S. Kraml, S. Kulkarni, U. Laa, A. Lessa, V. Magerl, J. Sonneveld, M. Traub & W. Waltenberger; «SModelS v1.1 user manual»; Comput. Phys. Comm. **227**, p. 72 (2018). 1701.06586. 89

[200] S. Kraml, S. Kulkarni, U. Laa, A. Lessa, W. Magerl, D. Proschofsky-Spindler & W. Waltenberger; «SModelS: a tool for interpreting simplified-model results from the LHC and its application to supersymmetry»; Eur. Phys. J. **C74**, p. 2868 (2014). 1312.4175. 89

[201] J. Dutta, S. Kraml, A. Lessa & W. Waltenberger; «SModelS extension with the CMS supersymmetry search results from Run 2»; (2018) 1803.02204. 89

[202] J. Alwall, R. Frederix, S. Frixione, V. Hirschi, F. Maltoni, O. Mattelaer, H. S. Shao, T. Stelzer, P. Torrielli & M. Zaro; «The automated computation of tree-level and next-to-leading order differential cross sections, and their matching to parton shower simulations»; JHEP **07**, p. 079 (2014). 1405.0301. 89, 91, 101

[203] E. Conte, B. Fuks & G. Serret; «MadAnalysis 5, A User-Friendly Framework for Collider Phenomenology»; Comput. Phys. Commun. **184**, p. 222–256 (2013). 1206.1599. 90, 101

[204] E. Conte, B. Dumont, B. Fuks & C. Wymant; «Designing and recasting LHC analyses with MadAnalysis 5»; Eur. Phys. J. **C74**, p. 3103 (2014). 1405.3982. 90

[205] B. Dumont, B. Fuks, S. Kraml, S. Bein, G. Chalons, E. Conte, S. Kulkarni, D. Sengupta & C. Wymant; «Toward a public analysis database for LHC new physics searches using MADANALYSIS 5»; Eur. Phys. J. **C75**, p. 56 (2015). 1407.3278. 90, 91

[206] I. Hinchliffe, F. E. Paige, M. D. Shapiro, J. Soderqvist & W. Yao; «Precision SUSY measurements at CERN LHC»; Phys. Rev. **D55**, p. 5520–5540 (1997). hep-ph/9610544. 91

[207] G. Chalons & H. Reyes-Gonzalez; «MadAnalysis 5 implementation of ATLAS-SUSY-16-07 (arXiv:1712.02332)»; (2018); http://doi.org/10.7484/INSPIREHEP.DATA.56DC.PPE2. 91

[208] T. Sjöstrand, S. Ask, J. R. Christiansen, R. Corke, N. Desai, P. Ilten, S. Mrenna, S. Prestel, C. O. Rasmussen & P. Z. Skands; «An Introduction to PYTHIA 8.2»; Comput. Phys. Commun. **191**, p. 159–177 (2015). 1410.3012. 91, 101

[209] J. de Favereau, C. Delaere, P. Demin, A. Giammanco, V. Lematre, A. Mertens & M. Selvaggi; «DELPHES 3, A modular framework for fast simulation of a generic collider experiment»; JHEP **02**, p. 057 (2014). 1307.6346. 91

[210] E. Conte & B. Fuks; «Confronting new physics theories to LHC data with MADANALYSIS 5»; Int. J. Mod. Phys. **A33**, p. 1830 027 (2018). 1808.00480. 91, 101

[211] W. Beenakker, R. Hopker, M. Spira & P. M. Zerwas; «Squark and gluino production at hadron colliders»; Nucl. Phys. **B492**, p. 51–103 (1997). hep-ph/9610490. 96

[212] https://www.uni-muenster.de/Physik.TP/~akule_01/nnllfast/doku.php. 96

[213] Zenodo dataset, "Data for Figs. 5 and 9 of arXiv:1812.09293", https://doi.org/10.5281/zenodo.2585684. 98

[214] H. P. Nilles; «Supersymmetry, Supergravity and Particle Physics»; Phys. Rept. **110**, p. 1–162 (1984). 99

[215] H. E. Haber & G. L. Kane; «The Search for Supersymmetry: Probing Physics Beyond the Standard Model»; Phys. Rept. **117**, p. 75–263 (1985). 99

[216] A. M. SIRUNYAN *et al.*; «Search for natural and split supersymmetry in proton-proton collisions at $\sqrt{s} = 13$ TeV in final states with jets and missing transverse momentum»; JHEP **05**, p. 025 (2018). 1802.02110. 99

[217] B. FUKS, M. KLASEN, D. R. LAMPREA & M. ROTHERING; «Gaugino production in proton-proton collisions at a center-of-mass energy of 8 TeV»; JHEP **10**, p. 081 (2012). 1207.2159. 99

[218] B. FUKS, M. KLASEN, D. R. LAMPREA & M. ROTHERING; «Revisiting slepton pair production at the Large Hadron Collider»; JHEP **01**, p. 168 (2014). 1310.2621. 99

[219] A. M. SIRUNYAN *et al.*; «Search for supersymmetric partners of electrons and muons in proton-proton collisions at $\sqrt{s} = 13$ TeV»; Phys. Lett. **B790**, p. 140–166 (2019). 1806.05264. 99, 100, 101, 107, 108, 109, 110

[220] M. AABOUD *et al.*; «Search for electroweak production of supersymmetric particles in final states with two or three leptons at $\sqrt{s} = 13$ TeV with the ATLAS detector»; Eur. Phys. J. **C78**, p. 995 (2018). 1803.02762. 99, 104

[221] M. AABOUD *et al.*; «Search for supersymmetry in events with four or more leptons in $\sqrt{s} = 13$ TeV *pp* collisions with ATLAS»; Phys. Rev. **D98**, p. 032 009 (2018). 1804.03602. 99

[222] M. AABOUD *et al.*; «Search for chargino-neutralino production using recursive jigsaw reconstruction in final states with two or three charged leptons in proton-proton collisions at $\sqrt{s} = 13$ TeV with the ATLAS detector»; Phys. Rev. **D98**, p. 092 012 (2018). 1806.02293. 99

[223] A. M. SIRUNYAN *et al.*; «Combined search for electroweak production of charginos and neutralinos in proton-proton collisions at $\sqrt{s} = 13$ TeV»; JHEP **03**, p. 160 (2018). 1801.03957. 99

[224] P. ATHRON *et al.*; «Combined collider constraints on neutralinos and charginos»; Eur. Phys. J. **C79**, p. 395 (2019). 1809.02097. 99

[225] V. D. BARGER, K.-m. CHEUNG, T. HAN & R. J. N. PHILLIPS; «Strong W^+W^+ scattering signals at *pp* supercolliders»; Phys. Rev. **D42**, p. 3052–3077 (1990). 99

[226] V. D. BARGER, K.-m. CHEUNG, T. HAN & D. ZEPPENFELD; «Single forward jet tagging and central jet vetoing to identify the leptonic WW decay mode of a heavy Higgs boson»; Phys. Rev. **D44**, p. 2701 (1991). [Erratum: Phys. Rev.D48,5444(1993)]. 99

[227] J. D. BJORKEN; «Rapidity gaps and jets as a new physics signature in very high-energy hadron hadron collisions»; Phys. Rev. **D47**, p. 101–113 (1993). 99

[228] R. S. FLETCHER & T. STELZER; «Rapidity gap signals in Higgs production at the SSC»; Phys. Rev. **D48**, p. 5162–5167 (1993). hep-ph/9306253. 99

[229] V. D. BARGER, R. J. N. PHILLIPS & D. ZEPPENFELD; «Mini - jet veto: A Tool for the heavy Higgs search at the LHC»; Phys. Lett. **B346**, p. 106–114 (1995). hep-ph/9412276. 99

[230] A. BANFI, P. F. MONNI, G. P. SALAM & G. ZANDERIGHI; «Higgs and Z-boson production with a jet veto»; Phys. Rev. Lett. **109**, p. 202 001 (2012). 1206.4998. 99

[231] T. BECHER, M. NEUBERT & L. ROTHEN; «Factorization and $N^3LL_p + NNLO$ predictions for the Higgs cross section with a jet veto»; JHEP **10**, p. 125 (2013). 1307.0025. 99

[232] I. W. STEWART, F. J. TACKMANN, J. R. WALSH & S. ZUBERI; «Jet p_T resummation in Higgs production at $NNLL' + NNLO$»; Phys. Rev. **D89**, p. 054 001 (2014). 1307.1808. 99

[233] P. MEADE, H. RAMANI & M. ZENG; «Transverse momentum resummation effects in W^+W^- measurements»; Phys. Rev. **D90**, p. 114 006 (2014). 1407.4481. 99

[234] P. JAISWAL & T. OKUI; «Explanation of the WW excess at the LHC by jet-veto resummation»; Phys. Rev. **D90**, p. 073 009 (2014). 1407.4537. 99

[235] P. F. MONNI & G. ZANDERIGHI; «On the excess in the inclusive W^+W^- to $l^+l^-\nu\bar{\nu}$ cross section»; JHEP **05**, p. 013 (2015). 1410.4745. 99, 103

[236] F. CAMPANARIO, R. ROTH & D. ZEPPENFELD; «QCD radiation in WH and WZ production and anomalous coupling measurements»; Phys. Rev. **D91**, p. 054 039 (2015). 1410.4840. 99

[237] S. GANGAL, M. STAHLHOFEN & F. J. TACKMANN; «Rapidity-Dependent Jet Vetoes»; Phys. Rev. **D91**, p. 054 023 (2015). 1412.4792. 99

[238] T. BECHER, R. FREDERIX, M. NEUBERT & L. ROTHEN; «Automated NNLL + NLO resummation for jet-veto cross sections»; Eur. Phys. J. **C75**, p. 154 (2015). 1412.8408. 99, 103

[239] S. GANGAL, J. R. GAUNT, M. STAHLHOFEN & F. J. TACKMANN; «Two-Loop Beam and Soft Functions for Rapidity-Dependent Jet Vetoes»; JHEP **02**, p. 026 (2017). 1608.01999. 99

[240] J. K. L. MICHEL, P. PIETRULEWICZ & F. J. TACKMANN; «Jet Veto Resummation with Jet Rapidity Cuts»; JHEP **04**, p. 142 (2019). 1810.12911. 99, 113

[241] I. W. STEWART, F. J. TACKMANN & W. J. WAALEWIJN; «The Beam Thrust Cross Section for Drell-Yan at NNLL Order»; Phys. Rev. Lett. **106**, p. 032 001 (2011). 1005.4060. 99

[242] C. F. BERGER, C. MARCANTONINI, I. W. STEWART, F. J. TACKMANN & W. J. WAALEWIJN; «Higgs Production with a Central Jet Veto at NNLL+NNLO»; JHEP **04**, p. 092 (2011). 1012.4480. 99

[243] T. BECHER & M. NEUBERT; «Factorization and NNLL Resummation for Higgs Production with a Jet Veto»; JHEP **07**, p. 108 (2012). 1205.3806. 99

[244] B. JAGER, A. KARLBERG & J. SCHELLER; «Parton-shower effects in electroweak $WZjj$ production at the next-to-leading order of QCD»; Eur. Phys. J. **C79**, p. 226 (2019). 1812.05118. 99, 103

[245] H. BAER, C.-h. CHEN, F. PAIGE & X. TATA; «Detecting Sleptons at Hadron Colliders and Supercolliders»; Phys. Rev. **D49**, p. 3283–3290 (1994). hep-ph/9311248. 99, 104

[246] H. BAER, C.-h. CHEN, F. PAIGE & X. TATA; «Signals for minimal supergravity at the CERN large hadron collider. 2: Multi - lepton channels»; Phys. Rev. **D53**, p. 6241–6264 (1996). hep-ph/9512383. 99, 104

[247] Yu. ANDREEV, S. BITYUKOV, N. KRASNIKOV & A. TOROPIN; «Using the l+ l- + E(T)(miss) + jet veto signature for slepton detection»; (2006). 99, 104

[248] F. J. TACKMANN, W. J. WAALEWIJN & L. ZEUNE; «Impact of Jet Veto Resummation on Slepton Searches»; JHEP **07**, p. 119 (2016). 1603.03052. 99, 104

[249] M. A. EBERT, S. LIEBLER, I. MOULT, I. W. STEWART, F. J. TACKMANN, K. TACKMANN & L. ZEUNE; «Exploiting jet binning to identify the initial state of high-mass resonances»; Phys. Rev. **D94**, p. 051901 (2016). 1605.06114. 99

[250] B. FUKS & R. RUIZ; «A comprehensive framework for studying W' and Z' bosons at hadron colliders with automated jet veto resummation»; JHEP **05**, p. 032 (2017). 1701.05263. 99, 101, 103

[251] S. PASCOLI, R. RUIZ & C. WEILAND; «Safe Jet Vetoes»; Phys. Lett. **B786**, p. 106–113 (2018). 1805.09335. 99, 103, 104, 106, 114, 118

[252] S. PASCOLI, R. RUIZ & C. WEILAND; «Heavy Neutrinos with Dynamic Jet Vetoes: Multilepton Searches at $\sqrt{s}$ = 14, 27, and 100 TeV»; (2018)1812.08750. 99, 101, 102, 103, 104, 106, 107, 113, 114, 118

[253] D. BINOSI & L. THEUSSL; «JaxoDraw: A Graphical user interface for drawing Feynman diagrams»; Comput. Phys. Commun. **161**, p. 76–86 (2004). hep-ph/0309015. 100

[254] M. J. BAKER & A. THAMM; «Leptonic WIMP Coannihilation and the Current Dark Matter Search Strategy»; JHEP **10**, p. 187 (2018). 1806.07896. 101

[255] A. ALLOUL, N. D. CHRISTENSEN, C. DEGRANDE, C. DUHR & B. FUKS; «FeynRules 2.0 - A complete toolbox for tree-level phenomenology»; Comput. Phys. Commun. **185**, p. 2250–2300 (2014). 1310.1921. 101

[256] C. DEGRANDE; «Automatic evaluation of UV and R2 terms for beyond the Standard Model Lagrangians: a proof-of-principle»; Comput. Phys. Commun. **197**, p. 239–262 (2015). 1406.3030. 101

[257] T. HAHN; «Generating Feynman diagrams and amplitudes with FeynArts 3»; Comput. Phys. Commun. **140**, p. 418–431 (2001). hep-ph/0012260. 101

[258] C. DEGRANDE, C. DUHR, B. FUKS, D. GRELLSCHEID, O. MATTELAER & T. REITER; «UFO - The Universal FeynRules Output»; Comput. Phys. Commun. **183**, p. 1201–1214 (2012). 1108.2040. 101

[259] S. FRIXIONE & B. R. WEBBER; «Matching NLO QCD computations and parton shower simulations»; JHEP **06**, p. 029 (2002). hep-ph/0204244. 101

[260] R. FREDERIX & S. FRIXIONE; «Merging meets matching in MC@NLO»; JHEP **12**, p. 061 (2012). 1209.6215. 101

[261] T. Sjostrand & M. van Zijl; ≪A Multiple Interaction Model for the Event Structure in Hadron Collisions≫; Phys. Rev. **D36**, p. 2019 (1987).   101

[262] T. Sjostrand & P. Z. Skands; ≪Multiple interactions and the structure of beam remnants≫; JHEP **03**, p. 053 (2004). `hep-ph/0402078`.   101

[263] P. Artoisenet, R. Frederix, O. Mattelaer & R. Rietkerk; ≪Automatic spin-entangled decays of heavy resonances in Monte Carlo simulations≫; JHEP **03**, p. 015 (2013). `1212.3460`.   101

[264] J. Alwall, C. Duhr, B. Fuks, O. Mattelaer, D. G. Öztürk & C.-H. Shen; ≪Computing decay rates for new physics theories with FeynRules and MadGraph 5 $_aMC@NLO$≫; Comput. Phys. Commun. **197**, p. 312–323 (2015). `1402.1178`.   101

[265] P. Skands, S. Carrazza & J. Rojo; ≪Tuning PYTHIA 8.1: the Monash 2013 Tune≫; Eur. Phys. J. **C74**, p. 3024 (2014). `1404.5630`.   101

[266] M. Cacciari, G. P. Salam & G. Soyez; ≪The anti-k_t jet clustering algorithm≫; JHEP **04**, p. 063 (2008). `0802.1189`.   101

[267] M. Cacciari, G. P. Salam & G. Soyez; ≪FastJet User Manual≫; Eur. Phys. J. **C72**, p. 1896 (2012). `1111.6097`.   101

[268] V. Bertone, S. Carrazza, N. P. Hartland & J. Rojo; ≪Illuminating the photon content of the proton within a global PDF analysis≫; SciPost Phys. **5**, p. 008 (2018). `1712.07053`.   101

[269] A. Buckley, J. Ferrando, S. Lloyd, K. Nordström, B. Page, M. Rüfenacht, M. Schönherr & G. Watt; ≪LHAPDF6: parton density access in the LHC precision era≫; Eur. Phys. J. **C75**, p. 132 (2015). `1412.7420`.   101

[270] B. Fuks, M. Klasen, D. R. Lamprea & M. Rothering; ≪Precision predictions for electroweak superpartner production at hadron colliders with Resummino≫; Eur. Phys. J. **C73**, p. 2480 (2013). `1304.0790`.   102

[271] M. Bonvini, S. Marzani, J. Rojo, L. Rottoli, M. Ubiali, R. D. Ball, V. Bertone, S. Carrazza & N. P. Hartland; ≪Parton distributions with threshold resummation≫; JHEP **09**, p. 191 (2015). `1507.01006`.   102

[272] J. Fiaschi & M. Klasen; ≪Slepton pair production at the LHC in NLO+NLL with resummation-improved parton densities≫; JHEP **03**, p. 094 (2018). `1801.10357`.   102

[273] J. F. Gunion, M. Herrero & A. Mendez; ≪The Role of Longitudinally Polarized W'999particlesmalls in Slepton Production and Decay≫; Phys. Rev. **D37**, p. 2533 (1988).   102

[274] G. C. Cho, K. Hagiwara, J. Kanzaki, T. Plehn, D. Rainwater & T. Stelzer; ≪Weak boson fusion production of supersymmetric particles at the CERN LHC≫; Phys. Rev. **D73**, p. 054 002 (2006). `hep-ph/0601063`.   102

[275] P. Konar & D. Zeppenfeld; ≪Next-to-leading order QCD corrections to slepton pair production via vector-boson fusion≫; Phys. Lett. **B647**, p. 460–465 (2007). `hep-ph/0612119`.   102

[276] F. Borzumati & K. Hagiwara; «Testing supersymmetry at the LHC through gluon-fusion production of a slepton pair»; JHEP **03**, p. 103 (2011). 0912.0454. 103

[277] J. M. Lindert, F. D. Steffen & M. K. Trenkel; «Direct stau production at hadron colliders in cosmologically motivated scenarios»; JHEP **08**, p. 151 (2011). 1106.4005. 103

[278] M. Dasgupta, F. Dreyer, G. P. Salam & G. Soyez; «Small-radius jets to all orders in QCD»; JHEP **04**, p. 039 (2015). 1411.5182. 103

[279] A. Banfi, F. Caola, F. A. Dreyer, P. F. Monni, G. P. Salam, G. Zanderighi & F. Dulat; «Jet-vetoed Higgs cross section in gluon fusion at $N^3LO+NNLL$ with small-R resummation»; JHEP **04**, p. 049 (2016). 1511.02886. 103

[280] M. Dasgupta, F. A. Dreyer, G. P. Salam & G. Soyez; «Inclusive jet spectrum for small-radius jets»; JHEP **06**, p. 057 (2016). 1602.01110. 103

[281] M. Dasgupta, L. Magnea & G. P. Salam; «Non-perturbative QCD effects in jets at hadron colliders»; JHEP **02**, p. 055 (2008). 0712.3014. 103

[282] T. Aaltonen *et al.*; «Search for Supersymmetry in $p\bar{p}$ Collisions at $\sqrt{s} = 1.96$-TeV Using the Trilepton Signature of Chargino-Neutralino Production»; Phys. Rev. Lett. **101**, p. 251 801 (2008). 0808.2446. 104

[283] G. Aad *et al.*; «Search for direct slepton and gaugino production in final states with two leptons and missing transverse momentum with the ATLAS detector in pp collisions at $\sqrt{s} = 7$ TeV»; Phys. Lett. **B718**, p. 879–901 (2013). 1208.2884. 104

[284] G. Aad *et al.*; «Search for direct production of charginos, neutralinos and sleptons in final states with two leptons and missing transverse momentum in pp collisions at $\sqrt{s} = 8$ TeV with the ATLAS detector»; JHEP **05**, p. 071 (2014). 1403.5294. 104

[285] V. Khachatryan *et al.*; «Searches for electroweak production of charginos, neutralinos, and sleptons decaying to leptons and W, Z, and Higgs bosons in pp collisions at 8 TeV»; Eur. Phys. J. **C74**, p. 3036 (2014). 1405.7570. 104

[286] G. Aad *et al.*; «Search for the direct production of charginos, neutralinos and staus in final states with at least two hadronically decaying taus and missing transverse momentum in pp collisions at $\sqrt{s} = 8$ TeV with the ATLAS detector»; JHEP **10**, p. 096 (2014). 1407.0350. 104

[287] G. Aad *et al.*; «Search for the electroweak production of supersymmetric particles in $\sqrt{s}=8$ TeV pp collisions with the ATLAS detector»; Phys. Rev. **D93**, p. 052 002 (2016). 1509.07152. 104

[288] A. M. Sirunyan *et al.*; «Search for electroweak production of charginos and neutralinos in multilepton final states in proton-proton collisions at $\sqrt{s} = 13$ TeV»; JHEP **03**, p. 166 (2018). 1709.05406. 104

[289] K. O. Mikaelian; «Photoproduction of Charged Intermediate Vector Bosons»; Phys. Rev. **D17**, p. 750 (1978). 106

[290] R. W. Brown, D. Sahdev & K. O. Mikaelian; «W+- Z0 and W+- gamma Pair Production in Neutrino e, p p, and anti-p p Collisions»; Phys. Rev. **D20**, p. 1164 (1979).   106

[291] K. O. Mikaelian, M. A. Samuel & D. Sahdev; «The Magnetic Moment of Weak Bosons Produced in p p and p anti-p Collisions»; Phys. Rev. Lett. **43**, p. 746 (1979).   106

[292] D.-p. Zhu; «Zeros in Scattering Amplitudes and the Structure of Nonabelian Gauge Theories»; Phys. Rev. **D22**, p. 2266 (1980).   106

[293] S. J. Brodsky & R. W. Brown; «Zeros in Amplitudes: Gauge Theory and Radiation Interference»; Phys. Rev. Lett. **49**, p. 966 (1982).   106

[294] R. W. Brown, K. L. Kowalski & S. J. Brodsky; «Classical Radiation Zeros in Gauge Theory Amplitudes»; Phys. Rev. **D28**, p. 624 (1983). [Addendum: Phys. Rev.D29,2100(1984)].   106

[295] U. Baur, T. Han & J. Ohnemus; «QCD corrections and nonstandard three vector boson couplings in W^+W^- production at hadron colliders»; Phys. Rev. **D53**, p. 1098–1123 (1996). `hep-ph/9507336`.   106

[296] T. Gehrmann, M. Grazzini, S. Kallweit, P. Maierhöfer, A. von Manteuffel, S. Pozzorini, D. Rathlev & L. Tancredi; «W^+W^- Production at Hadron Colliders in Next to Next to Leading Order QCD»; Phys. Rev. Lett. **113**, p. 212 001 (2014). `1408.5243`.   106

[297] A. M. Sirunyan *et al.*; «Search for top squarks decaying via four-body or chargino-mediated modes in single-lepton final states in proton-proton collisions at $\sqrt{s} = 13$ TeV»; JHEP **09**, p. 065 (2018). `1805.05784`.   107

[298] C. Collaboration; «2017 Tau Trigger Efficiencies»; .   107

[299] C. Collaboration; «Search for SSM W' production, in the lepton+MET final state at a center-of-mass energy of 13 TeV»; (2015).   107

[300] A. M. Sirunyan *et al.*; «Particle-flow reconstruction and global event description with the CMS detector»; JINST **12**, p. P10 003 (2017). `1706.04965`.   107

[301] S. Chatrchyan *et al.*; «Determination of Jet Energy Calibration and Transverse Momentum Resolution in CMS»; JINST **6**, p. P11 002 (2011). `1107.4277`.   107

[302] M. Aaboud *et al.*; «In situ calibration of large-radius jet energy and mass in 13 TeV protonproton collisions with the ATLAS detector»; Eur. Phys. J. **C79**, p. 135 (2019). `1807.09477`.   107

[303] C. G. Lester & D. J. Summers; «Measuring masses of semiinvisibly decaying particles pair produced at hadron colliders»; Phys. Lett. **B463**, p. 99–103 (1999). `hep-ph/9906349`.   108

[304] H.-C. Cheng & Z. Han; «Minimal Kinematic Constraints and m(T2)»; JHEP **12**, p. 063 (2008). `0810.5178`.   108

[305] M. Aaboud *et al.*; «Measurements of Higgs boson properties in the diphoton decay channel with 36 fb^{-1} of pp collision data at $\sqrt{s} = 13$ TeV with the ATLAS detector»; Phys. Rev. **D98**, p. 052 005 (2018). `1802.04146`.   113

[306] E. Bagnaschi, F. Brmmer, W. Buchmller, A. Voigt & G. Weiglein; ≪Vacuum stability and supersymmetry at high scales with two Higgs doublets≫; JHEP **03**, p. 158 (2016). `1512.07761`.   123

[307] H. E. Haber & R. Hempfling; ≪The Renormalization group improved Higgs sector of the minimal supersymmetric model≫; Phys. Rev. **D48**, p. 4280–4309 (1993). `hep-ph/9307201`.   125

Sophie Louise Soulsby Williamson   **12$^{\text{ème}}$ Septembre 2019**

Sujet : Phénoménologie et contraintes de collisionneur des modéles supersymétriques à l'ére Run 2 du LHC

Résumé : Il a longtemps été pensé que le modèle standard (MS) est une description incomplète de notre univers, mais les résultats expérimentaux obtenus jusqu'à présent ne confirment rien de plus. La supersymétrie minimale, concrétisée par le modéle standard supersymmétrique minimal (MSSM), est une extension compétitive du MS et a été bien étudiée, en particulier dans le contexte de modéles simplifiés, au niveau des collisionneurs. Cependant, les techniques de recherche actuelles n'utilisent peut-être pas de manière optimale la capacité du collisionneur à tester l'espace de paramètre accessible. Au lieu d'utiliser un veto statique sur le momentum du jet pour minimiser les processus d'arrière-plan indésirables dans les recherches de signaux, il peut être démontré que l'utilisation d'un veto au jet dynamique construit à partir de plusieurs mesures d'activité hadronique et leptonique peut augmenter le potentiel de découverte des balayages MSSM simplifiés. Dans le même temps, il est indéniable que les limites imposées aux modèles simplifiés ne représentent pas fidèlement des scénarios plus complexes - en particulier les modèles de supersymétrie non minimaux dans lesquels les signatures de désintégration sont modifiées par un spectre plus complexe de chargino et de neutralino. Les gauginos de Dirac (DG) constituent une extension non minimale bien motivée qui semble plus plausible que le MSSM, qui est de plus en plus contraint par les observations. Ce travail peut être divisé en deux parties: (1) il étudie comment le contenu en particules élargi des modèles DG peut modifier les limites actuelles de la masse de gluino et de squark du Run 2 du LHC, et (2) effectue une étude approfondie du secteur de Higgs dans de tels modèles, qui est automatiquement aligné en raison de la supersymétrie étendue qui relie les couplages de Yukawa aux couplages de jauge dans le secteur électrofaible.

Subject : Phenomenology and collider constraints of Supersymmetric models in the Run 2 era of the LHC

Abstract: It has long been thought that the Standard Model (SM) is an incomplete description of our universe, yet experimental results thus far do not confirm anything beyond it. Minimal supersymmetry, embodied by the minimal supersymmetric standard model (MSSM), is a competitive extension of the SM and has been well investigated, especially in the context of simplified models, at colliders. However, current search techniques may not be making optimal use of the collider's ability to test the accessible parameter space. Instead of using a static veto on jet momentum to minimise undesirable background processes in signal searches, it can be shown that employing a dynamic jet veto constructed out of several measures of hadronic and leptonic activity can heighten the discovery potential of simplified MSSM scans. At the same time, it cannot be denied that the limits placed on simplified models are not a true representation of more complex scenarios - especially non-minimal supersymmetry models where decay signatures are altered by a more complex chargino and neutralino spectrum. Dirac gauginos (DG) are a well-motivated non-minimal extension that restore the naturalness being lost by the ever more stringent constraints on the MSSM. Here this work looks down two avenues: it (1) investigates how the enlarged particle content of DG models can lead to altered bounds on current gluino and squark mass limits from Run 2 of the LHC, and (2) makes an in depth study of the Higgs sector in such models, which is automatically alligned owing to extended supersymmetry that links the Yukawa couplings to the gauge couplings in the electroweak sector.